PROSPECTIVE RADIOLABLED BOMBESIN CONJUGATES FOR PROSTATE CANCER IMAGING AND THERAPEUTIC AGENTS

A Dissertation

presented to

the Faculty of the Graduate School

at the University of Missouri-Columbia

In Partial Fulfillment

of the Requirements for the Degree

Doctor of Philosophy

---

by

STEPHANIE R. LANE

Dr. Silvia S. Jurisson and Dr. Charles J. Smith, Dissertation Supervisors

DECEMBER 2009

The undersigned, appointed by the dean of the Graduate School, have examined the dissertation entitled

PROSPECTIVE RADIOLABLED BOMBESIN CONJUGATES FOR PROSTATE CANCER IMAGING AGENTS

presented by Stephanie Lane,

a candidate for the degree of doctor of philosophy,

and hereby certify that, in their opinion, it is worthy of acceptance.

Professor Silvia Jurisson

Professor Charles Smith

Professor Timothy Hoffman

Professor David Robertson

Professor Carol Deakyne

To Earl

Thank you.

ACKNOWLEDGMENTS

At this time I would like to thank all of those who provided academic to me during my graduate school career. I would especially like to thank my advisor Dr. Silvia Jurisson. During my undergraduate studies, you introduced me to the field of radiochemistry. It was at that point that I found my career passion. Your enthusiasm for your work continues to amaze and inspire me. Thank you for always being there for me. I would also like to thank my advisor Dr. Jeff Smith. It has been a very fast few years working in your laboratory. I appreciate all the effort you have contributed towards molding me into a successful chemist. It has been a delight working with you. I thank the additional members on my committee, Dr. David Robertson, Dr. Timothy Hoffman and Dr. Carol Deakyne. I truly appreciate the time you have given me and your kind support.

I would also like to mention those with whom I have worked closely in the laboratory. Hendrik Engelbrecht, Bhadrasetty Veerendra, Prasant Nanda, Adam Prasanphanich and Kwamena Baidoo, thank you for showing me the ways of the lab. I couldn't have had more fun while working with you. Tammy Rold, thank you for your constant cheerfulness. Gary Sieckman, you have been a valuable asset to the lab's progress. Lixin Ma and Said Figueroa, we could not have obtained such beautiful images without your assistance.

Finally, I would like to thank Dr. Wynn Volkert. Thank you for the guidance you have given me.

TABLE OF CONTENTS

CHAPTER 2: SYNTHESIS OF RHENIUM(V) SCHIFF BASE COMPLEXES AND THEIR REARRANGEMENT WITH TRIPEHNYL PHOSPHINE

CHAPTER 4: COPPER-64 TETRAAMINE BOMBESIN CONJUGATES AS POTENTAIL DIAGNOSTIC IMAGING AGENTS

APPENDIX

CHAPTER 2 APPENDIX

CHAPTER 3 APPENDIX

CHAPTER 4 APPENDIX

LIST OF FIGURES

Figure Page

LIST OF TABLES

LIST OF ABBREVIATIONS

Abbreviation	Definition
3-D	Three-dimensional
A	Alanine
BBN	Bombesin
BFCA	Bifunctional chelate approach
Boc	Di-tert-butyl dicarbonate
CH_2Cl_2	Dichloromethane
$CHCl_3$	Chloroform
CT	Computed tomography
DIEA	Dissopropylethylamine
DMF	Dimethylformamide
DMSO	Dimethyl sulfoxide
DO2A	1,4,7,10-tetraazabicyclo[5.5.2]tetradecane-4,10-diyl)diacetic acid
DOTA	1,4,7,10-Tetraazacyclododecane-1,4,7,10-tetraacetic acid
DTPA	*N*-Ethyldiisopropylamine
ECD	1-Ethyl-3-[3-dimethylaminopropyl]carbodiimide hydrochloride
EDTA	Ethylenediamine tetraacetic acid
ESI-MS	Electrospray ionization-mass spectroscopy
ETOH	Ethanol
FDG	2-deoxy-2-[^{18}F]fluoro-D-glucose
FT-IR	Fourier transform infrared
Fmoc	9-Fluorenylmethyloxycarbonyl
G	Glycine
GRP	Gastrin-releasing peptide
GRPr	Gastrin-releasing peptide receptors
H	Histidine
HBTU	2-(1H-benzotriazole-1-yl)-*N,N,N',N'*-tetramethyluronium hexafluorophosphate
HEDP	Hydroxyethylidenediphosphonate
HMPAO	Hexamethylpropyleneamineoxime
HOBt	1-Hydroxybenzotriazole
HYNIC	Hydrazinonicotinamide
IC_{50}	Half maximal inhibitory concentration
L	Lysine
M	Methionine
MeCN	Acetonitrile
MES	2-[morpholino]ethanesulfonic acid

NH_4PF_6	Ammonium hexafluorophosphate
NMBR	Neuromedin B receptors
NMR	Nuclear magnetic resonance
NOTA	1,4,7-triazacyclononane-1,4,7-tracetic acid
NO2A	1,4,7-triazacyclononane-1,4-diacetic acid
ORTEP	Oak Ridge Thermal Ellipsoid Plot Program
PBS	Phosphate buffered saline
PET	Positron-emission tomography
PPh_3	Triphenylphosphine
Q	Glutamine
Sal_2en	*N*,*N*′-ethylenebis(salicylaldimine)
Sal_2phen	N,N′-O-phenylenebis(salicylaldimine)
SCID	Severe combined immunodeficient mice
SD	Standard deviation
SPECT	Single photon emission computed tomography
SPPS	Solid phase peptide synthesis
Sulfo-NHS	*N*-hydroxysulfosuccinimide
RP-HPLC	Reverse phase high performance liquid chromatography
$t_{½}$	Half-life
t-Bu	Tert-butyloxycarbonyl
TETA	1,4,8,11-tetraazacyclotetradecane-1,4,8,11-tetraacetic acid
TE2A	1,4,8,11-tetraazabicyclo[6.6.2]hexadecane-4,11-diyl)diacetic acid
TFA	Trifluoroacetic acid
TLC	Thin-layer chromatography
TIS	Triisopropylsilane
UV	Ultra violet
V	Valine
W	Tryptophan

PROSPECTIVE RADIOLABLED BOMBESIN CONJUGATES FOR PROSTATE CANCER IMAGING AND THERAPEUTIC AGENTS

Stephanie Lane

Professor Silvia S. Jurisson, Dissertation Advisor

Professor Charles J. Smith, Dissertation Advisor

ABSTRACT

An active area of prostate cancer research is in the synthesis of radiolabeled peptides for *in vivo* tumor imaging or therapy. This method is possible since specific receptors are expressed in high concentration on certain tumor tissue. One receptor that is expressed in high concentration on prostate cancer tissue is the gastrin-releasing peptide (GRP). The amphibian peptide, bombesin (BBN), has high affinity and specificity to the GRP receptors; therefore, when BBN is radiolabeled with an appropriate radionuclide, non-invasive prostate tumor images and therapy can be obtained. The aim of this research was to produce kinetically inert bifunctional chelate complexes that would effectively contain the radionuclide Rhenium-188 (^{188}Re), Technetium-99m (^{99m}Tc), Copper-64 (^{64}Cu) or Bismuth-213 (^{213}Bi).

My first aim was to produce kinetically inert rhenium Schiff base complexes, for the potential in developing ^{188}Re thearapeutic agents. Rhenium complexes with tetradentate Schiff base ligands have previously yielded both rearranged Re^{V} complexes and reduced Re^{III} complexes on reaction with tertiary phosphine ligands. To further understand this chemistry, the rigid diiminediphenol (N_2O_2) Schiff base-ligand sal_2phen (N,N´-O-phenylenebis(salicylaldimine)) was reacted with (n-Bu_4N)[$Re^{V}OCl_4$] to yield

trans-[$Re^{V}OCl(sal_2phen)$]•$CHCl_3$ (**1**). On reaction with triphenylphosphine (PPh_3), a rearranged Re^{V} product *cis*-[$ReO(PPh_3)(sal_2phen^*)]PF_6$•$CHCl_2$ (**2**) was isolated, in which one of the imines was reduced to the amine during the reaction; a reduced Re^{III} product *trans*-[$ReCl(PPh_3)(sal_2phen)$]•CH_2Cl_2 (**3**), and reduced Re^{III} product *trans*-$[Re(PPh_3)_2sal_2phen])^+$, was isolated. Reaction of sal_2phen with [$Re^{III}Cl_3(PPh_3)_2(MeCN)$] resulted in the isolation of [$ReCl_2(PPh_3)(sal_2phen)$]•2 CH_2Cl_2 (**4**). All compounds were characterized by ^{1}H NMR, ^{31}P NMR, FT-IR, and ESI-MS spectra. Complexes **1**, **2**, **3**, and **4** were also characterized by single crystal X-ray crystallography.

My second aim was to produce kinetically inert technetium tricarbonyl bifunctional chelate complexes for the potential in developing molecular imaging agents. Here, I report a synthetic approach toward design of a new tridentate amine ligand for the organometallic aqua-ion $[^{99m}Tc(H_2O)_3(CO)_3]^+$. The new chelating ligand framework, 2-(N,N´-Bis(tert-butoxycarbonyl)diethylenetriamine) acetic acid (DTMA), was synthesized from a diethylenetriamine precursor and fully characterized by mass spectrometry and nuclear magnetic resonance spectroscopy (^{1}H and ^{13}C). DTMA was conjugated to H_2N-(X)-BBN(7-14)NH_2, where X = β-Ala, GGG, GSG and SSS, by means of solid phase peptide synthesis. [DTMA-(X)-BBN(7-14)NH_2] conjugates were purified by RP-HPLC and characterized by ESI-MS. The new conjugates were radiolabeled with $[^{99m}Tc(H_2O)_3(CO)_3]^+$ produced *via* Isolink® radiolabeling kits to produce [$^{99m}Tc(CO)_3$-DTMA-(X)-BBN(7-14)NH_2]. Radiolabeled conjugates were purified by reversed-phase high performance chromatography. Effective receptor binding behavior was evaluated *in vitro* and *in vivo*. [$^{99m}Tc(CO)_3$-DTMA-(X)-BBN(7-14)NH_2] conjugates displayed very high affinity for the gastrin releasing peptide receptor *in vitro* and *in vivo*.

My third aim was to produce kinetically inert copper bifunctional chelate complexes for the potential in developing molecular imaging and therapy agents. Here, I report the development of novel [NO2A-X-BBN(7-14)NH_2] conjugates, where NO2A = 1,4,7-triazacyclononane-1,4-diacetic acid and X = PABA, β-Ala, 6-Ahx or 9-Anc. [NO2A-(X)-BBN(7-14)NH_2] conjugates were purified by RP-HPLC and characterized by ESI-MS. The novel conjugates were radiolabeled with [$^{64}CuCl_2$] to produce [^{64}Cu-NO2A-(X)-BBN(7-14)NH_2]. The NO2A chelator effectively stabilized Cu(II) under *in vivo* conditions. [^{64}Cu-NO2A-(X)-BBN(7-14)NH_2] conjugates showed affinity and specificity towards GRPr-positive tissue and had efficient localization and clearance properties. High-resolution microPET/microCT images were obtained for the [^{64}Cu-NO2A-(X)-BBN(7-14)NH_2] conjugates (where X = PABA, 6-Ahx, 8-Aoc, and 9-Anc) in PC-3 xenografted tumors in a SCID mouse model.

My fourth aim was to produce kinetically inert bismuth bifunctional chelate complexes for the potential in developing therapy agents. Here, I report the development of novel [CHX-A˝-(8-Aoc)-BBN(7-14)NH_2] conjugates, where CHX-A˝ = (*N*-[(*R*)-2-amino-3-(*p*-aminophenyl)propyl]-*trans*-(*S*,*S*)-cyclohexane-1,2-diamine-N,N,N′,N˝,N‴-pentaacetic acid). Conjugates were purified by RP-HPLC and characterized by ESI-MS. The conjugate was radiolabeled with [$^{205}BiI_3$], to produce [^{205}Bi-CHX-A˝-(8-Aoc)-BBN(7-14)NH_2]. The pharmacokinetics of the [^{205}Bi-CHX-A˝-(8-Aoc)-BBN(7-14)NH_2] conjugate was investigated in nude mice at 0.5, 1, 4, 8 and 24 h post-tail vein injection. Unfortunately, poor receptor-specific localization was observed.

CHAPTER 1: INTRODUCTION

1.1 NUCLEAR MEDICINE

Nuclear medicine utilizes the nuclear emissions of a radionuclide for imaging and therapy of disease. The area of nuclear medicine is a relatively new field of medicine, which incorporates chemistry, biology, and pathology. The first clinical application of nuclear medicine was in 1926 when Dr. Hermann Blumgart injected 1-6 mCi of bismuth-214 (^{214}Bi), also known as Radium C, to monitor blood flow by molecular imaging. The first therapeutic application of nuclear medicine was in 1937 when Dr. John Lawrence used phosphorous-32 (^{32}P) to treat leukemia. [1] Up until the late 1940's, the focus of nuclear medicine was on whole organ targeting by methods such as macroaggregate or colloidal uptake. After this time, the development of simple coordination complexes containing a radionuclide began to emerge. An example of such a radionuclide coordination complex is technetium-99m labeled DTPA for kidney. It was not until the late 1970's when nuclear medicine began to shift towards receptor-specific radiopharmaceutical targeting. [1] These types of molecular probes incorporate a radionuclide into a biological targeting molecule for receptor-specific uptake. The future of nuclear medicine now lies in these types of molecular probes that target cancer based on specific antigens, receptors, metabolic pathways and DNA. [2-3]

By specifically targeting cancer with biological targeting probes, it is hopeful that the radiolysis effect in normal tissue will be minimized. The types of biological molecules used for directing the radionuclide to target tissue include antibodies, antibody fragments, proteins and peptides. Examples of successful antibody-based

radiopharmaceuticals include Prostascint and Zevalin. Prostascint is the drug name for ^{111}In-labeled capromab pendetide. Capromab pendetide is a whole murine antibody that has high affinity to prostate specific antigen located on the prostate. By imaging these antigens, the reoccurrence or spread of the disease can be monitored. Zevalin is the drug name for ^{111}In- or ^{90}Y-labeled ibritumomab tiuxetan and is marketed by IDEC Pharmaceuticals. Ibritumomab tiuxetan is a murine monoclonal antibody that has high specificity to the CD20 antigen, which is located on non-Hodgkin's lymphoma. ^{111}In-Zevalin is used as a molecular imaging agent and ^{90}Y-Zevalin is used as a radiotherapeutic agent. [3] However, there are some drawbacks to using this type of biological targeting probe. Clinical studies have shown that the large size of antibodies (~150 kDa) and antibody fragments (~50-100 kDa) result in slow blood clearance, high tumor uptake, and modest tumor-to-background ratios. This results in long time intervals being required between the time the radiopharmaceutical is administered and the time of imaging. Antibodies or antibody fragments also tend to accumulate in nonspecific sites of inflammation. [4-5] Therefore, the effectiveness of antibodies and antibody fragments in nuclear medicine is drastically limited. Some of these unfavorable characteristics can be overcome by the use of smaller targeting vectors, such as proteins and peptides. Peptides are of specific focus since they can express binding affinities that are comparable or greater than those of antibodies, and their smaller size (~1 kDa) allows for faster tumor targeting, better tumor penetration, shorter blood circulation, and an overall better target-to-non-target ratio. [4-5] Examples of successful peptide-based radiopharmaceuticals include OctreoScan® and NeoTec®. OctreoScan® is the trade name for ^{111}In-labeled octreotide and is marketed by Mallinckrodt Medical, Inc. for imaging somatostatin

subtype-2 receptors which are expressed in high concentration in neuroendocrine tumors. NeoTec® is the trade name for ^{18}F-FDG (FDG = 2-deoxy-2-[^{18}F]fluoro-D-glucose). NeoTec® is used to target the gluc-1 transport, which is expressed in high concentration on metastatic cancer cells. [3]

1.2 RADIONUCLIDE CONSIDERATIONS

The radionuclide properties that need to be considered include: decay emissions, half-life, availability, chemical properties, and specific activity. [2] First, the main types of emissions used in nuclear medicine include the alpha particle (α, He^{2+} nucleus), beta particle (β^-, e^- ejected by nucleus), positron (β^+, e^+ ejected by nucleus which will undergo annihilation with an e^-, resulting in two 511 keV photons approximately 180° apart), and gamma ray (λ, photon emitted by nucleus). Gamma rays and annihilation photons can be used for imaging in nuclear medicine and β^- and α particles can be used for therapy in nuclear medicine. An alpha particle is the heaviest of the forms of radioactive emission; therefore, it travels a short distance before it deposits its energy. Typically, an alpha particle travels around 50-100 μm in tissue (5-10 cell diameters). The beta particle and positron are equal in mass, and can travel between 1 to 12 mm in tissue (100-1200 cell diameters). [6] A gamma ray and photon have no mass or charge. This allows for them to travel through a person's body. Second, the radionuclide half-life ($t_{½}$) is of importance. It needs to be sufficiently long for radiopharmaceutical production, blood circulation, clearance from non-target tissue, and imaging, but it must not be too long so that unnecessary radiation effects result. Third, the radionuclide's availability is of importance. Lack of radionuclide availability will limit the progress that can be made

from the radiopharmaceutical developed with it. Fourth, the radionuclide's fundamental chemical properties must be taken into consideration so that it can form a kinetically inert complex within the radiopharmaceutical and remain that way *in vivo*. Last, high specific activity is required. Specific activity can be defined as the number of radionuclide decays per unit mass of the radionuclide.

1.3 NUCLEAR IMAGING TECHNIQUES

The two nuclear imaging techniques include single photon emission computed tomography (SPECT) and positron emission tomography (PET). Both techniques are non-invasive physiological imaging techniques that quantitatively map radiopharmaceutical concentration. This is accomplished by first distributing a radiopharmaceutical drug into the patient's bloodstream. Adequate time is allotted for the gamma- or positron-emitting radiopharmaceutical to localize on the cell surface or in the target tissue. In SPECT, one or two gamma cameras rotate around the patient detecting the incident gamma photons. This data is then sent to a computer whereby a correlation can be made for the location the gamma ray originated from in the patient. In PET, gamma cameras surrounding the patient are arranged to detect the coincidence annihilation photons. Annihilation photons result when a positron encounters an electron, its antimatter. The masses from the positron are converted into two 0.511 MeV annihilation photons, which are emitted in opposite directions. When two photons are simultaneously detected 180° apart, a correlation can be made to a point where the annihilation occurred in the patient. Examples of diagnostic radionuclides include ^{99m}Tc, ^{64}Cu and ^{205}Bi.

1.4 RADIOTHERAPY

In radiotherapy, an alpha- or beta-emitting radionuclide is contained within the radiopharmaceutical. Upon decay, the particles result in the formation of free radicals or in the ionization of cell DNA. This is what leads to cell death. Most types of radiotherapy use β^- emitters due to their ability to penetrate tissue. Low energy β^- particles can travel a few cell diameters (sub-millimeter range), which can be useful for targeting small tumors with minimal collateral damage. However, if the emitted particle's energy is too low, insufficient irradiation of the target can result. High energy β^- particles can travel up to 3 millimeters, which can be useful for targeting large tumors such as lymphoma nodules. However, if the emitted particle's energy is too high, then the radiation dose is deposited outside of the target to normal tissue. [7] Examples of therapeutic radionuclides that emit β^- particles include ^{67}Cu, ^{90}Y, ^{111}In, ^{166}Ho, and ^{188}Re. Another type of radiotherapy uses α emitters due to their short path length of 0.05-0.10 millimeter. These types of radiopharmaceuticals can cause a high degree of cell killing within a very short distance, while limiting the radiation dose to the surrounding normal tissue. Examples of therapeutic radionuclides that emit α particles include ^{111}At and ^{213}Bi. [7]

1.5 BIFUNCTIONAL CHELATE APPROACH TOWARDS RADIOPHARMACEUTICAL DESIGN

The method of radiolabeling usually follows either the direct labeling approach or the indirect (bifunctional chelate approach, BFCA) labeling approach. The direct labeling approach is a comparatively short, facile, radiosynthetic approach, but it suffers from lack of specificity since the radiometal can coordinate to any site on the molecule, including

near or on the binding region of the biologically active compound, inhibiting receptor-binding. The BFCA involves coordination of radiometal to a bifunctional chelating moiety that is linked to a biologically active compound (antibody, antibody fragment, protein or peptide) via a pharmacokinetic modifier. (See Figure 1.1.) Therefore, the binding region of the biologically active compound should not be compromised.

The biological targeting vector is connected to a pharmacokinetic modifier. This not only distances the radiometallated complex from the binding region of the targeting vector, but it also provides the ability to modify the pharmacokinetics of the overall radiopharmaceutical. [8] For example, a more lipophilic spacer would lead to clearance through the liver, while a more hydrophilic spacer would lead to clearance through the kidneys. Typical pharmacokinetic modifiers include amino acids, aliphatic spacers, and polyethylene glycol (PEG) spacers.

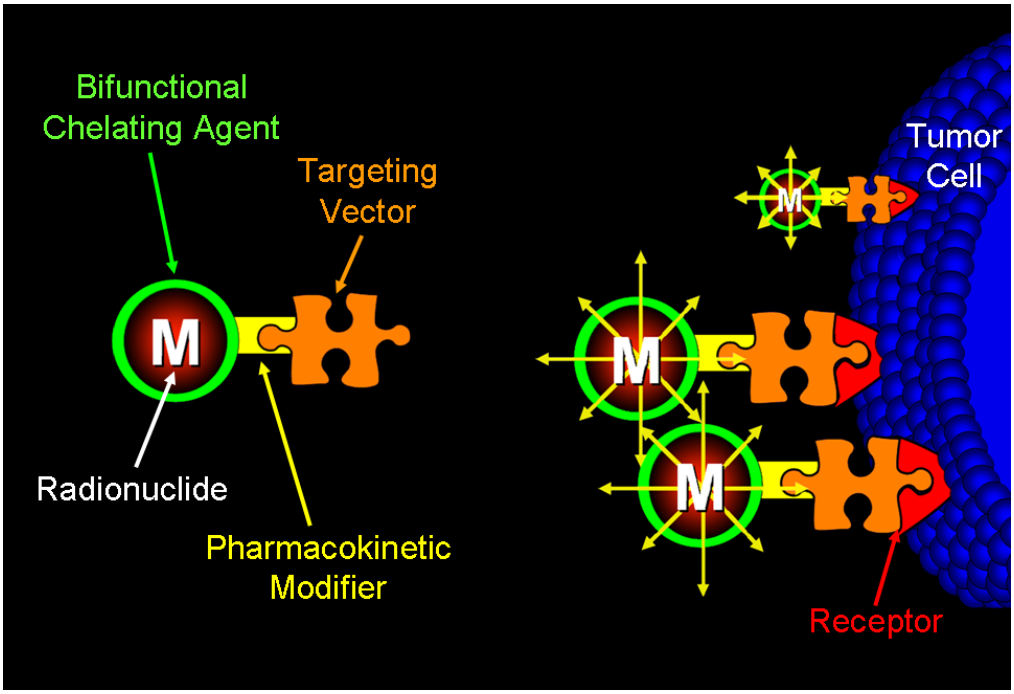

Figure 1.1: Schematic of the components and targeting of a site-directed radiopharmaceutical.

The chelate must effectively coordinate the radionuclide at low concentrations, result in high yield of a single product, produce a kinetically inert radionuclide complex under *in vivo* conditions, and be covalently linked to the biological targeting vector. [9] When deciding upon which chelate to use, it is important to consider the overall charge of the complex, the cavity size of the chelate in comparison to radionuclide radius, and the appropriate number of donor binding groups in the chelate. [10] An example of a successful bifunctional chelate is 1,4,7,10-tetraazacyclododecanetetraacetic acid (DOTA) for its ability to effectively contain +3 metal ions with four amine nitrogens and three of the carboxylic arms, while the fourth carboxylate arm is used to bind to the biological targeting vector.

1.6 BOMBESIN TARGETING OF GASTRIN-RELEASING PEPTIDE RECEPTORS

Bombesin (BBN) was first discovered by Erspamer and co-workers in 1971, from an extract in the skin of the frog, *Bombina bombina.* [11] BBN is the 14 amino acid amphibian peptide analog of the 27 amino acid mammalian regulatory gastrin-releasing peptide (GRP). (See Figure 1.2.) There are four known mammalian bombesin receptor subtypes, including BB1 (neuromedin B receptors, NMBR), BB2 (gastrin-releasing peptide receptors, GRPr), and BB3 (BRS-3). [12] BBN and GRP are neuroendocrine peptides that are involved in regulating exocrine secretion, smooth muscle contraction, and gastrointestinal hormone release. They also function as growth factors that stimulate growth in normal and neoplastic tissues of normal mouse pancreas, human prostate, breast, pancreatic, and small-cell lung cancer. [13]

BBN and GRP share a homologous 7 amino acid amidated C-terminus, [WAVGHLM-NH_2], which is necessary for receptor binding to GRPr. BBN(7-14)NH_2, [QWAVGHLM-NH_2], is of particular interest in nuclear medicine due to its smaller size, allowing for easier synthesis, and high affinity for the GRPr. Two approaches of BBN targeting can be utilized, including the antagonist and agonist approaches. When a BBN antagonistic radiopharmaceutical binds to a receptor, no signal is given to the cell, and the receptor/radiopharmaceutical complex is not internalized. Antagonists have been shown to have lower affinity than agonists, but they can be beneficial by preventing tumor-proliferation. [14] When a BBN agonistic radiopharmaceutical binds to a receptor, the receptor/radiopharmaceutical complex is internalized into the cell. This results in the trapping of the radionuclide inside of the cell and leads to high specific uptake and high target-to-nontarget ratios. [14]

In recent years, our group and others have focused upon development of site-directed molecular imaging agents targeting human cancers expressing the GRPr subtype. [15-16] These studies have been based primarily upon reports that specific human tumors tend to express the GRPr in very high numbers, therefore providing an approach to selectively target GRP receptor-expressing neoplasms with minimal accumulation in non-target collateral tissue. [13, 17]

GRP: H-A-P-V-S-V-G-G-G-T-V-L-A-K-M-Y-P-R-G-N-H-**W-A-V-G-H-L-M-NH_2**
BBN(1-14): E-G-Q-R-L-G-N-Q-**W-A-V-G-H-L-M-NH_2**
BBN(7-14): Q-**W-A-V-G-H-L-M-NH_2**

Figure 1.2: Amino acid sequence for GRP, BBN(1-14)NH_2, and BBN(7-14)NH_2. The GRP binding region is in bold.

1.7 GASTRIN-RELEASING PEPTIDE EXPRESSION ON PROSTATE CANCER

Markwalder and Reubi showed GRPr expression to be present in 30 of 30 cases who had primary prostate invasive cancer. Of those patients, 84% showed high or very high GRPr expression. Non-tumor prostate tissue and prostate enlargement caused by tissue overgrowth were shown to be either completely absent of or to have a low prevalence of GRP receptors. [18] Sun and co-workers found GRPr expression in 20 of 22 cases in those who had prostate cancer. [19] When focusing on the human prostate cancer cell line, PC-3, it is estimated that each cell contains 44,000 GRP receptors. [20] The findings of these combined studies make a sound argument for development of GRPr-specific diagnostic and therapeutic radiopharmaceuticals.

1.8 RHENIUM CHEMISTRY AND NUCLEAR PROPERTIES

Rhenium is a third-row transition metal in group 7 of the periodic table with an atomic number of 75. Rhenium's electron configuration is [Xe] $4f^{14}5d^{5}6s^{2}$, with seven valence electrons available for bonding. [21] Nine rhenium oxidation states are known, ranging from -1 to +7, with oxidation states of +4 and +7 being most common. This versatility in oxidation results in its dynamic coordination chemistry. There are various types of ligand systems that are used to complex rhenium, but the most common types are those with amine or amide nitrogen, thiolato sulfur, and oxide atoms. [9] Carbonyl or isocyanide back-donating groups are other types of ligand systems that have recently become prevalent in the literature. [9] Rhenium's main advantage is that it is a 'matched pair' to that of technetium, due to their chemical similarities. The work done with

rhenium can often be translated to technetium. Rhenium is also important since it is the therapeutic surrogate to the ^{99m}Tc imaging radionuclide.

Rhenium naturally occurs as stable Re-185 (37.4%) and Re-187 (62.6%), but the radioisotopes Re-186 and Re-188 can be produced. Rhenium-186 [$t_{1/2}$ = 89 h; β^-_{max} = 1.07 MeV (92.53%); λ_{avg} = 137 keV (7.47%)] and rhenium-188 [$t_{1/2}$ = 17 h; β^-_{max} = 2.12 MeV (85%); λ_{avg} = 155 keV (15%)] have application in therapeutic nuclear medicine. ^{186}Re has a mean range of 0.92 mm in tissue and ^{188}Re has a mean range of 2.43 mm in tissue. [7] When considering the $t_{½}$ and β^-_{max}, ^{186}Re delivers more radiation, in terms of rad/mCi, than does ^{188}Re. Two different production techniques are used to obtain the two rhenium isotopes. ^{186}Re can be produced by either neutron irradiation of ^{185}Re or by a (p,n) reaction on ^{186}W. ^{188}Re can be obtained carrier-free by using an ^{188}W/^{188}Re generator. [7] (See Table 1.1.)

1.9 TECHNETIUM CHEMISTRY AND NUCLEAR PROPERTIES

Technetium is a second-row transition metal in group 7 of the periodic table with atomic number 43. Technetium's electron configuration is [Kr] $4d^5 5s^2$, with seven valence electrons available for bonding. [21] Nine oxidation states of technetium are known, ranging from -1 to +7, with oxidation states of +4 and +7 being most common. This versatility in oxidation results in its dynamic coordination chemistry. There are various types of ligand systems that are used to complex technetium, but the most common types are those with amine nitrogens, amide nitrogens, thiolato sulphurs, phosphorous and oxo atoms. [9]

Technetium does not have any stable isotopes. The radionuclide that is utilized for nuclear medicine is technetium-99m. ^{99m}Tc [$t_{1/2}$ = 6.01 h; γ_{avg} = 140 keV (100%)] is the most widely used radionuclide in medicine. This is due to its short half-life, gamma ray emission energy, on-site availability and low cost. Tc-99m can be produced from a molybdenum-99 generator. (See Table 1.) The ^{99}Mo/^{99m}Tc generator consists of MoO_4^{2-}, which is adsorbed onto an alumina column. As the ^{99}Mo [$t_{½}$ = 66 h; β^- = 1.24 MeV; γ = 739.5 keV] undergoes beta decay to ^{99m}Tc, $^{99m}TcO_4^-$ accumulates on the alumina column. After about 24 h, maxium activity of $^{99m}TcO_4^-$ can be eluted off of the column with saline, while the doubly charged MoO_4^{2-} remains tightly bound to the column.

1.10 COPPER CHEMISTRY AND NUCLEAR PROPERTIES

Copper is a first-row transition metal in group 11 of the periodic table with an atomic number of 29. Copper's electron configuration is [Ar] $3d^{10}4s^1$, with eleven valence electrons available for bonding. Five oxidation states of copper are known, ranging from 0 to 4. Three oxidation states of copper are possible in aqueous solution. These are Cu(I), Cu(II), and Cu(III). Cu(II) forms the most kinetically inert complexes due to the d^9 electron configuration and crystal-field stabilization energy. [22] A wide variety of borderline-soft donors can effectively complex the Cu(II) atom, which include amines and imines. A variety of geometries are possible for Cu(II) complexes, including square planar, distorted square planar, trigonal pyramidal, square pyramidal, and distorted octahedral. [22]

Two radioisotopes of copper are important in nuclear medicine. These include ^{64}Cu and ^{67}Cu. Copper-64 [$t_{1/2}$ = 12.7 h; $E_{\beta^+}{}_{max}$ = 0.65 MeV (17.9%); $E_{\beta^-}{}_{max}$ = 0.57 MeV

(39%); electron capture (EC) (43.1%)] and Copper-67 [$t_{1/2}$ = 62 h; $E_{\beta^-}{}_{max}$ = 0.577 MeV (100%)] have applications in diagnostic (γ rays following β^- or annihilation photons following β^+ decay) and therapeutic (β^+ particles, β^- particles, and Auger electrons following EC) nuclear medicine. [7] (See Table 1.) The half-lives for ^{64}Cu and ^{67}Cu are suitable for radionuclide drug incorporation, drug circulation, and patient imaging or therapy. [23] ^{64}Cu can be produced at both a reactor and a cyclotron, but cyclotron-produced ^{64}Cu has many advantages, including very high specific activity (100 mCi/mg Cu). [7] For this work, ^{64}Cu was obtained by the ^{64}Ni(p,n)^{64}Cu nuclear reaction from either the MDS Nordion, Trace Life Sciences, or the University of Wisconsin-Madison cyclotron.

1.11 BISMUTH CHEMISTRY AND NUCLEAR PROPERTIES

Bismuth is a fifth-row post-transition metal in group 15 of the periodic table with atomic number 83. Bismuth's electron configuration is [Xe] $4f^{14}5d^{10}6s^26p^3$. Most of bismuth's chemistry can be interpreted from the three unpaired electrons in the 6 p-orbitals. Coordination numbers for bismuth include, 1, 2, 3, 4, 5, 6, 7, 8, 9, 10, and 12, with 3, 4, 5, and 6 being most common. The oxidation states of bismuth are -3, 0, +3 and +5, with +3 and +5 being most common. Bismuth's atomic radius is 1.50 Å, the six-coordinate Bi^{+3} ionic radius is 1.03 Å and the six-coordinate Bi^{+5} ionic radius is 0.76 Å. [24]

Bismuth has one non-radioactive isotope, ^{209}Bi, and multiple radioisotopes. Two bismuth radioisotopes that have potential application in nuclear medicine are ^{205}Bi and ^{213}Bi. Bismuth-205 [$t_{1/2}$ = 15.31 d; electron capture (EC) = 2.71 MeV (100%)] and

bismuth-213 [$t_{1/2}$ = 45.6 m; β^- = 1.42 MeV (97.8%); α = 5.87 MeV (2.2%)] have applications in diagnostic (λ) and therapeutic (β^- and α particles) nuclear medicine. (See Table 1.1.) The production of ^{205}Bi involves a (p,2n) reaction on enriched lead-206. The natural isotopes of lead include Pb-204 (1.4%), Pb-206 (24.1%), Pb-207 (22.1%) and Pb-208 (52.4%). [25] Therefore, if the enriched target has residual lead contamination with Pb-207, then ^{206}Bi will result. It is also known that ^{206}Bi production is 2.5 times more efficient than that of ^{205}Bi production. [26] ^{206}Bi [$t_{½}$ = 6.24 d; EC (100%)] is not an ideal radionuclide for nuclear medicine due to its high energy gammas of 516, 803, and 881 keV. ^{213}Bi can be produced from a ^{225}Ac/^{213}Bi generator, which can result in >25 mCi of high-grade ^{213}Bi from one elution. [27] The generator system also allows for the potential use in the clinical setting. The short half-life of ^{213}Bi is a challenge for drug incorporation, localization, and clearance, but its high linear energy transfer (LET) would be very beneficial in cell killing. [7] ^{213}Bi has a mean range of 0.06 mm in tissue. [7] For this work, non-radioactive bismuth-209 was used as the non-radioactive surrogate for Bi-205/Bi-213.

Table 1.1: Selected radionuclide production and decay properties.

Radionuclide	**Production**	**Decay**	**$E_\lambda/E_{\beta^-}/E_{\beta^+}/E_\alpha$ (keV)**	**$t_{½}$**
Cu-64	Cyclotron	EC, β^-, β^+	λ: 1345.8 β^-: 578 β^+: 651	12.7 h
Cu-67	Reactor or Cyclotron	β^-	β^-: 570	62 h
Tc-99m	^{99}Mo/^{99m}Tc Generator	IT	λ: 143	6.01 h
Re-186	Reactor or Cyclotron	β^- and λ	λ: 137.2 β^-: 1,071; 933	86 h
Re-188	^{188}W/^{188}Re Generator	β^- and λ	λ: 155 β^-: 2,118; 1,962	17 h
Bi-205	Cyclotron	EC	EC: 2,710	15.31 d
Bi-213	^{225}Ac/^{213}Bi Generator	β^-, λ and α	λ: 440.5; 323.7 β^-: 1,420; 1,020 α: 5,870; 5,550	45.6 min

1.12 REFERENCES

1. SNM. *Historical Timeline*. 2009 [cited 2009; Available from: http://interactive.snm.org/index.cfm PageID=1107&RPID=10.

2. Heeg, M.J. and S.S. Jurisson, *The Role of Inorganic Chemistry in the Development of Radiometal Agents for Cancer Therapy.* Accounts of Chemical Research, 1999. **32**(12): p. 1053-1060.

3. Imam, S.K., *Molecular Nuclear Imaging: The Radiopharmaceuticals (Review).* Cancer Biotherapy & Radiopharmaceuticals, 2005. **20**(2): p. 163-172.

4. Fischman, A.J., J.W. Babich, and H.W. Strauss, *A Ticket to Ride: Peptide Radiopharmaceuticals.* J Nucl Med, 1993. **34**(12): p. 2253-2263.

5. Sampson, C.B., ed. *Textbook of Radiopharmacy Theory and Practice; New Radiopharmaceuticals, 25.5 New Carrier Molecules*. 1994, Gordon and Breach: Amsterdam. 315-317.

6. Kassis, A.I. and S.J. Adelstein, *Considerations in The Selection of Radionuclides for Cancer Therapy*, in *Handbook of Radiopharmaceuticals*, M.J. Welch and C.S. Redvanly, Editors. 2003, John Wiley and Sons, Ltd: West Sussex. p. 767-793.

7. Eary, J.F. and W. Brenner, eds. *Nuclear Medicine Therapy*. 2007, Informa Healthcare USA, Inc.: New York.

8. Weiner, R.E. and M.L. Thakur, *Radiolabeled Peptides in Oncology: Role in Diagnosis and Treatment.* BioDrugs, 2005. **19**: p. 145-163.

9. Abram, U. and R. Alberto, *Technetium and rhenium: coordination chemistry and nuclear medical applications.* Journal of the Brazilian Chemical Society, 2006. **17**: p. 1486-1500.

10. Brechbiel, M.W., *Bifunctional Chelates for Metal Nuclides.* The Quarterly Journal of Nuclear Medicine and Molecular Imaging, 2008. **52**(2): p. 166-73.

11. Anastasi, A., V. Erspamer, and M. Bucci, *Isolation and structure of bombesin and alytesin, 2 analogous active peptides from the skin of the European amphibians Bombina and Alytes.* Experientia, 1971. **27**: p. 166-167.

12. Jensen, R.T., et al., *International Union of Pharmacology. LXVIII. Mammalian Bombesin Receptors: Nomenclature, Distribution, Pharmacology, Signaling, and Functions in Normal and Disease States.* Pharmacol Rev, 2008. **60**(1): p. 1-42.

13. Fleischmann, A., et al., *Bombesin Receptors in Distinct Tissue Compartments*

of Human Pancreatic Diseases. Laboratory Investigation, 2000. **80**(12): p. 1807-1817.

14. Knight, L.C., *Radiolabeled Peptides for Tumor Imaging*, in *Handbook of Radiopharmaceuticals*, M.J. Welch and C.S. Redvanly, Editors. 2003, John Wiley and Sons, Ltd.: West Sussex. p. 643-684.

15. García Garayoa, E., et al., *Chemical and biological characterization of new Re(CO)3/[99mTc](CO)3 bombesin analogues.* Nuclear Medicine and Biology, 2007. **34**(1): p. 17-28.

16. Lane, S.R., et al., *99mTc(CO)3-DTMA bombesin conjugates having high affinity for the GRP receptor.* Nuclear Medicine and Biology, 2008. **35**(3): p. 263-272.

17. West, S.D. and D.W. Mercer, *Bombesin-Induced Gastroprotection.* Annals of Surgery, 2005. **241**(2): p. 227-231.

18. Markwalder, R. and J.C. Reubi, *Gastrin-releasing Peptide Receptors in the Human Prostate: Relation to Neoplastic Transformation.* Cancer Res, 1999. **59**(5): p. 1152-1159.

19. Sun, B., et al., *Presence of receptors for bombesin/gastrin-releasing peptide and mRNA for three receptor subtypes in human prostate cancers.* The Prostate, 2000. **42**(4): p. 295-303.

20. Reile, H., P.E. Armatis, and A.V. Schally, *Characterization of high-affinity receptors for bombesin/gastrin releasing peptide on the human prostate cancer cell lines PC-3 and DU-145: Internalization of receptor bound ^{125}I-(Tyr$_4$) bombesin by tumor cells.* The Prostate, 1994. **25**(1): p. 29-38.

21. Peacock, R.D., *The Chemistry of Technetium and Rhenium*. 1966, Amsterdam: Elsevier Publishing Company.

22. Wadas, T.J., et al., *Copper Chelation Chemistry and its Role in Copper Radiopharmaceuticals.* Current Pharmaceutical Design, 2007. **13**: p. 3-16.

23. Blower, P.J., J.S. Lewis, and J. Zweit, *Copper radionuclides and radiopharmaceuticals in nuclear medicine.* Nuclear Medicine and Biology, 1996. **23**(8): p. 957-980.

24. Greenwood, N.N. and A. Earnshaw, *Chemistry of the Elements*. Second Edition ed. 2001, Oxford: Butterworth Heinemann.

25. Baum, E.M., H.D. Knox, and T.R. Miller, *Nuclides and Isotopes Chart of the Nuclides*. 16th Edition ed. 2002: Knolls Atomic Power Laboratory, Inc.

26. Fischer, R., et al., *205Bi/206Bi cyclotron production from Pb-isotopes for absorption studies in humans.* Applied Radiation and Isotopes, 1993. **44**(12): p. 1467-1472.

27. Zalutsky, M.R. and J.S. Lewis, *Radiolabeled Antibodies for Tumor Imaging and Therapy*, in *Handbook of Radiopharmaceuticals*, M.J. Welch and C.S. Redvanly, Editors. 2003, John Wiley and Sons, Ltd.: West Sussex. p. 685-714.

CHAPTER 2: SYNTHESIS OF RHENIUM(V) SCHIFF BASE COMPLEXES AND THEIR REARRANGEMENT WITH TRIPEHNYL PHOSPHINE

2.1 INTRODUCTION

2.1.1 Rhenium Schiff Base Complexes

Schiff base complexes contain a carbon-nitrogen double bond, where the nitrogen is connected to an aryl or alkyl group. (See Figure 2.1.) The first rhenium Schiff base complex was reported in 1979 by Middleton and co-workers. [1] Since then, a multitude of rhenium Schiff base complexes have been reported. One class of Schiff base ligands is the N_2O_2 tetradentate type. Upon chelation with rhenium, four possible configurations can result, but it is suggested that the ligand will lie in the equatorial plane with respect to the rhenium oxo core when less than five carbons are between the two imine nitrogens (configuration A). (See Figure 2.2.) The tetradentate coordination to the rhenium metal center results in the formation of three chelate rings, which assists in stabilizing the rhenium complex. [6] Rhenium complexes with tetradentate salicylaldehyde and tetradentate acetylacetone derived Schiff base ligands have

Figure 2.1: Basic Schiff base structure.

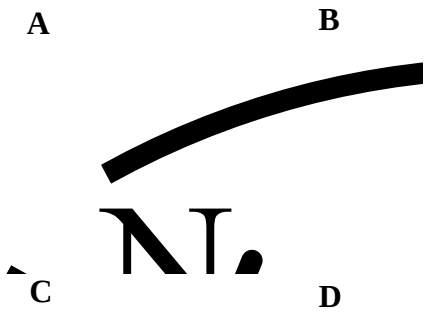

Figure 2.2: Possible rhenium-oxo complex formations with an N_2O_2 chelate.

been extensively studied for their potential use in nuclear medicine or commercial catalysis. [1-5]

2.1.2 Specific Aims

This work is focused on complexing rhenium with the chelate sal_2phen (N,N´-O-phenylenebis(salicylaldimine)). Sal_2phen is a tetradentate N_2O_2 ligand and will occupy four binding sites on the rhenium metal center. The two other sites on the rhenium metal center will be occupied by multiply-bound oxygen and a chloride atom. [$ReOCl(sal_2phen)$] will then be reacted with the moderate nucleophile, triphenyl phosphine (PPh_3) in the pursuit of obtaining a single Re(III) metal complex.

2.1.3 Preliminary Work

The potential of nuclear medical applications stems from the nuclear properties of Re-186 and Re-188. The bifunctional chelate approach is one technique that can be used to localize the radiation to specific sites in the body. This approach uses a chelate to effectively bind the metal center. It is imperative that the metal complex is kinetically inert in vivo so as to minimize non-target irradiation. Examples of such rhenium Schiff base complexes include *trans*-[$Re(H_2O)(acac_2en)$]Cl, *trans*-[$ReOCl(acac_2pn)$], [ReO(salen)(Solv)], and [ReO(salpn)(Solv)]. [1-2, 7] (See figure 2.3.) To enhance the kinetic stability of the *trans*-[$Re(H_2O)(acac_2en)$]Cl and *trans*-[$ReOCl(acac_2pn)$] complex, Benny and co-workers investigated the reduction of the Re(V) metal center to Re(III) by the addition of phosphines. Published results showed that phosphine addition resulted in either metal center reduction or ligand rearrangement to accommodate the phosphine.

The resulting product was dependent on the phosphine ligand and Schiff base ligand backbone. [7]

The potential of catalytic application stems from rhenium's catalytic activity, which is said to approach that of nickel and platinum. High-valent rhenium(V/VII) oxo complexes have been shown to be valuable as oxidation catalysts and in oxygen atom transfer (OAT)s. [3, 8] Rhenium catalysts have been shown to reduce ketones, aldehydes, and imines. Previous research has shown that rhenium tetradentate *N*,*N*′-ethylenebis(salicylaldimine) (sal_2en) complexes have utility for OAT, with their reactivity stemming from rhenium's high oxidation state and the cationic charge of the complex. [9] Two such examples include $[Re(O)(salen)(Solv)][B(C_6F_5)_4]$ and $[Re(O)(salpn)(Solv)][B(C_6F_5)_4]$. [3] These complexes have been shown to be air and moisture tolerant. In the presence of organosilanes, they result in hydrosilation of ketones and aldehydes. Abu-Omar and co-workers have reported that the $[Re(O)(salpn)(Solv)]^+$ complex resulted in higher catalytic activity than the $[Re(O)(salen)(Solv)]^+$ complex due

Figure 2.3: Examples of rhenium Schiff base complexes. Top left: [ReO(salen)X]. Top right: $[Re(H_2O)(acac_2en)]Cl$. Bottom left: [ReO(salpn)X]. Bottom right: $[ReOCl(acac_2pn)]$.

to the complex's geometry. Both $[Re(O)(salen)(Solv)]^+$ and $[Re(O)(salpn)(Solv)]^+$ resulted in the N_2O_2 donor atoms of the ligand occupying the equatorial plane, but with [Re(O)(salen)(Solv)], the solvent ligand is *trans* to the rhenium-oxo, whereas with [Re(O)(salpn)(Solv)], the solvent ligand is *cis* to the rhenium-oxo. The more labile *cis* solvent results in the higher catalytic activity of the rhenium metal center. [3]

2.2 EXPERIMENTAL

2.2.1 General Considerations

All chemicals were of reagent grade or better and solvents were degassed by flushing with N_2 for 30 min before using. All experiments were carried out under a nitrogen atmosphere unless otherwise noted. ^1H and ^{13}C NMR spectra were recorded on a Bruker 250 or 500 MHz instrument at 25°C in deuterated solvent (d^6-DMSO or d^6-$CDCl_3$) with TMS as an internal reference. The ^{31}P NMR spectra were recorded on a Bruker 250 MHz instrument at 25°C in deuterated solvent (d^6-DMSO or d^6-$CDCl_3$) with H_3PO_4 as an external reference. FT-IR spectra were recorded in the range of 4000-400 cm^{-1} as KBr pellets on a Nicolet Magna-IR spectrometer 550. Electrospray Ionization Mass Spectra (ESI-MS) were obtained on a Thermo Finnigan TSQ7000 triple-quadrupole instrument with an API2 source. Elemental analysis was performed by Quantitative Technologies Inc. (QTI; Whitehouse, NJ).

2.2.2 Materials

The starting compounds, [TBA]2.[$ReOCl_4$] and [$ReCl_3(PPh_3)_2(ACN)$] were prepared as reported in the literature. [14] The N_2O_2 Schiff base ligand, sal_2phen, was prepared by mixing the appropriate salicylaldehye and *o*-phenylenediamine in a 2:1 ratio in ethanol. The ligand was recrystalized from ethanol prior to use. [15]

2.2.3 *trans*-[$Re^{V}OCl(sal_2phen)$]•$CHCl_3$, (1)

(*n*-Bu_4)[$ReOCl_4$] (186 mg, 0.318 mmol) in $CHCl_3$ (10 mL) was added to a solution of sal_2phen (207 mg, 0.653 mmol) in ethanol (15 mL). The solution was refluxed for 3 hours under a nitrogen atmosphere and placed in a freezer overnight. The maroon product was collected by vacuum filtration. The product was washed with hot toluene and ether to remove any remaining starting material and byproducts. The solid product was dissolved in chloroform and placed in a screw-top vial with the cap slightly opened. After several days, dark brown crystals had formed. Yield: 75%. ^{1}H NMR [DMSO, 500 MHz; δ (ppm)]: 7.16 (1H), 7.26 (1H), 7.37 (1H), 7.50 (1H), 7.78 (1H), 7.82 (1H), 7.84 (1H), 7.95 (1H), 8.03 (1H), 8.16 (1H), 8.53 (1H), 8.60 (1H), 10.41 (1H), 10.42 (1H). ^{13}C NMR [DMSO, 250 MHz; δ (ppm)]: 179.43, 176.28, 173.29, 172.98, 151.47, 150.02, 141.00, 140.06, 139.82, 139.59, 131.44, 131.27, 122.31, 121.54, 121.45, 120.61, 119.56. IR (KBr, v in cm^{-1}): 951.36 (m, Re=O). MS (m/z): [$(M\text{-}Cl)^{+}$] 517.04 (517.07). Anal. Calcd (found) for $ReC_{20}H_{14}N_2O_3Cl$: C, 43.13 (43.36); H, 2.50 (2.91); N, 5.27 (5.06); Cl, 6.71 (6.40).

2.2.4 *cis*-[$Re^{V}O(PPh_3)(sal_2phen^*)]PF_6 \bullet CH_2Cl_2$, (2)

Triphenylphosphine (143 mg, 0.546 mmol) in CH_2Cl_2 (10 mL) was added to a solution of **1** (100 mg, 0.181 mmol) in ethanol (10 mL). The solution was refluxed for 2.5 hours under a nitrogen atmosphere, after which the solvent was removed under vacuum. The maroon-colored product was washed with hot hexane and ether to remove ligand by-products (i.e., phosphine oxide, sal_2phen fragments). NH_4PF_6 (11 mg, 0.067 mmol) was dissolved in CH_2Cl_2 (5 mL) and added to the product in CH_2Cl_2. Good quality crystals were obtained by the slow evaporation of $CDCl_3$ in an NMR tube at ambient temperature. Yield: 30%. ^{1}H NMR [$CDCl_3$, 500 MHz; δ (ppm)]: 3.96 (2H); 4.20 (1H); 6.65 (2H); 6.87 (2H); 6.95 (3H); 7.31 (3H); 7.44 (5H); 7.51 (4.5H); 7.64 (4.5H); 7.90 (1H); 8.55 (1H); 8.73 (1H). ^{31}P NMR [DMSO, 250 MHz; δ (ppm)]: 24.89. IR (KBr, ν in cm^{-1}): 951.39 (w, Re=O). MS (m/z): [Chloride dimer] 1597.78 (1597.32).

2.2.5 [$Re^{III}Cl_2(PPh_3)(salphen)] \bullet 2\ CHCl_3$, (3)

[$Re^{III}Cl_3(PPh_3)_2(MeCN)$] (50 mg, 0.063 mmol) in $CHCl_3$ (5 mL) was added to a solution of sal_2phen (20 mg, 0.063 mmol) in EtOH (5 mL). The orange-brown solution was refluxed for 2 hours, and filtered through a medium glass frit to remove the yellow unreacted sal_2phen starting material. The filtrate was then dried under vacuum and sonicated in toluene to remove the green-brown unreacted [$Re^{III}Cl_3(PPh_3)_2(MeCN)$] starting material. The purified product was then dissolved in $CDCl_3$ and placed in an NMR tube. Slow evaporation of the solvent resulted in crystal formation. Yield: 15%. ^{1}H NMR [DMSO, 500 MHz; δ (ppm)]: 7.54 (10H); 7.61 (14H). IR (KBr, ν in cm^{-1}): N/A. MS (m/z): [$(M)^+$] 693.13 (693.10); [$(M + Na)^+$] 751.16 (751.05).

2.2.6 *trans*-[$Re^{III}Cl(PPh_3)(sal_2phen)$]•2 CH_2Cl_2 (4)

Triphenylphosphine (74 mg, 0.282 mmol) in CH_2Cl_2 (5 mL) was added to **1** (50 mg, 0.091 mmol) in ethanol (20 mL). The burgundy solution was refluxed for 12 hours. The brown reaction mixture volume was reduced to dryness under vacuum. The dark brown solid was washed with toluene. The reaction mixture was filtered through a glass frit. The dark brown solid filtrate was washed with ether and then dried in air overnight. Small, orange crystals were obtained by slow exchange of dichloromethane to hexane in a scintillation vial. Yield: 10%. ^{1}H NMR [$CDCl_3$, 500 MHz; δ (ppm)]: -22.44 (2H); -9.18 (2H); -6.68 (2H); 3.46 (2H); 7.30 (2H); 7.61 (6H); 7.90 (6H); 8.26 (3H); 21.65 (2H); 30.89 (2H). IR (KBr, ν in cm^{-1}): N/A. MS (m/z): [($M^{+\bullet}$)] 798.05 (798.12).

2.2.7 *trans*-[$Re^{III}(PPh_3)_2(sal_2phen)]^+$, (5)

Triphenylphosphine (1.47 g, 5.61 mmol) was added to **1** (1 g, 1.81 mmol) in ethanol (10 mL). The burgundy solution was refluxed for 12 hours. The reaction mixture volume was reduced to dryness in vacuum. The grey solid was washed with toluene that resulted in a red-brown solid once filtered through a glass frit. The solid filtrate was washed with ether and then dried in air. Yield: 10%. ^{1}H NMR [DMSO, 250 MHz; δ (ppm)]: -22.51 (d; 1.77 H); -8.88 (t; 1.72 H); -7.47 (d; 1.72 H); 1.42 (s; 1.91 H); 2.48 (t; 0.51 H); 3.14 (d; 1.08 H); 6.68 (d; 11.60 H); 7.25 (t; 12.11 H); 7.75 (m; 3.54 H); 8.43 (t; 6 H); 20.26 (t; 1.72 H); 30.52 (d; 1.77). IR (KBr, ν in cm^{-1}): N/A. MS (m/z): [(M^+)] 1025.20; calcd 1025.24.

2.2.8 X-ray Structure Determinations and Refinements for 1-4

Intensity data was obtained at -100 °C on a Bruker SMART CCD area detector system using the *ö* scan technique with Mo Kα radiation from a graphite monochromator. Intensities were corrected for Lorentz and polarization effects. Equivalent reflections were merged, and absorption corrections were made using the multiscan method. [16] The space group, lattice parameters, and other parameters are summarized in Table 2.1. Structures were solved by direct methods and refined by full-matrix least-squares using the SHELX suite of software with the aid of X-Seed. [16-18] All non-hydrogen atoms were refined with anisotropic thermal parameters. The hydrogen atoms were placed at calculated positions and included in the refinements using a riding model, with fixed isotropic *U*. Final difference maps contained no features of chemical significance.

Table 2.1. X-ray crystal data, data collection parameters, and refinement parameters for **1, 2, 3**, and **4**.

	1	**2**	**3**	**4**
formula	$C_{20}H_{14}ClN_2O_3Re{\bullet}CHCl_3$	$C_{38.5}H_{31}N_2O_3PRe^{+}\ PF_6^{-}{\bullet}CH_2Cl_2$	$C_{31}H_{24}N_2OPCl_2Re{\bullet}2.5\ CHCl_3$	$C_{38}H_{29}ClN_2O_2PRe{\bullet}2\ CH_2Cl_2$
fw	671.35	968.25	1027.01	968.10
Crystal system	Orthorhombic	Orthorhombic	Triclinic	Monoclinic
space group	Pbca	Pnn2	P-1	P 21/c
a (Å)	19.4392(14)	21.0703(15)	11.1410(8)	23.0805(7)
b (Å)	10.9257(8)	11.3780(8)	11.5874(8)	13.1946(4)
c (Å)	21.4868(15)	15.0859(11)	17.7337(12)	25.9868(8)
α (Å)	90	90	91.854(1)	90
β (°)	90	90	108.169(1)	104.4470(10)
λ (Å)	90	90	115.297(1)	90
V (Å ^{3})	4563.5(6)	3616.7(4)	1929.7(2)	7663.7(4)
Z	8	4	2	8
ρ_{calc} (g/cm^3)	1.954	1.778	1.768	1.678
T (K)	173(2)	173(2)	173(2)	173(2)
μ (mm^{-1})	5.820	3.595	3.879	3.600
λ source (Å)	0.71073	0.71073	0.71073	0.71073
R(*F*)	0.0350	0.0374	0.0517	0.0398
Rw(*F*)^2	0.0886	0.0608	0.1143	0.0666
GoF	1.046	1.013	1.104	1.032

$R = (\Sigma||F_O| - |F_C||/\Sigma|F_O|)$. $R_W = [\Sigma\varpi(|F_O^2| - |F_C^2|)^2/\Sigma\varpi(|F_O^2|^2]^{1/2}$

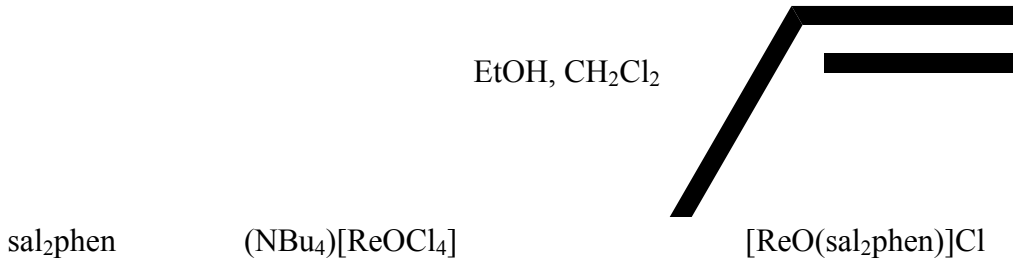

Figure 2.4: Formation of Re^{V} complex, $[ReO(sal_2phen)]Cl$.

2

1

4

5

Figure 2.5: Formation of Re^{V} and Re^{III} phosphine complexes after triphenylphosphine addition to $[ReO(sal_2phen)]Cl$.

2.3 RESULTS AND DISCUSSION

The reaction of (n-Bu_4N)[$ReOCl_4$] with the Schiff base ligand sal_2phen yielded the monomeric [ReO(sal_2phen)]Cl compound in high yield (75%). (See Figure 2.4.) The X-ray crystal structure of **1** showed that the equatorial plane was occupied by the N_2O_2 donor atoms of the ligand. This differs from the crystals obtained by Gerber et al, [19] where the equatorial plane was occupied by one ligand-oxygen donor atom, two ligand-nitrogen donor atoms, and the coordinating chloride donor atom. The difference of structure could have resulted due to the reaction solvent used and the reaction time.

The sal_2phen ligand's rigidity and electron delocalization capabilities were further investigated to see if a single Re^{III} complex could be produced in high yield. The first method used to obtain a Re-sal_2phen complex utilized the reaction of **1** with tertiary, monodentate triphenyl phosphine (PPh_3) in a 3.1:1 ratio. Depending on reaction time and solvent volume, this method resulted in the formation of monosubstituted phosphine Re^{V} oxo compound, **2**, where one of the imines had been reduced to an amine; a monosubstituted phosphine Re^{III} chloride compound, **4**; or a disubstituted phosphine Re^{III} compound, **5**. (See Figure 2.5.) The second method used to obtain a Re-sal_2phen complex was by the addition of [$Re^{III}Cl_3(PPh_3)_2$(MeCN)] to the sal_2phen ligand in a 1:1 ratio. This

3

Figure 2.6: Formation of Re^{III} phosphine complexes after [$ReCl_3(PPh_3)_2$(MeCN)] addition to sal_2phen.

method resulted in the formation of a monosubstituted phosphine Re^{III} chloride complex, **3**. (See Figure 2.6.)

Initially, infrared and nuclear magnetic resonance spectra helped to suggest product formation, but the mass spectral analysis and X-ray crystal structures confirmed these suggestions. All phosphine products were obtained in low yields, 10-30%, and were difficult to separate due to having only slightly different chemical properties. Since the purpose of this work was to obtain a single species in high yield, limited efforts were put forth in the separation techniques. Therefore, the purpose of this work is to show the dynamic chemistry of Re and how the steric hindrance on the amine backbone was not able to afford a Re^{III} complex without complication or ligand fragmentation.

2.4 CHARACTERIZATION

2.4.1 General Characterization

ESI-MS showed the expected cationic rhenium isotope patterns of **1-5**, confirming their identity. ESI-MS data for the crude product of **5** suggests the synthesis of three products, including $[Re^{III}(PPh_3)sal_2phen]^{+\bullet}$ at 763.11 (763.15), $[Re^{III}(PPh_3)(MeOH)sal_2phen+H]^{+}$ at 795.17 (794.17), and $[Re^{III}(PPh_3)(MeCN)sal_2phen]^{+}$ at 804.14 (803.17). Elemental analysis was performed for **1**. The FT-IR spectra for **1** and **2** showed the medium strength band at ~950 cm^{-1}, which corresponds to the Re=O stretch. This band was not seen in complexes **3-5**, supporting that the Re=O had been substituted.

2.4.2 NMR Characterization

Unique ^{1}H NMR splitting patterns were observed for each of the five complexes. Proton identification was difficult in complexes **2-5** due to the multiple aromatic protons. Proton identification for the Re^{III} complexes **4** and **5** was even more difficult due to the fast relaxation of the unpaired electrons, [20] with a splitting pattern exhibited in an expanded window (-50 to 50 ppm). A single peak in the ^{31}P NMR was observed in the Re^{V} complexes **2** (24.89 ppm) and **3** (23.83 ppm). These phosphorous signals are down-field from where unbound triphenylphosphine (-6 ppm) and up-field from where triphenylphosphine oxide (29.8 ppm) would normally be found. No phosphorous signals were observed for complexes **4**, and **5**, as is to be expected for the paramagnetic Re^{III} complexes. [20]

2.4.3 X-Ray Crystallography

The Re^{V} complexes, *trans*-[$Re^{V}OCl(sal_2phen)$], **1**, *cis*-[$Re^{V}O(PPh_3)(sal_2phen^*)]PF_6 \bullet CH_2Cl_2$, **2**, *cis*-[$Re^{V}Cl_2(PPh_3)(salphen)$], **3**, and the Re^{III} complex, *trans*-[$Re^{III}Cl(PPh_3)(sal_2phen)$], **4**, were characterized by X-ray crystallography (Figures 2.7-2.10). All four complexes had a distorted octahedral geometry. For complexes **1** and **4**, the Re=O (1.66 Å), Re-Cl (2.45 – 2.56 Å), Re-P (2.41 – 2.42 Å), Re-N (2.02 – 2.06 Å), and Re-O (1.99 – 2.02 Å) bond distances were as expected. However, the isolation of the singly reduced sal_2phen complex *cis*-[$Re^{V}O(PPh_3)(sal_2phen^*)]PF_6 \bullet CH_2Cl_2$, **2,** and the doubly reduced salphen complex *cis*-[$Re^{V}Cl_2(PPh_3)(salphen)$], **3,** were somewhat unexpected. In comparing these complexes with those of the sal_2en type, the distorted octahedral geometry for complex **1** was similar

to that of $[ReO(salen)H_2O][B(C_6F_5)_4]$ and the distorted octahedral geometry for complexes **2-4** were similar to related structures. [7] From using this sal_2en ligand as a reference, the sal_2phen ligand degradation in complex **3** was not expected. The bond angles and distance for **1-4** are summarized in Table 2.2.

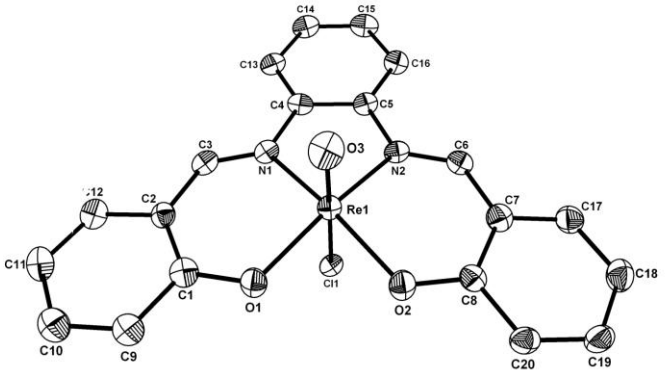

Figure 2.7. ORTEP representation of *trans*-$[ReOCl(sal_2phen)]\bullet CHCl_3$ with 50% probability ellipsoids.

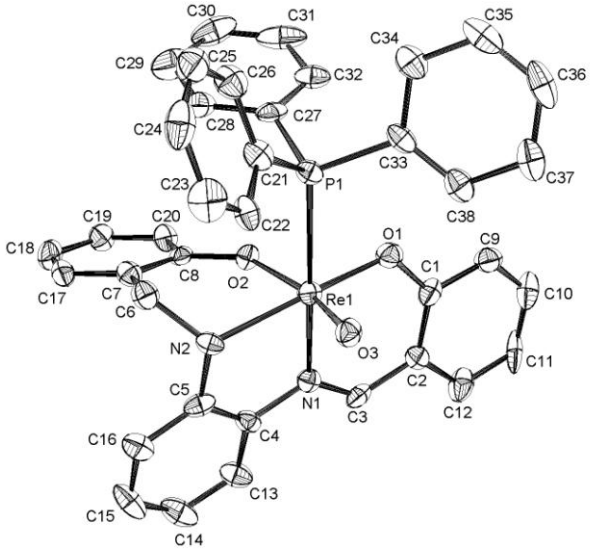

Figure 2.8. ORTEP representation of *cis*-$[ReO(PPh_3)(sal_2phen)]PF_6\bullet CH_2Cl_2$ with 50% probability ellipsoids.

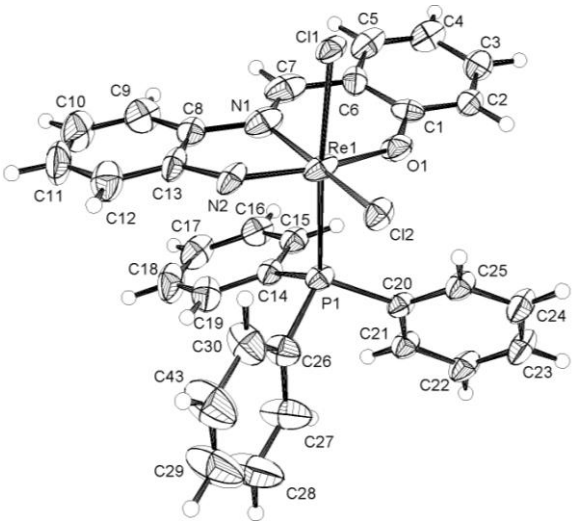

Figure 2.9. ORTEP representation of $[ReCl_2(PPh_3)(salphen)]$ with 50% probability ellipsoids.

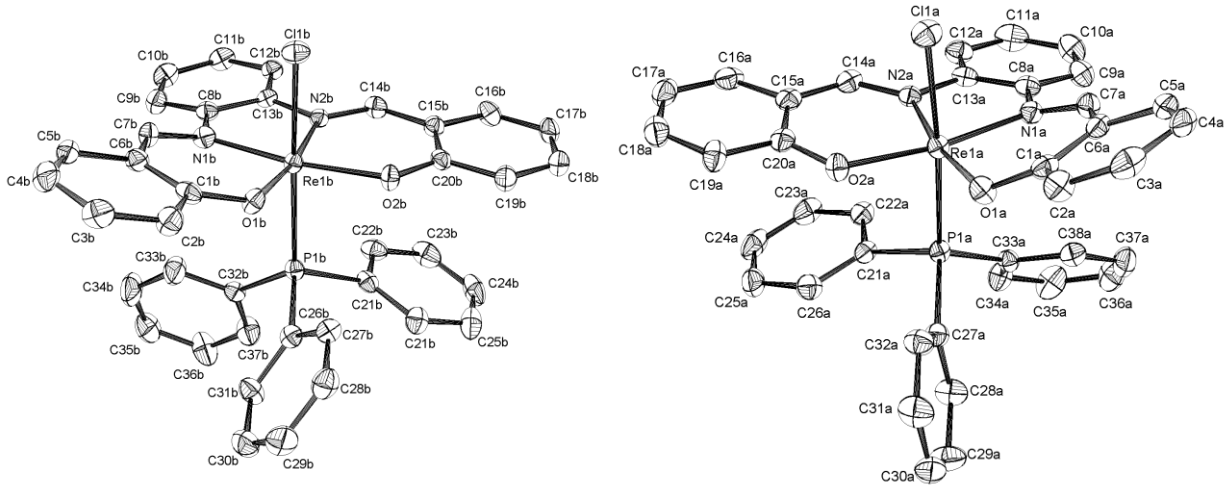

Figure 2.10. ORTEP representation of *trans*-$[ReCl(PPh_3)(sal_2phen)]$ with 50% probability ellipsoids.

Table 2.2. Selected bond angles (°) and distances (Å) for **1**, **2**, **3**, **4a,** and **4b**.

	1	**2**	**3**	**4a**	**4b**
Re-N1	2.061(3)	2.087(5)	2.209(7)	2.026(4)	2.024(4)
Re-N2	2.054(3)	2.199(5)	1.775(6)	2.037(4)	2.032(3)
Re-O1	1.990(3)	1.973(4)	1.890(5)	2.02(3)	1.996(3)
Re-O2	1.990(3)	1.943(3)	--	2.001(3)	2.011(3)
Re-O3	1.665(3)	1.697(4)	--	--	--
Re-P1	--	2.4923(16)	2.4244(16)	2.4128(11)	2.4218(12)
Re-Cl1	2.568(1)	--	2.4421(15)	2.4550(11)	2.4563(11)
Re-Cl2	--	--	2.3621(15)	--	--
N1-C3/C7	1.294(5)	1.283(8)	1.234(11)	1.318(6)	1.317(5)
N2-	1.299(5)	1.511(7)	--	1.312(6)	1.308(5)
O1-Re-O2	85.28(12)	91.61(19)	--	97.14(12)	96.08(11)
O1-Re-N1	94.27(13)	92.08(17)	84.8(2)	90.28(13)	91.20(13)
O1-Re-N2	163.34(14)	168.84(16)	157.8(2)	170.48(13)	171.35(12)
O1-Re-O3	100.29(15)	102.69(17)			
O1-Re-	83.04(10)		87.86(14)	86.85(9)	86.29(9)
O1-Re-			100.01(15)		
O1-Re-P1		82.92(12)	87.03(14)	93.94(9)	88.85(9)
O2-Re-N1	161.21(13)	84.50(17)		170.81(13)	171.64(13)
O2-Re-N2	94.10(12)	80.15(19)		91.29(13)	91.22(12)
O2-Re-O3	102.90(14)	165.6(2)			
O2-Re-	82.02(10)			87.88(9)	89.84(9)
O2-Re-P1		88.14(10)		87.90(9)	87.00(9)
N1-Re-N2	80.99(13)	79.72(18)	73.4(3)	80.92(14)	81.21(14)
N1-Re-O3	95.68(15)	96.48(18)			
N1-Re-	79.29(10)		87.07(17)	87.13(10)	86.51(10)
N1-Re-P1		170.99(13)	92.61(16)	97.01(10)	97.29(10)
N1-Re-			173.38(17)		
N2-Re-O3	96.08(15)	85.88(18)			
N2-Re-	80.38(10)		95.19(17)	89.06(9)	89.10(10)
N2-Re-P1		104.15(13)	89.60(17)	90.77(9)	96.19(10)
N2-Re-			101.99(18)		
O3-Re-P1		91.95(13)			
P1-Re-Cl1			174.89(6)	175.77(4)	173.89(4)
P1-Re-Cl2			92.14(5)		
Cl1-Re-			88.61(5)		

2.4.3.1 Crystallography of *trans*-[$Re^{V}OCl(sal_2phen)$]•$CHCl_3$

Compound **1** had a distorted octahedral geometry with the tetradente N_2O_2 ligand occupying the equatorial plane and a Cl coordinated *trans* to the Re=O group in the axial position. This structure differs from that of the previously published [$ReOCl(sal_2mp)$], [19] where the Re=O was *cis* to the chloride. For compound **1**, the Re was set 0.3093(17) Å above the equatorial plane defined by the N_2O_2 donors towards the oxo group as is typically found in Re^{V} mono-oxo complexes. The *trans* O=Re-Cl angle deviated slightly from linear at 174.21(11)º and fell well within the range observed for similar complexes.[21] The bond lengths and angles in complex **1** are near their expected values. [2, 19] The N1-Re-N2 "bite-angle" was 80.99(13)º and the *cis*-O-Re-N angles for the N_2O_2 ligand were 94.27(13)º and 94.10(12)º respectively. The equatorial Re-O (1.990(3) Å), Re-N (2.054-2.061(3) Å), as well as the axial Re=O (1.655(3) Å) bond distances were consistent with similar Re^{V} oxo Schiff base complexes. [2, 19] For comparison, the *trans* Re-Cl bond (2.568(1) Å) was slightly longer than that of *cis*-[$ReOCl(sal_2mp)$] (2.420(1) Å) and of *trans*-[$ReOCl(acac_2pn)$] (2.468(2) and 2.464(2) Å). [2, 19] This elongation is attributed to the *trans* influence of the oxo moiety and could be further enhanced by the more efficient donation of electron density to the Re atom by the sal_2phen ligand. The planar two carbon backbone led to a N1-Re-N2 angle of 80.99(13)º compared to the 86.0(1)º in *cis*-[$ReOCl(sal_2mp)$] and the 96.2(2)-96.4(2)º induced by the 3 carbon backbone complex, *trans*-[$ReO(acac_2pn)Cl$]. [1, 13] Structure **1** also has hydrogen bonding interactions (2.715 – 2.818 Å) between the O and or Cl coordinated to the Re and the H atoms on the phenyl moieties in the equatorial plane. The exact atom involved in the hydrogen bonding is unclear due to the disorder resulting in altering O and Cl

atoms in the axial position. The H atom on the chloroform molecule (H21) also has hydrogen bonding interactions (2.417-2.421 Å) with the coordinated sal_2phen oxygen atoms. No rearrangement was observed in complex **1**.

2.4.3.2 Crystallography of *cis*-[$Re^{V}O(PPh_3)(sal_2phen^*)]PF_6 \bullet CH_2Cl_2$

The X-ray crystal structure of **2** illustrates the asymmetric coordination of the sal_2phen ligand. This is a result of the equatorial coordination of the phosphine ligand *cis* to the Re^{V} oxo group (Figure 2.8) and the reduction of one imine to an amine. This is very different from what was observed in previous work with $acac_2$en and $acac_2$pn complexes, where there was no imine reduction. [7] Three equatorial coordination sites of the *cis*-[$Re^{V}O(PPh_3)(sal_2phen^*)]PF_6 \bullet CH_2Cl_2$ complex were occupied by one oxygen and two nitrogen donor atoms from the sal_2phen ligand, while the remaining phenolic oxygen donor (from the reduced amine fragment) coordinated in the axial position *trans* to the Re=O group. This resulted in a distorted octahedral conformation with the Re atom set 0.1517(20) Å above the equatorial plane toward the oxo group. The Re=O bond distance was 1.697(4) Å, which corresponds to a Re-oxo multiple bond. The "bite-angle" of N1-Re-N2 was 79.72(18)º, which was in line with other five-membered ring systems. [2, 7, 9] The equatorial *cis*-O1-Re-N1 angle was found to be 92.08(17)º, and the *cis*-O2-Re-N2 bond angle, *trans* to the Re=O, was 80.15(19)º. The difference in the equatorial and *trans* angles were in line with the angles observed in similarly rearranged complexes. [7] The Re-O and Re-N bond distances were 1.943(3)-1.973(4) Å and 2.087(5)-2.199(5) Å respectively. The larger Re-N bond distance of 2.199(5) Å is typical for Re-amide bonds. [22] The Re-P bond distance was 2.4923(16) Å and was within ranges of Re^{V}-P bond

lengths. [7, 9] The Re^{V} core (O2-Re-O3) deviated slightly from linear at 165.6(2)°. An extensive hydrogen interaction network was observed between the PF_6 anion and the complex, with distances ranging from 2.171 to 2.870 Å. The CH_2Cl_2 solvent molecule also had hydrogen interaction ranging from 2.628 to 2.833 Å.

2.4.3.3 Crystallography of $[Re^{V}Cl_2(PPh_3)(salphen)]\bullet 2.5\ CHCl_3$

Compound **3** had a slightly distorted octahedral geometry with the Re atom set 0.0199 Å above the equatorial plane towards the chloride. One oxygen and two nitrogen donor atoms from the fragmented tridentate N_2O Schiff base ligand (salphen) occupied three equatorial coordination sites. This ligand consisted of one salicylic moiety linked to one diaminobenzene and is thought to be the remnant of a reduced sal_2phen ligand in which the imine was completely reduced to an amine, resulting in the loss of the second salicylic moiety. The reduction of the imine could have led to the oxidation of the Re^{III} starting material to Re^{V}. One other possibility could be the oxidative addition of the formed amine to the Re^{III} center to yield the Re^{V}-imido core. The remaining equatorial position was occupied by a Cl atom and the axial core (PPh_3-Re-Cl) was made up by a PPh_3 molecule with a second *trans*- coordinated Cl atom. The Re^{V} core (PPh_3-Re-Cl) deviated slightly from linear at 174.89(6)º. This deviation is similar to that of the Re^{V} cores (PPh_3-Re-Cl) of the tridentate phosphine complexes, *cis*-[Re(apa)Cl_2(PPh_3)], at 173.36(5)º and *cis*-[Re(mps)Cl_2(PPh_3)], at 173.15(3)º. [23-24] The *cis*-N1-Re-N2 "bite-angle" for complex **2** was 73.4(3)º and falls within the range of the similar tridentate complexes, *cis*-[Re(apa)Cl_2(PPh_3)], at 70.1(3)º and *cis*-[Re(mps)Cl_2(PPh_3)], at 76.7(1)º. [23-24] The N1-Re-O1 angle forming a six-membered ring was 84.8(2)º. This angle falls

within the range of angles observed for similar rings in the equatorial plane of 82.6(1)-87.7(3)º. [23-24] The Re-O bond distances for the equatorial oxygen atom was 1.890(5) Å and is comparable to the values observed in the literature of 1.866(4) and 1.928(2) Å for similar tridentate ligands. [23-24] The Re-N bond distances in the equatorial plane were 1.775(6) and 2.209(7) Å, respectively. The shorter Re-N2 bond of 1.775(6) Å agreed with the formation of a Re-imido bond. [24] The Re-N1 bond of 2.209(7) Å was quite similar to the 2.199(5) Å reported for complex **2**. This could imply that the remaining imine in the salphen ligand could also have been reduced to an amine. Closer examination of the N1-C7 bond of 1.234(11) Å does indicate the presence of an imine bond (-N=C-). The Re-P bond of 2.4244(16) Å is in close agreement with the Re-P bond of 2.429(2) observed in *cis*-[Re(apa)Cl_2(PPh_3)] by Gerber *et al*. [24] The Re-Cl bond length *trans* to the PPh_3 was longer than the *cis*-Re-Cl bond length, and is attributed to the *trans* influence of the PPh_3 moiety. The chloroform molecule had some hydrogen interactions of 2.783 – 2.863 Å with the two Cl atoms coordinated to the Re. The Cl atoms also had some hydrogen interactions with hydrogen atoms on adjacent phenyl groups of 2.833 – 2.860 Å.

2.4.3.4 Crystallography of *trans*-[$Re^{III}Cl(PPh_3)(sal_2phen)$]·2 CH_2Cl_2

Two independent molecules of **4** (4a and 4b) were found within the unit cell. The sal_2phen ligand occupied the equatorial plane where the Re atom was set 0.0723(16) Å above the plane. The PPh_3 was oriented *trans* to the Cl moiety in the axial position. The Re^{III} core (PPh_3-Re-Cl) deviated slightly from linear at 175.77(4)º and 173.89(4)º for both molecules. These complexes had very similar bond distances and bond angles. For

4a, the *cis*-N1-Re-N2 "bite-angle" was 80.92(14)º and the six-membered *cis*-O-Re-N angles were 90.28(13) and 91.29(13)º. For **4b**, the *cis*-N1-Re-N2 "bite-angle" was found to be 81.21(14)º. The *cis*-O-Re-N angles were 91.20(13) and 91.22(12)º. For both complexes the Re-O bond distances for the equatorially bound oxygen atoms were 1.996(3)-2.011(3) Å. The Re-N bond distances in the equatorial plane were 2.024(4)-2.037(4) Å. The Re-P bond lengths in the axial positions ranged from 2.4128(11) - 2.4218(12) Å and were shorter than the Re-P bonds of the *trans*-$[Re^{III}(PPh_3)_2(acac_2en)]PF_6$ complexes at 2.4820(11) - 2.4992(11) Å. [7] The Re-Cl bonds were 2.4550(11) - 2.4563(11) Å and were within the range of Re-Cl bond lengths. The CH_2Cl_2 solvent molecule had hydrogen interactions of 2.847 Å with the Cl atom and of 2.844 Å with the phenyl groups coordinated to PPh_3. The bound Cl atom also showed a hydrogen interaction of 2.870 Å with a hydrogen atom on the phenyl group of an adjacent PPh_3.

2.6 CONCLUSIONS

The reaction of $(n\text{-}Bu_4N)[Re^{V}OCl_4]$ with the Schiff base ligand sal_2phen yielded the monomeric $[Re^{V}O(sal_2phen)]Cl$ compound. The reaction of $[Re^{V}O(sal_2phen)]Cl$ with triphenyl phosphine resulted in *cis*-$[Re^{V}O(PPh_3)(sal_2phen^*)]PF_6 \bullet CHCl_2$, *trans*-$[Re^{III}Cl(PPh_3)(sal_2phen)] \bullet CH_2Cl_2$, and *trans*-$[Re^{III}(PPh_3)_2sal_2phen])^+$ in low yield. The reaction of sal_2phen with $[Re^{III}Cl_3(PPh_3)_2(MeCN)]$ resulted in $[ReCl_2(PPh_3)(sal_2phen)] \bullet 2\ CH_2Cl_2$ in low yield. The sal_2phen ligand's delocalized electron density did not assist in the reduction of Re^{V} to Re^{III}. The Re atom seemed to be too large for the planar containment in the sal_2phen ligand. Since the sal_2phen ligand was not able to withstand

rearrangement, along with the low yields and difficulty in separation, the extension of this work towards ^{186}Re radiotracer studies will not be pursued.

2.7 FUTURE STUDIES

Future $^{186/188}$Re radiopharmaceuticals must effectively contain the radioactive atom so as to minimize non-target irradiation. Attempts to reduce a Re(V) metal center in a [ReO(schiff base)]X complex to obtain the more kinetically inert Re(III) metal center has proved to be difficult. The lower oxidation state was desired due to its d^4 electron configuration being more kinetically inert than that of Re(V), with a d^2 electron configuration. An alternative to Re(III) chemistry is with Re(I) chemistry. Re(I) is even more kinetically inert than Re(III) since it has a low-spin d^6 electron configuration. The aqua ion complex, $[^{186/188}Re(H_2O)_3(CO)_3]^+$, is air stable and labeling can be performed in either organic or aqueous solvent. A wide variety of chelating ligand frameworks can stabilize the cationic Re(I) metal center under *in vivo* conditions. The future of Re(I) tricarbonyl complexes seems endless.

2.8 REFERENCES

1. Van Bommel, K.J.C., et al., *Rhenium(V) - Salen Complexes: Configurational Control and Ligand Exchange.* Inorganic Chemistry, 1998. **37**(17): p. 4197-4203.

2. Benny, P.D., et al., *Synthesis and characterization of novel rhenium(V) tetradentate N_2O_2 Schiff base monomer and dimer complexes.* Inorganic Chemistry, 2003. **42**(20): p. 6519-6527.

3. Du, G. and M.M. Abu-Omar, *Catalytic Hydrosilation of Carbonyl Compounds with Cationic Oxorhenium(V) Salen.* Organometallics, 2006. **25**: p. 4920-4923.

4. Gerber, T.I.A., D. Luzipo, and P. Mayer, *A rhenium(V) complex containing a terdentate chelate with an imido donor atom: Synthesis and structure of $[Re(aps)I(PPh_3)_2]I$ (H_3aps = N-(2-aminophenyl)-salicylideneimine).* Journal of Coordination Chemistry, 2006. **59**(10): p. 1149-1155.

5. Ison, E.A., et al., *Synthesis of Cationic Oxorhenium Salen Complexes via μ-Oxo Abstraction and Their Activity in Catalytic Reductions.* Inorganic Chemistry, 2006. **45**(6): p. 2385-2387.

6. Luo, H., et al., *Rhenium and technetium complexes from pentadentate (N3O2) and tetradentate (N_2O_2) Schiff base ligands.* Canadian Journal of Chemistry, 1995. **73**(12): p. 2272-2281.

7. Benny, P.D., et al., *Reactivity of rhenium(V) oxo Schiff base complexes with phosphine ligands: Rearrangement and reduction reactions.* Inorganic Chemistry, 2005. **44**(7): p. 2381-2390.

8. Sachse, A., et al., *Rhenium(V) Oxo Complexes with Acetylacetone Derived Schiff Bases: Structure and Catalytic Epoxidation.* Inorganic Chemistry, 2007. **46**(17): p. 7129-7135.

9. Ison, E.A., et al., *Synthesis of Cationic Rhenium(VII) Oxo Imido Complexes and Their Tunability Towards Oxygen Atom Transfer.* Journal of the American Chemical Society, 2007. **129**(5): p. 1167-1178.

10. Greenwood, N.N. and A. Earnshaw, *Manganese, Technetium and Rhenium*, in *Chemistry of the Elements*. 2001, Butterworth Heinemann: Oxford. p. 1040-1069.

11. Bottomley, L.A., P. E. Wojciechowski, and G.N. Holder, *Voltammetry of monomeric and dimeric oxorhenium(V) complexes of Schiff base ligands N,N'-ethylenebis(acetylacetone)diimine, N,N'-ethylene(salicylidene)diimine and N,N'-phenylenebis(salicylidene)diimine.* Inorganica Chimica Acta, 1997. **255**(1): p. 149-155.

12. de C.T. Carrondo, M.A.A.F., et al., *A novel linear OReOReOReO system: The synthesis and x-ray structure of di-oxo-bis{[N,N'-ethylenebis(acetylacetiminatol)] oxorhenium(V)} [N,N'-ethylenebis(acetylacetiminato)] rhenium(V) perrhenate.* Inorganica Chimica Acta, 1980. **44**(C).

13. Tisato, F., et al., *Rhenium(V) oxo complexes with schiff base ligands containing four or five coordination sites. X-ray molecular structure of [N,N'-3-azapentane-1,5-diylbis(salicylideneiminato)(3-)-O,O',N,N',N'']oxorhenium(V).* Inorganica Chimica Acta, 1991. **189**(1): p. 97-103.

14. Chat, J.R., G. A., *Complex compounds of tertiary phosphines and a tertiary arsine with rhenium(V), rhenium(III), and rhenium(II).* Journal of the Chemical Society 1962: p. 4019.

15. Pillai, M.R.A., C.L. Barnes, and E.O. Schlemper, *Dinuclear complexes of rhenium(V) with amine-phenol ligands: Synthesis, characterization and x-ray crystal structures.* Polyhedron, 1994. **13**(4): p. 701-708.

16. Sheldrick, G.M., *SHELXS-97, Crystal Structure Solution.* Crystal Structure Solution, 1997. **University of Göttingen: Germany**.

17. Barbour, L., Journal of Supramolecular Chemistry, 2001. **1**: p. 189-191.

18. Sheldrick, G.M., *Crystal Structure Refinement.* SHELXL-97, 1997. **University of Göttingen: Germany**.

19. Gerber, T.I.A., D. Luzipo, and P. Mayer, *Different coordination modes of tetradentate Schiff bases in monomeric and dimeric oxorhenium(V) complexes.* Journal of Coordination Chemistry, 2005. **58**(16): p. 1505-1512.

20. Pearson, C. and A. Beauchamp, *^{1}H NMR study of monomeric chloro-rhenium(III) complexes with triarylphosphines and nitriles.* Inorganica Chimica Acta, 1995. **237**(1-2): p. 13-18.

21. Marmion, M.E., et al., *Preparation and characterization of technetium complexes with Schiff base and phosphine coordination. 1. complexes of technetium-99g and -99m with substituted acac$_2$en and trialkyl phosphines (where acac$_2$en = N,N'-ethylenebis[acetylacetone iminato]).* Nuclear Medicine and Biology, 1999. **26**(7): p. 755-770.

22. Hegetschweiler, K., et al., *1,3,5-Trideoxy-1,3,5-tris((2-hydroxybenzyl)amino)-cis-inositol, a novel multidentate ligand providing various N,O coordination sites. Structure of the rhenium(V) complex.* Inorganic Chemistry, 1992. **31**(20): p. 4027-4028.

23. Booysen, I., et al., *Synthesis and characterization of a neutral rhenium(V) complex containing a tridentate chelate with an imido donor atom.* Journal of Coordination Chemistry, 2007. **60**(16): p. 1771-1776.

24. Gerber, T.I.A., D.G. Luzipo, and P. Mayer, *Coordination of a tridentate imido-amino-phenolate chelate to rhenium(V).* Journal of Coordination Chemistry, 2006. **59**(16): p. 1801-1805.

CHAPTER 3: TECHNETIUM-99m TRICARBONYL TRIAMINE BOMBESIN CONJUGATES AS POTENTIAL DIAGNOSTIC IMAGING AGENTS

3.1 INTRODUCTION

3.1.1 Technetium(I) Organometallic Aqua Complex

Up until 1998, the pursuit of designing a technetium-based radiopharmaceutical consisted mostly of tetradentate N and S ligands used to stabilize a Tc(V) core. A new focus in technetium was established when Alberto and co-workers introduced the air and water stable Tc(I) organometallic aqua complex, $[^{99m}Tc(OH_2)_3(CO)_3]^+$. The main attraction of technetium tricarbonyl chemistry is due to the ease of reducing pertechnetate from a +7 oxidation state to a +1 oxidation state. The +1 oxidation state is more kinetically inert due to its d^6 electron configuration. The dynamics behind the tricarbonyl complex are that the three CO ligands are substitutionally inert while the three water molecules are substitutionally labile. Even after chelation of the technetium tricarbonyl metal center, it remains inert. It is this stability that allows for potential applications in nuclear medicine. [8]

Initially, the synthesis of $[^{99m}Tc(OH_2)_3(CO)_3]^+$ was performed by the addition of $[^{99m}TcO_4]^-$ in saline (0.9% $NaCl/H_2O$) to a vial containing sodium borohydride, which acted as a reducing agent. The vial was sealed, placed under 1 atm of carbon monoxide gas, and heated for 30 min at 75ºC. Although the resulting Tc(I) product was ideal, the clinical usefulness was not, due to the multi-step, high-pressure synthetic route required. An alternative synthetic route was discovered by Alberto in 2001, which created a new

avenue for the successful radiolabeling of biological targeting vectors with Tc(I). In place of carbon monoxide, potassium boranocarbonate is used, which generates carbon monoxide in situ. The boranocarbonate also acted as the reducing agent. [9]

The success from this work ultimately resulted in one-step kit production of $[^{99m}Tc(OH_2)_3(CO)_3]^+$. Today, kits are manufactured by Mallinckrodt under the name Isolink®. Each kit contains sodium-boranocarbonate (4.5 mg), sodium tetraborate•$10H_2O$ (2.8 mg), sodium tartrate•$2H_2O$ (8.5 mg), and sodium carbonate (7.15 mg) in a sealed vial. [10]

3.1.2 Specific Aims

The use of radiolabeled BBN targeting vectors to selectively target receptor-expressing tumors offers innovative diagnostic and treatment strategies for patients suffering from specific human cancers such as breast or prostate. [1-4] ^{99m}Tc is a versatile radiometal used in molecular imaging of human tumors due to its ideal physical properties ($t_{½}$ = 6 h and 140 keV gamma emission), on-site availability from a $^{99}Mo/^{99m}Tc$ generator, and diverse labeling chemistry. [5-6] ^{99m}Tc has proven its utility in nuclear medicine by its use in ~85% of all diagnostic procedures in clinical nuclear medicine. [7]

This work is focused on complexing the technetium tricarbonyl with the bifunctional chelate DTMA (2-(N, N´-Bis(tert-butoxycarbonyl)diethylenetriamine) Acetic Acid). DTMA is a tridentate ligand and will occupy the three binding sites on the *fac*-$[^{99m}Tc(CO)_3]^+$ metal fragment. Novel [DTMA-(X)-BBN(7-14)NH_2] conjugates will be synthesized for the purpose of targeting gastrin releasing peptide receptor-positive

tissues. The effect of the spacing moiety will be investigated by using spacers of increasing hydrophilicity. The [DTMA-(X)-BBN(7-14)NH_2] conjugates will be labeled with *fac*-[$^{99m}Tc(CO)_3]^+$. *In vitro* assays will be performed to determine the affinity of the [DTMA-(X)-BBN(7-14)NH_2] and [$^{99m}Tc(CO)_3$-DTMA-(X)-BBN(7-14)NH_2] complexes. The assays that will be performed include inhibitory concentration at 50% (IC_{50}) and internalization/efflux. If the [$^{99m}Tc(CO)_3$-DTMA-(X)-BBN(7-14)NH_2] complexes are found to have good *in vitro* stability and uptake, *in vivo* biodistribution studies will be performed in normal CF-1 mice.

3.1.3 Preliminary Work

Studies have shown bi- and tridentate ligands that are comprised of primary, secondary, and aromatic amines to be effective chelators for the low-valent metal center, providing the stability necessary for *in vivo* molecular imaging of human tumor tissue. [6, 11-12] Chelate systems that consist of medium hard ligands, such as nitrogen (imidazoles, pyridines, and amines), oxygen (carboxylate), sulphur (thione and thiether), and phosphorous, have been widely used in coordinating ^{99m}Tc to produce *in vivo* kinetically inert complexes. [15]

Histidine was one of the first chelates studied for its ability to chelate the technetium tricarbonyl complex. This chelate was of interest due to its small size, donor atoms, and its ability to coordinate in a facial manor. From this study, it was found that histidine could chelate the technetium tricarbonyl complex at ligand concentrations that are almost stoichiometric with ^{99m}Tc concentrations after 60 min at 75ºC. [8] The

realization that radioconjugates of this caliber could be produced in one step without further purification led to an explosion of interest in this area of radiochemistry.

3.2 EXPERIMENTAL

3.2.1 Materials

All chemicals were purchased from Aldrich Chemical Company (St. Louis, MO3.7) and used without further purification. American Chemical Society (ACS) certified solvents were purchased from Fisher Scientific (Pittsburgh, PAf) and used without further purification. All procedures and results have been previously published and have approval for publication in this dissertation (Lane, SR, et al. 2008. Journal of Nuclear Medicine and Biology, 35(3): 263-272). [14]

3.2.2 Synthesis of *N, N´-Bis*(*tert*-butoxycarbonyl)diethylenetriamine

BOC-ON (4.46 g, 18.1 mmol) dissolved in THF (250 mL) was slowly added dropwise to diethylenetriamine (0.933 g, 9.04 mmol) in THF (10 mL) at <0ºC (ice, NaCl, and $(CH_3)_2CO$). The reaction mixture was stirred overnight after which solvent was removed under reduced pressure. Ligand precursor was purified by flash column chromatography using a 4 x 45 cm column packed half-full with silica gel (particle size 63-200). Methylene chloride (600 mL) was used to remove reaction by-products, followed by 98.5% CH_2Cl_2/1.5% MeOH (600 mL), and then 100% MeOH (1000 mL). TLC, run on alumina backed silica gel TLC plates, in 98.5% CH_2Cl_2/1.5% MeOH, was used to determine the progress of the separation. MeOH fractions were collected from the

column and solvent was removed *in vacuo* to give a yellow oil (5.38 g, 98%). **^{1}H NMR** [$CDCl_3$, 500 MHz, RT, δ(ppm)] ((-O-C-**CH_3**)$_3$, s, 18H) 1.409, (-NH-**CH_2**-CH_2-NH-CH_2-**CH_2**-NH-, t, 4H) 2.675, (-NH-CH_2-**CH_2**-NH-**CH_2**-CH_2-NH-, m, 4H) 3.169, (-CO-**NH**-CH_2-CH_2-**NH**-, s) 5.083. **^{13}C NMR** [$CDCl_3$, 500 MHz, RT, δ(ppm)] ((-O-C-**CH_3**)$_3$) 28.31, (-NH-**CH_2**-CH_2-NH-CH_2-**CH_2**-NH-) 40.16, (-NH-CH_2-**CH_2**-NH-**CH_2**-CH_2-NH-) 48.70, (-**C**-$(CH_3)_3$) 79.03, (-**COO**-C-$(CH_3)_3$) 156.10. **Mass spectrum (HR-FAB MS)**: Anal Calc. for $C_{14}H_{29}N_3O_4$ ($M+Li^+$): 311.2346. Found: 311.2357.

3.2.3 Synthesis of *N, N´-Bis*(*tert*-butoxycarbonyl)diethylenetriamine Ethyl Bromoester

BOC-DTMA (2.29 g, 7.41 mmol) was dissolved in MeCN (35 mL). To this solution was added ethyl bromoacetate (1.025 mL, 9.26 mmol), KI (1.51 g, 9.10 mmol), and triethylamine (5 mL). The solution was refluxed for 48 h. (See Figure 3.1.) The orange-cream colored solution was filtered through filter paper to remove excess salt, and was washed with MeCN. Removal of solvent under reduced pressure afforded the product as a clear yellow oil (2.79 g, 95%). **^{1}H NMR** [$CDCl_3$, 500 MHz, RT, δ(ppm)] (-COO-CH_2-**CH_3**, t, 3H) 1.174, (-COO-C-(**CH_3**)$_3$, s, 18H) 1.351, (-NH-**CH_2**-CH_2-N-CH_2-**CH_2**-NH-, t, 4H) 2.623, (-NH-CH_2-**CH_2**-N-**CH_2**-CH_2-NH-, m, 4H) 3.052, (-N-**CH_2**-COO-CH_2-CH_3, s, 2H) 3.259, (-COO-**CH_2**-CH_3, q, 2H) 4.069, (-**NH**-CH_2-CH_2-N-CH_2-CH_2-**NH**-, s, 2H) 5.180. **^{13}C NMR** [$CDCl_3$, 250 MHz, RT, δ(ppm)] (-COO-CH_2-**CH_3**) 14.05, (-COO-**$(CH_3)_3$**) 28.28, (-NH-**CH_2**-CH_2-N-CH_2-**CH_2**-NH-) 38.45, (-NH-CH_2-**CH_2**-N-**CH_2**-CH_2-NH-) 53.99, (-COO-**CH_2**-CH_3) 55.08, (-N-**CH_2**-COO-CH_2-CH_3) 60.51, (-

COO-**C**-$(CH_3)_3$) 78.88, (-**COO**-C-$(CH_3)_3$) 156.04, (-**COO**-CH_2-CH_3) 171.56). **Mass spectrum (ESI-MS)**: Anal Calc. for $C_{18}H_{36}N_3O_6$ (M^+): 390.26. Found: 390.1.

3.2.4 Synthesis of 2-(N, N´-Bis(tert-butoxycarbonyl)diethylenetriamine) Acetic Acid

To BOC-DTMA-ester (2.50 g, 6.42 mmol) in MeOH (15 mL) was added 10% NaOH solution (~8 mL) until the final pH of the solution was adjusted to 11. The solution was stirred for 3 h and dried under reduced pressure. (See Figure 3.1.) The product was dissolved in water (10 mL). A saturated solution of citric acid was added to the dissolved product until a pH of 5 was obtained. Ethyl acetate (40 mL) was added to the solution while stirring. The aqueous and organic solutions were separated *via* separatory funnel. The ethyl acetate layer was washed with water a total of three times and dried over sodium sulfate. The organic layer was dried *in vacuo* to afford a white solid. The product was washed with diethyl ether and centrifuged. The supernatant was decanted and the white powder was dried overnight under reduced pressure (0.63 g, 27%). **^{1}H NMR** [MeOD, 500 MHz, RT, δ(ppm)] (-COO-C-(**CH_3)$_3$**, s, 18H) 1.360, (-NH-

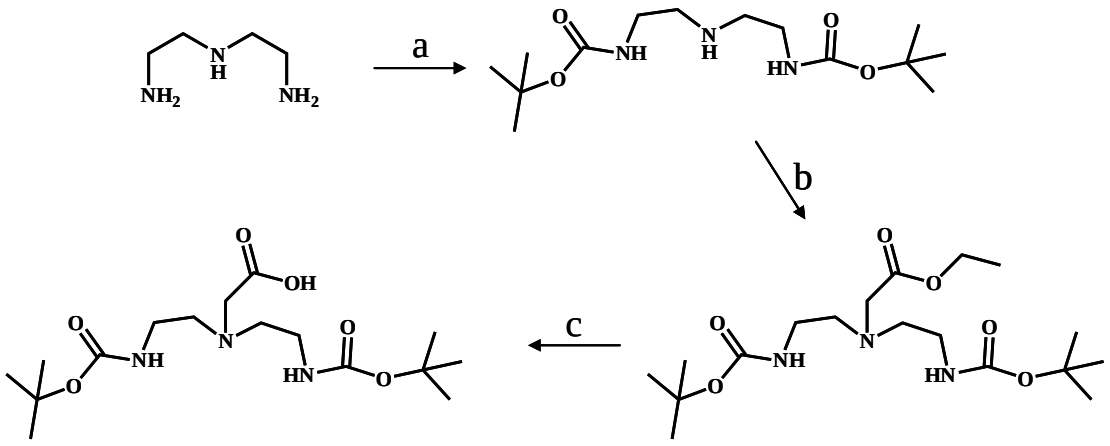

FIGURE 3.1: Synthesis of BOC-DTMA-acid. (a) BOC-ON, THF, 0ºC, 4 h; (b) $BrCH_2COOC_2H_5$, $N(Et)_3$, KI, CH_3CN, Δ, 6 h; (c) MeOH, 5% NaOH, RT, 3 h.

CH_2-CH_2-N-CH_2-**CH_2**-NH-, m, 4H) 3.149, (-NH-CH_2-**CH_2**-N-**CH_2**-CH_2-NH-, m, 4H) 3.288, (-N-**CH_2**-COOH, s, 2H) 3.575. **^{13}C NMR** [MeOD, 500 MHz, RT, δ(ppm)] (-COO-**$(CH_3)_3$**) 28.28, (-NH-**CH_2**-CH_2-N-CH_2-**CH_2**-NH-) 37.22, (-NH-CH_2-**CH_2**-N-**CH_2**-CH_2-NH-) 56.15, (-N-**CH_2**-COOH) 57.81, (-COO-**C**-$(CH_3)_3$) 80.84, (-**COO**-C-$(CH_3)_3$) 158.75, (-**COOH**) 170.81. **Mass spectrum (ESI-MS)**: Anal Calc. for $C_{16}H_{31}N_3O_6$ (M^++Li): 368.24. **Found:** 368.2.

3.2.5 Synthesis of [DTMA-(X)-BBN(7-14)NH_2] Peptide Conjugates

[DTMA-(X)-BBN(7-14)NH_2] conjugates were synthesized on a Perkin-Elmer-Applied Biosystem model 432A automated peptide synthesizer employing traditional Fmoc chemistry, where X denotes the linker (GGG, GSG, SSS, or β-Ala) and BBN(7-14)NH_2 denotes the amino acid sequence, Q-W-A-V-G-H-L-M-NH_2. (See Figure 3.2.) Rink Amide MBHA resin (25μmol), Fmoc-protected amino acids (75μmol), and DTMA (75μmol) were utilized for SPPS. A cocktail of thioanisol, water, ethanedithiol and trifluoracetic acid in a ratio of 2:1:1:36 was used to cleave the peptide from the resin, followed by peptide precipitation in methyl-t-butyl ether. Crude peptide conjugates were obtained in 80-85% yield. The crude peptide-conjugates were purified by reversed-phase high performance liquid chromatography (RP-HPLC) and solvents were removed *in vacuo* using a SpeedVac concentrator (Labconco, Kansas City, MO). Negative ion mode ESI-MS was used to compare calculated to experimental molecular ion peaks. The calculated and experimental masses for the [DTMA-(X)-BBN(7-14)NH_2] conjugates were as follows: X=GGG (1255.7, 1254.4), X=GSG (1285.6, 1284.9), X=SSS (1345.5, 1344.7), and X=β-Ala (1153.6, 1152.7).

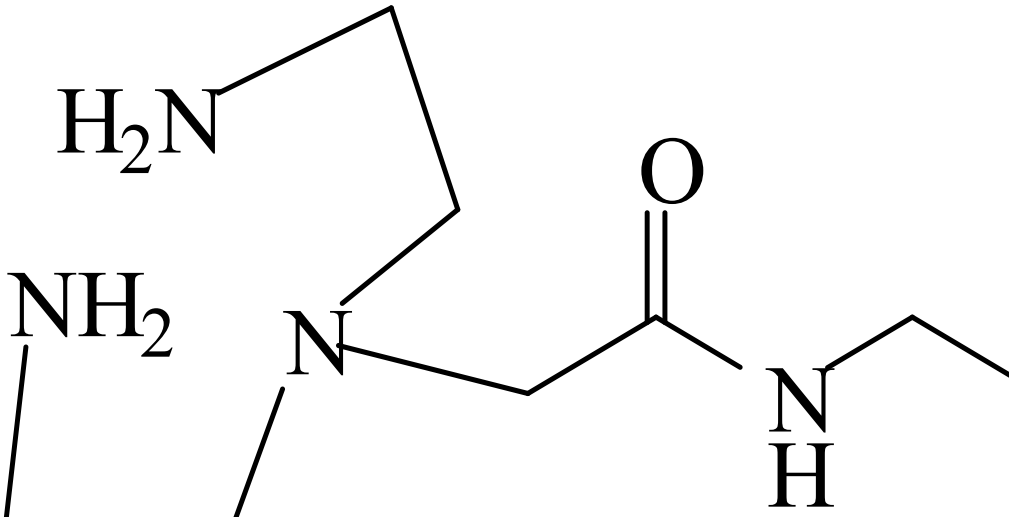

FIGURE 3.2: Structure of DTMA-(X)-BBN(7-14)NH_2, where X= GGG (top), GSG, SSS and β-Ala (bottom).

FIGURE 3.3: Radiolabeling scheme for $[^{99m}Tc(CO)_3$-DTMA-(X)-BBN(7-14)$NH_2]^+$ conjugates. (a) Isolink® kit, 120 μL 0.1N HCl, 100°C, 25 min; (b) peptide conjugate, 80°C, 1 h.

3.2.6 Radiolabeling of [DTMA-(X)-BBN(7-14)NH_2] Conjugates With $[^{99m}Tc(H_2O)_3(CO)_3]^+$

Na[$^{99m}TcO_4$] was eluted from a $^{99m}Tc/^{99}Mo$ generator (Mallinckrodt Medical, Inc., St. Louis, MO) using 0.9% saline. The $[^{99m}Tc(H_2O)_3(CO)_3]^+$ precursor was synthesized by adding $[^{99m}TcO_4]^-$ generator eluent (1 mL) to an Isolink® kit (Tyco Healthcare, St. Louis, MO), heating for 30 min in a water bath, and then adding 0.1 M HCl (120 µL). The $[^{99m}Tc(H_2O)_3(CO)_3]^+$ (500 µL) was added to a test tube containing purified peptide conjugate (100 µg, 74.3-86.7 nmol) and heated at 80ºC for 1 h. (See Figure 3.3.) Radiolabeled conjugates were purified by RP-HPLC and were collected into 100 µL of 1 mg/mL bovine serum albumin (BSA) stabilizing agent prior to *in vitro* and *in vivo* evaluation.

3.2.7 RP-HPLC Analyses of Metallated and Non-Metallated [DTMA-(X)-BBN(7-14)NH_2] Conjugates

RP-HPLC analyses of radiolabeled and non-radiolabeled compounds were performed on a Shimadzu SCL-10A system equipped with a Shimadzu SPD-10A UV-Vis tunable absorbance detector (set at λ=280 nm), an Eppendorf TC-50 column heater, and a radiometric in-line EG&G ORTEC NaI solid scintillation detector. HPLC grade solvents were purchased from Fisher Scientific (Pittsburg, PA). Purification of non-metallated conjugates was performed on a semi-preparative reversed-phase C-18 column (Phenomenex Jupiter Proteo, 250 x 10.00mm, 10µm). Radiolabeling investigations were performed using an analytical reversed-phase C-18 column (Phenomenex Jupiter Proteo, 250 x 4.60 mm, 5 µm). The solvent system was H_2O/0.1% TFA (A) and CH_3CN/0.1%

TFA (B). The gradient system began at 95% A and 5% B. From 0 to 25 minutes, the solvent increased linearly to 30% A and 70% B. From 25 to 30 minutes, the solvent increased to 5% A and 95% B.

3.2.8 ESI- and HR-FAB MS

High-resolution fast atom bombardment mass spectrometry (HR-FAB MS) analyses of the non-conjugated ligand and ligand intermediates were performed by the Washington University Mass Spectrometry Resource (St. Louis, MO), a NIH Research Resource (Grant No. P41RR0954). Characterization of the non-metallated peptide conjugates by ESI-MS was performed by SynBioSci (Livermore, CA).

3.2.9 *In Vitro* Analysis of $[^{99m}Tc\text{-}(CO)_3\text{-DTMA-(X)-BBN(7-14)}NH_2]^+$

3.2.9.1 Stability Study in Phosphate Buffered Saline

The stability of radiometallated peptide conjugates was assessed in phosphate buffered saline (PBS) after 0, 1, 4, and 24 h incubation periods at room temperature (RT). RP-HPLC was used to assess the stability for each of the metallated conjugates. To assess the stability of the new conjugates to transmetallation reactions, histidine challenge experiments were performed. Briefly, each of the conjugates was incubated in 10^{-3} M histidine solution and analyzed by RP-HPLC. Assessment of stability was determined at 24 h post-incubation with histidine solution.

3.2.9.2 Competitive Displacement Binding Assay

The IC_{50} of DTMA-(X)-BBN(7-14)NH_2 was established by competitive displacement cell binding assays using radiolabeled [^{125}I-(Tyr^4)-BBN] as the radioligand. Briefly, $3x10^4$ cells (in D-MEM/F-12K media containing 0.01 M MEM and 2% BSA, pH=5.5) were incubated with 20,000 counts per minute [^{125}I-(Tyr^4)-BBN] ($8.2x10^{-15}$ mol, $8.14x10^4$ GBq/mmol ($2.20x10^3$ Ci/mmol)) at 37ºC. Non-radiolabeled peptide conjugate was added at a steadily increasing concentration and allowed to incubate for an additional minute at 37ºC. The solution was aspirated, and the cells were rinsed with cold media. Cell-associated radioactivity was determined using a Packard Riastar gamma counter.

3.2.9.3 Internalization and Externalization Assays

The internalization studies were conducted by incubating $3x10^4$ cells (in D-MEM/F-12K media containing 0.01 M MEM and 2% BSA, pH=5.5) in the presence of 20,000 counts per minute [^{99m}Tc(CO)$_3$-DTMA-(X)-BBN(7-14)NH_2]$^+$ ($3.45x10^{-17}$ mol, $1.94x10^7$ GBq/mmol ($5.23x10^5$ Ci/mmol) at 37ºC. At 10, 20, 30, 45, 60, 90, and 120 min post-incubation, the cells were aspirated, washed (0.2 N acetic acid/0.5 M NaCl (pH=2.5)), and counted on a Packard Riastar gamma counter. The externalization studies were completed after an initial 40 min internalization period. The cells were washed at RT, resuspended in media, and incubated a second time. At 0, 20, 40, 60, 90, 120, and 150 min post-incubation, the cells were washed with media and acetic acid/saline (pH=2.5 at 4ºC) and counted on a Packard Riastar gamma counter.

3.2.10 *In Vivo* Analysis of $[^{99m}Tc\text{-}(CO)_3\text{-}DTMA\text{-}(X)\text{-}BBN(7\text{-}14)NH_2]^+$

The pharmacokinetics of the $[^{99m}Tc(CO)_3\text{-}DTMA\text{-}(X)\text{-}BBN(7\text{-}14)NH_2]^+$ conjugates were determined in normal CF-1 and tumor-bearing PC-3 mouse models (n=5). All animal studies were conducted in accordance with the highest standards of care as outlined in the NIH guide for Care and Use of Laboratory Animals and the Policy and Procedures for Animal Research at the Harry S. Truman Memorial Veterans' Hospital. SCID mice bearing xenografted human PC-3 tumors were used to determine the ability to target tumor tissue *in vivo*. For studies involving tumor-bearing mice, four to 5-week old female ICR SCID outbred mice were obtained from Taconic (Germantown, NY). The mice were housed five animals per cage in sterile micro-isolator cages in a temperature- and humidity-controlled room with a 12 h light/12 h dark schedule. The animals were fed autoclaved rodent chow (Ralston Purina Company, St. Louis, MO) and water *ad libitum*. Animals were anesthetized for injections with isoflurane (Baxter Healthcare Corp., Deerfield, IL) at a rate of 2.5% with 0.4 L oxygen through a non-rebreathing anesthesia vaporizer. Human prostate PC-3 cells were injected on the bilateral subcutaneous flank with $5x10^6$ cells in a suspension of 100 μL normal sterile saline per injection site. PC-3 cells were allowed to grow two to three weeks post inoculation, developing tumors ranging in mass from 0.02-1.30 grams. Briefly, the mice were injected *via* the tail vein with 185 kBq (5 μCi) of conjugate in 100 μL of isotonic saline. Mice were euthanized at specific time-points. Tissues, organs, and urine were excised, weighed, and counted in a NaI well counter. The percent injected dose (% ID) and the percent injected dose per gram (% ID/g) were calculated. The whole blood volume was assumed to be 6.5% of the total body weight, allowing for the % ID in whole blood.

3.3 RESULTS AND DISCUSSION

DTMA was synthesized in good yield from a three step procedure according to Figure 3.1. ^{1}H and ^{13}C NMR and HR-FAB MS characterization were performed on all purified reaction intermediates. DTMA peptide conjugates (Figure 3.2) were synthesized by SPPS, purified by RP-HPLC, and characterized by ESI-MS (Table 3.1). Radiolabeled conjugates were synthesized in a two step procedure, according to Figure 3.3. Radiolabeling yields were optimized by adjusting the pH of the solution containing the peptide conjugate and tricarbonyl precursor. Radiolabeled conjugates were afforded in ~90% yield. Single radiolabeled products were isolated by RP-HPLC (Figure 3.4) and were stable over 24 h. Radiolabeled conjugates were also stable to 10^{-3} M histidine solution for periods ≤ 24 h. [14]

In vivo analysis of [DTMA-(X)-BBN(7-14)NH_2] conjugates was performed in human prostate PC-3 tumor cells. IC_{50} values for [DTMA-(X)-BBN(7-14)NH_2] conjugates were determined using [^{125}I-(Tyr^4)-BBN] as the gold standard. (See Figure 3.5.) Single nanomolar IC_{50} values were obtained for all of the non-metallated conjugates (GGG (2.58±1.3 nmol), GSG (0.65±0.3 nmol), SSS (0.77±0.2 nmol), β-Ala (0.29±0.2 nmol)), demonstrating the high affinity of these BBN(7-14)NH_2-conjugates for the GRPr. Internalization and externalization studies of [^{99m}Tc(CO)$_3$-DTMA-(X)-BBN(7-14)NH_2]$^+$ conjugates in human prostate PC-3 tumor cells is shown in Figure 3.6 and Figure 3.7. It is clearly shown that the [^{99m}Tc(CO)$_3$-DTMA-(β-Ala)-BBN(7-14)NH_2]$^+$ conjugate exhibited rapid internalization with 18.7±3% internalized in 3x10^4 cells at 45 min. Internalization of conjugate increased slightly to 23.8±3% at 120 min post-incubation. The [^{99m}Tc(CO)$_3$-DTMA-(X)-BBN(7-14)NH_2]$^+$ conjugates, where

TABLE 3.1: Electrospray mass spectrometry values of DTMA-(X)-BBN(7-14)NH_2 conjugates.

DTMA-X-BBN(7-14)	Molecular Formula	Calculated	Experimental
X=β-ala	$C_{52}H_{83}N_{17}O_{11}S$	1153.6	1152.7
X=GGG	$C_{55}H_{89}N_{19}O_{13}S$	1255.6	1254.4
X=GSG	$C_{56}H_{91}N_{19}O_{14}S$	1285.6	1284.9
X=SSS	$C_{58}H_{95}N_{19}O_{16}S$	1346.5	1344.7

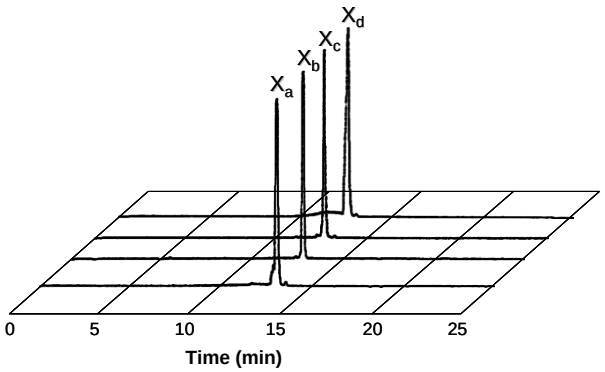

FIGURE 3.4: HPLC chromatographic profiles of [^{99m}Tc(CO)$_3$-DTMA-(X)-BBN(7-14)NH_2]$^+$ conjugates, where X_a = β-Ala (13.0 min), X_b = GGG (12.7 min), X_c = GSG (12.6 min), and X_d = SSS (12.5 min).

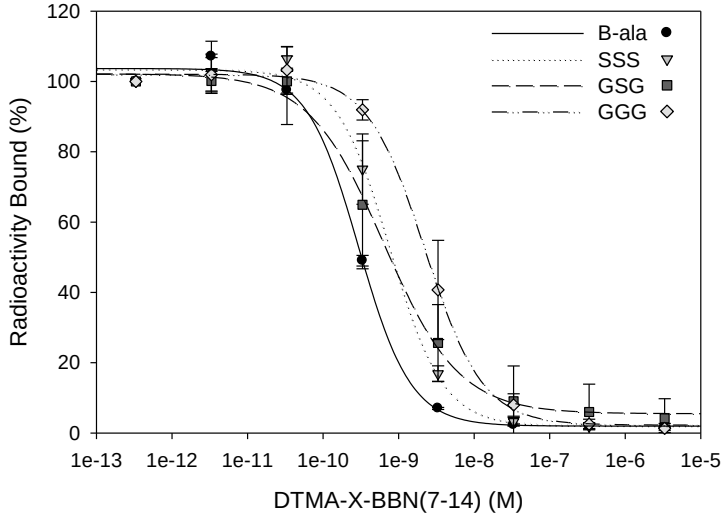

FIGURE 3.5: IC_{50} data of DTMA-(X)-BBN(7-14)NH_2 peptides versus bound [^{125}I-Tyr^4-BBN] conjugate, for X=β-Ala (0.28±0.2 nM), GGG (2.56±1.3 nM), GSG (0.68±0.3 nM), and SSS (0.74±0.2 nM).

X=GGG, GSG, and SSS, did not internalize at the same rate as [^{99m}Tc(CO)$_3$-DTMA-(β-Ala)-BBN(7-14)NH$_2$]$^+$, with only 2.37±1%, 6.59±4%, and 11.46±3% internalizing at 120 min, respectively. [^{99m}Tc(CO)$_3$-DTMA-(β-Ala)-BBN(7-14)NH$_2$]$^+$ conjugate also exhibited favorable externalization properties from PC-3 cells, where after 90 min incubation in media, 90.1±12% remained internalized in the cells. [^{99m}Tc(CO)$_3$-DTMA-(X)-BBN(7-14)NH$_2$]$^+$ conjugates, where X=GGG, GSG, and SSS, externalized more rapidly than [^{99m}Tc(CO)$_3$-DTMA-(β-Ala)-BBN(7-14)NH$_2$]$^+$, with only 57.0±17%, 51.3±9%, and 74.7±11% of administered tracer remaining in PC-3 cells at the end of the 90 min incubation period. [14] (Error was omitted in Figures 3.6 and 3.7 for clarity. The average internalization error was 2.3% for X=β-Ala, 0.8% for GGG, 2.8% for GSG, and 1.65% for SSS. The average externalization error was 9.8% for X=β-Ala, 37.3% for GGG, 12.1% for GSG, and 12.5% for SSS.

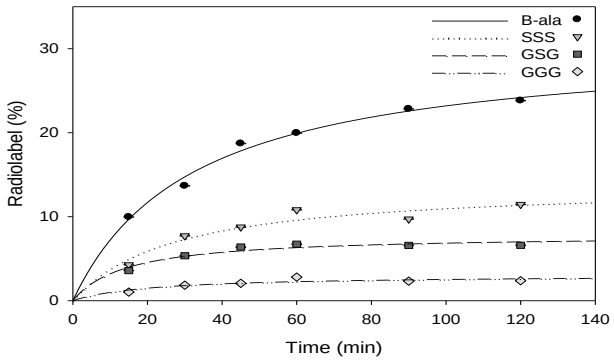

FIGURE 3.6: Internalization data, percentage of [^{99m}Tc(CO)$_3$-DTMA-(X)-BBN(7-14)NH$_2$]$^+$ conjugates cell-associated radioactivity internalized versus time, for X=β-Ala (solid line), SSS (dotted line), GSG (dashed line), GGG (intermittently dashed line). (Error of ~20%.)

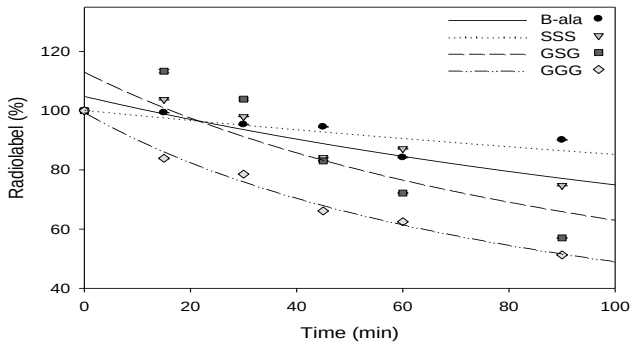

FIGURE 3.7: Externalization data, percentage of initial [^{99m}Tc(CO)$_3$-DTMA-(X)-BBN(7-14)NH$_2$]$^+$ conjugates remaining internalized versus time for X=β-Ala (solid line), SSS (dotted line), GSG (dashed line), GGG (intermittently dashed line). (Error of ~20%.)

In vivo analysis of $[^{99m}Tc(CO)_3$-DTMA-(X)-BBN(7-14)$NH_2]^+$ conjugates was first performed in normal CF-1 mice. The mice were sacrificed at 1 h p.i., and tissues and organs were excised and counted in a NaI well counter. The results of biodistribution studies are summarized in Table 3.2. Rapid clearance from blood was observed for all of the conjugates at 1 h p.i., with the exception of the conjugate where X=SSS, with a blood retention of 2.73±0.40% ID/g. Excretion of the conjugates varied. The more hydrophilic serine-containing pharmacokinetic modifiers emptied primarily *via* the renal-urinary excretion system. On the other hand, the hydrophobic conjugates, where X= β-Ala and GGG, were excreted primarily *via* the hepatobiliary system. High affinity of conjugates to GRP receptor-expressing pancreas was shown in this study. The pancreas uptake in normal mice was 19.42±4.31% ID/g for X=β-Ala, 10.36±0.90% ID/g for X=GGG, 15.48±5.25% ID/g for X=GSG, and 8.00±0.88% ID/g for X=SSS. Blocking studies, in which high levels of cold BBN(1-14) were administered 15 min prior to the $[^{99m}Tc(CO)_3$-DTMA-(X)-BBN(7-14)$NH_2]^+$ conjugate, reduced the % ID/g uptake/retention in normal pancreas by a factor of 8-10. This clearly identifies the affinity of these conjugates for the GRPr. Table 3.3 summarizes the results of biodistribution studies for the $[^{99m}Tc(CO)_3$-DTMA-(β-Ala)-BBN(7-14)$NH_2]^+$ conjugate in SCID mice bearing xenografted, human, PC-3 tumors at 1, 4, and 24 h p.i. The conjugate's rate of clearance from whole blood was very rapid, with only 0.73±0.60% ID at 1 h p.i., 0.37±.24% ID at 4 h p.i., and 0.11±0.04% ID at 24 h p.i. remaining in tissue. The average tumor uptake for the $[^{99m}Tc(CO)_3$-DTMA-(β-Ala)-BBN(7-14)$NH_2]^+$ conjugate was 0.95±0.15% ID/g at 1 h p.i., 0.52±0.10% ID/g at 4 h p.i., and 0.13±0.07% ID/g at 24 h p.i. Receptor-mediated

pancreatic uptake was 8.20±2.38% ID/g at 1 h p.i., 8.27±2.47% ID/g at 4 h p.i., and 4.12±1.23% ID/g at 24 h p.i. [14]

TABLE 3.2: Biodistribution of $[^{99m}Tc(CO)_3$-DTMA-(X)-BBN(7-14)$NH_2]^+$ conjugates in CF-1 normal mice at 1 h p.i. (n = 5, % ID/g ± SD).

Tissue/Organ	X=β-ala	X=GGG	X=GSG	X=SSS
Bladder	0.65(0.38)	1.17(0.81)	1.41(1.58)	3.52(2.77)
Heart	0.15(0.04)	1.86(029)	0.40(0.21)	1.58(0.15)
Lungs	0.26(0.04)	0.46(0.10)	0.49(0.27)	2.55(0.28)
Liver	7.48(0.87)	9.52(1.29)	5.49(2.12)	6.38(0.96)
Kidney	3.49(0.65)	2.30(0.50)	3.39(2.0)	6.37(0.30)
Spleen	1.16(0.17)	0.47(0.08)	1.09(0.54)	0.97(0.12)
Stomach	1.03(0.50)	2.27(1.23)	0.96(0.42)	0.82(0.26)
S. Intestine	20.52(2.73)	16.97(2.93)	5.92(1.85)	5.07(0.79)
L. Intestine	3.37(1.00)	9.14(2.55)	4.07(0.91)	1.81(0.50)
Muscle	0.12(0.06)	0.20(0.07)	0.11(0.07)	0.43(0.06)
Bone	0.30(0.16)	0.19(0.04)	0.23(0.08)	0.80(0.22)
Brain	0.03(0.01)	0.02(0.01)	0.03(0.02)	0.21(0.15)
Pancreas	19.43(4.31)	10.36(0.90)	15.48(5.25)	8.00(0.88)
Blood	0.22(0.02)	0.17(0.04)	0.32(0.13)	2.73(0.40)
Urine	41.37(2.77)	38.31(23.68)	63.75(13.03)	57.69(4.04)

TABLE 3.3: Biodistribution of $[^{99m}Tc(CO)_3$-DTMA-(β-Ala)-BBN(7-14)$NH_2]^+$ conjugate in PC-3 tumor-bearing SCID mice at 1, 4, 24 h p.i. (n = 5, % ID/g ± SD).

Tissues/Organ	1 Hour	4 Hour	24 Hour
Bladder	0.94 (1.25)	0.29 (0.22)	0.00 (0.00)
Heart	0.28 (0.04)	0.18 (0.02)	0.16 (0.31)
Lungs	0.56 (0.07)	0.29 (0.07)	0.10 (0.12)
Liver	5.38 (1.30)	1.99 (0.40)	0.64 (0.19)
Kidney	3.05 (0.51)	1.92 (0.76)	0.48 (0.20)
Spleen	0.38 (0.10)	0.43 (0.19)	0.26 (0.27)
Stomach	0.93 (0.65)	0.39 (0.19)	1.96 (4.08)
S. Intestine	25.36 (4.73)	2.19 (1.00)	0.85 (0.93)
L. Intestine	1.75 (0.63)	50.63 (27.45)	2.08 (3.62)
Muscle	0.16 (0.03)	0.06 (0.01)	0.02 (0.03)
Bone	0.24 (0.07)	0.13 (0.06)	0.00 (0.00)
Brain	0.03 (0.00)	0.03 (0.01)	0.00 (0.01)
Pancreas	8.20 (2.38)	8.27 (2.47)	4.12 (1.23)
Blood	0.73 (0.60)	0.37 (0.24)	0.11 (0.04)
Urine	50.50 (3.07)	57.64 (10.44)	94.01 (5.04)
Tumor # 1	0.92 (0.17)	0.47 (0.11)	0.11 (0.07)
Tumor # 2	0.98 (0.12)	0.56 (0.09)	0.14 (0.07)

3.4 CONCLUSION

In this study, the DTMA ligand was synthesized by conventional methods and conjugated to the N-terminal primary amine of [H_2N-(X)-BBN(7-14)NH_2]. [DTMA-(X)-BBN(7-14)NH_2] conjugates were produced and displayed good selectivity and affinity for the GRPr. Competitive displacement of [^{125}I-(Tyr^4)-BBN] from human prostate PC-3 cells by DTMA-(X)-BBN(7-14)NH_2 showed that the [DTMA-(X)-BBN(7-14)NH_2] conjugates had very high affinity to the GRPr expressed on this cell line. $[^{99m}Tc(CO)_3$-DTMA-(X)-BBN(7-14)$NH_2]^+$ conjugates were produced in high radiochemical yield

using the Isolink® $[^{99m}Tc(H_2O)_3(CO)_3]^+$ kit. Their affinity for the GRPr was tested *in vitro* and *in vivo*. $[^{99m}Tc(CO)_3$-DTMA-(β-Ala)-BBN(7-14)$NH_2]^+$ showed the highest degree of receptor-mediated pancreatic accumulation at 1 h p.i. in normal CF-1 mice and favorable *in vitro* internalization in PC-3 cells. Therefore, this conjugate was selected for further studies in PC-3 tumor-bearing SCID mouse model. Experimental results for $[^{99m}Tc(CO)_3$-DTMA-(β-Ala)-BBN(7-14)$NH_2]^+$ in PC-3 tumor-bearing mice were not nearly as favorable as was expected. Average tumor uptake for the $[^{99m}Tc(CO)_3$-DTMA-(β-Ala)-BBN(7-14)$NH_2]^+$ conjugate was 0.95±0.15% ID/g at 1 h p.i. This value is somewhat low when compared to the SCID mouse PC-3 tumor uptake of up to 3.7% ID/g at 1 h p.i. exhibited by $[^{99m}Tc(CO)_3(X)$-Dpr-$(Ser)_3]$BBN(7-14)$NH_2]$, where X = H_2O or $P(CH_2OH)_3$. [16]

3.5 FUTURE STUDIES

3.5.1 Alternative Chelate

A more hydrophilic chelate might be able to counterbalance the strongly hydrophobic properties of the tricarbonyl. One suggestion might be to maintain the frame of the DTMA chelate, but modify it with the addition of a furan ring on the backbone between each of the secondary and primary amines. This would lead to increased hydrophilicity while retaining the characteristics of the amines.

FIGURE 3.8: Modified DTMA chelate with enhanced hydrophilicity.

3.5.2 Alternative Bombesin Analogs

Modification of [BBN(7-14)NH_2] to improve receptor targeting ability is also one possibility. For example, Schweinsberg and co-workers have synthesized [^{99m}Tc-$(CO)_3$-Ala(NTG)-βAla-βAla-BBN(7-14)NH_2], where Leu^{13} and Met^{14} have been replaced by Cha and Nle, respectively. This peptide modification has been reported to increase metabolic stability in human plasma and PC-3 cells. [17] It is also possible to use bombesin antagonists since they have recently been shown to have equivalent if not superior uptake values when compared to bombesin agonists. Cescato and co-workers have explored the use of the antagonist, [N_4-[D-Phe^6,Leu-NHEt^{13},*des*-Met^{14}]bombesin(6-14)] (Demobesin 1). Their results showed comparable in vitro binding to that of the agonists, [BBN(1-14)NH_2] and [N_4-[Pro^1,Tyr^4,Nle^{14}]bombesin] (Demobesin 4), in GRP receptor-transfected HEK293 cells, PC-3 cells, and human prostate cancer specimens. In PC-3 cells at 4h and 24h, [^{99m}Tc-Demobesin 1] uptake was 4- and 2-fold better than that of [^{99m}Tc-Demobesin 4]. In fact, when compared in PC-3 tumors, [^{99m}Tc-Demobesin 1] labels GRP receptors more intensely and longer than any GRPr agonist. [18] Reubi and others suggest that GRPR antagonists might be the future in bombesin radiopharmaceuticals. [19-20]

3.6 REFERENCES:

1. Fleischmann, A., et al., *Bombesin Receptors in Distinct Tissue Compartments of Human Pancreatic Diseases.* Laboratory Investigation, 2000. **80**(12): p. 1807-1817.

2. García Garayoa, E., et al., *Chemical and biological characterization of new Re(CO)3/[99mTc](CO)3 bombesin analogues.* Nuclear Medicine and Biology, 2007. **34**(1): p. 17-28.

3. Montet, X., et al., *Enzyme-based visualization of receptor-ligand binding in tissues.* Lab Invest, 2006. **86**(5): p. 517-525.

4. West, S.D. and D.W. Mercer, *Bombesin-Induced Gastroprotection.* Annals of Surgery, 2005. **241**(2): p. 227-231.

5. Marti, N., et al., *Comparative Studies of Substitution Reactions of Rhenium(I) Dicarbonyl−Nitrosyl and Tricarbonyl Complexes in Aqueous Media.* Inorganic Chemistry, 2005. **44**(17): p. 6082-6091.

6. Veerendra, B., et al., *Synthesis, Radiolabeling and In vitro GRP Receptor Targeting Studies of ^{99m}Tc-Triaza-X-BBN[7-14]NH_2 (X=Serylserylserine, Glycylglycylglycine, Glycylserylglycine, or Beta Alanine).* Synthesis and Reactivity in Inorganic, Metal-Organic, and Nano-Metal Chemistry, 2006. **36**(6): p. 481 - 491.

7. Brookhaven. *The Technetium-99m Generator*. 2009 [cited 2009; Available from: http://www.bnl.gov/bnlweb/history/tc-99m.asp.

8. Alberto, R., et al., *Basic aqueous chemistry of [M(OH2)3(CO)3]+ (M=Re, Tc) directed towards radiopharmaceutical application.* Coordination Chemistry Reviews, 1999. **190-192**: p. 901-919.

9. Alberto, R., et al., *Synthesis and Properties of Boranocarbonate: A Convenient in Situ CO Source for the Aqueous Preparation of [99mTc(OH2)3(CO)3]+.* Journal of the American Chemical Society, 2001. **123**(13): p. 3135-3136.

10. Alberto, R., et al., *A Novel Organometallic Aqua Complex of Technetium for the Labeling of Biomolecules: Synthesis of [99mTc(OH2)3(CO)3]+ from [99mTcO4]- in Aqueous Solution and Its Reaction with a Bifunctional Ligand.* Journal of the American Chemical Society, 1998. **120**(31): p. 7987-7988.

11. Abram, U. and R. Alberto, *Technetium and rhenium: coordination chemistry and nuclear medical applications.* Journal of the Brazilian Chemical Society, 2006. **17**: p. 1486-1500.

12. Prasanphanich, A.F., et al., *[64Cu-NOTA-8-Aoc-BBN(7-14)NH2] targeting vector for positron-emission tomography imaging of gastrin-releasing peptide receptor-expressing tissues.* Proceedings of the National Academy of Sciences, 2007. **104**(30): p. 12462-12467.

13. Prasanphanich, A.F., et al., *The Effects of Linking Substituents on the In Vivo Behavior of Site-Directed, Peptide-based, Diagnostic Radiopharmaceuticals.* In Vivo, 2007. **21**: p. 1-16.

14. Lane, S.R., et al., *99mTc(CO)3-DTMA bombesin conjugates having high affinity for the GRP receptor.* Nuclear Medicine and Biology, 2008. **35**(3): p. 263-272.

15. Vitor, R.F., et al., *Rhenium(I)- and technetium(I) tricarbonyl complexes anchored by bifunctional pyrazole-diamine and pyrazole-dithioether chelators.* Journal of Organometallic Chemistry, 2004. **689**(25): p. 4764-4774.

16. Smith, C.J., et al., *Radiochemical Investigations of Gastrin-releasing Peptide Receptor-specific [99mTc(X)(CO)3-Dpr-Ser-Ser-Ser-Gln-Trp-Ala-Val-Gly-His-Leu-Met-(NH2)] in PC-3, Tumor-bearing, Rodent Models: Syntheses, Radiolabeling, and in Vitro/in Vivo Studies where Dpr = 2,3-Diaminopropionic acid and X = H2O or P(CH2OH)3.* Cancer Res, 2003. **63**(14): p. 4082-4088.

17. Schweinsberg, C., et al., *Novel Glycated [99mTc(CO)3]-Labeled Bombesin Analogues for Improved Targeting of Gastrin-Releasing Peptide Receptor-Positive Tumors.* Bioconjugate Chemistry, 2008. **19**(12): p. 2432-2439.

18. Cescato, R., et al., *Bombesin Receptor Antagonists May Be Preferable to Agonists for Tumor Targeting.* J Nucl Med, 2008. **49**(2): p. 318-326.

19. Karra, S.R., et al., *99mTc-Labeling and in Vivo Studies of a Bombesin Analogue with a Novel Water-Soluble Dithiadiphosphine-Based Bifunctional Chelating Agent.* Bioconjugate Chemistry, 1999. **10**(2): p. 254-260.

20. Reubi, J.C. and H.R. Maecke, *Peptide-Based Probes for Cancer Imaging.* J Nucl Med, 2008. **49**(11): p. 1735-1738.

CHAPTER 4: COPPER-64 TETRAAMINE BOMBESIN CONJUGATES AS POTENTAIL DIAGNOSTIC IMAGING AGENTS

4.1 INTRODUCTION

4.1.1 Copper Chemistry

Three oxidation states of copper are possible in aqueous solution. These are Cu(I), Cu(II), and Cu(III). Cu(II) forms the most kinetically inert complexes due to the d^9 electron configuration and crystal-field stabilization energy. [1] A wide variety of borderline-soft donors can effectively complex the Cu(II) atom, which include amines and imines. A variety of geometries are possible for Cu(II) complexes, including square planar, distorted square planar, trigonal pyramidal, square pyramidal, and distorted octahedral. [1]

4.1.2 Specific Aims

The work described herein is focused on complexing copper-64 with the polyamino polycarboxylate chelate NOTA. Previous work has shown that NOTA formed a 6-coordinate distorted prismatic complex with copper. Metal bonds were formed between three amines and three carboxylates of the chelate. [16] No reactive groups was left uncoordinated. When NOTA is utilized as a BFCA, one of the carboxylic acid arms is bound to a biological targeting moiety. This change in the chelate is denoted by the acronym NO2A, which will be used in place of NOTA.

Novel [NO2A-(X)-BBN(7-14)NH_2] conjugates were synthesized for the purpose of targeting gastrin releasing peptide receptor-positive tissues. (See Figure 4.1) The effect of the spacing moiety was investigated by using spacers of increasing length. The [NO2A-(X)-BBN(7-14)NH_2] conjugates were labeled with cold $CuCl_2$ and radiolabelled with $^{64}CuCl_2$. *In vitro* assays were performed to determine the affinity of the [Cu-NO2A-(X)-BBN(7-14)NH_2] and [NO2A-(X)-BBN(7-14)NH_2] complexes. The assays that were performed include inhibitory concentration at 50% (IC_{50}) and internalization/efflux. The stability of the [^{64}Cu-NOTA-X-BBN(7-14)NH_2] complexes were investigated in human serum albumin (HSA) to determine the potential for transchelation to serum proteins. *In vivo* studies were performed. Biodistribution studies were first performed in normal CF-1 mice, followed by PC-3 tumor-bearing SCID mice. For those conjugates that showed high tumor uptake and favorable pharmacokinetic properties, maximum intensity microPET/CT images were obtained.

4.1.2 Preliminary Work

Polyaza macrocyclic polycarboxylates have been investigated for the purpose of chelating Cu(II) for use in nuclear medicine. Such examples include DOTA (1,4,7,10-

Figure 4.1: Structure of [Cu-NO2A-(X)-BBN(7-14)NH_2].

tetraazacyclodecane-1,4,7,10-tetraacetic acid), TETA (1,4,8,11-tetraazacyclotetradecane-1,4,8,11-tetraacetic acid), DO2A (1,4,7,10-tetraazabicyclo[5.5.2]tetradecane-4,10-diyl)diacetic acid), TE2A (1,4,8,11-tetraazabicyclo[6.6.2]hexadecane-4,11-diyl)diacetic acid), and NOTA (1,4,7-triazacyclononane-1,4,7-tracetic acid). [1-2] (See Figure 4.2). These small chelate structures provide a rigid, pre-oriented backbone, which results in more stable complexes than those of linear or branched amines. [3] The chelate ring size, along with the number of amine donors and carboxylic arms, can be selected to complement copper, allowing to adjust for better *in vivo* stability of the complex. [4-5]

Another benefit of this type of copper complex is its Cu[chelate]$^-$ formation constant, which is comparable to the linear polyaza polycarboxylate, EDTA: Cu[EDTA]$^-$ (18.9±0.1), Cu[NOTA]$^-$ (21.63±0.03), Cu[DOTA]$^-$ (22.2±0.2), Cu[TETA]$^-$ (21.6±0.2), [6] and Cu[DO2A]$^-$ (18.87). [7] DOTA has been one of the most studied chelator for binding ^{64}Cu. The DOTA bifunctional chelate (BFC) binds Cu(II) with four amines and two carboxylate arms of the chelate, while the third carboxylate arm binds the biological moiety and the fourth carboxylate arm remains unbound. [1] Garrison and co-workers studied one such complex in PC-3 cells and PC-3 tumor bearing SCID mice. The *in vitro* studies showed their [^{64}Cu-DOTA-(8-Aoc)-BBN(7-14)NH_2] complex to have an IC_{50} value of 1.44±0.08 nM, and a maximum internalization of about 2.3% activity at 2 hours. [8] At 4 and 24 h, the *in vivo* studies showed high uptake in the tumor

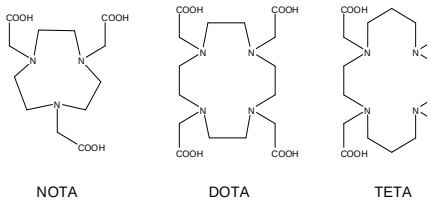

Figure 4.2: Examples of polyaza macrocyclic polycarboxylate chelates.

(3.00±1.10 %ID/g, 3.88±1.40 %ID/g) and pancreas (12.16±1.34 %ID/g, 3.65±0.44 %ID/g). At the same time points, uptake in the kidney (5.43±0.90 %ID/g, 4.58±0.95 %ID/g) and liver (8.98±2.74 %ID/g, 7.80±1.51 %ID/g) were also high, which could potentially cause high background radiation, and lower contrast PET images. [8] Complete biodistribution for [^{64}Cu-DOTA-(8-Aoc)-BBN(7-14)NH_2] can be found in Table 4.1. Fused microPET/CT images of the complex were taken in SCID mice bearing PC-3 tumors and imaged at 24 h p.i. (see Figure 4.3). [8] (Permission was granted for the use of Figure 4.3 and Figure 4.4. The original images are copyright protected and can be found in the article: Garrison, J.C., et al., *In Vivo Evaluation and Small-Animal PET/CT of a Prostate Cancer Mouse Model Using ^{64}Cu Bombesin Analogs: Side-by-Side Comparison of the CB-TE2A and DOTA Chelation Systems.* J Nucl Med, 2007. **48**(8): p. 1327-1337.)

Table 4.1: Biodistribution data for [^{64}Cu-DOTA-(8-Aoc)-BBN(7-14)NH_2] in PC-3 tumor bearing SCID mice at 1, 4 and 24 h p.i. [8]

^{64}Cu-DOTA-Aoc-BBN(7-14)NH_2			
Tissue/Organ	1 h	4 h	24 h
Excretion	44.63(9.15)	49.77(8.19)	67.84(5.43)
Heart	2.05(1.45)	1.63(0.73)	2.69(1.09)
Lungs	2.96(1.84)	3.27(1.31)	3.55(1.17)
Liver	9.56(5.20)	8.98(2.74)	7.80(1.51)
Kidney	8.46(2.79)	5.43(0.90)	4.58(0.95)
Spleen	2.52(1.59)	3.57(2.23)	3.59(2.48)
Stomach	2.30(0.96)	2.46(0.95)	1.68(0.59)
S.Intestine	13.45(2.08)	5.04(1.07)	2.84(0.48)
L.Intestine	5.58(2.84)	16.29(3.81)	3.78(0.85)
Muscle	0.65(0.37)	0.26(0.14)	0.46(0.21)
Bone	1.12(0.66)	0.79(0.35)	1.15(0.59)
Pancreas	13.81(2.69)	12.16(1.34)	3.65(0.44)
Tumor	3.48 ± 0.90	3.00 ± 1.10	3.88(1.40)
Blood	1.22 ± 0.62	0.76 ± 0.46	0.90(0.48)

*All data presented as %ID/g(SD), except excretion data (%ID(SD)). (n=5).

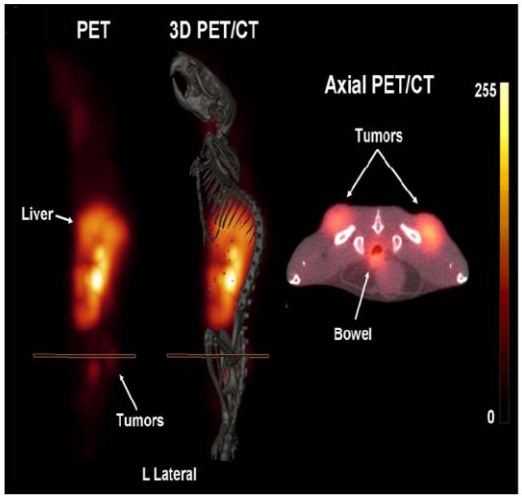

Figure 4.3: MicroPET, MicroPET/CT, and microPET/CT axial cross section images of [^{64}Cu-DOTA-(8-Aoc)-BBN(7-14)NH_2]. Images were performed in PC-3 tumor bearing SCID mice at 24 h p.i. [8]

^{64}Cu-DOTA's *in vivo* instability led to the search for a better Cu(II)-chelate. Therefore, the TETA chelate was investigated due to its similarities to DOTA, in hopes of retaining tumor specific uptake and improving the complex's kinetic stability. TETA differs from DOTA by having an increased ring size. The less strained binding conformation of Cu-TETA was predicted to contribute to increased kinetic stability, but transchelation *in vivo* was observed. [1, 9] One study performed by Bass and co-workers performed biodistribution and metabolism studies with ^{64}Cu-TETA-OC in Sprague-Dawley rats. They showed that ~70% of ^{64}Cu was transchelated in the liver by 20 h p.i. [10] The disappointing kinetic stability with the ^{64}Cu-DOTA and ^{64}Cu-TETA complexes led to the design of new cross-bridged (CB) analogues, DO2A and TE2A. [11-12] By bridging an ethylene moiety between non-adjacent ring nitrogens, Cu(II) complex rigidity was expected and observed. [9, 13-14] In one article, Boswell and co-workers compared metabolism studies of ^{64}Cu-DOTA, ^{64}Cu-DO2A, ^{64}Cu-TETA, and ^{64}Cu-TE2A in male Lewis rats. At 4 hours, the *in vivo* transchelation to serum proteins was measured for ^{64}Cu-DOTA (90.3±0.5%), ^{64}Cu-DO2A (61±14%), ^{64}Cu-TETA (75±9%), and ^{64}Cu-TE2A (13±6%). The CB chelates showed less transchelation and were significantly more kinetically inert. [13]

Garrison and co-workers recently performed studies with ^{64}Cu-TE2A-8-Aoc-BBN(7-14)NH_2. *In vitro* studies for this conjugate showed an IC_{50} value of 0.48±0.01 nM, and maximum internalization of activity of ~8% at 2 hours. At 4 and 24 h, the *in vivo* studies showed uptake in the tumor was 1.32±0.49 %ID/g and 0.28±0.21 %ID/g, and uptake in the pancreas to be 2.18±0.71 %ID/g and 0.18±0.14 %ID/g. At the same time points, the kidney uptake and accumulation was 1.88±0.53 %ID/g and 0.28±0.22 %ID/g.

Liver uptake and accumulation was 0.64±0.08 %ID/g and 0.21±0.06 %ID/g. [8] The complete biodistribution for ^{64}Cu-TE2A-8-Aoc-BBN(7-14)NH_2 can be found in Table 4.2. Fused microPET/CT images of the complex were taken in SCID mice bearing PC-3 tumors and imaged at 24 h p.i. (see Figure 4.4). The ^{64}Cu-TE2A complex produced a highly-resolved microPET image. [8]

Although the CB macrocycles showed improved biodistribution *in vivo* and improved kinetic stability when compared to non-CB chelates, there is still a great need for developing more stable ^{64}Cu complexes with improved radiosynthetic techniques. [1] One chelate that has recently reemerged and has shown great potential for ^{64}Cu binding is NOTA. When ^{64}Cu-NOTA is bound to the biological targeting moiety, the Cu atom is bound by three amines and two carboxylate arms, while the third carboxylate arm is covalently linked to the 8-Aoc-BBN(7-14)NH_2. [15]

Table 4.2: Biodistribution data for [^{64}Cu-TE2A-(8-Aoc)-BBN(7-14)NH_2] in PC-3 tumor bearing SCID mice at 1, 4 and 24 h p.i. [8]

^{64}Cu-TE2A-Aoc-BBN(7-14)NH_2			
Tissue/Organ	1 h	4 h	24 h
Excretion	60.38(2.16)	77.88(6.58)	98.60(0.28)
Heart	0.09(0.08)	0.08(0.08)	0.10(0.09)
Lungs	0.60(0.19)	0.22(0.15)	0.15(0.08)
Liver	2.15(0.26)	0.64(0.08)	0.21(0.06)
Kidney	5.26(0.58)	1.88(0.53)	0.28(0.22)
Spleen	0.68(0.53)	0.16(0.16)	0.56(0.30)
Stomach	0.94(0.27)	1.65(2.63)	0.05(0.04)
S.Intestine	13.17(1.21)	1.78(0.57)	0.11(0.04)
L.Intestine	3.52(1.12)	17.70(7.06)	0.20(0.08)
Muscle	0.26(0.15)	0.10(0.07)	0.22(0.17)
Bone	0.58(0.41)	0.39(0.25)	0.29(0.10)
Pancreas	17.66(2.00)	2.18(0.71)	0.18(0.14)
Tumor	2.65(1.05)	1.32(0.49)	0.28(0.21)
Blood	0.51(0.14)	0.06(0.05)	0.05(0.03)

*All data presented as %ID/g(SD), except excretion data (%ID(SD)). (n=5).

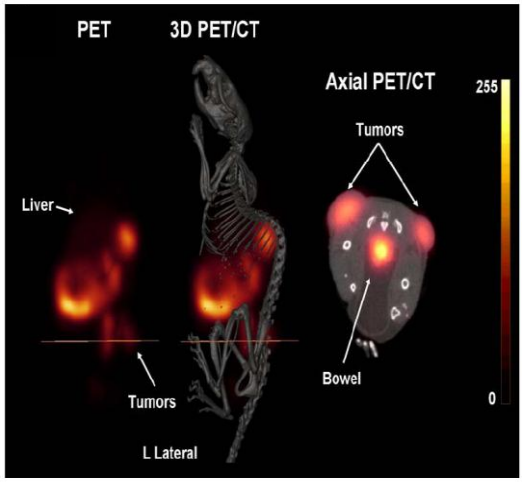

Figure 4.4: MicroPET, MicroPET/CT, and microPET/CT axial cross section images of [^{64}Cu-TE2A-(8-Aoc)-BBN(7-14)NH_2]. Images were performed in PC-3 tumor bearing SCID mice at 24 h p.i. [8]

Prasanphanich and co-workers have recently performed studied with ^{64}Cu-NOTA-8-Aoc-BBN(7-14)NH_2. *In vitro* studies showed an IC_{50} value of 3.1±0.5 nM. *In vivo* biodistribution studies at 1, 4 and 24 h showed uptake in the tumor was 1.64±0.15 %ID/g and 1.01±0.20 %ID/g. Uptake and accumulation in the pancreas was 7.46±1.06 %ID/g and 1.88±0.29 %ID/g. Kidney uptake and retention was 0.96±0.20 %ID/g and 0.47±0.12 %ID/g. Liver uptake and accumulation was 1.22±0.12 %ID/g and 0.68±0.21 %ID/g. The complete biodistribution for ^{64}Cu-NOTA-Aoc-BBN(7-14)NH_2 is shown in Table 4.3. [2] Fused microPET/CT images of the complex were taken in SCID mice bearing PC-3 tumors and imaged at 24 h p.i. (see Figure 4.5). (Permission was granted for the use of Figure 4.5. The original image is copyright protected from the article: Prasanphanich, A.F., et al., *[^{64}Cu-NOTA-8-Aoc-BBN(7-14)NH_2] targeting vector for positron-emission tomography imaging of gastrin-releasing peptide receptor-expressing tissues.* Proceedings of the National Academy of Sciences, 2007. **104**(30): p. 12462-12467.) The

Table 4.3: Biodistribution data for [^{64}Cu-NOTA-(8-Aoc)-BBN(7-14)NH_2] in PC-3 tumor-bearing SCID mice at 1, 4 & 24h p.i. [2]

^{64}Cu-NOTA-Aoc-BBN(7-14)NH_2			
Tissue/Organ	1 h	4 h	24 h
Bladder	2.81(1.48)	0.47(0.74)	1.02(0.44)
Heart	0.36(0.16)	0.22(0.05)	0.31(0.14)
Lungs	0.82(0.28)	0.41(0.08)	0.35(0.16)
Liver	1.58(0.40)	1.22(0.12)	0.68(0.21)
Kidney	3.79(1.09)	0.96(0.20)	0.47(0.12)
Spleen	0.81(0.20)	0.44(0.14)	0.44(0.14)
Stomach	1.23(0.34)	0.49(0.22)	0.19(0.10)
S.Intestine	9.88(2.71)	1.63(0.56)	0.34(0.08)
L.Intestine	3.85(2.37)	9.93(3.36)	0.50(0.12)
Muscle	0.25(.09)	0.04(0.02)	0.12(0.06)
Bone	0.32(0.12)	0.15(0.14)	0.42(0.31)
Brain	0.05(0.02)	0.03(0.01)	0.07(0.01)
Pancreas	26.89(7.22)	7.46(1.06)	1.88(0.29)
Tumor	3.59(0.73)	1.64(0.15)	1.01(0.20)
Blood	0.59(0.19)	0.17(0.09)	0.09(0.05)

*All data presented as %ID/g(SD), except excretion data (%ID(SD)). (n=5).

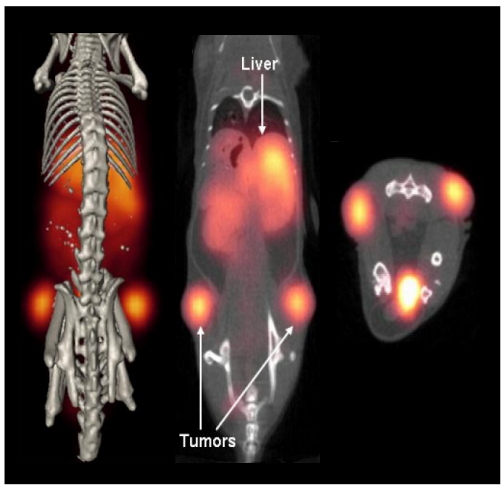

Figure 4.5: MicroPET/CT, MicroPET, and microPET/CT axial cross section image of [^{64}Cu-NOTA-(8-Aoc)-BBN(7-14)NH_2]. Images were performed in PC-3 tumor bearing SCID mice at 24 h p.i. [2]

^{64}Cu-NOTA complex produced a highly-resolved microPET image. This was largely due to the improved tumor to organ ratios and fast blood clearance. In addition, the small uptake of reactivity in the liver at 1 h p.i. suggests little or no *in vivo* dissociation of ^{64}Cu. [2]

4.2 EXPERIMENTAL

4.2.1 Materials

Chemicals were purchased from Aldrich Chemical Company (St. Louis, MO) and American Chemical Society (ACS) certified solvents were purchased from Fisher Scientific (Pittsburg, PA). All were used without further purification.

4.2.2 1,4,7-Triazacyclononane 1,4,7-triacetic Acid

NOTA was synthesized as previously reported by Bevilacqua and co-workers. [6] In brief, α-chloroacetic acid and 1,4,7-triazacyclononane were reacted in a 3:1 ratio with stirring on ice, followed by refluxing for 12 h. The volume was reduced to half by roto-evaporation. The product was isolated by crystallization at pH 3 and characterized by ^{1}H and ^{13}C NMR, and ESI-MS.

4.2.3 [(X)-BBN(7-14)NH_2] Peptide Conjugates

[(X)-BBN(7-14)NH_2] conjugates were synthesized on a Liberty automatic microwave peptide synthesizer employing traditional F-moc chemistry, where X denotes the linker, PABA, β-Ala, 5-Ava, 6-Ahx, or 9-Anc (see Figure 4.6), and BBN(7-14)NH_2

denotes the amino acid sequence, Q-W-A-V-G-H-L-M-NH_2. Rink Amide MBHA resin (0.1 mmol) and F-moc-protected amino acids (0.2 mmol) were utilized for SPPS. A cocktail of 1,2-ethanedithiol (EDT), water, triisopropylsilane (TIS), and trifluoracetic acid (TFA) in a ratio of 2.5:2.5:1:94 was used to cleave the peptide from the resin, followed by peptide precipitation in methyl-t-butyl ether. Crude peptide conjugates were obtained in ~80% yield. The crude peptide-conjugates were purified by reversed-phase high performance liquid chromatography (RP-HPLC) and solvents were removed *in vacuo* using a SpeedVac concentrator (Labconco, Kansas City, MO). Matrix-assisted laser desorption/ionization time-of-flight mass spectrometry (MALDI TOF MS) was used to compare calculated to experimental molecular ion peaks. The calculated and experimental masses, in Daltons, for the [(X)-BBN(7-14)NH_2] conjugates were as follows: X = PABA (1059.5, 1059.5), X = β-Ala (1012.2, 1012.4), X = 5-Ava (1040.3, 1040.6), X = 6-Ahx (1056.6, 1053.5), and X = 9-Anc (1095.6, 1095.6).

Figure 4.6: Pharmacokinetic modifier structures of PABA, β-Ala, 5-Ava, 6-Ahx, 8-Aoc and 9-Anc.

4.2.4 [NO2A-X-BBN(7-14)NH_2] Peptide Conjugates

NOTA, 1,4,7-triazacyclononane-1,4,7-triacetic acid, was conjugated via an active ester to the peptide-conjugate to produce [NO2A-(X)-BBN(7-14)NH_2] conjugates. This method has been previously published by Prasanphanich, et al. [2] In brief, 2-[morpholino]ethanesulfonic acid (MES) buffer (pH 4.7), NOTA, Sulfo-NHS (*N*-

hydroxysulfosuccinimide), and EDC (1-Ethyl-3-[3-dimethylaminopropyl]carbodiimide hydrochloride) were stirred at room temperature. The desired peptide, dissolved in phosphate buffered solution (PBS), was then added to the active ester solution in MES buffer. The NO2A conjugate was isolated by RP-HPLC. Nanospray quadrupole time-of-flight mass spectrometry (QqTOF-MS) was used to confirm the identity of the conjugates. The calculated and experimental masses for the [NO2A-(X)-BBN(7-14)NH_2] conjugates were as follows: X = PABA (1344.7, 1344.7), X = β-Ala (1295.6, 1295.7), X = 5-Ava (1325.7, 1325.6), X = 6-Ahx (1338.7, 1338.8), and X = 9-Anc (1380.7, 1380.7).

4.2.5 [^{63}Cu-NO2A-X-BBN(7-14)NH_2] and [^{64}Cu-NO2A-X-BBN(7-14)NH_2]

The ^{63}Cu-NO2A-X-BBN(7-14)NH_2 complexes were synthesized by adding $^{63}CuCl_2$ (1 mg, 7.4 μmol) to a plastic tube containing purified peptide conjugate (100 μg, 74.3-86.7 nmol) and heated at 80ºC for 1 h. 1 M DTPA solution (25 μL, 25 μmol) was added to complex unbound copper. Metallated conjugates were purified by RP-HPLC. QqTOF MS was used to compare calculated to experimental molecular ion peaks. The calculated and experimental masses for the [^{63}Cu-NO2A-(X)-BBN(7-14)NH_2] conjugates were as follows: X = PABA (1404.6, 1404.6), X = β-Ala (1356.6, 1356.6), X = 5-Ava (1384.6, 1384.6), X = 6-Ahx (1398.6, 1398.6), and X = 9-Anc (1440.7, 1440.7). RP-HPLC fractions were collected into 1 mg/mL bovine serum albumin (BSA) stabilizing agent and ascorbic acid (25 μg) prior to *in vivo* evaluation.

$^{64}CuCl_2$ was obtained from either MDS Nordion (Vancouver, Canada), Trace Life Sciences (Denton, TX), or University of Wisconsin (Madison, WI). The [^{64}Cu-NO2A-(X)-BBN(7-14)NH_2] conjugates were synthesized by adding $^{64}CuCl_2$ (7 mCi) to a plastic

tube containing purified peptide conjugate (100 μg, 74.3-86.7 nmol) and heated at 80ºC for 1 h. 10 mM DTPA solution (50 μL, 0.5 nmol) was added to complex unbound radioactivity. Radiolabeled conjugates were then purified by RP-HPLC and collected into 1 mg/mL BSA stabilizing agent (100 μL) and ascorbic acid (25 μg) prior to *in vitro* and *in vivo* evaluation.

4.2.6 RP-HPLC Analyses of [(X)-BBN(7-14)NH_2], [NO2A-(X)-BBN(7-14)NH_2], [^{63}Cu-NO2A-(X)-BBN(7-14)NH_2], and [^{64}Cu-NO2A-(X)-BBN(7-14)NH_2] Conjugates

RP-HPLC analyses of radiolabeled and non-radiolabeled compounds were performed on a Shimadzu SCL-10A system equipped with a Shimadzu SPD-10A UV-Vis tunable absorbance detector (set at λ=280 nm), an Eppendorf TC-50 column heater, and a radiometric in-line EG&G ORTEC NaI solid scintillation detector. Purification of [(X)-BBN(7-14)NH_2] and [NO2A-(X)-BBN(7-14)NH_2] conjugates were performed on a semi-preparative reversed-phase C18 column (Phenomenex Jupiter Proteo, 250 x 10.00 mm, 10 μm). Purification of [^{64}Cu-NO2A-(X)-BBN(7-14)NH_2] was performed on an analytical reverse-phase C18 column (Phenomenex Jupiter Proteo, 250 x 4.60 mm, 5 μm). The solvent system used was H_2O/0.1% TFA (A) and CH_3CN/0.1% TFA (B). The gradient system began at 75% A and 25% B. From 0 to 15 minutes, the solvent increased linearly to 65% A and 35% B. From 15 to 17 minutes, the solvent increased to 5% A and 95% B. The flow rate was set at 5 mL/min for the semi-preparative and 1.5 mL/min for the analytical RP-HPLC.

4.2.7 MALDI TOF-MS and QqTOF-MS

MALDI TOF was performed by SynBioSci (Livermore, CA) and QqTOF-MS was performed by the Charles W. Gehrke Proteomics Center of the University of Missouri (Columbia, MO). MALDI TOF-MS was used to analyze the non-conjugated peptides. QqTOF-MS was used to analyze the non-metallated and metallated peptide conjugates.

4.2.8 *In Vitro* Analysis of [^{64}Cu-NO2A-X-BBN(7-14)NH_2]

4.2.8.1 Stability Study in Human Serum Albumin

Radiolabeled peptide conjugates were synthesized as previously mentioned above. Upon RP-HPLC purification, the [^{64}Cu-NO2A-(X)-BBN(7-14)NH_2] conjugates were collected in human serum albumin (HSA) stabilizing agent (500 μL) and ascorbic acid (25 μg). Acetonitrile was removed under a steady stream of nitrogen. The conjugates' stability was assessed by analytical RP-HPLC after 0, 2, 6, and 24 h incubation periods at 37ºC in a 5% carbon dioxide chamber.

4.2.8.2 Competitive Displacement Binding Assay

The IC_{50} of [NO2A-(X)-BBN(7-14)NH_2] was established by competitive displacement cell binding assays using radiolabeled [^{125}I-(Tyr^4)-BBN] as the radioligand. Briefly, $3x10^4$ cells (in D-MEM/F-12K media containing 0.01 M MEM and 2% BSA, pH=5.5) were incubated with 20,000 counts per minute of [^{125}I-(Tyr^4)-BBN] ($8.2x10^{-15}$ mol, $8.14x10^4$ GBq/mmol ($2.20x10^3$ Ci/mmol)) at 37ºC. Non-radiolabeled peptide

conjugate was added at a steadily increasing concentration and allowed to incubate for an additional minute at 37ºC. The solution was aspirated, and the cells were rinsed with cold media. Cell-associated radioactivity was determined using a Packard Riastar gamma counter. The K_i value was calculated by using the Cheng-Prusoff equation. [17]

4.2.8.3 Internalization and Externalization Assay

The internalization studies were conducted by incubating $3x10^4$ cells (in D-MEM/F-12K media containing 0.01 M MEM and 2% BSA, pH=5.5) in the presence of 20,000 counts per minute of [^{64}Cu-NO2A-(X)-BBN(7-14)NH_2] ($3.45x10^{-17}$ mol, $1.94x10^7$ GBq/mmol ($5.23x10^5$ Ci/mmol) at 37ºC. At 10, 20, 30, 45, 60, 90, and 120 min post-incubation, the cells were aspirated, washed (0.2 N acetic acid/0.5 M NaCl (pH = 2.5)), and counted on a Packard Riastar gamma counter. The externalization studies were completed after an initial 40 min internalization period. The cells were washed at RT, resuspended in media, and incubated a second time. At 0, 20, 40, 60, 90, 120, and 150 min post-incubation, the cells were washed with media and acetic acid/saline (pH=2.5 at 4ºC) and counted on a Packard Riastar gamma counter.

4.2.9 *In Vivo* Analysis of [^{64}Cu-NO2A-X-BBN(7-14)NH_2]

The pharmacokinetics of the [^{64}Cu-NO2A-(X)-BBN(7-14)NH_2] conjugates were determined in normal CF-1 and tumor-bearing PC-3 SCID mouse models (n=5). All animal studies were conducted in accordance with the highest standards of care as outlined in the NIH guide for Care and Use of Laboratory Animals and the Policy and Procedures for Animal Research at the Harry S. Truman Memorial Veterans' Hospital.

For studies involving tumor-bearing mice, four to five-week old female ICR SCID outbred mice were obtained from Taconic (Germantown, NY). The mice were housed five animals per cage in sterile micro isolator cages in a temperature- and humidity-controlled room with a 12 h light/12 h dark schedule. The animals were fed autoclaved rodent chow (Ralston Purina Company, St. Louis, MO) and water *ad libitum*. Animals were anesthetized for injections with isoflurane (Baxter Healthcare Corp., Deerfield, IL) at a rate of 2.5% with 0.4 L oxygen through a non-rebreathing anesthesia vaporizer. Human prostate PC-3 cells were injected on the bilateral subcutaneous flank with $5x10^6$ cells in a suspension of 100 μL normal sterile saline per injection site. PC-3 cells were allowed to grow two to three weeks post inoculation, developing tumors ranging in mass from 0.02-0.65 grams. For the biodistribution studies, the mice were injected *via* the tail vein with 40-240 kBq (1.1-6.5 μCi) of conjugate in 100 μL of isotonic saline. Mice were euthanized at specific time-points. Tissues, organs, and urine were excised, weighed, and counted in a NaI well counter. The percent injected dose (% ID) and the percent injected dose per gram (% ID/g) were calculated. The whole blood volume was assumed to be 6.5 % of the total body weight, allowing for the % ID in whole blood to be determined. For imaging studies, the mice were injected *via* the tail vein with 111-185 kBq (3-5 mCi) of conjugate in 100 μL of isotonic saline.

4.3 RESULTS AND DISCUSSION

The [NO2A-(X)-BBN(7-14)NH_2] and [^{63}Cu-NO2A-(X)-BBN(7-14)NH_2] conjugates were fully characterized by RP-HPLC and mass spectrometry (Table 4.4). The preparation of [^{64}Cu-NO2A-(X)-BBN(7-14)NH_2] conjugates were performed as

Table 4.4: [NO2A-(X)-BBN(7-14)NH_2] and [^{63}Cu-NO2A-(X)-BBN(7-14)NH_2] characterization by RP-HPLC (min) and ESI-mass spectrometry (Da).

Spacer Group (X)	**β-Ala**	**5-Ava**	**6-Ahx**	**8-Aoc**	**9-Anc**	**PABA**
Calculated MW	1295.6	1325.7	1338.7	1366.7	1380.7	1344.7
ESI-MS MW	1295.7	1325.6	1338.8	1366.7	1380.7	1344.7
Calculated MW (Cu)	1356.6	1384.6	1398.6	1426.6	1440.7	1404.6
ESI-MS MW (Cu)	1356.6	1384.6	1398.6	1426.7	1440.7	1404.6
Formula	$C_{58}H_{89}N_{17}O_{15}S$	$C_{60}H_{93}N_{17}O_{15}S$	$C_{61}H_{95}N_{17}O_{15}S$	$C_{63}H_{99}N_{17}O_{15}S$	$C_{64}H_{101}N_{17}O_{15}S$	$C_{62}H_{89}N_{17}O_{15}S$
Formula (Cu)	$C_{58}H_{87}CuN_{17}O_{15}S$	$C_{60}H_{91}CuN_{17}O_{15}S$	$C_{61}H_{93}CuN_{17}O_{15}S$	$C_{63}H_{97}CuN_{17}O_{15}S$	$C_{64}H_{99}CuN_{17}O_{15}S$	$C_{62}H_{87}CuN_{17}O_{15}S$
HPLC t_R	6.6	5.7	6.2	9.6	11.2	7.3
HPLC t_R (^{64}Cu)	5.6	5.8	5.9	8.9	10.3	6.3

previously reported. The [^{64}Cu-NO2A-(X)-BBN(7-14)NH_2] conjugates were characterized by radiometric RP-HPLC retention time, and were obtained in >90 % yield. Stability studies were performed with [^{64}Cu-NO2A-(X)-BBN(7-14)NH_2] conjugates in HSA over 24 h. Stability was determined by the quantification of the [^{64}Cu-NO2A-(X)-BBN(7-14)NH_2] radiometric RP-HPLC peak area. Conjugates were >80% stable for up to 24 h.

Binding assays were performed with [Cu-NO2A-(X)-BBN(7-14)NH_2] and [^{63}Cu-NO2A-(X)-BBN(7-14)NH_2] in PC-3 cells bearing GRP receptors to determine the binding affinity. The K_i values for the [NO2A-(X)-BBN(7-14)NH_2] conjugates with aliphatic spacers ranged from 1.99±0.17 to 6.24±0.67 nm, with a slight trend of decreasing K_i value with increasing spacer length. The K_i value for [NO2A-PABA-BBN(7-14)NH_2] was 4.61±1.54 nm. The K_i values for the [^{63}Cu-NO2A-(X)-BBN(7-14)NH_2] conjugates with aliphatic spacers varied slightly from their counterparts, with values ranging from 4.10±2.14 to 6.98±1.99 nm. No trend between K_i and increasing spacer length was observed for these conjugates. The K_i value for [^{63}Cu-NO2A-PABA-BBN(7-14)NH_2] varied from that of the non-metallated conjugate, with a K_i value of 15.45±2.88 nm. (See Table 4.5.)

Table 4.5: Inhibitory concentration 50% (IC_{50}) in vitro cell assays in PC-3 cells.

	NO2A-X-BBN(7-14)NH_2	^{63}Cu-NO2A-X-BBN(7-14)NH_2
X=β-Ala	6.24±0.67	6.53±2.47
X=5-Ava	2.74±0.17	5.43±0.96
X=6-Ahx	2.85±0.15	6.98±1.99
X=8-Aoc	1.99±0.25	4.10±2.14
X=9-Anc	1.99±0.17	6.75±1.70
X=PABA	4.61±1.54	15.45±2.88

Internalization and externalization of [^{64}Cu-NO2A-(X)-BBN(7-14)NH_2] conjugates were assayed in PC-3 cells. Although the [^{64}Cu-NO2A-(X)-BBN(7-14)NH_2] conjugates showed slow internalization (ranging from 3.5 to 3.7% at 90 min post-incubation, a high retention of the conjugates was observed (ranging from 86 to 100% at 90 min).

Biodistribution study results for [^{64}Cu-NO2A-(X)-BBN(7-14)NH_2] conjugates in normal CF-1 mice are summarized in Table 4.6. The mice were sacrified at 1 h p.i., and the tissues and organs were excised and counted in a NaI well counter. Rapid clearance from the blood was observed for all conjugates, ranging from 0.17±0.05 to 0.29±0.09 % ID/g at 1 h p.i. Excretion of the PABA conjugate varied significantly from the aliphatic conjugates. The more hydrophilic PABA conjugate emptied primarily via the renal-urinary excretion system, while the aliphatic conjugates were excreted by both the renal-urinary system and the hepatobiliary system. Liver uptake increased linearly with increasing spacer length, with values of 1.29±0.20% ID/g for X = β-Ala, 1.33±0.37% ID/g for X = 5-Ava, 1.24±0.19% ID/g for X=6-Ahx, 1.54±0.59% ID/g for 8-Aoc, and 2.35±0.50% ID/g 9-Anc. The PABA conjugate exhibited a much lower liver accumulation, with only 0.70±0.08% ID/g remaining at 1 h p.i. Specific targeting of the GRP receptors was observed for all conjugates, with pancreas uptake increasing linearly with increasing aliphatic spacer length, with 15.10±1.93% ID/g for X = β-Ala, 11.33±2.32% ID/g for X = 5-Ava, 26.87±5.01% ID/g for X=6-Ahx, 26.95±3.18% ID/g for X=8-Aoc and 22.80±2.96% ID/g for X=9-Anc. The pancreas uptake for the X=PABA conjugate was 30.63±3.26% ID/g.

Four conjugates were further investigated in SCID mice bearing xenografted, human, PC-3 tumors at 1, 4 and 24 h p.i. The conjugates chosen were X = 6-Ahx, 8-Aoc, 9-Anc, and PABA. Results are summarized in Table 4.7 and 4.8. Clearance from blood was slower than that observed in the CF-1 mice. At 1 h p.i., blood retention ranged from 0.69±0.17 to 0.93±0.41% ID/g. At 24 h p.i., blood retention ranged from 0.12±0.02 to 0.23±0.35% ID/g. Specific targeting of the GRP receptors was observed for all conjugates. Receptor-mediated pancreatic uptake at 24 h p.i. was 2.19±0.32% ID/g for X=6-Ahx, 1.88±0.29% ID/g for X=8-Aoc, 1.20±0.15% ID/g for X=9-Anc and 8.93±1.81% ID/g for X=PABA. The average tumor uptake at 24 h p.i. for the [^{64}Cu-NO2A-(X)-BBN(7-14)NH_2] conjugates was 1.14±0.53% ID/g for X=6-Ahx, 1.01±0.20% ID/g for X=8-Aoc, 0.62±0.09% ID/g for X=9-Anc and 2.54±0.63% ID/g for X=PABA.

High-quality, high-contrast microPET/CT images were obtained in SCID mice bearing xenografted, human, PC-3 tumor at 18 h p.i. (See Figure 4.7.) The microPET/CT images showed that the PABA conjugate had superior tumor targeting and retention. The 6-Ahx and 8-Aoc conjugates also showed significant tumor uptake. The 9-Anc conjugate showed lower tumor and higher liver uptake when compared to that of the 6-Ahx and 8-Aoc conjugates.

Table 4.6: [^{64}Cu-NO2A-(X)-BBN(7-14)NH_2] biodistribution results in CF-1 normal mice at 1 h p.i.

	β-ala	5-Ava	6-Ahx	8-Aoc	9-Anc	PABA
Bladder	2.02±2.52	1.13±0.46	3.25±6.20	0.96±0.42	0.40±0.29	1.35±1.19
Heart	0.18±0.13	0.13±0.06	0.20±0.18	0.30±0.05	0.40±0.16	0.13±0.07
Lung	0.47±0.06	0.35±0.08	0.58±0.18	0.62±0.11	0.97±0.21	0.26±0.08
Liver	1.29±0.20	1.33±0.37	1.24±0.19	1.54±0.59	2.35±0.50	0.70±0.08
Kidneys	2.86±0.99	2.24±0.69	2.64±0.41	2.92±0.64	2.35±0.24	3.80±1.11
Spleen	0.71±0.12	0.45±0.21	1.11±0.46	1.15±0.14	0.86±0.28	1.44±0.27
Stomach	0.95±0.53	2.54±3.64	1.010±0.10	1.43±0.57	0.90±0.35	2.82±2.67
S. Intestine	5.85±0.68	5.07±1.74	8.41±1.26	10.83±1.10	15.52±4.23	8.01±2.04
L. Intestine	2.43±0.85	1.75±0.24	3.27±0.68	2.14±0.35	5.70±7.28	5.75±1.44
Muscle	0.05±0.07	0.07±0.06	0.11±0.11	0.12±0.02	0.16±0.09	0.09±0.06
Bone	0.22±0.18	0.10±0.08	0.41±0.37	0.38±0.07	0.48±0.24	0.28±0.25
Brain	0.03±0.02	0.01±0.01	0.03±0.02	0.037±0.01	0.05±0.03	0.03±0.02
Pancreas	15.10±1.93	11.33±2.32	26.87±5.02	26.95±3.18	22.80±2.96	30.63±3.26
Blood	0.29±0.19	0.18±0.04	0.17±0.05	0.29±0.09	0.28±0.11	0.19±0.03

Table 4.7: [^{64}Cu-NO2A-(X)-BBN(7-14)NH_2] biodistribution results in PC-3 tumor-bearing SCID mice at 1, 4 and 24h p.i., where X = 6-Ahx or 8-Aoc*. * = [2]

	6-Ahx				8-Aoc		
	1h	4h	24h		1h	4h	24h
Bladder	1.47±0.82	0.38±0.30	0.59±0.80		2.81±1.48	0.47±0.74	1.02±0.44
Heart	0.50±0.11	0.36±0.18	0.40±0.16		0.36±0.16	0.22±0.05	0.31±0.14
Lung	0.94±0.22	0.71±0.14	0.75±0.14		0.82±0.28	0.41±0.08	0.35±0.16
Liver	2.49±0.72	2.04±0.27	1.29±0.08		1.58±0.40	1.22±0.12	0.68±0.21
Kidneys	4.52±0.41	1.59±0.15	1.20±0.33		3.79±1.09	0.96±0.20	0.47±0.12
Spleen	2.15±1.09	1.98±0.53	0.64±0.39		0.81±0.20	0.44±0.14	0.44±0.14
Stomach	1.21±0.21	0.82±0.31	0.34±0.09		1.23±0.34	0.49±0.22	0.19±0.10
S. Intestine	6.62±0.67	1.94±0.35	0.64±0.13		9.88±2.71	1.63±0.56	0.34±0.08
L. Intestine	2.26±0.32	8.69±1.61	1.10±0.18		3.85±2.37	9.93±3.36	0.50±0.12
Muscle	0.12±0.05	0.05±0.06	0.11±0.09		0.25±0.09	0.04±0.02	0.12±0.06
Bone	0.41±0.22	0.26±0.21	0.18±0.19		0.32±0.12	0.15±0.14	0.42±0.31
Brain	0.06±0.04	0.03±0.02	0.05±0.03		0.05±0.02	0.03±0.01	0.07±0.01
Pancreas	13.59±1.81	9.06±0.91	2.19±0.32		26.89±7.22	7.46±1.06	1.88±0.29
Tumor #1	2.60±0.59	1.80±0.44	1.10±0.54		3.68±0.75	1.69±0.24	0.99±0.25
Tumor #2	2.83±0.59	1.98±0.17	1.18±0.51		3.49±0.71	1.59±0.05	1.02±0.14
Blood	0.71±0.09	0.27±0.04	0.08±0.04		0.59±0.19	0.17±0.09	0.09±0.05
Carcass	0.45±0.07	0.16±0.03	0.12±0.01		0.51±0.09	0.14±0.01	0.06±0.02
Feces			7.06±3.04				6.36±2.01

Table 4.8: [^{64}Cu-NO2A-(X)-BBN(7-14)NH_2] biodistribution results in PC-3 tumor-bearing SCID mice at 1, 4 and 24h p.i., where X = 9-Anc or PABA.

	9-Anc				PABA		
	1h	4h	24h		1h	4h	24h
Bladder	2.49±2.00	0.52±0.60	0.64±0.59		5.30±7.16	0.25±0.17	0.19±0.15
Heart	0.51±0.16	0.26±0.19	0.06±0.02		0.48±0.26	0.18±0.09	0.24±0.15
Lung	1.10±0.24	0.46±0.25	0.35±0.17		0.87±0.29	0.35±0.09	0.51±0.14
Liver	2.47±0.57	1.78±0.54	1.37±0.52		1.22±0.17	1.00±0.11	1.23±0.25
Kidneys	6.77±1.76	1.66±0.92	0.77±0.27		6.58±3.85	1.11±0.25	0.91±0.20
Spleen	2.21±2.21	0.71±0.36	0.75±0.37		0.93±0.30	0.82±0.21	0.71±0.29
Stomach	1.52±0.45	0.79±0.38	0.53±0.49		2.04±0.33	1.10±0.36	0.39±0.17
S. Intestine	20.40±6.15	6.61±8.34	0.65±0.47		8.46±1.33	2.93±0.50	1.01±0.14
L. Intestine	3.72±1.19	30.18±13.86	1.61±0.83		2.79±0.25	9.49±2.36	1.09±0.28
Muscle	0.25±0.10	0.06±0.04	0.08±0.09		0.27±0.12	0.05±0.03	0.05±0.04
Bone	0.57±0.31	0.18±0.14	0.24±0.25		0.43±0.15	0.15±0.08	0.06±0.07
Brain	0.06±0.03	0.02±0.01	0.05±0.04		0.07±0.01	0.03±0.01	0.03±0.02
Pancreas	20.76±4.24	4.03±1.07	1.20±0.15		37.34±4.83	22.50±3.13	8.93±1.81
Tumor #1	3.36±0.79	1.13±0.19	0.61±0.09		5.68±1.39	3.86±0.37	2.59±0.47
Tumor #2	4.10±1.67	0.85±0.32	0.63±0.10		6.42±0.91	3.46±0.71	2.49±0.79
Blood	0.69±0.17	0.38±0.25	0.14±0.07		0.93±0.41	0.11±0.02	0.12±0.02
Carcass	0.63±0.19	0.16±0.06	0.11±0.05		0.73±0.30	0.16±0.02	0.11±0.02
Feces			43.61±16.48				9.40±2.27

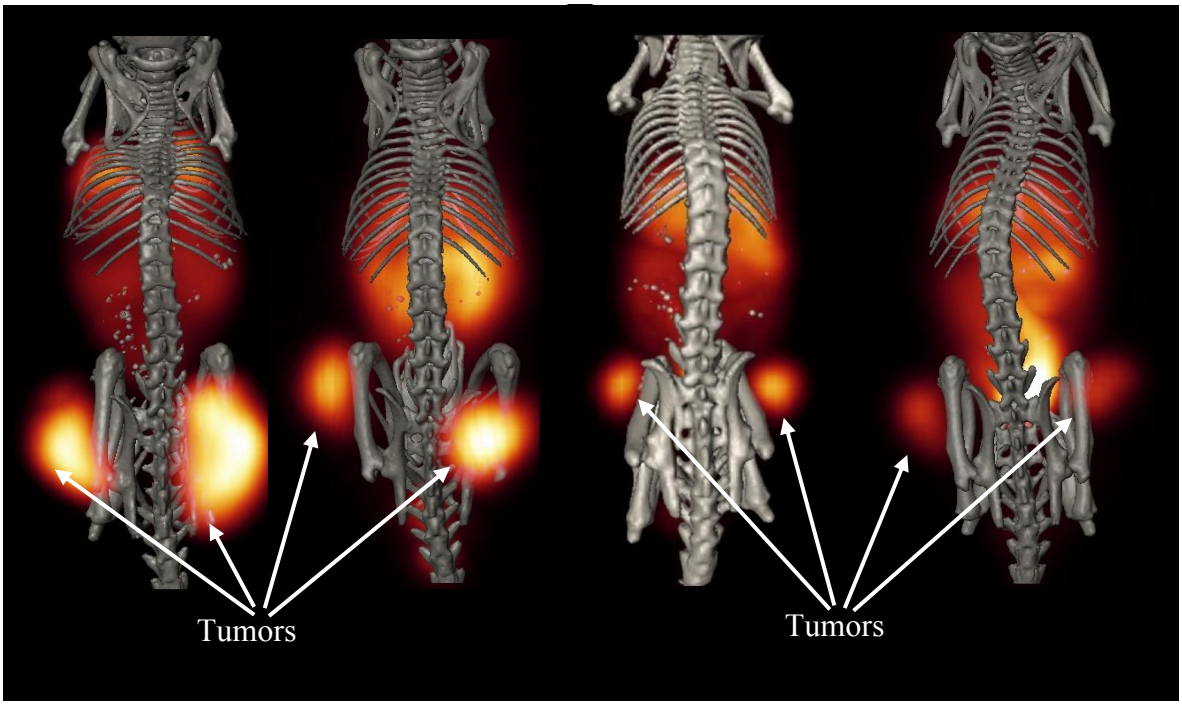

Figure 4.7: [^{64}Cu-NO2A-(X)-BBN(7-14)NH_2] maximum intensity microPET/CT coronal images of PC-3 tumor-bearing SCID mice at 18h p.i. Left to right, X = PABA, 6-Ahx, 8-Aoc*, and 9-Anc. * = [2].

4.4 CONCLUSION

The [^{64}Cu-NO2A-(X)-BBN(7-14)NH_2] results obtained from this study agree with previously published results that the copper metal center was effectively stabilized under *in vivo* conditions using the NO2A chelator. [2] Our data clearly showed that the pharmacokinetic modifier affects the binding affinity and clearance properties of the radiolabeled peptide. Increasing the carbon-spacer length past eight carbons does not show to be beneficial, as tumor uptake begins to decrease and liver uptake increases. The copper-64 microPET/CT image obtained from the [^{64}Cu-NO2A-(PABA)-BBN(7-14)NH_2] conjugate is far superior to any other previously published image. Future studies with the PABA conjugate are necessary to determine its worth as a PET imaging agent for GRP receptor-positive tumors.

4.5 FUTURE STUDIES

4.5.1 Toxicity Studies

Future studies include toxicology studies of [^{64}Cu-NO2A-(PABA)-BBN(7-17)NH_2] in mice. This would involve a specific amount of drug to be administrated to mice over a time period of 2 to 6 weeks. The mice would be sacrificed at various times during the trial and the organs would be examined to determine the negative side-effects. Median lethal dose (LD_{50}) studies could also be performed to determine the radiolabelled conjugate dose required to kill half the mice in the test population. Due to current regulation on animal research, cell culture and computer modeling might be substituted for the use of mice. [19]

4.5.2 Investigate Stability of 5- vs. 6-coordinate NOTA Copper Analogs

Electrochemistry will be performed on both the 6-coordinate Cu-NOTA complex and a 5-coordinate Cu-NO2A analog to determine if there is a difference in the reduction potential of the metal center. This will assist in the determination of the overall stability of the metallated complex. The NO2A analog, 1.4-bis(carboxvmethvl)-7-methyl-1,4,7-triazacyclononane, will be synthesized similarly to previously reported procedures. [20] Labeling procedures will be similar to that of non-radioactive labeling of [NOTA-X-BBN(7-14)NH_2], except that the purified complex will not be collected in BSA. Electrochemistry studies will be performed by cyclic voltammetry, as previously reported. [21] In brief, studies will be performed under an argon atmosphere. A glassy carbon disk working electrode, platinum auxiliary electrode, and silver/silver chloride

reference electrode will be used. Samples of NOTA and the NOTA analogue will be run in 0.1 M aqueous sodium acetate with the pH adjusted to 7.0 with glacial acetic acid.

It is hypothesized that the Cu-NO2A complex will be easier to reduce due the availability of the open site on the metal center. This study will also determine if the reduction of the copper metal center in the Cu-NO2A analog is reversible. If this is found true, then an alternative chelate will be investigated for improved copper chelation.

4.5.3 Alternative NOTA Chelate

Alternative NOTA chelates could be used for copper chelation. One option is to use the NOTA derivative S-2-(4-Isothiocyanatobenzyl)-1,4,7-triazacyclononane-1,4,7-triacetic acid (p-SCN-Bn-NOTA). (See Figure 4.8.) This chelate is available from Macrocyclics. All carboxylic groups and amine donors would be available to bind to copper, while the functionalization off of the backbone would allow for peptide conjugation. No spacing moiety would be necessary as the backbone mimics PABA.

Figure 4.8: Structure of p-SCN-Bn-NOTA.

4.5.4 Alternative Spacers

The [^{64}Cu-NOTA-(PABA)-BBN(7-14)NH_2] conjugate showed the best tumor to tissue ratios out of all of the conjugates. At 1, 4 and 24 h p.i., the tumor to liver ratio was 5.0, 3.66 and 2.07 and tumor to kidney ratio was 0.92, 3.30 and 2.79. Modification to the

spacer might assist in producing complexes with more desirable pharmacokinetic properties. One possibility is use a PABA derivative containing a polyethylene glycol (PEG) chain. (See Figure 4.9.) The addition of the PEG spacer would increase the lipophilicity of the complex, which could possibly assist the complex's cellular internalization or hinder tumor imaging with higher liver accumulation and retention. Either way, the results from this change would not be known until tested.

Figure 4.9: Possible PABA analogs to consider for alternative studies.

4.6 REFERENCES

1. Wadas, T.J., et al., *Copper Chelation Chemistry and its Role in Copper Radiopharmaceuticals.* Current Pharmaceutical Design, 2007. **13**: p. 3-16.

2. Prasanphanich, A.F., et al., *[^{64}Cu-NOTA-8-Aoc-BBN(7-14)NH$_2$] targeting vector for positron-emission tomography imaging of gastrin-releasing peptide receptor-expressing tissues.* Proceedings of the National Academy of Sciences, 2007. **104**(30): p. 12462-12467.

3. Zompa, L.J., *Metal complexes of cyclic triamines. 2. Stability and electronic spectra of nickel(II), copper(II), and zinc(II) complexes containing nine- through twelve-membered cyclic triamine ligands.* Inorganic Chemistry, 2002. **17**(9): p. 2531-2536.

4. Cacheris, W.P., S.K. Nickle, and A.D. Sherry, *Thermodynamic study of lanthanide complexes of 1,4,7-triazacyclononane-N,N',N''-triacetic acid and 1,4,7,10-tetraazacyclododecane-N,N',N'',N'''-tetraacetic acid.* Inorganic Chemistry, 2002. **26**(6): p. 958-960.

5. Cortes, S., et al., *Potentiometry and NMR studies of 1,5,9-triazacyclododecane-N,N',N''-triacetic acid and its metal ion complexes.* Inorganic Chemistry, 2002. **29**(1): p. 5-9.

6. Bevilacqua, A., et al., *Equilibrium and thermodynamic study of the aqueous complexation of 1,4,7-triazacyclononane-N,N',N''-triacetic acid with protons, alkaline-earth-metal cations, and copper(II).* Inorganic Chemistry, 1987. **26**(16): p. 2699-2706.

7. Zompa, L.J., *Metal complexes of cyclic triamines. 2. Stability and electronic spectra of nickel(II), copper(II), and zinc(II) complexes containing nine- through twelve-membered cyclic triamine ligands.* Inorganic Chemistry, 1978. **17**(9): p. 2531-2536.

8. Garrison, J.C., et al., *In Vivo Evaluation and Small-Animal PET/CT of a Prostate Cancer Mouse Model Using 64Cu Bombesin Analogs: Side-by-Side Comparison of the CB-TE2A and DOTA Chelation Systems.* J Nucl Med, 2007. **48**(8): p. 1327-1337.

9. Jones-Wilson, T.M., et al., *The in vivo behavior of copper-64-labeled azamacrocyclic complexes.* Nuclear Medicine and Biology, 1998. **25**(6): p. 523-530.

10. Bass, L.A., et al., *In Vivo Transchelation of Copper-64 from TETA-Octreotide to Superoxide Dismutase in Rat Liver.* Bioconjugate Chemistry, 2000. **11**(4): p. 527-532.

11. Weisman, G.R., et al., *Cross-bridged cyclam. Protonation and lithium cation (Li^+) complexation in a diamond-lattice cleft.* Journal of the American Chemical Society, 1990. **112**(23): p. 8604-8605.

12. Weisman, G.R., et al., *Synthesis and Transition-Metal Complexes of New Cross-Bridged Tetraamine Ligands.* Chemical Communications, 1996(8): p. 947-948.

13. Boswell, C.A., et al., *Comparative in Vivo Stability of Copper-64-Labeled Cross-Bridged and Conventional Tetraazamacrocyclic Complexes.* Journal of Medicinal Chemistry, 2004. **47**(6): p. 1465-1474.

14. Sun, X., et al., *Radiolabeling and In Vivo Behavior of Copper-64-Labeled Cross-Bridged Cyclam Ligands.* Journal of Medicinal Chemistry, 2002. **45**(2): p. 469-477.

15. Wieghardt, K., et al., *1,4,7-Triazacyclononane-N,N',N''-triacetate (TCTA), a new hexadentate ligand for divalent and trivalent metal ions. Crystal structures of $[Cr^{III}(TCTA)]$, $[Fe^{III}(TCTA)]$, and $Na[Cu^{II}(TCTA)]\bullet 2Na\bullet 8H_2O$.* Inorganic Chemistry, 1982. **21**(12): p. 4308-4314.

16. Vab der Merwe, M.J., J.C.A. Boeyens, and R.D. Hancock, *Optimum ligand hole sizes for stabilizing nickel(III). Structure of the nickel(III) complex of 1,4,7-triazacyclononane-N,N',N''-triacetate.* Inorganic Chemistry, 1983. **22**(24): p. 3489-3490.

17. Yung-Chi, C. and W.H. Prusoff, *Relationship between the inhibition constant (KI) and the concentration of inhibitor which causes 50 per cent inhibition (I_{50}) of an enzymatic reaction.* Biochemical Pharmacology, 1973. **22**(23): p. 3099-3108.

18. Hoffman, T.J., et al., *Novel Series of ^{111}In-Labeled Bombesin Analogs as Potential Radiopharmaceuticals for Specific Targeting of Gastrin-Releasing Peptide Receptors Expressed on Human Prostate Cancer Cells.* J Nucl Med, 2003. **44**(http://jnm.snmjournals.org/cgi/content/abstract/44/5/823 May 1, 2003): p. 823-831.

19. Saha, G.B., *Quality Control of Radiopharmaceuticals*, in *Fundamentals of Nuclear Pharmacy*. 2004, Springer: New York. p. 173-174.

20. Storr, T., et al., *Novel Carbohydrate-Appended Metal Complexes for Potential Use in Molecular Imaging.* Chemistry - A European Journal, 2005. **11**(1): p. 195-203.

21. Benny, P.D., et al., *Reactivity of Rhenium(V) Oxo Schiff Base Complexes with Phosphine Ligands: Rearrangement and Reduction Reactions.* Inorganic Chemistry, 2005. **44**(7): p. 2381-2390.

22. Schweinsberg, C., et al., *Novel Glycated [^{99m}Tc(CO)$_3$]-Labeled Bombesin Analogues for Improved Targeting of Gastrin-Releasing Peptide Receptor-Positive Tumors.* Bioconjugate Chemistry, 2008. **19**(12): p. 2432-2439.

23. Cescato, R., et al., *Bombesin Receptor Antagonists May Be Preferable to Agonists for Tumor Targeting.* J Nucl Med, 2008. **49**(2): p. 318-326.

24. Reubi, J.C. and H.R. Maecke, *Peptide-Based Probes for Cancer Imaging.* J Nucl Med, 2008. **49**(11): p. 1735-1738.

CHAPTER 5: BISMUTH CHX-A´´ BOMBESIN CONJUGATES AS PRECURSOR TOWARDS THERAPEUTIC AGENTS

5.1 INTRODUCTION

5.1.1 Radiotherapy

Radiotherapy can be used to treat cancer in a variety of ways. It can be utilized as the sole treatment of cancer, a method to reduce the size of cancer before surgery, a method to treat the local spread of cancer, or as a method to slow down tumor growth to relieve pain. Therapeutic radiopharmaceuticals contain an α- or β-emitting radionuclide. Upon decay of the radionuclide, the particles will result in ionization of cellular DNA. It is the ill repair of the DNA that leads to cell death. Currently, most radiotherapeutic agents utilize β-particle emission due to the β-particle's ability to penetrate tissue. [1] An example of a high-energy β-emitting radiopharmaceutical commonly used in radiotherapy is ^{90}Y-ibritumomab Tiuxetan (Zevalin®). [2] This radiopharmaceutical consists of a murine monoclonal anti-CD20 antibody linked to DTPA, which effectively complexes Y-90 ($t_{½}$ = 64 h; β_{max} = 2.27 MeV; $range_{mean}$ = 2.76 mm). [1-2] The high-energy β-particles can travel several millimeters in tissue and result in a homogeneous dose to the surrounding tissue. An example of an intermediate-energy β-emitting radiopharmaceutical commonly used in radiotherapy is ^{131}I-tositumomab (Bexxar®). [2] This radiopharmaceutical consists of a murine monoclonal anti-CD20 antibody linked to DTPA, which effectively complexes I-131 ($t_{½}$ = 193 h; β_{max} = 0.61 MeV; $range_{mean}$ = 0.4 mm). [1-2] The intermediate-energy β-particles deposit their energy over a shorter path

length (a few cell diameters), which can reduce the radiation burden on surrounding healthy tissue. Both Zevalin® and Bexxar® are FDA approved to treat non-Hodgkin's lymphoma. [2] Alpha-emitting radionuclides have not played a large role in radiotherapeutic agents, but interest in their potential use has risen over the last 10 years. Examples of α-emitters currently being pursued for use in radiotherapy include Bi-213 ($t_{½}$ = 0.78 h; α_{max} = 5.8 MeV; $Range_{mean}$ = 0.06 mm) and At-211 ($t_{½}$ = 7.2 h; α_{max} = 5.9 MeV; $Range_{mean}$ = 0.06 mm). When comparing linear energy transfer (LET) of β-particle emitters and α-particle emitters, the high LET α-particle results in higher tumor-specific cell killing and lower irradiation to surrounding healthy tissue than the low LET β-particle. [1] High energy α-particles (4-9 MeV) are of particular interest since they deposit large amounts of energy over a short distance of 40-100 μm in tissue. It is estimated that it takes only 3-6 alpha particles (of energy 4-9 MeV) to effectively kill a cell due to its dense track of ionizing radiation. [3]

Peptide-based radiotherapy has become of recent interest as it has advantages over antibody-based radiotherapy. When comparing peptides to antibodies, peptide-based radiopharmaceuticals result in faster blood clearance, which can lead to reduced bone marrow toxicity, better tissue diffusion and higher tumor uptake. Ease of synthesis and the potential to optimize the peptide's affinity are also advantages over antibodies, since peptides are more tolerant of harsh radiolabeling conditions such as temperature and pH. [4-5]

5.1.2 Bismuth Chemistry

Although bismuth is a p-block element in the periodic table, its properties are associated with metallic and metalloid behavior. This is due to its low electronegativity on the Pauling scale (2.02) and its low ionization energies (i.e., first ionization energy is 703.2 kJ/mol). [6] Therefore, bismuth forms stable complexes with amine and carboxylate ligands. Bismuth is most stable in the +3 oxidation state and prefers to be eight-coordinate.

5.1.3 Specific Aims

As mentioned earlier, an active area of cancer research is in the synthesis of radiolabeled peptides for *in vivo* tumor imaging and therapy. These agents specifically target tumor cells by their high specificities for receptors on the cells' surface. One method used to radiolabel peptides is known as the bifunctional chelate approach (BFCA). This approach utilizes a chelate to stabilize the radiometal and minimize the chance of transchelation or oxidation. The BFCA is one approach that can be utilized in

Figure 5.1: Chemical structure of CHX-A′′ and maleimido- CHX-A′′.

prostate cancer imaging since the cancer over-expresses gastrin-releasing peptide (GRP) receptors. Bombesin (BBN) has high affinity and specificity to the GRP receptors. [7-8] When BBN is radiolabeled with ^{205}Bi, non-invasive prostate tumor images can be obtained.

The work described herein was performed at the National Cancer Institute (Bethesda, MD) in collaboration with Dr. Martin Brechbiel. The proposed study was focused on complexing bismuth-213 with the maleimido derivative of the bifunctional macrocyclic amine chelate CHX-A´´ (see Figure 1), which was linked to the bombesin peptide, BBN(7-14)NH_2, *via* a spacing moiety. A novel [CHX-A´´-(X)-BBN(7-14)NH_2] conjugate was synthesized, where X = 8-Aoc. The tethering moiety was chosen due to previous reports showing favorable pharmacokinetics. The [CHX-A´´-(8-Aoc)-BBN(7-14)NH_2] conjugate was labeled with $^{205}BiI_3$, a surrogate for $^{213}BiI_3$. RP-HPLC separation techniques were investigated. The pharmacokinetics of the [^{205}Bi-CHX-A´´-(8-Aoc)-BBN(7-14)NH_2] conjugate was investigated in nude mice at 0.5, 1, 4, 8 and 24 h post-tail vein injection.

5.1.4 Previous Studies

The bifunctional chelates that have been explored for stable coordination of Bi(III) are typically based on acyclic and macrocyclic polyaminocarboxylate chelates. Examples include ethylenediamine tetraacetic acid (EDTA), diethylenetriamine pentaacetic acid (DTPA) and 1,4,7,10-tetraazacyclododecane-*N*,*N*´,*N*´´,*N*´´´-tetraacetic acid (DOTA). (See Figure 2.) Stability constants for the acyclic complexes are as follows: Bi-EDTA (27.8) and Bi-DTPA (35.6). [9] The Bi(III) metal center prefers to be

8-coordinate over 6-coordinate. [9] The stability constant for the 8-coordinate Bi-DOTA complex is 30.3, which is lower than that for the DTPA complex. [10] Even though the macrocyclic effect can improve metal complex stability, a decrease was observed due to the stereochemical constraints of the rigid DOTA chelate. Other limitations with the DOTA chelate include its slow complexation of the metal. This is a major issue when working with a radionuclide that has a half-life of ≤60 minutes. [9] Therefore, non-macrocyclic bifunctional chelates were pursued. Brechbiel and co-workers have investigated DTPA derivates, and one has particular interest due to its improved bismuth complexation and stability. This DTPA derivative is *N*-[(*R*)-2-amino-3-(*p*-aminophenyl)propyl]-*trans*-(*S*,*S*)-cyclohexane-1,2-diamine-N,N,N′,N′′,N′′′-pentaacetic acid) (CHX-A′′). (See Figure 2.) The C-4 methyl substituent on the backbone of the CHX-A′′ sterically hinders metal transchelation, while the *trans*-cyclohexyl moiety on the CHX-A′′ backbone increases steric rigidity, improving the orientation of the chelating groups. [11] In 2002, clinical trials were performed with ^{213}Bi-CHX-A′′ conjugated to HuM195, a humanized anti-CD33 monoclonal antibody. This was the first clinical antibody trial containing an α-emitting radionuclide. [9]

Figure 5.2: Chemical structure of EDTA, DTPA and DOTA.

5.2 EXPERIMENTAL

5.2.1 Materials

Chemicals were purchased from Aldrich Chemical Company (St. Louis, MO) and American Chemical Society (ACS) certified solvents were purchased from Fisher Scientific (Pittsburg, PA). All were used without further purification. The CHX-A´´ chelate was obtained from Dr. Martin Brechbiel at the National Cancer Institute (Bethesda, MD). Bi-205 was obtained from cyclotron production at the PET Department, Clinical Center, at the NIH (Bethesda, MD).

5.2.2 Synthesis of [(8-Aoc)-BBN(7-14)NH_2]

The [(8-Aoc)-BBN(7-14)NH_2] conjugate was synthesized on a Liberty automatic microwave peptide synthesizer employing traditional F-moc chemistry, where BBN(7-14)NH_2 denotes the amino acid sequence, Q-W-A-V-G-H-L-M-NH_2. Rink Amide MBHA resin (0.1 mmol) and F-moc-protected amino acids (0.2 mmol) were utilized for SPPS. A cocktail of 1,2-ethanedithiol (EDT), water, triisopropylsilane (TIS), and trifluoracetic acid (TFA) in a ratio of 2.5:2.5:1:94 was used to cleave the peptide from the resin, followed by peptide precipitation in methyl-t-butyl ether. The crude peptide conjugate was obtained in ~80% yield. The crude peptide-conjugate was purified by reversed-phase high performance liquid chromatography (RP-HPLC). The solvent system used was H_2O/0.1% TFA (A) and CH_3CN/0.1% TFA (B). The gradient system began at 75% A and 25% B. From 0 to 15 minutes, the solvent increased linearly to 65% A and 35% B. From 15 to 17 minutes, the solvent increased to 5% A and 95% B. The flow rate

was set at 5 mL/min for the semi-preparative and 1.5 mL/min for the analytical RP-HPLC. Solvents were removed *in vacuo* using a SpeedVac concentrator (Labconco, Kansas City, MO). Matrix-assisted laser desorption/ionization time-of-flight mass spectrometry (MALDI TOF MS) was used to compare calculated to experimental molecular ion peaks. The calculated and experimental mass for the [(8-Aoc)-BBN(7-14)NH_2] conjugate were 1081.6 Da and 1082.5 Da, respectively.

5.2.3 Synthesis of [CHX-A´´-(8-Aoc)-BBN(7-14)NH_2]

CHX-A´´, *N*-[(*R*)-2-amino-3-(*p*-aminophenyl)propyl]-*trans*-(*S*,*S*)-cyclohexane-1,2-diamine-N,N,N´,N´´,N´´´-pentaacetic acid) was conjugated via an active maleimido group to the peptide-conjugate to produce the [CHX-A´´-(8-Aoc)-BBN(7-14)NH_2] conjugate. In a glass test tube, CHX-A´´ (57.5 mg, 55.1 μmol) was added to [(8-Aoc)-BBN(7-14)NH_2] (5.5 mg, 5.1 μmol) in a 11:1 molar ratio. After the addition of DMF (1 mL) to the test tube, the reaction mixture was stirred at room temperature for 6 h. The reaction mixture was then transferred to a 10 mL centrifuge tube. Cold ethyl ether (~7 mL) was added to the reaction mixture, which resulted in the crude product precipitating from solution. The solution was centrifuged for 5 min, after which the liquid was decanted from the solid. The process of the addition of ethyl ether followed by centrifugation and decantation was repeated two times. The crude residue was allowed to dry overnight on the bench. Once dry, the crude product was transferred to a glass test tube and dissolved in neat TFA (1 mL) to cleave the t-butyl protecting groups on the chelate. The solution was stirred for 30 min in an ice bath, followed by stirring at room temperature for 1 h. Peptide conjugate precipitation was performed by the addition of

cold methyl t-butyl ether. The solution was centrifuged for 5 min, after which the liquid was decanted from the solid. This process of the addition of ether followed by centrifugation and decantation was repeated two times. The crude residue was allowed to dry overnight on the bench. The crude peptide-conjugate was purified by RP-HPLC. The solvent system used was H_2O with 0.1% TFA (A) and CH_3CN with 0.1% TFA (B). The gradient system began at 100% A and 0% B. From 0 to 40 minutes, the solvent increased linearly to 55% A and 45% B. From 40 to 42 minutes, the solvent increased to 5% A and 95% B. The flow rate was set at 5 mL/min for the semi-preparative and 1.5 mL/min for the analytical RP-HPLC. Purified product was obtained in a 50% yield. Matrix-assisted laser desorption/ionization time-of-flight mass spectrometry (MALDI TOF MS) was used to compare calculated to experimental molecular ion peaks. The calculated and experimental mass for the [CHX-A´´-(8-Aoc)-BBN(7-14)NH_2] conjugate was 1742.87 Da and 1743.98 Da.

5.2.4 Production of a Bi-213 Generator

$^{225}AcCl_3$ was obtained from Oak Ridge Natl. Laboratories (Oak Ridge, TN). $^{225}AcCl_3$ (1.92 mCi) in 0.1 M HNO_3 was added to the cation exchange resin AGMP-50 resin (200-400 mesh, 1 mL) in a 50 mL glass vial. The resin solution was stirred for 45 min, after which the resin was transferred via pipette to a plastic column (5 x 2 cm). The column was then rinsed with 0.1 M HNO_3 (1 mL), followed by 1 M

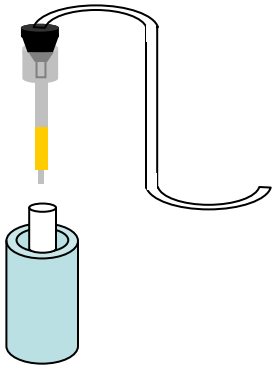

Figure 5.3: $^{225}Ac/^{213}Bi$ generator set-up.

HNO_3 (1 mL), 0.1 M HNO_3 (1 mL), and four times with 0.02 M HNO_3 (1 mL). Next, the slow addition of 0.2 M HNO_3 (3 mL) was performed via a syringe-tubing system to the column. (See Figure 3.) Addition of 0.1 M HI (0.5 mL) was then performed via a clean syringe using the syringe-tubing system. A clean tube was placed under the column. Three, 5 mL volumes of air were added to the column via the syringe-tubing system to remove all solvent from the column. A second, clean tube was placed under the column. The Bi-213 was eluted from the column by the addition of 0.1 M HI (1.5 mL). The generator yielded up to 925 MBq (25 mCi) of Bi-213 every 5 to 6 hours and can be eluted for up to 2 weeks.

5.2.5 Radiolabeling [CHX-A´´-(8-Aoc)-BBN(7-14)NH_2] with $^{205}BiI_3$

^{205}Bi was produced using a CS30 cyclotron (PET Department, Clinical Center, NIH). [^{205}Bi-CHX-A´´-(8-Aoc)-BBN(7-14)NH_2] was synthesized by adding $^{205}BiI_3$ (400 μCi) to a plastic tube containing 5 M NH_4OAc (60 μL), ascorbic acid (50 μL of 220 mg/mL water) and purified peptide conjugate (20 μg, 11.5 nmol). The pH of the solution was ~5.5. The reaction mixture was stirred at room temperature for 30 min. 0.1 M EDTA (4 mL, 400 nmol) was added to the solution to complex any unbound radioactivity. The radiolabeled conjugate was purified by RP-HPLC on a C-18 column (Phenomenex Jupiter Proteo, 90Å, 250 x 4.60 mm, 4 μm). Two RP-HPLC gradient systems were developed to effectively separate the radiolabeled and non-labeled peptide conjugate. Both gradient systems were composed of 10 mM ammonium acetate (A) and acetonitrile (B). The isocratic system was a steady flow of 25% B over 60 min. The second gradient second was a steady flow of 28% B over 30 min. (The RP-HPLC column used was a

Phenomenex, Jupiter 4μ Proteo, 90Å, 250 x 4.6 mm.) Purified RP-HPLC fractions were collected into 1 mg/mL bovine serum albumin (BSA) stabilizing agent and ascorbic acid (25 μg) prior to *in vivo* evaluation. The acetonitrile was removed by placing the collected fraction under a steady stream of argon for 10 min.

5.2.6 *In Vivo* Analysis of [^{205}Bi-CHX-A´´-(8-Aoc)-BBN(7-14)NH_2]

The pharmacokinetics of the [^{205}Bi-CHX-A´´-(8-Aoc)-BBN(7-14)NH_2] conjugate were determined in nude mouse models bearing PC-3 tumor (n=5). All animal studies were conducted in accordance with the highest standards of care as outlined in the NIH guide for Care and Use of Laboratory Animals. For the biodistribution studies, the mice were injected *via* the tail vein with 78.44-83.62 kBq (2.12-2.26 μCi) of conjugate in 100 μL of isotonic saline. Mice were euthanized at 0, 1, 4, 8, and 24 h time-points. Tissues, organs, and urine were excised, weighed, and counted in a γ-scintillation counter (1480 Wizard, Perkin-Elmer). The percent injected dose (% ID) and the percent injected dose per gram (% ID/g) were calculated. The whole blood volume was assumed to be 6.5 % of the total body weight, allowing for the % ID in whole blood.

5.3 RESULTS AND DISCUSSION

^{225}Ac/^{213}Bi generator production was performed as a learning experiment so that new skills and techniques could be obtained. I demonstrated efficient Bi-213 elution. This is a rare skill to learn as few facilities in the United States perform studies with this radionuclide.

[CHX-A′′-(8-Aoc)-BBN(7-14)NH_2] was synthesized in good yield and was characterized by RP-HPLC and HR-FAB MS. The [^{205}Bi-CHX-A′′-(8-Aoc)-BBN(7-14)NH_2] conjugate was characterized by radiometric RP-HPLC. Effective separation of the cold and radiolabelled conjugate was obtained, where the radiolabelled conjugate eluted at 18 min and the cold conjugate eluted at 19 min. (See Figure 4.) *In vivo* analysis of [^{205}Bi-CHX-A′′-(8-Aoc)-BBN(7-14)NH_2] was performed in normal nude mice. The mice were sacrificed at 0.5, 1, 4, 8 and 24 h p.i., and tissues and organs were excised and counted. The results of the biodistribution study in nude mice are summarized in Table 1. Rapid clearance from the blood was observed with only 0.022±0.005 % ID remaining at 24 h. Specific binding to the GRP receptors located in the mouse pancreas was not observed, and no trend in the pancreas uptake was observed. Pancreas uptake values were found to be 1.28±0.65, 0.96±0.28, 0.57±0.04, 1.09±0.35 and 0.59±0.09 at 0.5, 1, 4, 8 and 24 h p.i. However, a trend was observed with the kidneys. The kidneys had the highest % ID/g at all time points, but decreased over time. Kidney uptake values were 3.24±1.10, 3.26±0.58, 1.69±0.42, 1.42±0.28 and 0.83±0.17 % ID/g at 0.5, 1, 4, 8, and 24 h respectively.

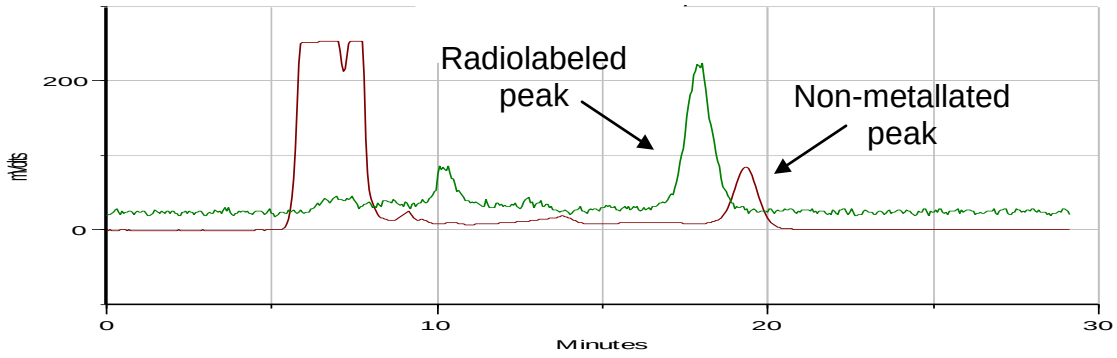

Figure 5.4: Radiometric RP-HPLC of [^{205}Bi-CHX-A′′-(8-Aoc)-BBN(7-14)NH_2] overlaid with UV RP-HPLC of [^{205}Bi-CHX-A′′-(8-Aoc)-BBN(7-14)NH_2].

Table 5.1: [^{205}Bi-CHX-A′′-(8-Aoc)-BBN(7-14)NH_2] biodistribution data at 0.5, 1, 4, 8 and 24 h p.i. (%ID/g (SD)).

	0.5h	1h	4h	8h	24h
Blood	0.55±0.42	0.22±0.11	0.045±0.01	0.05±0.01	0.02±0.005
Tumor	1.06±0.50	0.93±0.18	0.30±0.04	0.28±0.05	0.26±0.12
Liver	0.47±0.13	0.94±1.16	0.23±0.03	0.18±0.02	0.11±0.03
Spleen	1.45±1.01	1.24±0.51	0.55±0.30	0.59±0.19	0.31±0.08
Kidney	3.24±1.10	3.26±0.58	1.69±0.42	1.42±0.28	0.83±0.17
Lung	0.63±0.30	0.36±0.09	0.13±0.02	0.15±0.02	0.08±0.01
Heart	0.38±0.12	0.26±0.05	0.16±0.07	0.21±0.02	0.10±0.02
Femur	0.71±0.20	0.62±0.14	0.33±0.09	0.48±0.12	0.26±0.06
Pancreas	1.28±0.65	0.96±0.28	0.57±0.04	1.09±0.35	0.59±0.09
Tail	1.47±0.39	1.47±0.52	0.20±0.08	0.22±0.05	0.10±0.03

5.4 CONCLUSION

The [^{205}Bi-CHX-A′′-(8-Aoc)-BBN(7-14)NH_2] conjugate was investigated for its potential in delivering alpha radiation to GRP receptor-positive cancer tissue. Previous studies have shown that the BBN(7-14)NH_2 peptide conjugate has high specificity and affinity to the GRP receptor. The CHX-A′′ bifunctional chelate was used due to its superior binding affinity to bismuth. The 8-Aoc aliphatic spacer was used since it has shown optimal pharmacokinetic properties when used in similar bifunctional systems, such as the [^{64}Cu-NOTA-(8-Aoc)-BBN(7-14)NH_2] conjugate. [12] Unfortunately, the pre-existing 5-carbon linker off of the CHX-A′′ functionalized backbone was overlooked. Upon the linking of CHX-A′′ to [(8-Aoc)-BBN(7-14)NH_2], the true spacer length became 13 carbons long. Previous studies have shown that a spacing moiety of 3 to 8 carbons in length is optimal for GRP receptor targeting. [13-14] I expect that the

long spacer formed within the [^{205}Bi-CHX-A´´-(8-Aoc)-BBN(7-14)NH_2] conjugate was simply too long, resulting in the fast clearance of the radioconjugate.

5.5 FUTURE STUDIES

[CHX-A´´-(X)-BBN(7-14)NH_2] conjugates, where X = no spacer, β-Ala, or PABA, will be synthesized. These conjugates will be metallated with cold BiI_3. Inhibitory binding at 50% (IC_{50}) will be performed in human prostate PC-3 cells to determine receptor binding affinity of the conjugates. The [CHX-A´´-(X)-BBN(7-14)NH_2] will then be radiolabelled with $^{205}BiI_3$ and internalization and externalization assays will be performed in PC-3 cells. The results from these preliminary studies could be used to determine if a shorter spacer, or no spacer, would lead to improved pharmacokinetics of the overall conjugate.

5.6 REFERENCES

1. Eary, J.F. and W. Brenner, eds. *Nuclear Medicine Therapy*. 2007, Informa Healthcare USA, Inc.: New York.

2. Saha, G.B., *Fundamentals of Nuclear Pharmacy*. 2004, New York: Springer.

3. Milenic, D.E., et al., *In Vivo Evaluation of Bismuth-Labeled Monoclonal Antibody Comparing DTPA-Derived Bifunctional Chelates.* Cancer Biotherapy & Radiopharmaceuticals, 2001. **16**(2): p. 133-146.

4. Reubi, J.C. and H.R. Maecke, *Peptide-Based Probes for Cancer Imaging.* The Journal of Nuclear Medicine, 2008. **49**(11): p. 1735-1738.

5. Tweedle, M.F., *Peptide-Targeted Diagnostics and Radiotherapeutics.* Accounts of Chemical Research, 2009. **42**(7): p. 958-968.

6. Norman, N.C., ed. *Chemistry of Arsenic Antimony and Bismuth*. Arsenic, antimony and bismuth: some general properties and aspects of periodicity. 1998, Thomson Science: London.

7. Fleischmann, A., et al., *Bombesin Receptors in Distinct Tissue Compartments of Human Pancreatic Diseases.* Laboratory Investigation, 2000. **80**(12): p. 1807-1817.

8. West, S.D. and D.W. Mercer, *Bombesin-Induced Gastroprotection.* Annals of Surgery, 2005. **241**(2): p. 227-231.

9. Brechbiel, M.W., *Bifunctional chelates for metal nuclides.* The Quarterly Journal of Nuclear Medicine and Molecular Imaging, 2008. **52**(2): p. 166-173.

10. Csajbok, E., et al., *Equilibrium, ^{1}H and ^{13}C NMR Spectroscopy, and X-ray Diffraction Studies on the Complexes Bi(DOTA)- and Bi(DO3A-Bu).* Inorganic Chemistry, 2003. **42**(7): p. 2342-2349.

11. Brechbiel, M.W. and O.A. Gansow, *Synthesis of C-functionalized trans-cyclohexyldiethylenetriaminepenta-acetic acids for labelling of monoclonal antibodies with the bismuth-212 α-particle emitter.* Perkin Transactions 1 1992(9): p. 1173-1178.

12. Prasanphanich, A.F., et al., *[^{64}Cu-NOTA-8-Aoc-BBN(7-14)NH_2] targeting vector for positron-emission tomography imaging of gastrin-releasing peptide receptor-expressing tissues.* Proceedings of the National Academy of Sciences, 2007. **104**(30): p. 12462-12467.

13. Hoffman, T.J., et al., *Novel Series of ^{111}In-Labeled Bombesin Analogs as Potential Radiopharmaceuticals for Specific Targeting of Gastrin-Releasing Peptide Receptors Expressed on Human Prostate Cancer Cells.* J Nucl Med, 2003. **44**(5): p. 823-831.

14. Smith, C.J., et al., *Radiochemical Investigations of $^{99m}Tc-N_3S$-X-BBN[7−14]NH_2: An in Vitro/in Vivo Structure−Activity Relationship Study Where X = 0-, 3-, 5-, 8-, and 11-Carbon Tethering Moieties.* Bioconjugate Chemistry, 2002. **14**(1): p. 93-102.

APPENDIX:

Appendix 1.1: Crystal structure data and refinement for *trans*-[$ReCl(PPh_3)(sal_2phen)]•2CH_2Cl_2$.

```
_audit_creation_method            SHELXL-97
_chemical_name_systematic

_chemical_name_common
_chemical_melting_point
_chemical_formula_moiety
'C38 H30 N2 O3 P Re 1+, P F6 1-, 0.5(C H2 Cl2)'
_chemical_formula_sum
'C38.50 H31 N2 O3 F6 P2 Cl Re'
_chemical_formula_weight          967.24

loop_
 _atom_type_symbol
 _atom_type_description
 _atom_type_scat_dispersion_real
 _atom_type_scat_dispersion_imag
 _atom_type_scat_source
'C'  'C'   0.0033   0.0016
'International Tables Vol C Tables 4.2.6.8 and 6.1.1.4'
'H'  'H'   0.0000   0.0000
'International Tables Vol C Tables 4.2.6.8 and 6.1.1.4'
'N'  'N'   0.0061   0.0033
'International Tables Vol C Tables 4.2.6.8 and 6.1.1.4'
'O'  'O'   0.0106   0.0060
'International Tables Vol C Tables 4.2.6.8 and 6.1.1.4'
'F'  'F'   0.0171   0.0103
'International Tables Vol C Tables 4.2.6.8 and 6.1.1.4'
'P'  'P'   0.1023   0.0942
'International Tables Vol C Tables 4.2.6.8 and 6.1.1.4'
'Cl'  'Cl'   0.1484   0.1585
'International Tables Vol C Tables 4.2.6.8 and 6.1.1.4'
'Re'  'Re'  -1.0185   7.2310
'International Tables Vol C Tables 4.2.6.8 and 6.1.1.4'

_symmetry_cell_setting            orthorhombic
_symmetry_space_group_name_H-M    Pnn2

loop_
 _symmetry_equiv_pos_as_xyz
 'x, y, z'
 '-x, -y, z'
```

'-x+1/2, y+1/2, z+1/2'
'x+1/2, -y+1/2, z+1/2'

_cell_length_a 21.0703(15)
_cell_length_b 11.3780(8)
_cell_length_c 15.0859(11)
_cell_angle_alpha 90.00
_cell_angle_beta 90.00
_cell_angle_gamma 90.00
_cell_volume 3616.7(4)
_cell_formula_units_Z 4
_cell_measurement_temperature 173(2)
_cell_measurement_reflns_used 7142
_cell_measurement_theta_min 2.4
_cell_measurement_theta_max 26.9

_exptl_crystal_description red
_exptl_crystal_colour needle
_exptl_crystal_size_max 0.40
_exptl_crystal_size_mid 0.05
_exptl_crystal_size_min 0.05
_exptl_crystal_density_meas
_exptl_crystal_density_diffrn 1.776
_exptl_crystal_density_method 'not measured'
_exptl_crystal_F_000 1904
_exptl_absorpt_coefficient_mu 3.595
_exptl_absorpt_correction_type multi-scan
_exptl_absorpt_correction_T_min 0.50
_exptl_absorpt_correction_T_max 0.85
_exptl_absorpt_process_details

Data were corrected for decay and absorption using the program SADABS (Sheldrick, G. M. (2003). SADABS. Version 2.10. University of Göttingen, Germany).

_exptl_special_details

_diffrn_ambient_temperature 173(2)
_diffrn_radiation_wavelength 0.71073
_diffrn_radiation_type MoK\a
_diffrn_radiation_source 'fine-focus sealed tube'
_diffrn_radiation_monochromator graphite
_diffrn_measurement_device_type 'Bruker SMART CCD area detector'
_diffrn_measurement_method 'omega scans'
_diffrn_detector_area_resol_mean

_diffrn_standards_number
_diffrn_standards_interval_count
_diffrn_standards_interval_time
_diffrn_standards_decay_% 0.0
_diffrn_reflns_number 25028
_diffrn_reflns_av_R_equivalents 0.0589
_diffrn_reflns_av_sigmaI/netI 0.0765
_diffrn_reflns_limit_h_min -22
_diffrn_reflns_limit_h_max 26
_diffrn_reflns_limit_k_min -14
_diffrn_reflns_limit_k_max 14
_diffrn_reflns_limit_l_min -19
_diffrn_reflns_limit_l_max 19
_diffrn_reflns_theta_min 1.66
_diffrn_reflns_theta_max 27.17
_reflns_number_total 7838
_reflns_number_gt 6143
_reflns_threshold_expression >2sigma(I)

_computing_data_collection 'SMART (Bruker, 1998)'
_computing_cell_refinement 'SAINT (Bruker, 1998)'
_computing_data_reduction 'SAINT (Bruker, 1998)'
_computing_structure_solution 'SHELXS-97 (Sheldrick, 1997)'
_computing_structure_refinement 'SHELXL-97 (Sheldrick, 1997)'
_computing_molecular_graphics 'ORTEP-III (Burnett & Johnson, 1996)'
_computing_publication_material 'CIFTAB (Sheldrick, 1997)'

_refine_special_details

Refinement of F^2^ against ALL reflections. The weighted R-factor wR and goodness of fit S are based on F^2^, conventional R-factors R are based on F, with F set to zero for negative F^2^. The threshold expression of F^2^ > 2sigma(F^2^) is used only for calculating R-factors(gt) etc. and is not relevant to the choice of reflections for refinement. R-factors based on F^2^ are statistically about twice as large as those based on F, and R-factors based on ALL data will be even larger.

_refine_ls_structure_factor_coef Fsqd
_refine_ls_matrix_type full
_refine_ls_weighting_scheme calc
_refine_ls_weighting_details
'calc w=1/[\s^2^(Fo^2^)+(0.0074P)^2^+0.0000P] where P=(Fo^2^+2Fc^2^)/3'
_atom_sites_solution_primary direct
_atom_sites_solution_secondary difmap
_atom_sites_solution_hydrogens geom

```
_refine_ls_hydrogen_treatment     noref
_refine_ls_extinction_method      none
_refine_ls_extinction_coef
_refine_ls_abs_structure_details
 'Flack H D (1983), Acta Cryst. A39, 876-881'
_refine_ls_abs_structure_Flack    0.014(7)
_refine_ls_number_reflns          7838
_refine_ls_number_parameters      485
_refine_ls_number_restraints      1
_refine_ls_R_factor_all           0.0604
_refine_ls_R_factor_gt            0.0377
_refine_ls_wR_factor_ref          0.0676
_refine_ls_wR_factor_gt           0.0621
_refine_ls_goodness_of_fit_ref    1.014
_refine_ls_restrained_S_all       1.014
_refine_ls_shift/su_max           0.000
_refine_ls_shift/su_mean          0.000

loop_
 _atom_site_label
 _atom_site_type_symbol
 _atom_site_fract_x
 _atom_site_fract_y
 _atom_site_fract_z
 _atom_site_U_iso_or_equiv
 _atom_site_adp_type
 _atom_site_occupancy
 _atom_site_symmetry_multiplicity
 _atom_site_calc_flag
 _atom_site_refinement_flags
 _atom_site_disorder_assembly
 _atom_site_disorder_group
Re1 Re 0.378610(8) 0.419692(16) 0.33461(3) 0.02195(6) Uani 1 1 d . . .
Cl1 Cl 0.46231(11) 0.1079(3) 0.7584(2) 0.1060(11) Uani 1 1 d . . .
P1 P 0.27885(8) 0.52477(14) 0.37457(10) 0.0239(4) Uani 1 1 d . . .
F1 F 0.5000 0.5000 0.7853(5) 0.239(9) Uani 1 2 d S . .
O1 O 0.34806(19) 0.4463(4) 0.2125(3) 0.0287(10) Uani 1 1 d . . .
N1 N 0.4528(2) 0.3134(4) 0.2905(3) 0.0220(11) Uani 1 1 d . . .
C1 C 0.3829(3) 0.4278(5) 0.1388(4) 0.0277(14) Uani 1 1 d . . .
F2 F 0.4815(4) 0.6317(5) 0.6866(4) 0.139(3) Uani 1 1 d . . .
O2 O 0.33175(15) 0.2730(3) 0.3433(4) 0.0219(8) Uani 1 1 d . . .
N2 N 0.4154(2) 0.3556(4) 0.4625(3) 0.0238(11) Uani 1 1 d . . .
C2 C 0.4407(3) 0.3663(5) 0.1353(4) 0.0286(15) Uani 1 1 d . . .
P3 P 0.5000 0.0000 0.08951(18) 0.0425(7) Uani 1 2 d S . .
F3 F 0.4339(4) 0.4525(9) 0.6796(7) 0.180(4) Uani 1 1 d . . .
O3 O 0.42322(17) 0.5412(3) 0.3544(3) 0.0272(11) Uani 1 1 d . . .
```

C3 C 0.4708(3) 0.3108(6) 0.2093(5) 0.0267(17) Uani 1 1 d . . .
H3 H 0.5082 0.2671 0.1970 0.032 Uiso 1 1 calc R . .
F4 F 0.5000 0.5000 0.5819(5) 0.119(3) Uani 1 2 d S . .
C4 C 0.4837(3) 0.2458(5) 0.3582(3) 0.0234(15) Uani 1 1 d . . .
F5 F 0.5491(2) 0.1090(4) 0.0918(3) 0.0591(12) Uani 1 1 d . . .
C5 C 0.4659(3) 0.2704(6) 0.4443(5) 0.0268(18) Uani 1 1 d . . .
F6 F 0.45808(19) 0.0620(4) 0.1641(3) 0.0507(11) Uani 1 1 d . . .
C6 C 0.3660(3) 0.3041(5) 0.5245(4) 0.0288(15) Uani 1 1 d . . .
H6A H 0.3859 0.2881 0.5828 0.035 Uiso 1 1 calc R . .
H6B H 0.3317 0.3624 0.5338 0.035 Uiso 1 1 calc R . .
F7 F 0.4583(2) 0.0624(4) 0.0156(3) 0.0735(15) Uani 1 1 d . . .
C7 C 0.3376(3) 0.1918(5) 0.4889(4) 0.0253(14) Uani 1 1 d . . .
C8 C 0.3210(3) 0.1820(5) 0.4001(4) 0.0207(13) Uani 1 1 d . . .
C9 C 0.3573(3) 0.4735(6) 0.0593(4) 0.0314(15) Uani 1 1 d . . .
H9 H 0.3193 0.5183 0.0609 0.038 Uiso 1 1 calc R . .
C10 C 0.3870(4) 0.4534(6) -0.0200(4) 0.0392(18) Uani 1 1 d . . .
H10 H 0.3686 0.4827 -0.0730 0.047 Uiso 1 1 calc R . .
C11 C 0.4428(5) 0.3919(6) -0.0242(5) 0.043(2) Uani 1 1 d . . .
H11 H 0.4630 0.3795 -0.0797 0.052 Uiso 1 1 calc R . .
C12 C 0.4693(3) 0.3484(6) 0.0517(4) 0.0400(18) Uani 1 1 d . . .
H12 H 0.5078 0.3053 0.0482 0.048 Uiso 1 1 calc R . .
C13 C 0.5305(2) 0.1605(5) 0.3407(6) 0.0320(13) Uani 1 1 d . . .
H13 H 0.5419 0.1421 0.2814 0.038 Uiso 1 1 calc R . .
C14 C 0.5590(3) 0.1049(6) 0.4096(5) 0.0427(19) Uani 1 1 d . . .
H14 H 0.5900 0.0463 0.3978 0.051 Uiso 1 1 calc R . .
C15 C 0.5441(4) 0.1315(6) 0.4970(5) 0.0424(19) Uani 1 1 d . . .
H15 H 0.5660 0.0938 0.5442 0.051 Uiso 1 1 calc R . .
C16 C 0.4971(3) 0.2133(6) 0.5151(5) 0.0344(17) Uani 1 1 d . . .
H16 H 0.4860 0.2309 0.5747 0.041 Uiso 1 1 calc R . .
C17 C 0.3278(3) 0.0976(5) 0.5443(4) 0.0278(15) Uani 1 1 d . . .
H17 H 0.3398 0.1037 0.6049 0.033 Uiso 1 1 calc R . .
C18 C 0.3010(3) -0.0052(6) 0.5141(5) 0.0363(17) Uani 1 1 d . . .
H18 H 0.2941 -0.0691 0.5535 0.044 Uiso 1 1 calc R . .
C19 C 0.2843(3) -0.0143(6) 0.4258(4) 0.0304(15) Uani 1 1 d . . .
H19 H 0.2659 -0.0849 0.4042 0.036 Uiso 1 1 calc R . .
C20 C 0.2943(3) 0.0787(5) 0.3690(4) 0.0269(13) Uani 1 1 d . . .
H20 H 0.2829 0.0720 0.3083 0.032 Uiso 1 1 calc R . .
C21 C 0.2714(3) 0.5867(5) 0.4850(4) 0.0283(14) Uani 1 1 d . . .
C22 C 0.3243(3) 0.6205(5) 0.5308(4) 0.0305(16) Uani 1 1 d . . .
H22 H 0.3652 0.6075 0.5060 0.037 Uiso 1 1 calc R . .
C23 C 0.3190(4) 0.6734(6) 0.6128(5) 0.0408(18) Uani 1 1 d . . .
H23 H 0.3562 0.6954 0.6442 0.049 Uiso 1 1 calc R . .
C24 C 0.2608(4) 0.6943(6) 0.6493(5) 0.0426(19) Uani 1 1 d . . .
H24 H 0.2575 0.7321 0.7052 0.051 Uiso 1 1 calc R . .
C25 C 0.2067(4) 0.6604(6) 0.6045(5) 0.0388(18) Uani 1 1 d . . .
H25 H 0.1661 0.6747 0.6298 0.047 Uiso 1 1 calc R . .

C26 C 0.2115(3) 0.6063(6) 0.5240(4) 0.0357(17) Uani 1 1 d . . .
H26 H 0.1742 0.5817 0.4940 0.043 Uiso 1 1 calc R . .
C27 C 0.2121(3) 0.4255(6) 0.3642(4) 0.0285(16) Uani 1 1 d . . .
C28 C 0.1969(3) 0.3497(6) 0.4340(5) 0.0364(17) Uani 1 1 d . . .
H28 H 0.2207 0.3533 0.4875 0.044 Uiso 1 1 calc R . .
C29 C 0.1482(3) 0.2704(6) 0.4266(6) 0.052(2) Uani 1 1 d . . .
H29 H 0.1389 0.2188 0.4743 0.062 Uiso 1 1 calc R . .
C30 C 0.1132(3) 0.2656(7) 0.3505(8) 0.053(3) Uani 1 1 d . . .
H30 H 0.0790 0.2116 0.3457 0.064 Uiso 1 1 calc R . .
C31 C 0.1274(3) 0.3383(8) 0.2815(6) 0.054(2) Uani 1 1 d . . .
H31 H 0.1030 0.3336 0.2286 0.064 Uiso 1 1 calc R . .
C32 C 0.1766(3) 0.4192(6) 0.2866(5) 0.0338(17) Uani 1 1 d . . .
H32 H 0.1858 0.4695 0.2380 0.041 Uiso 1 1 calc R . .
C33 C 0.2629(3) 0.6520(5) 0.3026(4) 0.0273(15) Uani 1 1 d . . .
C34 C 0.2021(3) 0.7045(5) 0.3058(4) 0.0347(18) Uani 1 1 d . . .
H34 H 0.1694 0.6716 0.3415 0.042 Uiso 1 1 calc R . .
C35 C 0.1911(4) 0.8049(6) 0.2559(5) 0.0432(19) Uani 1 1 d . . .
H35 H 0.1500 0.8392 0.2552 0.052 Uiso 1 1 calc R . .
C36 C 0.2392(4) 0.8554(6) 0.2073(4) 0.043(2) Uani 1 1 d . . .
H36 H 0.2311 0.9256 0.1750 0.051 Uiso 1 1 calc R . .
C37 C 0.2988(4) 0.8058(6) 0.2046(5) 0.0423(19) Uani 1 1 d . . .
H37 H 0.3316 0.8400 0.1701 0.051 Uiso 1 1 calc R . .
C38 C 0.3099(3) 0.7035(6) 0.2541(4) 0.0340(16) Uani 1 1 d . . .
H38 H 0.3511 0.6694 0.2539 0.041 Uiso 1 1 calc R . .
C39 C 0.5000 0.0000 0.8206(7) 0.050(3) Uani 1 2 d S . .
H39A H 0.5318 0.0381 0.8594 0.060 Uiso 0.50 1 calc PR . .
H39B H 0.4682 -0.0381 0.8594 0.060 Uiso 0.50 1 calc PR . .
P2 P 0.5000 0.5000 0.68681(16) 0.0349(6) Uani 1 2 d S . .

loop_
 _atom_site_aniso_label
 _atom_site_aniso_U_11
 _atom_site_aniso_U_22
 _atom_site_aniso_U_33
 _atom_site_aniso_U_23
 _atom_site_aniso_U_13
 _atom_site_aniso_U_12
Re1 0.02210(10) 0.01754(9) 0.02620(9) -0.0003(2) 0.0003(2) -0.00022(10)
Cl1 0.0456(15) 0.145(3) 0.128(2) 0.079(2) -0.0091(15) -0.0140(16)
P1 0.0237(9) 0.0211(8) 0.0268(8) -0.0012(7) -0.0021(7) 0.0027(7)
F1 0.64(3) 0.057(6) 0.017(4) 0.000 0.000 -0.094(10)
O1 0.026(2) 0.026(3) 0.034(3) 0.0008(19) 0.0013(19) 0.0015(19)
N1 0.022(3) 0.019(3) 0.025(3) -0.001(2) -0.001(2) -0.002(2)
C1 0.032(4) 0.024(3) 0.027(3) 0.001(3) 0.009(3) -0.001(3)
F2 0.281(10) 0.051(4) 0.085(5) 0.012(3) 0.053(5) 0.049(5)
O2 0.0249(18) 0.0205(18) 0.020(2) -0.002(2) 0.000(2) -0.0057(14)

N2 0.020(3) 0.022(3) 0.028(3) -0.002(2) -0.002(2) 0.006(2)
C2 0.026(4) 0.029(4) 0.030(4) 0.007(3) 0.004(3) 0.005(3)
P3 0.0513(19) 0.0389(17) 0.0374(16) 0.000 0.000 0.0131(14)
F3 0.082(6) 0.202(9) 0.254(11) -0.017(8) 0.034(6) -0.064(6)
O3 0.030(2) 0.022(2) 0.030(3) 0.0023(18) 0.0016(19) -0.0013(16)
C3 0.022(4) 0.024(4) 0.035(4) 0.001(3) 0.012(3) -0.002(3)
F4 0.243(11) 0.061(5) 0.054(5) 0.000 0.000 -0.069(6)
C4 0.020(3) 0.021(3) 0.029(4) 0.001(3) -0.006(2) -0.002(2)
F5 0.059(3) 0.043(3) 0.076(3) 0.012(2) 0.020(2) -0.002(2)
C5 0.020(4) 0.023(4) 0.037(4) -0.008(3) 0.004(3) -0.005(3)
F6 0.053(3) 0.050(3) 0.049(3) -0.015(2) 0.006(2) 0.005(2)
C6 0.031(4) 0.030(4) 0.024(3) -0.001(3) -0.004(3) -0.001(3)
F7 0.097(4) 0.073(4) 0.050(3) -0.002(3) -0.013(3) 0.040(3)
C7 0.027(4) 0.023(3) 0.026(3) -0.001(3) -0.001(3) 0.004(3)
C8 0.015(3) 0.021(3) 0.025(3) 0.001(3) 0.006(3) 0.003(2)
C9 0.025(4) 0.040(4) 0.029(4) 0.000(3) 0.001(3) 0.002(3)
C10 0.063(5) 0.025(4) 0.030(4) 0.005(3) 0.009(4) -0.005(4)
C11 0.084(7) 0.027(4) 0.019(4) 0.010(3) 0.016(4) -0.001(4)
C12 0.052(5) 0.034(4) 0.034(4) 0.003(3) 0.022(4) 0.008(4)
C13 0.029(3) 0.033(3) 0.034(3) -0.009(5) -0.006(5) 0.007(2)
C14 0.041(4) 0.031(4) 0.056(5) -0.005(4) -0.016(4) 0.013(3)
C15 0.053(5) 0.039(4) 0.036(4) -0.001(3) -0.025(4) 0.007(4)
C16 0.030(4) 0.036(4) 0.037(4) -0.001(3) -0.008(3) 0.002(3)
C17 0.029(4) 0.027(4) 0.027(3) 0.007(3) -0.003(3) 0.001(3)
C18 0.039(4) 0.026(4) 0.044(4) 0.014(3) 0.008(3) 0.000(3)
C19 0.032(4) 0.025(4) 0.034(4) 0.002(3) -0.003(3) -0.005(3)
C20 0.033(3) 0.016(3) 0.032(3) 0.001(3) 0.000(2) 0.000(3)
C21 0.035(4) 0.015(3) 0.035(3) -0.003(3) 0.000(3) 0.004(3)
C22 0.040(4) 0.021(3) 0.030(4) 0.006(3) -0.003(3) 0.002(3)
C23 0.054(5) 0.031(4) 0.038(4) -0.011(3) -0.008(4) -0.012(4)
C24 0.073(6) 0.025(4) 0.030(4) -0.001(3) 0.010(4) -0.005(4)
C25 0.043(5) 0.031(4) 0.042(4) 0.005(3) 0.009(4) 0.006(4)
C26 0.040(4) 0.032(4) 0.035(4) -0.003(3) -0.002(3) 0.006(3)
C27 0.018(3) 0.028(3) 0.040(4) -0.004(3) 0.007(3) 0.007(3)
C28 0.025(4) 0.031(4) 0.053(5) 0.002(3) 0.003(3) 0.002(3)
C29 0.038(5) 0.026(4) 0.091(7) -0.004(4) 0.014(4) -0.005(4)
C30 0.033(4) 0.045(4) 0.082(9) -0.024(5) 0.017(5) -0.015(3)
C31 0.025(5) 0.070(6) 0.065(6) -0.041(5) -0.004(4) 0.011(4)
C32 0.024(4) 0.038(4) 0.039(4) -0.013(4) 0.001(3) 0.008(4)
C33 0.033(4) 0.019(3) 0.029(3) -0.003(3) -0.009(3) 0.006(3)
C34 0.044(4) 0.024(4) 0.037(4) -0.004(3) -0.004(3) 0.006(3)
C35 0.051(5) 0.038(4) 0.041(4) -0.007(4) -0.018(4) 0.017(4)
C36 0.078(6) 0.015(4) 0.035(4) -0.001(3) -0.024(4) -0.002(4)
C37 0.061(5) 0.028(4) 0.038(4) 0.008(3) -0.005(4) -0.001(4)
C38 0.041(4) 0.025(4) 0.036(4) 0.001(3) -0.006(3) 0.002(3)
C39 0.045(6) 0.075(7) 0.030(8) 0.000 0.000 -0.014(5)

P2 0.0437(17) 0.0324(15) 0.0286(14) 0.000 0.000 -0.0079(12)

_geom_special_details

All esds (except the esd in the dihedral angle between two l.s. planes)
are estimated using the full covariance matrix. The cell esds are taken
into account individually in the estimation of esds in distances, angles
and torsion angles; correlations between esds in cell parameters are only
used when they are defined by crystal symmetry. An approximate (isotropic)
treatment of cell esds is used for estimating esds involving l.s. planes.

loop_
_geom_bond_atom_site_label_1
_geom_bond_atom_site_label_2
_geom_bond_distance
_geom_bond_site_symmetry_2
_geom_bond_publ_flag
Re1 O3 1.699(4) .
Re1 O2 1.943(3) .
Re1 O1 1.974(4) .
Re1 N1 2.086(5) .
Re1 N2 2.203(5) .
Re1 P1 2.4923(16) .
Cl1 C39 1.738(6) .
P1 C27 1.810(7) .
P1 C21 1.815(6) .
P1 C33 1.840(6) .
F1 P2 1.486(7) .
O1 C1 1.349(7) .
N1 C3 1.282(8) .
N1 C4 1.435(7) .
C1 C2 1.405(8) .
C1 C9 1.414(8) .
F2 P2 1.548(5) .
O2 C8 1.364(7) .
N2 C5 1.465(8) .
N2 C6 1.517(7) .
C2 C12 1.412(8)
C2 C3 1.432(9) .
P3 F7 1.587(5) 2_655
P3 F7 1.587(5) .
P3 F6 1.596(4) 2_655
P3 F6 1.596(4) .
P3 F5 1.615(4) .
P3 F5 1.615(4) 2_655

F3 P2 1.497(7) .
C3 H3 0.9500 .
F4 P2 1.583(8) .
C4 C5 1.381(9) .
C4 C13 1.407(7) .
C5 C16 1.413(10) .
C6 C7 1.510(8) .
C6 H6A 0.9900 .
C6 H6B 0.9900 .
C7 C17 1.375(8)
C7 C8 1.389(8) .
C8 C20 1.384(8)
C9 C10 1.369(9)
C9 H9 0.9500 .
C10 C11 1.368(11) .
C10 H10 0.9500 .
C11 C12 1.367(10)
C11 H11 0.9500 .
C12 H12 0.9500 .
C13 C14 1.357(10)
C13 H13 0.9500 .
C14 C15 1.389(10)
C14 H14 0.9500 .
C15 C16 1.386(9)
C15 H15 0.9500 .
C16 H16 0.9500 .
C17 C18 1.376(9)
C17 H17 0.9500 .
C18 C19 1.381(9)
C18 H18 0.9500 .
C19 C20 1.378(8)
C19 H19 0.9500 .
C20 H20 0.9500 .
C21 C22 1.368(8)
C21 C26 1.410(9)
C22 C23 1.379(8)
C22 H22 0.9500 .
C23 C24 1.365(9)
C23 H23 0.9500 .
C24 C25 1.379(9)
C24 H24 0.9500 .
C25 C26 1.366(9)
C25 H25 0.9500 .
C26 H26 0.9500 .
C27 C32 1.392(8)
C27 C28 1.398(9)

C28 C29 1.371(9)
C28 H28 0.9500 .
C29 C30 1.366(14)
C29 H29 0.9500 .
C30 C31 1.363(12)
C30 H30 0.9500 .
C31 C32 1.389(10)
C31 H31 0.9500 .
C32 H32 0.9500 .
C33 C38 1.363(9)
C33 C34 1.415(8)
C34 C35 1.389(9)
C34 H34 0.9500 .
C35 C36 1.375(10)
C35 H35 0.9500 .
C36 C37 1.378(10)
C36 H36 0.9500 .
C37 C38 1.402(9)
C37 H37 0.9500 .
C38 H38 0.9500 .
C39 Cl1 1.738(6) 2_655
C39 H39A 0.9900 .
C39 H39B 0.9900 .
P2 F3 1.497(7) 2_665
P2 F2 1.548(5) 2_665

loop_
 _geom_angle_atom_site_label_1
 _geom_angle_atom_site_label_2
 _geom_angle_atom_site_label_3
 _geom_angle
 _geom_angle_site_symmetry_1
 _geom_angle_site_symmetry_3
 _geom_angle_publ_flag
O3 Re1 O2 165.6(2) .
O3 Re1 O1 102.66(17)
O2 Re1 O1 91.64(19) .
O3 Re1 N1 96.48(18) .
O2 Re1 N1 84.53(17) .
O1 Re1 N1 92.06(18) .
O3 Re1 N2 85.50(18) .
O2 Re1 N2 80.53(19) .
O1 Re1 N2 169.18(17)
N1 Re1 N2 79.84(18) .
O3 Re1 P1 91.93(13) .
O2 Re1 P1 88.12(10) .

O1 Re1 P1 82.94(12) .
N1 Re1 P1 170.99(14)
N2 Re1 P1 104.09(13)
C27 P1 C21 104.7(3) .
C27 P1 C33 107.4(3) .
C21 P1 C33 102.7(3) .
C27 P1 Re1 109.6(2) .
C21 P1 Re1 118.8(2) .
C33 P1 Re1 112.8(2) .
C1 O1 Re1 124.6(4) . .
C3 N1 C4 122.2(5) . .
C3 N1 Re1 122.6(5) .
C4 N1 Re1 115.1(4) .
O1 C1 C2 125.5(5) . .
O1 C1 C9 115.7(5) . .
C2 C1 C9 118.8(5) . .
C8 O2 Re1 141.1(4) .
C5 N2 C6 111.0(5) . .
C5 N2 Re1 108.1(4) .
C6 N2 Re1 115.3(3) .
C1 C2 C12 118.4(6) .
C1 C2 C3 125.0(6) . .
C12 C2 C3 116.3(6) .
F7 P3 F7 90.7(4) 2_65
F7 P3 F6 89.5(2) 2_655 2_655
F7 P3 F6 179.7(3) . 2_655
F7 P3 F6 179.7(3) 2_655 .
F7 P3 F6 89.5(2) . .
F6 P3 F6 90.2(3) 2_655
F7 P3 F5 90.2(3) 2_655
F7 P3 F5 91.5(3) . .
F6 P3 F5 88.3(2) 2_655
F6 P3 F5 90.0(2) . .
F7 P3 F5 91.5(3) 2_655 2_655
F7 P3 F5 90.2(3) . 2_655
F6 P3 F5 90.0(2) 2_655 2_655
F6 P3 F5 88.3(2) . 2_655
F5 P3 F5 177.6(4) . 2_655
N1 C3 C2 127.2(7) . .
N1 C3 H3 116.4 . .
C2 C3 H3 116.4 . .
C5 C4 C13 120.4(6)
C5 C4 N1 115.9(5) .
C13 C4 N1 123.7(6)
C4 C5 C16 119.4(6)
C4 C5 N2 120.6(6) .

C16 C5 N2 120.0(6)
C7 C6 N2 112.3(5) .
C7 C6 H6A 109.2 . .
N2 C6 H6A 109.2 . .
C7 C6 H6B 109.2 . .
N2 C6 H6B 109.2 . .
H6A C6 H6B 107.9
C17 C7 C8 119.1(6)
C17 C7 C6 120.2(5)
C8 C7 C6 120.8(5) .
O2 C8 C20 119.9(5)
O2 C8 C7 120.2(6) .
C20 C8 C7 119.8(5)
C10 C9 C1 120.3(6)
C10 C9 H9 119.8 . .
C1 C9 H9 119.8 . .
C11 C10 C9 121.2(7) .
C11 C10 H10 119.4 . .
C9 C10 H10 119.4 . .
C12 C11 C10 119.8(7)
C12 C11 H11 120.1 . .
C10 C11 H11 120.1 . .
C11 C12 C2 121.4(7) .
C11 C12 H12 119.3 . .
C2 C12 H12 119.3 . .
C14 C13 C4 119.2(8)
C14 C13 H13 120.4 . .
C4 C13 H13 120.4 . .
C13 C14 C15 121.7(7)
C13 C14 H14 119.1 . .
C15 C14 H14 119.1 . .
C16 C15 C14 119.7(6)
C16 C15 H15 120.2 . .
C14 C15 H15 120.2 . .
C15 C16 C5 119.5(7) .
C15 C16 H16 120.2 . .
C5 C16 H16 120.2 . .
C7 C17 C18 121.5(6)
C7 C17 H17 119.3 . .
C18 C17 H17 119.3 .
C17 C18 C19 119.2(6)
C17 C18 H18 120.4 . .
C19 C18 H18 120.4 . .
C20 C19 C18 120.2(6)
C20 C19 H19 119.9 . .
C18 C19 H19 119.9 . .

C19 C20 C8 120.2(6) . .
C19 C20 H20 119.9 . .
C8 C20 H20 119.9 . .
C22 C21 C26 118.3(6) . .
C22 C21 P1 120.2(5) . .
C26 C21 P1 121.5(5) . .
C21 C22 C23 120.6(7) . .
C21 C22 H22 119.7 . .
C23 C22 H22 119.7 . .
C24 C23 C22 120.7(7) . .
C24 C23 H23 119.6 . .
C22 C23 H23 119.6 . .
C23 C24 C25 119.7(7) . .
C23 C24 H24 120.1 . .
C25 C24 H24 120.1 . .
C26 C25 C24 120.0(7) . .
C26 C25 H25 120.0 . .
C24 C25 H25 120.0 . .
C25 C26 C21 120.6(7) . .
C25 C26 H26 119.7 . .
C21 C26 H26 119.7 . .
C32 C27 C28 118.6(6) . .
C32 C27 P1 121.5(5) . .
C28 C27 P1 119.8(5) . .
C29 C28 C27 121.0(7) . .
C29 C28 H28 119.5 . .
C27 C28 H28 119.5 . .
C30 C29 C28 120.0(8) . .
C30 C29 H29 120.0 . .
C28 C29 H29 120.0 . .
C31 C30 C29 120.0(7) . .
C31 C30 H30 120.0 . .
C29 C30 H30 120.0 . .
C30 C31 C32 121.6(8) . .
C30 C31 H31 119.2 . .
C32 C31 H31 119.2 . .
C31 C32 C27 118.8(7) . .
C31 C32 H32 120.6 . .
C27 C32 H32 120.6 . .
C38 C33 C34 119.7(6) . .
C38 C33 P1 121.5(5) . .
C34 C33 P1 118.5(5) . .
C35 C34 C33 118.6(7) . .
C35 C34 H34 120.7 . .
C33 C34 H34 120.7 . .
C36 C35 C34 120.7(7) . .

C36 C35 H35 119.6 . .
C34 C35 H35 119.6 . .
C35 C36 C37 121.0(7) . .
C35 C36 H36 119.5 . .
C37 C36 H36 119.5 . .
C36 C37 C38 118.5(7) . .
C36 C37 H37 120.8 . .
C38 C37 H37 120.8 . .
C33 C38 C37 121.4(7) . .
C33 C38 H38 119.3 . .
C37 C38 H38 119.3 . .
Cl1 C39 Cl1 114.6(7) 2_655 .
Cl1 C39 H39A 108.6 2_655 .
Cl1 C39 H39A 108.6 . .
Cl1 C39 H39B 108.6 2_655 .
Cl1 C39 H39B 108.6 . .
H39A C39 H39B 107.6 . .
F1 P2 F3 94.2(4) . 2_665
F1 P2 F3 94.2(4) . .
F3 P2 F3 171.6(8) 2_665 .
F1 P2 F2 90.1(2) . 2_665
F3 P2 F2 96.6(5) 2_665 2_665
F3 P2 F2 83.4(5) . 2_665
F1 P2 F2 90.1(2) . .
F3 P2 F2 83.4(5) 2_665 .
F3 P2 F2 96.6(5) . .
F2 P2 F2 179.8(5) 2_665 .
F1 P2 F4 180.000(3) . .
F3 P2 F4 85.8(4) 2_665 .
F3 P2 F4 85.8(4) . .
F2 P2 F4 89.9(2) 2_665 .
F2 P2 F4 89.9(2) . .

loop_
 _geom_torsion_atom_site_label_1
 _geom_torsion_atom_site_label_2
 _geom_torsion_atom_site_label_3
 _geom_torsion_atom_site_label_4
 _geom_torsion
 _geom_torsion_site_symmetry_1
 _geom_torsion_site_symmetry_2
 _geom_torsion_site_symmetry_3
 _geom_torsion_site_symmetry_4
 _geom_torsion_publ_flag
O3 Re1 P1 C27 -179.6(3) . . . .
O2 Re1 P1 C27 -14.0(3) . . . .

O1 Re1 P1 C27 77.8(2) . . . .
N1 Re1 P1 C27 21.2(9) . . . .
N2 Re1 P1 C27 -93.8(3) . . . .
O3 Re1 P1 C21 -59.4(3) . . . .
O2 Re1 P1 C21 106.2(3) . . . .
O1 Re1 P1 C21 -162.0(3) . . . .
N1 Re1 P1 C21 141.4(9) . . . .
N2 Re1 P1 C21 26.4(3) . . . .
O3 Re1 P1 C33 60.8(2) . . . .
O2 Re1 P1 C33 -133.6(3) . . . .
O1 Re1 P1 C33 -41.7(2) . . . .
N1 Re1 P1 C33 -98.4(9) . . . .
N2 Re1 P1 C33 146.6(2) . . . .
O3 Re1 O1 C1 78.9(4) . . . .
O2 Re1 O1 C1 -102.8(4) . . . .
N1 Re1 O1 C1 -18.2(4) . . . .
N2 Re1 O1 C1 -59.4(11) . . . .
P1 Re1 O1 C1 169.3(4) . . . .
O3 Re1 N1 C3 -87.5(5) . . . .
O2 Re1 N1 C3 107.0(5) . . . .
O1 Re1 N1 C3 15.5(5) . . . .
N2 Re1 N1 C3 -171.7(5) . . . .
P1 Re1 N1 C3 71.6(11) . . . .
O3 Re1 N1 C4 90.8(4) . . . .
O2 Re1 N1 C4 -74.7(4) . . . .
O1 Re1 N1 C4 -166.2(4) . . . .
N2 Re1 N1 C4 6.6(4) . . . .
P1 Re1 N1 C4 -110.1(9) . . . .
Re1 O1 C1 C2 13.2(8) . . . .
Re1 O1 C1 C9 -168.0(4) . . . .
O3 Re1 O2 C8 -8.5(10) . . . .
O1 Re1 O2 C8 178.2(6) . . . .
N1 Re1 O2 C8 86.3(6) . . . .
N2 Re1 O2 C8 5.7(5) . . . .
P1 Re1 O2 C8 -98.9(5) . . . .
O3 Re1 N2 C5 -101.8(4) . . . .
O2 Re1 N2 C5 81.7(4) . . . .
O1 Re1 N2 C5 37.6(11) . . . .
N1 Re1 N2 C5 -4.4(4) . . . .
P1 Re1 N2 C5 167.3(3) . . . .
O3 Re1 N2 C6 133.4(4) . . . .
O2 Re1 N2 C6 -43.1(4) . . . .
O1 Re1 N2 C6 -87.2(10) . . . .
N1 Re1 N2 C6 -129.2(4) . . . .
P1 Re1 N2 C6 42.5(4) . . . .
O1 C1 C2 C12 176.1(6) . . . .

C9 C1 C2 C12 -2.6(9) . . . .
O1 C1 C2 C3 1.7(10) . . . .
C9 C1 C2 C3 -177.0(6) . . . .
C4 N1 C3 C2 174.4(6) . . . .
Re1 N1 C3 C2 -7.4(10) . . . .
C1 C2 C3 N1 -4.5(11) . . . .
C12 C2 C3 N1 -179.0(7) . . . .
C3 N1 C4 C5 170.5(6) . . . .
Re1 N1 C4 C5 -7.8(6) . . . .
C3 N1 C4 C13 -8.2(9) . . . .
Re1 N1 C4 C13 173.5(4) . . . .
C13 C4 C5 C16 3.0(9) . . . .
N1 C4 C5 C16 -175.8(5) . . . .
C13 C4 C5 N2 -177.4(5) . . . .
N1 C4 C5 N2 3.8(8) . . . .
C6 N2 C5 C4 129.0(6) . . . .
Re1 N2 C5 C4 1.7(7) . . . .
C6 N2 C5 C16 -51.4(7) . . . .
Re1 N2 C5 C16 -178.7(5) . . . .
C5 N2 C6 C7 -56.7(6) . . . .
Re1 N2 C6 C7 66.6(5) . . . .
N2 C6 C7 C17 137.3(6) . . . .
N2 C6 C7 C8 -42.7(8) . . . .
Re1 O2 C8 C20 -164.5(4) . . . .
Re1 O2 C8 C7 14.5(9) . . . .
C17 C7 C8 O2 -178.2(5) . . . .
C6 C7 C8 O2 1.8(9) . . . .
C17 C7 C8 C20 0.7(9) . . . .
C6 C7 C8 C20 -179.3(5) . . . .
O1 C1 C9 C10 -176.1(6) . . . .
C2 C1 C9 C10 2.8(9) . . . .
C1 C9 C10 C11 -1.8(10) . . . .
C9 C10 C11 C12 0.6(11) . . . .
C10 C11 C12 C2 -0.5(11) . . . .
C1 C2 C12 C11 1.5(10) . . . .
C3 C2 C12 C11 176.4(7) . . . .
C5 C4 C13 C14 -1.7(9) . . . .
N1 C4 C13 C14 177.0(6) . . . .
C4 C13 C14 C15 -1.2(10) . . . .
C13 C14 C15 C16 2.7(11) . . . .
C14 C15 C16 C5 -1.3(11) . . . .
C4 C5 C16 C15 -1.5(10) . . . .
N2 C5 C16 C15 178.9(6) . . . .
C8 C7 C17 C18 -1.1(9) . . . .
C6 C7 C17 C18 178.9(6) . . . .
C7 C17 C18 C19 0.8(10) . . . .

C17 C18 C19 C20 -0.2(10) . . . .
C18 C19 C20 C8 -0.2(9) . . . .
O2 C8 C20 C19 178.9(5) . . . .
C7 C8 C20 C19 -0.1(9) . . . .
C27 P1 C21 C22 150.1(5) . . . .
C33 P1 C21 C22 -97.9(5) . . . .
Re1 P1 C21 C22 27.4(6) . . . .
C27 P1 C21 C26 -32.8(6) . . . .
C33 P1 C21 C26 79.2(6) . . . .
Re1 P1 C21 C26 -155.5(4) . . . .
C26 C21 C22 C23 -0.6(9) . . . .
P1 C21 C22 C23 176.6(5) . . . .
C21 C22 C23 C24 -0.8(10) . . . .
C22 C23 C24 C25 1.2(10) . . . .
C23 C24 C25 C26 -0.1(10) . . . .
C24 C25 C26 C21 -1.3(10) . . . .
C22 C21 C26 C25 1.6(9) . . . .
P1 C21 C26 C25 -175.5(5) . . . .
C21 P1 C27 C32 137.9(5) . . . .
C33 P1 C27 C32 29.2(6) . . . .
Re1 P1 C27 C32 -93.6(5) . . . .
C21 P1 C27 C28 -44.5(6) . . . .
C33 P1 C27 C28 -153.2(5) . . . .
Re1 P1 C27 C28 83.9(5) . . . .
C32 C27 C28 C29 0.2(10) . . . .
P1 C27 C28 C29 -177.4(5) . . . .
C27 C28 C29 C30 -0.9(11) . . . .
C28 C29 C30 C31 1.1(12) . . . .
C29 C30 C31 C32 -0.7(12) . . . .
C30 C31 C32 C27 0.1(10) . . . .
C28 C27 C32 C31 0.1(9) . . . .
P1 C27 C32 C31 177.7(5) . . . .
C27 P1 C33 C38 -140.7(5) . . . .
C21 P1 C33 C38 109.2(5) . . . .
Re1 P1 C33 C38 -19.9(6) . . . .
C27 P1 C33 C34 46.3(5) . . . .
C21 P1 C33 C34 -63.8(5) . . . .
Re1 P1 C33 C34 167.1(4) . . . .
C38 C33 C34 C35 2.9(9) . . . .
P1 C33 C34 C35 176.0(5) . . . .
C33 C34 C35 C36 -2.8(9) . . . .
C34 C35 C36 C37 2.1(10) . . . .
C35 C36 C37 C38 -1.2(10) . . . .
C34 C33 C38 C37 -2.2(10) . . . .
P1 C33 C38 C37 -175.1(5) . . . .
C36 C37 C38 C33 1.3(10) . . . .

_diffrn_measured_fraction_theta_max 0.999
_diffrn_reflns_theta_full 27.17
_diffrn_measured_fraction_theta_full 0.999
_refine_diff_density_max 0.882
_refine_diff_density_min -0.782
_refine_diff_density_rms 0.108

Appendix 1.2: Crystal structure data and refinement for [$ReCl_2(PPh_3)$(salphen)].

Identification code	ReSalP3
Empirical formula	C40 H33 Cl5 N2 O2 P Re
Formula weight	968.10
Temperature	173(2) K
Wavelength	0.71073 A
Crystal system, space group	Monoclinic, P 21/c
Unit cell dimensions	a = 23.0805(7) A alpha = 90 deg. b = 13.1946(4) A beta = 104.4470(10) deg. c = 25.9868(8) A gamma = 90 deg.
Volume	7663.7(4) A^3
Z, Calculated density	8, 1.678 Mg/m^3
Absorption coefficient	3.600 mm^-1
F(000)	3824
Crystal size	0.55 x 0.10 x 0.05 mm
Theta range for data collection	1.62 to 27.13 deg.
Limiting indices	-29<=h<=29, -16<=k<=16, -33<=l<=33
Reflections collected / unique	53711 / 16877 [R(int) = 0.0494]
Completeness to theta = 27.13	99.5 %
Absorption correction	Semi-empirical from equivalents
Max. and min. transmission	0.84 and 0.50
Refinement method	Full-matrix least-squares on F^2
Data / restraints / parameters	16877 / 0 / 919
Goodness-of-fit on F^2	1.032

Final R indices [I>2sigma(I)] R1 = 0.0398, wR2 = 0.0666

R indices (all data) R1 = 0.0625, wR2 = 0.0715

Largest diff. peak and hole 1.486 and -1.161 e.A^-3

Table 2. Atomic coordinates (x 10^4) and equivalent isotropic displacement parameters (A^2 x 10^3) for resalp3.
U(eq) is defined as one third of the trace of the orthogonalized Uij tensor.

	x	y	z	U(eq)
C(46)	3533(2)	9583(4)	181(2)	28(1)
Re(1A)	338(1)	1103(1)	1530(1)	19(1)
Cl(1A)	-566(1)	618(1)	1807(1)	29(1)
P(1A)	1179(1)	1651(1)	1206(1)	19(1)
O(1A)	295(1)	-262(2)	1187(1)	24(1)
N(1A)	815(2)	508(3)	2226(1)	21(1)
C(1A)	317(2)	-1145(3)	1436(2)	24(1)
O(2A)	-194(1)	1832(2)	915(1)	24(1)
N(2A)	405(2)	2362(3)	1995(1)	20(1)
C(2A)	65(2)	-1986(4)	1133(2)	28(1)
C(3A)	74(2)	-2930(4)	1361(2)	31(1)
C(4A)	353(2)	-3072(4)	1898(2)	30(1)
C(5A)	605(2)	-2260(4)	2200(2)	27(1)
C(6A)	591(2)	-1270(3)	1987(2)	22(1)
C(7A)	847(2)	-465(4)	2344(2)	25(1)
C(8A)	1045(2)	1260(4)	2623(2)	23(1)
C(9A)	1474(2)	1078(4)	3094(2)	30(1)
C(10A)	1651(2)	1845(4)	3459(2)	35(1)
C(11A)	1403(2)	2808(4)	3354(2)	39(1)
C(12A)	995(2)	3007(4)	2875(2)	29(1)
C(13A)	818(2)	2237(4)	2510(2)	23(1)
C(14A)	95(2)	3197(3)	1865(2)	25(1)
C(15A)	-317(2)	3394(3)	1365(2)	25(1)
C(16A)	-607(2)	4350(4)	1302(2)	32(1)
C(17A)	-1010(2)	4634(4)	844(2)	36(1)
C(18A)	-1140(2)	3957(4)	416(2)	33(1)
C(19A)	-865(2)	3035(4)	449(2)	29(1)
C(20A)	-449(2)	2727(3)	919(2)	23(1)
C(21A)	1078(2)	2999(3)	1043(2)	22(1)

C(22A)	1191(2)	3732(3)	1440(2)	26(1)
C(23A)	1060(2)	4741(4)	1311(2)	34(1)
C(24A)	813(2)	5026(4)	797(2)	40(1)
C(25A)	688(2)	4302(4)	401(2)	35(1)
C(26A)	822(2)	3294(4)	522(2)	28(1)
C(27A)	1282(2)	1080(3)	591(2)	23(1)
C(28A)	1813(2)	1216(4)	446(2)	31(1)
C(29A)	1887(2)	812(4)	-26(2)	41(1)
C(30A)	1439(2)	263(4)	-348(2)	34(1)
C(31A)	911(2)	110(4)	-205(2)	35(1)
C(32A)	829(2)	523(4)	261(2)	28(1)
C(33A)	1917(2)	1513(3)	1661(2)	20(1)
C(34A)	2068(2)	555(4)	1890(2)	29(1)
C(35A)	2622(2)	388(4)	2229(2)	38(1)
C(36A)	3034(2)	1166(4)	2352(2)	41(1)
C(37A)	2895(2)	2101(4)	2118(2)	42(1)
C(38A)	2342(2)	2273(4)	1770(2)	32(1)
Re(1B)	4424(1)	7625(1)	1524(1)	17(1)
Cl(1B)	5414(1)	7138(1)	2070(1)	25(1)
P(1B)	3478(1)	8020(1)	907(1)	19(1)
O(1B)	4426(1)	6300(2)	1154(1)	21(1)
N(1B)	4086(2)	6965(3)	2090(1)	21(1)
C(1B)	4354(2)	5394(3)	1341(2)	22(1)
O(2B)	4816(1)	8425(2)	1045(1)	22(1)
N(2B)	4437(2)	8847(3)	2002(1)	17(1)
C(2B)	4441(2)	4559(4)	1031(2)	28(1)
C(3B)	4387(2)	3582(4)	1196(2)	30(1)
C(4B)	4243(2)	3393(4)	1679(2)	32(1)
C(5B)	4138(2)	4194(3)	1981(2)	25(1)
C(6B)	4183(2)	5213(3)	1822(2)	23(1)
C(7B)	4063(2)	5981(3)	2167(2)	23(1)
C(8B)	3966(2)	7664(3)	2474(2)	21(1)
C(9B)	3644(2)	7429(4)	2843(2)	27(1)
C(10B)	3585(2)	8154(4)	3219(2)	29(1)
C(11B)	3849(2)	9096(4)	3217(2)	27(1)
C(12B)	4145(2)	9358(3)	2834(2)	21(1)
C(13B)	4186(2)	8650(3)	2447(2)	18(1)
C(14B)	4666(2)	9734(3)	1944(2)	22(1)
C(15B)	4916(2)	10031(3)	1515(2)	21(1)
C(16B)	5100(2)	11057(3)	1506(2)	28(1)
C(17B)	5335(2)	11432(4)	1110(2)	31(1)
C(18B)	5394(2)	10788(4)	701(2)	31(1)
C(19B)	5222(2)	9793(4)	692(2)	26(1)
C(20B)	4983(2)	9383(3)	1093(2)	20(1)
C(21B)	3467(2)	9334(3)	682(2)	21(1)
C(22B)	3420(2)	10104(4)	1035(2)	29(1)

C(23B)	3454(2)	11107(4)	892(2)	36(1)
C(24B)	3529(2)	11353(4)	398(2)	38(1)
C(25B)	3568(2)	10598(4)	44(2)	37(1)
C(26B)	3361(2)	7248(3)	305(2)	22(1)
C(27B)	3856(2)	7047(4)	94(2)	26(1)
C(28B)	3792(2)	6421(4)	-341(2)	31(1)
C(29B)	3250(2)	5973(4)	-563(2)	38(1)
C(30B)	2763(2)	6160(4)	-365(2)	37(1)
C(31B)	2820(2)	6800(4)	72(2)	29(1)
C(32B)	2771(2)	7887(3)	1097(2)	20(1)
C(33B)	2705(2)	7133(4)	1442(2)	43(2)
C(34B)	2160(2)	6983(5)	1566(2)	54(2)
C(35B)	1683(2)	7588(4)	1346(2)	41(1)
C(36B)	1738(2)	8336(4)	998(2)	42(1)
C(37B)	2283(2)	8494(4)	880(2)	35(1)
Cl(1S)	2025(1)	7981(2)	3255(1)	94(1)
C(1S)	1897(3)	7087(6)	3713(3)	76(2)
Cl(2S)	2501(1)	6267(2)	3914(1)	91(1)
C(2S)	2860(3)	4087(6)	518(3)	73(2)
Cl(3S)	2466(1)	4704(2)	909(1)	92(1)
C(3S)	4162(3)	3074(5)	-891(2)	61(2)
Cl(4S)	2368(1)	3554(2)	-43(1)	98(1)
C(4S)	7268(3)	9113(5)	1931(3)	68(2)
Cl(5S)	4431(1)	3302(2)	-228(1)	108(1)
Cl(6S)	3386(1)	3265(2)	-1120(1)	84(1)
Cl(7S)	7525(2)	9760(2)	2516(1)	157(2)
Cl(8S)	6537(1)	9435(2)	1634(1)	77(1)

Table 3. Bond lengths [A] and angles [deg] for resalp3.

C(46)-C(21B)	1.388(6)
C(46)-C(25B)	1.394(7)
Re(1A)-O(2A)	2.001(3)
Re(1A)-O(1A)	2.002(3)
Re(1A)-N(1A)	2.026(4)
Re(1A)-N(2A)	2.037(4)
Re(1A)-P(1A)	2.4128(11)
Re(1A)-Cl(1A)	2.4550(11)
P(1A)-C(33A)	1.824(4)
P(1A)-C(21A)	1.829(5)
P(1A)-C(27A)	1.836(4)
O(1A)-C(1A)	1.327(5)
N(1A)-C(7A)	1.318(6)
N(1A)-C(8A)	1.434(6)

C(1A)-C(2A)	1.400(6)
C(1A)-C(6A)	1.424(6)
O(2A)-C(20A)	1.320(5)
N(2A)-C(14A)	1.312(6)
N(2A)-C(13A)	1.446(6)
C(2A)-C(3A)	1.377(7)
C(3A)-C(4A)	1.398(7)
C(4A)-C(5A)	1.368(6)
C(5A)-C(6A)	1.415(6)
C(6A)-C(7A)	1.437(6)
C(8A)-C(9A)	1.391(6)
C(8A)-C(13A)	1.395(6)
C(9A)-C(10A)	1.377(7)
C(10A)-C(11A)	1.393(7)
C(11A)-C(12A)	1.385(7)
C(12A)-C(13A)	1.380(6)
C(14A)-C(15A)	1.428(6)
C(15A)-C(16A)	1.419(6)
C(15A)-C(20A)	1.427(6)
C(16A)-C(17A)	1.367(7)
C(17A)-C(18A)	1.400(7)
C(18A)-C(19A)	1.364(7)
C(19A)-C(20A)	1.412(6)
C(21A)-C(26A)	1.390(6)
C(21A)-C(22A)	1.392(6)
C(22A)-C(23A)	1.388(6)
C(23A)-C(24A)	1.367(7)
C(24A)-C(25A)	1.383(7)
C(25A)-C(26A)	1.384(7)
C(27A)-C(28A)	1.382(6)
C(27A)-C(32A)	1.385(6)
C(28A)-C(29A)	1.386(7)
C(29A)-C(30A)	1.364(7)
C(30A)-C(31A)	1.373(7)
C(31A)-C(32A)	1.385(6)
C(33A)-C(38A)	1.382(6)
C(33A)-C(34A)	1.403(6)
C(34A)-C(35A)	1.379(7)
C(35A)-C(36A)	1.382(7)
C(36A)-C(37A)	1.376(7)
C(37A)-C(38A)	1.388(7)
Re(1B)-O(1B)	1.996(3)
Re(1B)-O(2B)	2.011(3)
Re(1B)-N(1B)	2.024(4)
Re(1B)-N(2B)	2.032(3)
Re(1B)-P(1B)	2.4218(12)

Re(1B)-Cl(1B)	2.4563(11)
P(1B)-C(21B)	1.828(5)
P(1B)-C(32B)	1.829(4)
P(1B)-C(26B)	1.829(4)
O(1B)-C(1B)	1.317(5)
N(1B)-C(7B)	1.317(5)
N(1B)-C(8B)	1.438(5)
C(1B)-C(2B)	1.409(6)
C(1B)-C(6B)	1.421(6)
O(2B)-C(20B)	1.318(5)
N(2B)-C(14B)	1.308(5)
N(2B)-C(13B)	1.440(5)
C(2B)-C(3B)	1.373(6)
C(3B)-C(4B)	1.400(6)
C(4B)-C(5B)	1.374(6)
C(5B)-C(6B)	1.419(6)
C(6B)-C(7B)	1.426(6)
C(8B)-C(9B)	1.385(6)
C(8B)-C(13B)	1.404(6)
C(9B)-C(10B)	1.399(6)
C(10B)-C(11B)	1.385(7)
C(11B)-C(12B)	1.383(6)
C(12B)-C(13B)	1.393(6)
C(14B)-C(15B)	1.431(6)
C(15B)-C(16B)	1.421(6)
C(15B)-C(20B)	1.431(6)
C(16B)-C(17B)	1.370(6)
C(17B)-C(18B)	1.393(7)
C(18B)-C(19B)	1.370(6)
C(19B)-C(20B)	1.404(6)
C(21B)-C(22B)	1.392(6)
C(22B)-C(23B)	1.382(7)
C(23B)-C(24B)	1.376(7)
C(24B)-C(25B)	1.375(7)
C(26B)-C(31B)	1.378(6)
C(26B)-C(27B)	1.410(6)
C(27B)-C(28B)	1.377(6)
C(28B)-C(29B)	1.375(7)
C(29B)-C(30B)	1.370(7)
C(30B)-C(31B)	1.394(6)
C(32B)-C(33B)	1.372(6)
C(32B)-C(37B)	1.382(6)
C(33B)-C(34B)	1.388(7)
C(34B)-C(35B)	1.365(8)
C(35B)-C(36B)	1.367(7)
C(36B)-C(37B)	1.383(6)

Cl(1S)-C(1S)	1.752(7)
C(1S)-Cl(2S)	1.740(7)
C(2S)-Cl(3S)	1.727(7)
C(2S)-Cl(4S)	1.756(7)
C(3S)-Cl(5S)	1.706(6)
C(3S)-Cl(6S)	1.758(6)
C(4S)-Cl(7S)	1.714(7)
C(4S)-Cl(8S)	1.724(7)

C(21B)-C(46)-C(25B)	119.6(5)
O(2A)-Re(1A)-O(1A)	97.14(12)
O(2A)-Re(1A)-N(1A)	170.81(13)
O(1A)-Re(1A)-N(1A)	90.28(13)
O(2A)-Re(1A)-N(2A)	91.29(13)
O(1A)-Re(1A)-N(2A)	170.48(13)
N(1A)-Re(1A)-N(2A)	80.92(14)
O(2A)-Re(1A)-P(1A)	87.90(9)
O(1A)-Re(1A)-P(1A)	93.94(9)
N(1A)-Re(1A)-P(1A)	97.01(10)
N(2A)-Re(1A)-P(1A)	90.77(9)
O(2A)-Re(1A)-Cl(1A)	87.88(9)
O(1A)-Re(1A)-Cl(1A)	86.85(9)
N(1A)-Re(1A)-Cl(1A)	87.13(10)
N(2A)-Re(1A)-Cl(1A)	89.06(9)
P(1A)-Re(1A)-Cl(1A)	175.77(4)
C(33A)-P(1A)-C(21A)	107.0(2)
C(33A)-P(1A)-C(27A)	102.7(2)
C(21A)-P(1A)-C(27A)	103.5(2)
C(33A)-P(1A)-Re(1A)	116.54(14)
C(21A)-P(1A)-Re(1A)	107.81(14)
C(27A)-P(1A)-Re(1A)	118.11(15)
C(1A)-O(1A)-Re(1A)	125.5(3)
C(7A)-N(1A)-C(8A)	121.3(4)
C(7A)-N(1A)-Re(1A)	124.8(3)
C(8A)-N(1A)-Re(1A)	113.2(3)
O(1A)-C(1A)-C(2A)	117.4(4)
O(1A)-C(1A)-C(6A)	123.1(4)
C(2A)-C(1A)-C(6A)	119.5(4)
C(20A)-O(2A)-Re(1A)	127.6(3)
C(14A)-N(2A)-C(13A)	121.7(4)
C(14A)-N(2A)-Re(1A)	125.2(3)
C(13A)-N(2A)-Re(1A)	113.1(3)
C(3A)-C(2A)-C(1A)	121.0(5)
C(2A)-C(3A)-C(4A)	120.3(4)
C(5A)-C(4A)-C(3A)	119.4(4)
C(4A)-C(5A)-C(6A)	122.3(5)

C(5A)-C(6A)-C(1A)	117.4(4)
C(5A)-C(6A)-C(7A)	117.7(4)
C(1A)-C(6A)-C(7A)	124.8(4)
N(1A)-C(7A)-C(6A)	125.5(4)
C(9A)-C(8A)-C(13A)	119.5(4)
C(9A)-C(8A)-N(1A)	124.6(4)
C(13A)-C(8A)-N(1A)	115.9(4)
C(10A)-C(9A)-C(8A)	120.2(5)
C(9A)-C(10A)-C(11A)	119.9(5)
C(12A)-C(11A)-C(10A)	120.2(5)
C(13A)-C(12A)-C(11A)	119.7(5)
C(12A)-C(13A)-C(8A)	120.4(4)
C(12A)-C(13A)-N(2A)	124.5(4)
C(8A)-C(13A)-N(2A)	115.2(4)
N(2A)-C(14A)-C(15A)	125.7(4)
C(16A)-C(15A)-C(20A)	117.1(4)
C(16A)-C(15A)-C(14A)	117.0(4)
C(20A)-C(15A)-C(14A)	125.8(4)
C(17A)-C(16A)-C(15A)	122.9(5)
C(16A)-C(17A)-C(18A)	118.8(5)
C(19A)-C(18A)-C(17A)	121.0(5)
C(18A)-C(19A)-C(20A)	121.1(5)
O(2A)-C(20A)-C(19A)	117.4(4)
O(2A)-C(20A)-C(15A)	123.5(4)
C(19A)-C(20A)-C(15A)	119.1(4)
C(26A)-C(21A)-C(22A)	118.9(4)
C(26A)-C(21A)-P(1A)	119.8(4)
C(22A)-C(21A)-P(1A)	120.9(4)
C(23A)-C(22A)-C(21A)	119.9(5)
C(24A)-C(23A)-C(22A)	120.9(5)
C(23A)-C(24A)-C(25A)	119.7(5)
C(24A)-C(25A)-C(26A)	120.1(5)
C(25A)-C(26A)-C(21A)	120.5(5)
C(28A)-C(27A)-C(32A)	119.0(4)
C(28A)-C(27A)-P(1A)	120.0(4)
C(32A)-C(27A)-P(1A)	121.0(3)
C(27A)-C(28A)-C(29A)	120.3(5)
C(30A)-C(29A)-C(28A)	120.3(5)
C(29A)-C(30A)-C(31A)	120.0(5)
C(30A)-C(31A)-C(32A)	120.2(5)
C(27A)-C(32A)-C(31A)	120.2(4)
C(38A)-C(33A)-C(34A)	118.6(4)
C(38A)-C(33A)-P(1A)	124.1(4)
C(34A)-C(33A)-P(1A)	117.2(3)
C(35A)-C(34A)-C(33A)	120.5(5)
C(34A)-C(35A)-C(36A)	120.2(5)

C(37A)-C(36A)-C(35A)	119.6(5)
C(36A)-C(37A)-C(38A)	120.6(5)
C(33A)-C(38A)-C(37A)	120.4(5)
O(1B)-Re(1B)-O(2B)	96.08(11)
O(1B)-Re(1B)-N(1B)	91.20(13)
O(2B)-Re(1B)-N(1B)	171.64(13)
O(1B)-Re(1B)-N(2B)	171.35(12)
O(2B)-Re(1B)-N(2B)	91.22(12)
N(1B)-Re(1B)-N(2B)	81.21(14)
O(1B)-Re(1B)-P(1B)	88.85(9)
O(2B)-Re(1B)-P(1B)	87.00(9)
N(1B)-Re(1B)-P(1B)	97.29(10)
N(2B)-Re(1B)-P(1B)	96.19(10)
O(1B)-Re(1B)-Cl(1B)	86.29(9)
O(2B)-Re(1B)-Cl(1B)	89.84(9)
N(1B)-Re(1B)-Cl(1B)	86.51(10)
N(2B)-Re(1B)-Cl(1B)	89.10(10)
P(1B)-Re(1B)-Cl(1B)	173.89(4)
C(21B)-P(1B)-C(32B)	103.65(19)
C(21B)-P(1B)-C(26B)	105.5(2)
C(32B)-P(1B)-C(26B)	103.1(2)
C(21B)-P(1B)-Re(1B)	110.74(14)
C(32B)-P(1B)-Re(1B)	121.20(15)
C(26B)-P(1B)-Re(1B)	111.27(15)
C(1B)-O(1B)-Re(1B)	127.0(3)
C(7B)-N(1B)-C(8B)	120.2(4)
C(7B)-N(1B)-Re(1B)	125.0(3)
C(8B)-N(1B)-Re(1B)	113.9(3)
O(1B)-C(1B)-C(2B)	116.7(4)
O(1B)-C(1B)-C(6B)	124.4(4)
C(2B)-C(1B)-C(6B)	118.9(4)
C(20B)-O(2B)-Re(1B)	127.7(3)
C(14B)-N(2B)-C(13B)	120.6(4)
C(14B)-N(2B)-Re(1B)	125.8(3)
C(13B)-N(2B)-Re(1B)	113.5(3)
C(3B)-C(2B)-C(1B)	121.2(4)
C(2B)-C(3B)-C(4B)	120.6(4)
C(5B)-C(4B)-C(3B)	119.4(4)
C(4B)-C(5B)-C(6B)	121.7(4)
C(5B)-C(6B)-C(1B)	118.2(4)
C(5B)-C(6B)-C(7B)	116.7(4)
C(1B)-C(6B)-C(7B)	125.1(4)
N(1B)-C(7B)-C(6B)	125.6(4)
C(9B)-C(8B)-C(13B)	120.4(4)
C(9B)-C(8B)-N(1B)	124.5(4)
C(13B)-C(8B)-N(1B)	115.1(4)

C(8B)-C(9B)-C(10B)	119.5(4)
C(11B)-C(10B)-C(9B)	119.4(4)
C(12B)-C(11B)-C(10B)	121.6(4)
C(11B)-C(12B)-C(13B)	119.1(4)
C(12B)-C(13B)-C(8B)	119.6(4)
C(12B)-C(13B)-N(2B)	124.8(4)
C(8B)-C(13B)-N(2B)	115.6(4)
N(2B)-C(14B)-C(15B)	126.0(4)
C(16B)-C(15B)-C(20B)	117.8(4)
C(16B)-C(15B)-C(14B)	117.0(4)
C(20B)-C(15B)-C(14B)	125.2(4)
C(17B)-C(16B)-C(15B)	122.2(4)
C(16B)-C(17B)-C(18B)	119.1(4)
C(19B)-C(18B)-C(17B)	120.9(4)
C(18B)-C(19B)-C(20B)	121.5(4)
O(2B)-C(20B)-C(19B)	117.4(4)
O(2B)-C(20B)-C(15B)	124.0(4)
C(19B)-C(20B)-C(15B)	118.5(4)
C(46)-C(21B)-C(22B)	119.4(4)
C(46)-C(21B)-P(1B)	121.9(3)
C(22B)-C(21B)-P(1B)	118.6(4)
C(23B)-C(22B)-C(21B)	120.2(5)
C(24B)-C(23B)-C(22B)	120.4(5)
C(25B)-C(24B)-C(23B)	119.9(5)
C(24B)-C(25B)-C(46)	120.4(5)
C(31B)-C(26B)-C(27B)	118.7(4)
C(31B)-C(26B)-P(1B)	122.7(3)
C(27B)-C(26B)-P(1B)	118.5(3)
C(28B)-C(27B)-C(26B)	120.1(4)
C(29B)-C(28B)-C(27B)	120.1(4)
C(30B)-C(29B)-C(28B)	120.7(5)
C(29B)-C(30B)-C(31B)	119.7(5)
C(26B)-C(31B)-C(30B)	120.6(4)
C(33B)-C(32B)-C(37B)	118.4(4)
C(33B)-C(32B)-P(1B)	119.9(4)
C(37B)-C(32B)-P(1B)	121.6(3)
C(32B)-C(33B)-C(34B)	120.6(5)
C(35B)-C(34B)-C(33B)	120.2(5)
C(34B)-C(35B)-C(36B)	120.0(5)
C(35B)-C(36B)-C(37B)	119.8(5)
C(32B)-C(37B)-C(36B)	120.9(5)
Cl(2S)-C(1S)-Cl(1S)	111.3(4)
Cl(3S)-C(2S)-Cl(4S)	110.6(4)
Cl(5S)-C(3S)-Cl(6S)	113.5(3)
Cl(7S)-C(4S)-Cl(8S)	111.0(4)

Symmetry transformations used to generate equivalent atoms:

Table 4. Anisotropic displacement parameters (A^2 x 10^3) for resalp3.
The anisotropic displacement factor exponent takes the form:
-2 pi^2 [h^2 a*^2 U11 + ... + 2 h k a* b* U12]

	U11	U22	U33	U23	U13	U12
C(46)	26(3)	28(3)	32(3)	3(2)	12(2)	3(2)
Re(1A)	21(1)	14(1)	20(1)	-1(1)	4(1)	-2(1)
Cl(1A)	26(1)	25(1)	37(1)	-2(1)	11(1)	-5(1)
P(1A)	22(1)	15(1)	20(1)	-2(1)	4(1)	-1(1)
O(1A)	34(2)	17(2)	22(2)	-3(1)	6(1)	-4(1)
N(1A)	21(2)	22(2)	20(2)	0(2)	5(2)	1(2)
C(1A)	25(2)	20(2)	28(3)	-4(2)	11(2)	1(2)
O(2A)	25(2)	21(2)	23(2)	-1(1)	1(1)	0(1)
N(2A)	18(2)	21(2)	23(2)	2(2)	7(2)	-2(2)
C(2A)	31(3)	23(3)	30(3)	-4(2)	6(2)	-4(2)
C(3A)	32(3)	17(3)	46(3)	-13(2)	15(2)	-6(2)
C(4A)	36(3)	13(2)	46(3)	4(2)	22(3)	4(2)
C(5A)	32(3)	23(3)	31(3)	3(2)	15(2)	6(2)
C(6A)	21(2)	19(3)	29(3)	-1(2)	8(2)	3(2)
C(7A)	22(2)	27(3)	24(3)	4(2)	4(2)	2(2)
C(8A)	22(2)	25(3)	22(2)	-2(2)	7(2)	-4(2)
C(9A)	32(3)	31(3)	25(3)	1(2)	4(2)	-2(2)
C(10A)	37(3)	42(3)	22(3)	-1(2)	-2(2)	-4(3)
C(11A)	44(3)	42(4)	31(3)	-14(3)	9(3)	-13(3)
C(12A)	35(3)	26(3)	28(3)	-6(2)	12(2)	-3(2)
C(13A)	24(2)	26(3)	20(2)	-3(2)	9(2)	-6(2)
C(14A)	24(3)	19(3)	33(3)	-2(2)	12(2)	-3(2)
C(15A)	22(2)	22(3)	33(3)	3(2)	14(2)	-3(2)
C(16A)	38(3)	27(3)	39(3)	0(2)	23(3)	3(2)
C(17A)	32(3)	30(3)	51(3)	14(3)	18(3)	10(2)
C(18A)	24(3)	35(3)	39(3)	14(3)	4(2)	-1(2)
C(19A)	22(3)	25(3)	37(3)	5(2)	1(2)	-1(2)
C(20A)	16(2)	23(3)	30(3)	3(2)	8(2)	-3(2)
C(21A)	21(2)	15(2)	31(3)	2(2)	11(2)	0(2)
C(22A)	24(2)	22(3)	33(3)	1(2)	10(2)	-1(2)
C(23A)	37(3)	17(3)	52(4)	-4(2)	19(3)	-1(2)

C(24A)	35(3)	19(3)	71(4)	10(3)	24(3)	7(2)
C(25A)	34(3)	32(3)	38(3)	13(3)	9(2)	7(2)
C(26A)	31(3)	25(3)	29(3)	0(2)	10(2)	-1(2)
C(27A)	27(3)	20(2)	23(2)	1(2)	9(2)	1(2)
C(28A)	28(3)	36(3)	28(3)	-8(2)	7(2)	-11(2)
C(29A)	34(3)	56(4)	38(3)	-9(3)	18(3)	-3(3)
C(30A)	41(3)	36(3)	25(3)	-7(2)	9(2)	5(2)
C(31A)	37(3)	40(3)	25(3)	-12(2)	1(2)	-9(2)
C(32A)	27(3)	34(3)	24(3)	-3(2)	7(2)	-3(2)
C(33A)	22(2)	20(2)	18(2)	0(2)	4(2)	0(2)
C(34A)	26(3)	31(3)	31(3)	2(2)	10(2)	2(2)
C(35A)	30(3)	39(3)	44(3)	10(3)	7(3)	11(3)
C(36A)	27(3)	48(4)	41(3)	-2(3)	-4(2)	6(3)
C(37A)	25(3)	40(4)	54(4)	-12(3)	-1(3)	-6(2)
C(38A)	28(3)	25(3)	39(3)	-1(2)	4(2)	0(2)
Re(1B)	20(1)	14(1)	18(1)	-1(1)	6(1)	1(1)
Cl(1B)	23(1)	26(1)	25(1)	-1(1)	3(1)	6(1)
P(1B)	20(1)	16(1)	20(1)	-1(1)	6(1)	0(1)
O(1B)	32(2)	12(2)	19(2)	0(1)	8(1)	4(1)
N(1B)	23(2)	17(2)	22(2)	-2(2)	5(2)	3(2)
C(1B)	21(2)	17(2)	26(3)	-7(2)	2(2)	-1(2)
O(2B)	27(2)	19(2)	23(2)	0(1)	13(1)	-3(1)
N(2B)	18(2)	17(2)	17(2)	0(2)	4(2)	0(2)
C(2B)	37(3)	22(3)	26(3)	-2(2)	9(2)	0(2)
C(3B)	40(3)	20(3)	28(3)	-8(2)	4(2)	6(2)
C(4B)	46(3)	16(3)	32(3)	2(2)	4(2)	1(2)
C(5B)	31(3)	21(3)	21(2)	2(2)	3(2)	-3(2)
C(6B)	25(2)	18(2)	22(2)	-2(2)	3(2)	-1(2)
C(7B)	26(2)	18(3)	25(2)	2(2)	8(2)	-2(2)
C(8B)	21(2)	21(2)	19(2)	-2(2)	3(2)	1(2)
C(9B)	33(3)	24(3)	25(3)	1(2)	11(2)	0(2)
C(10B)	33(3)	34(3)	23(3)	-2(2)	13(2)	5(2)
C(11B)	33(3)	26(3)	22(3)	-6(2)	9(2)	7(2)
C(12B)	25(2)	18(2)	20(2)	-3(2)	4(2)	0(2)
C(13B)	20(2)	18(2)	15(2)	0(2)	3(2)	3(2)
C(14B)	25(2)	15(2)	25(3)	-4(2)	5(2)	1(2)
C(15B)	20(2)	20(2)	22(2)	1(2)	5(2)	0(2)
C(16B)	31(3)	19(3)	33(3)	-6(2)	7(2)	-5(2)
C(17B)	31(3)	21(3)	38(3)	8(2)	4(2)	-9(2)
C(18B)	28(3)	37(3)	29(3)	9(2)	7(2)	-7(2)
C(19B)	27(3)	25(3)	27(3)	2(2)	9(2)	-3(2)
C(20B)	15(2)	18(2)	25(2)	3(2)	3(2)	0(2)
C(21B)	13(2)	19(2)	30(3)	0(2)	5(2)	2(2)
C(22B)	23(3)	28(3)	31(3)	-2(2)	0(2)	3(2)
C(23B)	34(3)	21(3)	49(3)	-8(2)	3(3)	2(2)
C(24B)	29(3)	17(3)	65(4)	10(3)	9(3)	-1(2)

C(25B)	33(3)	33(3)	49(3)	14(3)	19(3)	2(2)
C(26B)	25(2)	18(2)	22(2)	0(2)	6(2)	2(2)
C(27B)	27(3)	27(3)	22(3)	2(2)	4(2)	-1(2)
C(28B)	38(3)	32(3)	27(3)	0(2)	16(2)	2(2)
C(29B)	59(4)	32(3)	25(3)	-12(2)	14(3)	-6(3)
C(30B)	43(3)	39(3)	30(3)	-8(2)	10(2)	-16(3)
C(31B)	27(3)	27(3)	32(3)	-8(2)	10(2)	-6(2)
C(32B)	18(2)	22(3)	22(2)	-2(2)	6(2)	0(2)
C(33B)	23(3)	51(4)	52(4)	28(3)	3(3)	-3(2)
C(34B)	34(3)	65(4)	63(4)	31(3)	14(3)	-12(3)
C(35B)	28(3)	49(4)	51(3)	-1(3)	19(3)	-7(3)
C(36B)	25(3)	28(3)	74(4)	5(3)	17(3)	6(2)
C(37B)	27(3)	26(3)	51(3)	8(2)	10(2)	5(2)
Cl(1S)	54(1)	108(2)	105(2)	33(1)	-10(1)	-1(1)
C(1S)	51(4)	76(6)	104(6)	-12(5)	26(4)	-19(4)
Cl(2S)	80(1)	69(1)	111(2)	4(1)	0(1)	8(1)
C(2S)	50(4)	71(5)	97(6)	15(4)	16(4)	22(4)
Cl(3S)	130(2)	79(2)	84(1)	4(1)	56(1)	5(1)
C(3S)	68(4)	72(5)	49(4)	2(3)	29(3)	29(4)
Cl(4S)	150(2)	63(1)	74(1)	-6(1)	13(1)	-7(1)
C(4S)	73(5)	58(5)	65(5)	-1(4)	0(4)	14(4)
Cl(5S)	93(2)	178(3)	58(1)	-47(2)	31(1)	-23(2)
Cl(6S)	61(1)	71(1)	118(2)	-22(1)	19(1)	17(1)
Cl(7S)	206(3)	65(2)	125(2)	-20(1)	-101(2)	27(2)
Cl(8S)	53(1)	81(1)	92(1)	-19(1)	6(1)	11(1)

Table 5. Hydrogen coordinates (x 10^4) and isotropic displacement parameters (A^2 x 10^3) for resalp3.

	x	y	z	U(eq)
H(46)	3553	9064	-68	33
H(2A)	-114	-1904	764	34
H(3A)	-111	-3487	1152	37
H(4A)	368	-3727	2053	36
H(5A)	796	-2364	2564	33
H(7A)	1057	-650	2694	29
H(9A)	1646	423	3165	36
H(10A)	1941	1717	3782	42
H(11A)	1513	3330	3611	47
H(12A)	838	3671	2797	35

H(14A)	148	3717	2125	29
H(16A)	-517	4814	1591	39
H(17A)	-1198	5278	817	43
H(18A)	-1424	4141	98	40
H(19A)	-954	2594	151	35
H(22A)	1357	3542	1799	31
H(23A)	1143	5240	1583	41
H(24A)	729	5720	713	48
H(25A)	510	4496	44	42
H(26A)	737	2799	248	33
H(28A)	2130	1588	670	37
H(29A)	2251	917	-126	49
H(30A)	1492	-14	-670	41
H(31A)	602	-281	-427	43
H(32A)	461	425	356	34
H(34A)	1785	18	1810	34
H(35A)	2721	-265	2380	46
H(36A)	3410	1057	2595	49
H(37A)	3182	2632	2195	50
H(38A)	2254	2918	1607	38
H(2B)	4540	4673	702	34
H(3B)	4447	3031	979	36
H(4B)	4218	2717	1797	39
H(5B)	4033	4062	2306	30
H(7B)	3956	5764	2480	27
H(9B)	3466	6780	2840	32
H(10B)	3366	8002	3474	35
H(11B)	3827	9574	3484	32
H(12B)	4317	10012	2835	25
H(14B)	4665	10227	2211	26
H(16B)	5058	11498	1784	33
H(17B)	5455	12121	1114	37
H(18B)	5557	11043	425	38
H(19B)	5266	9372	408	31
H(22B)	3364	9940	1375	34
H(23B)	3425	11629	1136	43
H(24B)	3554	12043	302	45
H(25B)	3620	10770	-297	44
H(27B)	4233	7344	251	31
H(28B)	4124	6298	-487	37
H(29B)	3212	5529	-858	46
H(30B)	2388	5855	-524	44
H(31B)	2483	6929	209	34
H(33B)	3035	6709	1596	52
H(34B)	2119	6459	1805	64
H(35B)	1312	7489	1435	49

H(36B)	1404	8745	837	50
H(37B)	2323	9028	646	42
H(1S1)	1826	7443	4027	91
H(1S2)	1533	6691	3549	91
H(2S1)	3109	3546	728	88
H(2S2)	3129	4573	404	88
H(3S1)	4256	2366	-966	73
H(3S2)	4370	3525	-1092	73
H(4S1)	7295	8375	2002	82
H(4S2)	7523	9273	1687	82

Table 6. Torsion angles [deg] for resalp3.

O(2A)-Re(1A)-P(1A)-C(33A)	166.40(18)
O(1A)-Re(1A)-P(1A)-C(33A)	-96.59(18)
N(1A)-Re(1A)-P(1A)-C(33A)	-5.81(19)
N(2A)-Re(1A)-P(1A)-C(33A)	75.14(19)
Cl(1A)-Re(1A)-P(1A)-C(33A)	162.7(5)
O(2A)-Re(1A)-P(1A)-C(21A)	46.21(18)
O(1A)-Re(1A)-P(1A)-C(21A)	143.23(18)
N(1A)-Re(1A)-P(1A)-C(21A)	-126.00(19)
N(2A)-Re(1A)-P(1A)-C(21A)	-45.05(19)
Cl(1A)-Re(1A)-P(1A)-C(21A)	42.5(6)
O(2A)-Re(1A)-P(1A)-C(27A)	-70.52(19)
O(1A)-Re(1A)-P(1A)-C(27A)	26.50(19)
N(1A)-Re(1A)-P(1A)-C(27A)	117.3(2)
N(2A)-Re(1A)-P(1A)-C(27A)	-161.8(2)
Cl(1A)-Re(1A)-P(1A)-C(27A)	-74.2(6)
O(2A)-Re(1A)-O(1A)-C(1A)	-147.4(3)
N(1A)-Re(1A)-O(1A)-C(1A)	27.2(3)
N(2A)-Re(1A)-O(1A)-C(1A)	4.8(10)
P(1A)-Re(1A)-O(1A)-C(1A)	124.3(3)
Cl(1A)-Re(1A)-O(1A)-C(1A)	-59.9(3)
O(2A)-Re(1A)-N(1A)-C(7A)	126.4(8)
O(1A)-Re(1A)-N(1A)-C(7A)	-17.6(3)
N(2A)-Re(1A)-N(1A)-C(7A)	158.8(4)
P(1A)-Re(1A)-N(1A)-C(7A)	-111.6(3)
Cl(1A)-Re(1A)-N(1A)-C(7A)	69.3(3)
O(2A)-Re(1A)-N(1A)-C(8A)	-44.1(10)
O(1A)-Re(1A)-N(1A)-C(8A)	171.9(3)
N(2A)-Re(1A)-N(1A)-C(8A)	-11.8(3)
P(1A)-Re(1A)-N(1A)-C(8A)	77.9(3)
Cl(1A)-Re(1A)-N(1A)-C(8A)	-101.3(3)
Re(1A)-O(1A)-C(1A)-C(2A)	156.8(3)

Re(1A)-O(1A)-C(1A)-C(6A)	-24.4(6)
O(1A)-Re(1A)-O(2A)-C(20A)	165.0(3)
N(1A)-Re(1A)-O(2A)-C(20A)	21.3(10)
N(2A)-Re(1A)-O(2A)-C(20A)	-10.6(3)
P(1A)-Re(1A)-O(2A)-C(20A)	-101.3(3)
Cl(1A)-Re(1A)-O(2A)-C(20A)	78.4(3)
O(2A)-Re(1A)-N(2A)-C(14A)	8.1(3)
O(1A)-Re(1A)-N(2A)-C(14A)	-144.3(7)
N(1A)-Re(1A)-N(2A)-C(14A)	-167.0(3)
P(1A)-Re(1A)-N(2A)-C(14A)	96.0(3)
Cl(1A)-Re(1A)-N(2A)-C(14A)	-79.8(3)
O(2A)-Re(1A)-N(2A)-C(13A)	-174.8(3)
O(1A)-Re(1A)-N(2A)-C(13A)	32.8(9)
N(1A)-Re(1A)-N(2A)-C(13A)	10.1(3)
P(1A)-Re(1A)-N(2A)-C(13A)	-86.9(3)
Cl(1A)-Re(1A)-N(2A)-C(13A)	97.3(3)
O(1A)-C(1A)-C(2A)-C(3A)	179.6(4)
C(6A)-C(1A)-C(2A)-C(3A)	0.7(7)
C(1A)-C(2A)-C(3A)-C(4A)	-2.2(7)
C(2A)-C(3A)-C(4A)-C(5A)	1.7(7)
C(3A)-C(4A)-C(5A)-C(6A)	0.4(7)
C(4A)-C(5A)-C(6A)-C(1A)	-1.8(6)
C(4A)-C(5A)-C(6A)-C(7A)	177.4(4)
O(1A)-C(1A)-C(6A)-C(5A)	-177.5(4)
C(2A)-C(1A)-C(6A)-C(5A)	1.3(6)
O(1A)-C(1A)-C(6A)-C(7A)	3.3(7)
C(2A)-C(1A)-C(6A)-C(7A)	-178.0(4)
C(8A)-N(1A)-C(7A)-C(6A)	175.0(4)
Re(1A)-N(1A)-C(7A)-C(6A)	5.2(6)
C(5A)-C(6A)-C(7A)-N(1A)	-172.3(4)
C(1A)-C(6A)-C(7A)-N(1A)	6.9(7)
C(7A)-N(1A)-C(8A)-C(9A)	21.6(6)
Re(1A)-N(1A)-C(8A)-C(9A)	-167.5(3)
C(7A)-N(1A)-C(8A)-C(13A)	-159.2(4)
Re(1A)-N(1A)-C(8A)-C(13A)	11.7(4)
C(13A)-C(8A)-C(9A)-C(10A)	3.2(7)
N(1A)-C(8A)-C(9A)-C(10A)	-177.6(4)
C(8A)-C(9A)-C(10A)-C(11A)	-0.5(7)
C(9A)-C(10A)-C(11A)-C(12A)	-2.4(7)
C(10A)-C(11A)-C(12A)-C(13A)	2.5(7)
C(11A)-C(12A)-C(13A)-C(8A)	0.2(7)
C(11A)-C(12A)-C(13A)-N(2A)	-178.8(4)
C(9A)-C(8A)-C(13A)-C(12A)	-3.1(6)
N(1A)-C(8A)-C(13A)-C(12A)	177.7(4)
C(9A)-C(8A)-C(13A)-N(2A)	176.0(4)
N(1A)-C(8A)-C(13A)-N(2A)	-3.2(5)

C(14A)-N(2A)-C(13A)-C(12A)	-10.4(6)
Re(1A)-N(2A)-C(13A)-C(12A)	172.3(3)
C(14A)-N(2A)-C(13A)-C(8A)	170.5(4)
Re(1A)-N(2A)-C(13A)-C(8A)	-6.7(4)
C(13A)-N(2A)-C(14A)-C(15A)	179.2(4)
Re(1A)-N(2A)-C(14A)-C(15A)	-4.0(6)
N(2A)-C(14A)-C(15A)-C(16A)	-179.8(4)
N(2A)-C(14A)-C(15A)-C(20A)	-1.6(7)
C(20A)-C(15A)-C(16A)-C(17A)	1.7(6)
C(14A)-C(15A)-C(16A)-C(17A)	-180.0(4)
C(15A)-C(16A)-C(17A)-C(18A)	-0.6(7)
C(16A)-C(17A)-C(18A)-C(19A)	-1.0(7)
C(17A)-C(18A)-C(19A)-C(20A)	1.2(7)
Re(1A)-O(2A)-C(20A)-C(19A)	-172.5(3)
Re(1A)-O(2A)-C(20A)-C(15A)	8.8(6)
C(18A)-C(19A)-C(20A)-O(2A)	-178.8(4)
C(18A)-C(19A)-C(20A)-C(15A)	0.0(6)
C(16A)-C(15A)-C(20A)-O(2A)	177.3(4)
C(14A)-C(15A)-C(20A)-O(2A)	-0.8(7)
C(16A)-C(15A)-C(20A)-C(19A)	-1.4(6)
C(14A)-C(15A)-C(20A)-C(19A)	-179.5(4)
C(33A)-P(1A)-C(21A)-C(26A)	137.9(4)
C(27A)-P(1A)-C(21A)-C(26A)	29.9(4)
Re(1A)-P(1A)-C(21A)-C(26A)	-96.0(3)
C(33A)-P(1A)-C(21A)-C(22A)	-49.5(4)
C(27A)-P(1A)-C(21A)-C(22A)	-157.6(4)
Re(1A)-P(1A)-C(21A)-C(22A)	76.5(4)
C(26A)-C(21A)-C(22A)-C(23A)	-1.6(6)
P(1A)-C(21A)-C(22A)-C(23A)	-174.2(3)
C(21A)-C(22A)-C(23A)-C(24A)	0.9(7)
C(22A)-C(23A)-C(24A)-C(25A)	0.5(7)
C(23A)-C(24A)-C(25A)-C(26A)	-1.2(8)
C(24A)-C(25A)-C(26A)-C(21A)	0.5(7)
C(22A)-C(21A)-C(26A)-C(25A)	0.9(7)
P(1A)-C(21A)-C(26A)-C(25A)	173.6(4)
C(33A)-P(1A)-C(27A)-C(28A)	-37.5(4)
C(21A)-P(1A)-C(27A)-C(28A)	73.7(4)
Re(1A)-P(1A)-C(27A)-C(28A)	-167.3(3)
C(33A)-P(1A)-C(27A)-C(32A)	143.5(4)
C(21A)-P(1A)-C(27A)-C(32A)	-105.3(4)
Re(1A)-P(1A)-C(27A)-C(32A)	13.7(4)
C(32A)-C(27A)-C(28A)-C(29A)	0.9(8)
P(1A)-C(27A)-C(28A)-C(29A)	-178.1(4)
C(27A)-C(28A)-C(29A)-C(30A)	-1.0(8)
C(28A)-C(29A)-C(30A)-C(31A)	0.1(8)
C(29A)-C(30A)-C(31A)-C(32A)	0.9(8)

C(28A)-C(27A)-C(32A)-C(31A)	0.1(7)
P(1A)-C(27A)-C(32A)-C(31A)	179.1(4)
C(30A)-C(31A)-C(32A)-C(27A)	-1.0(8)
C(21A)-P(1A)-C(33A)-C(38A)	-10.4(4)
C(27A)-P(1A)-C(33A)-C(38A)	98.2(4)
Re(1A)-P(1A)-C(33A)-C(38A)	-131.0(4)
C(21A)-P(1A)-C(33A)-C(34A)	172.9(3)
C(27A)-P(1A)-C(33A)-C(34A)	-78.5(4)
Re(1A)-P(1A)-C(33A)-C(34A)	52.3(4)
C(38A)-C(33A)-C(34A)-C(35A)	1.9(7)
P(1A)-C(33A)-C(34A)-C(35A)	178.8(4)
C(33A)-C(34A)-C(35A)-C(36A)	0.5(7)
C(34A)-C(35A)-C(36A)-C(37A)	-2.2(8)
C(35A)-C(36A)-C(37A)-C(38A)	1.5(8)
C(34A)-C(33A)-C(38A)-C(37A)	-2.7(7)
P(1A)-C(33A)-C(38A)-C(37A)	-179.3(4)
C(36A)-C(37A)-C(38A)-C(33A)	1.0(8)
O(1B)-Re(1B)-P(1B)-C(21B)	-137.14(17)
O(2B)-Re(1B)-P(1B)-C(21B)	-40.99(17)
N(1B)-Re(1B)-P(1B)-C(21B)	131.80(18)
N(2B)-Re(1B)-P(1B)-C(21B)	49.91(18)
Cl(1B)-Re(1B)-P(1B)-C(21B)	-99.9(4)
O(1B)-Re(1B)-P(1B)-C(32B)	101.24(19)
O(2B)-Re(1B)-P(1B)-C(32B)	-162.61(19)
N(1B)-Re(1B)-P(1B)-C(32B)	10.2(2)
N(2B)-Re(1B)-P(1B)-C(32B)	-71.71(19)
Cl(1B)-Re(1B)-P(1B)-C(32B)	138.5(4)
O(1B)-Re(1B)-P(1B)-C(26B)	-20.12(17)
O(2B)-Re(1B)-P(1B)-C(26B)	76.03(18)
N(1B)-Re(1B)-P(1B)-C(26B)	-111.18(18)
N(2B)-Re(1B)-P(1B)-C(26B)	166.93(18)
Cl(1B)-Re(1B)-P(1B)-C(26B)	17.1(4)
O(2B)-Re(1B)-O(1B)-C(1B)	162.9(3)
N(1B)-Re(1B)-O(1B)-C(1B)	-12.9(3)
N(2B)-Re(1B)-O(1B)-C(1B)	15.6(10)
P(1B)-Re(1B)-O(1B)-C(1B)	-110.2(3)
Cl(1B)-Re(1B)-O(1B)-C(1B)	73.5(3)
O(1B)-Re(1B)-N(1B)-C(7B)	13.5(4)
O(2B)-Re(1B)-N(1B)-C(7B)	-137.0(8)
N(2B)-Re(1B)-N(1B)-C(7B)	-162.3(4)
P(1B)-Re(1B)-N(1B)-C(7B)	102.5(4)
Cl(1B)-Re(1B)-N(1B)-C(7B)	-72.7(4)
O(1B)-Re(1B)-N(1B)-C(8B)	-177.2(3)
O(2B)-Re(1B)-N(1B)-C(8B)	32.3(10)
N(2B)-Re(1B)-N(1B)-C(8B)	7.0(3)
P(1B)-Re(1B)-N(1B)-C(8B)	-88.2(3)

Cl(1B)-Re(1B)-N(1B)-C(8B)	96.6(3)
Re(1B)-O(1B)-C(1B)-C(2B)	-172.9(3)
Re(1B)-O(1B)-C(1B)-C(6B)	8.5(6)
O(1B)-Re(1B)-O(2B)-C(20B)	-175.5(3)
N(1B)-Re(1B)-O(2B)-C(20B)	-25.1(11)
N(2B)-Re(1B)-O(2B)-C(20B)	-0.1(3)
P(1B)-Re(1B)-O(2B)-C(20B)	96.0(3)
Cl(1B)-Re(1B)-O(2B)-C(20B)	-89.2(3)
O(1B)-Re(1B)-N(2B)-C(14B)	145.4(7)
O(2B)-Re(1B)-N(2B)-C(14B)	-2.2(4)
N(1B)-Re(1B)-N(2B)-C(14B)	174.2(4)
P(1B)-Re(1B)-N(2B)-C(14B)	-89.3(3)
Cl(1B)-Re(1B)-N(2B)-C(14B)	87.6(3)
O(1B)-Re(1B)-N(2B)-C(13B)	-32.2(10)
O(2B)-Re(1B)-N(2B)-C(13B)	-179.7(3)
N(1B)-Re(1B)-N(2B)-C(13B)	-3.3(3)
P(1B)-Re(1B)-N(2B)-C(13B)	93.2(3)
Cl(1B)-Re(1B)-N(2B)-C(13B)	-89.9(3)
O(1B)-C(1B)-C(2B)-C(3B)	178.9(4)
C(6B)-C(1B)-C(2B)-C(3B)	-2.5(7)
C(1B)-C(2B)-C(3B)-C(4B)	-0.2(7)
C(2B)-C(3B)-C(4B)-C(5B)	2.1(7)
C(3B)-C(4B)-C(5B)-C(6B)	-1.3(7)
C(4B)-C(5B)-C(6B)-C(1B)	-1.3(7)
C(4B)-C(5B)-C(6B)-C(7B)	179.8(4)
O(1B)-C(1B)-C(6B)-C(5B)	-178.3(4)
C(2B)-C(1B)-C(6B)-C(5B)	3.1(6)
O(1B)-C(1B)-C(6B)-C(7B)	0.5(7)
C(2B)-C(1B)-C(6B)-C(7B)	-178.1(4)
C(8B)-N(1B)-C(7B)-C(6B)	-178.8(4)
Re(1B)-N(1B)-C(7B)-C(6B)	-10.1(6)
C(5B)-C(6B)-C(7B)-N(1B)	179.4(4)
C(1B)-C(6B)-C(7B)-N(1B)	0.6(7)
C(7B)-N(1B)-C(8B)-C(9B)	-21.5(6)
Re(1B)-N(1B)-C(8B)-C(9B)	168.7(4)
C(7B)-N(1B)-C(8B)-C(13B)	160.2(4)
Re(1B)-N(1B)-C(8B)-C(13B)	-9.6(5)
C(13B)-C(8B)-C(9B)-C(10B)	-5.6(7)
N(1B)-C(8B)-C(9B)-C(10B)	176.2(4)
C(8B)-C(9B)-C(10B)-C(11B)	0.0(7)
C(9B)-C(10B)-C(11B)-C(12B)	3.4(7)
C(10B)-C(11B)-C(12B)-C(13B)	-1.1(7)
C(11B)-C(12B)-C(13B)-C(8B)	-4.5(6)
C(11B)-C(12B)-C(13B)-N(2B)	174.8(4)
C(9B)-C(8B)-C(13B)-C(12B)	7.9(6)
N(1B)-C(8B)-C(13B)-C(12B)	-173.7(4)

C(9B)-C(8B)-C(13B)-N(2B)	-171.5(4)
N(1B)-C(8B)-C(13B)-N(2B)	6.9(5)
C(14B)-N(2B)-C(13B)-C(12B)	2.0(6)
Re(1B)-N(2B)-C(13B)-C(12B)	179.7(3)
C(14B)-N(2B)-C(13B)-C(8B)	-178.7(4)
Re(1B)-N(2B)-C(13B)-C(8B)	-1.0(4)
C(13B)-N(2B)-C(14B)-C(15B)	-178.5(4)
Re(1B)-N(2B)-C(14B)-C(15B)	4.1(6)
N(2B)-C(14B)-C(15B)-C(16B)	175.4(4)
N(2B)-C(14B)-C(15B)-C(20B)	-3.3(7)
C(20B)-C(15B)-C(16B)-C(17B)	0.1(7)
C(14B)-C(15B)-C(16B)-C(17B)	-178.7(4)
C(15B)-C(16B)-C(17B)-C(18B)	0.2(7)
C(16B)-C(17B)-C(18B)-C(19B)	0.0(7)
C(17B)-C(18B)-C(19B)-C(20B)	-0.3(7)
Re(1B)-O(2B)-C(20B)-C(19B)	-176.9(3)
Re(1B)-O(2B)-C(20B)-C(15B)	0.8(6)
C(18B)-C(19B)-C(20B)-O(2B)	178.3(4)
C(18B)-C(19B)-C(20B)-C(15B)	0.6(7)
C(16B)-C(15B)-C(20B)-O(2B)	-178.0(4)
C(14B)-C(15B)-C(20B)-O(2B)	0.7(7)
C(16B)-C(15B)-C(20B)-C(19B)	-0.4(6)
C(14B)-C(15B)-C(20B)-C(19B)	178.3(4)
C(25B)-C(46)-C(21B)-C(22B)	1.9(7)
C(25B)-C(46)-C(21B)-P(1B)	-175.0(4)
C(32B)-P(1B)-C(21B)-C(46)	-124.4(4)
C(26B)-P(1B)-C(21B)-C(46)	-16.4(4)
Re(1B)-P(1B)-C(21B)-C(46)	104.2(4)
C(32B)-P(1B)-C(21B)-C(22B)	58.7(4)
C(26B)-P(1B)-C(21B)-C(22B)	166.7(3)
Re(1B)-P(1B)-C(21B)-C(22B)	-72.8(4)
C(46)-C(21B)-C(22B)-C(23B)	-1.7(7)
P(1B)-C(21B)-C(22B)-C(23B)	175.3(4)
C(21B)-C(22B)-C(23B)-C(24B)	0.6(7)
C(22B)-C(23B)-C(24B)-C(25B)	0.3(8)
C(23B)-C(24B)-C(25B)-C(46)	0.0(8)
C(21B)-C(46)-C(25B)-C(24B)	-1.1(7)
C(21B)-P(1B)-C(26B)-C(31B)	-103.1(4)
C(32B)-P(1B)-C(26B)-C(31B)	5.4(4)
Re(1B)-P(1B)-C(26B)-C(31B)	136.8(4)
C(21B)-P(1B)-C(26B)-C(27B)	81.4(4)
C(32B)-P(1B)-C(26B)-C(27B)	-170.1(4)
Re(1B)-P(1B)-C(26B)-C(27B)	-38.7(4)
C(31B)-C(26B)-C(27B)-C(28B)	0.6(7)
P(1B)-C(26B)-C(27B)-C(28B)	176.2(4)
C(26B)-C(27B)-C(28B)-C(29B)	-1.3(7)

C(27B)-C(28B)-C(29B)-C(30B)	1.5(8)
C(28B)-C(29B)-C(30B)-C(31B)	-0.9(8)
C(27B)-C(26B)-C(31B)-C(30B)	0.0(7)
P(1B)-C(26B)-C(31B)-C(30B)	-175.4(4)
C(29B)-C(30B)-C(31B)-C(26B)	0.1(8)
C(21B)-P(1B)-C(32B)-C(33B)	-158.5(4)
C(26B)-P(1B)-C(32B)-C(33B)	91.6(4)
Re(1B)-P(1B)-C(32B)-C(33B)	-33.6(5)
C(21B)-P(1B)-C(32B)-C(37B)	25.2(4)
C(26B)-P(1B)-C(32B)-C(37B)	-84.7(4)
Re(1B)-P(1B)-C(32B)-C(37B)	150.1(3)
C(37B)-C(32B)-C(33B)-C(34B)	0.2(8)
P(1B)-C(32B)-C(33B)-C(34B)	-176.2(5)
C(32B)-C(33B)-C(34B)-C(35B)	0.0(10)
C(33B)-C(34B)-C(35B)-C(36B)	0.8(10)
C(34B)-C(35B)-C(36B)-C(37B)	-1.7(9)
C(33B)-C(32B)-C(37B)-C(36B)	-1.2(8)
P(1B)-C(32B)-C(37B)-C(36B)	175.1(4)
C(35B)-C(36B)-C(37B)-C(32B)	2.0(9)

Symmetry transformations used to generate equivalent atoms:

Table 7. Least squares planes for resalp3.

Least-squares planes (x,y,z in crystal coordinates) and deviations from them
(* indicates atom used to define plane)

- 21.3893 (0.0096) x - 3.1861 (0.0140) y + 13.2527 (0.0246) z = 1.0352 (0.0046)

* 0.0102 (0.0017) N1A
* -0.0101 (0.0017) N2A
* -0.0090 (0.0015) O1A
* 0.0089 (0.0015) O2A
-0.0806 (0.0016) Re1A
2.3738 (0.0019) Cl1A
-2.4848 (0.0019) P1A

Rms deviation of fitted atoms = 0.0096

18.4958 (0.0157) x - 2.9880 (0.0144) y + 8.7373 (0.0273) z = 7.3078 (0.0139)

Angle to previous plane (with approximate esd) = 58.09 (0.07)

* -0.0052 (0.0017) N1B
*   0.0051 (0.0017) N2B
*   0.0046 (0.0015) O1B
* -0.0045 (0.0015) O2B
   -0.0723 (0.0016) Re1B
    2.3822 (0.0019) Cl1B
   -2.4794 (0.0019) P1B

Rms deviation of fitted atoms = 0.0049

Appendix 1.3: Crystal structure data and refinement for *cis*-[$ReO(PPh_3)(sal_2phen)$]•PF_6•0.5CH_2Cl_2.

Identification code	ReOPPH3Sal
Empirical formula	C38.50 H31 N2 O3 F6 P2 Cl Re
Formula weight	967.24
Temperature	173(2) K
Wavelength	0.71073 A
Crystal system, space group	Orthorhombic, Pnn2
Unit cell dimensions	a = 21.0703(15) A alpha = 90 deg. b = 11.3780(8) A beta = 90 deg. c = 15.0859(11) A gamma = 90 deg.
Volume	3616.7(4) A^3
Z, Calculated density	4, 1.776 Mg/m^3
Absorption coefficient	3.595 mm^-1
F(000)	1904
Crystal size	0.40 x 0.05 x 0.05 mm
Theta range for data collection	1.66 to 27.17 deg.
Limiting indices	-22<=h<=26, -14<=k<=14, -19<=l<=19
Reflections collected / unique	25028 / 7838 [R(int) = 0.0589]
Completeness to theta = 27.17	99.9 %
Absorption correction	Semi-empirical from equivalents
Max. and min. transmission	0.85 and 0.50
Refinement method	Full-matrix least-squares on F^2
Data / restraints / parameters	7838 / 1 / 485

Goodness-of-fit on F^2 1.014

Final R indices [I>2sigma(I)] R1 = 0.0377, wR2 = 0.0621

R indices (all data) R1 = 0.0604, wR2 = 0.0676

Absolute structure parameter 0.014(7)

Largest diff. peak and hole 0.882 and -0.782 e.A^-3

Table 2. Atomic coordinates (x 10^4) and equivalent isotropic displacement parameters (A^2 x 10^3) for reopph. U(eq) is defined as one third of the trace of the orthogonalized Uij tensor.

	x	y	z	U(eq)
Re(1)	3786(1)	4197(1)	3346(1)	22(1)
Cl(1)	4623(1)	1079(3)	7584(2)	106(1)
P(1)	2789(1)	5248(1)	3746(1)	24(1)
F(1)	5000	5000	7853(5)	239(9)
O(1)	3481(2)	4463(4)	2125(3)	29(1)
N(1)	4528(2)	3134(4)	2905(3)	22(1)
C(1)	3829(3)	4278(5)	1388(4)	28(1)
F(2)	4815(4)	6317(5)	6866(4)	139(3)
O(2)	3318(2)	2730(3)	3433(4)	22(1)
N(2)	4154(2)	3556(4)	4625(3)	24(1)
C(2)	4407(3)	3663(5)	1353(4)	29(2)
P(3)	5000	0	895(2)	43(1)
F(3)	4339(4)	4525(9)	6796(7)	180(4)
O(3)	4232(2)	5412(3)	3544(3)	27(1)
C(3)	4708(3)	3108(6)	2093(5)	27(2)
F(4)	5000	5000	5819(5)	119(3)
C(4)	4837(3)	2458(5)	3582(3)	23(2)
F(5)	5491(2)	1090(4)	918(3)	59(1)
C(5)	4659(3)	2704(6)	4443(5)	27(2)
F(6)	4581(2)	620(4)	1641(3)	51(1)
C(6)	3660(3)	3041(5)	5245(4)	29(2)
F(7)	4583(2)	624(4)	156(3)	74(2)
C(7)	3376(3)	1918(5)	4889(4)	25(1)
C(8)	3210(3)	1820(5)	4001(4)	21(1)
C(9)	3573(3)	4735(6)	593(4)	31(2)

C(10)	3870(4)	4534(6)	-200(4)	39(2)
C(11)	4428(5)	3919(6)	-242(5)	43(2)
C(12)	4693(3)	3484(6)	517(4)	40(2)
C(13)	5305(2)	1605(5)	3407(6)	32(1)
C(14)	5590(3)	1049(6)	4096(5)	43(2)
C(15)	5441(4)	1315(6)	4970(5)	42(2)
C(16)	4971(3)	2133(6)	5151(5)	34(2)
C(17)	3278(3)	976(5)	5443(4)	28(2)
C(18)	3010(3)	-52(6)	5141(5)	36(2)
C(19)	2843(3)	-143(6)	4258(4)	30(2)
C(20)	2943(3)	787(5)	3690(4)	27(1)
C(21)	2714(3)	5867(5)	4850(4)	28(1)
C(22)	3243(3)	6205(5)	5308(4)	31(2)
C(23)	3190(4)	6734(6)	6128(5)	41(2)
C(24)	2608(4)	6943(6)	6493(5)	43(2)
C(25)	2067(4)	6604(6)	6045(5)	39(2)
C(26)	2115(3)	6063(6)	5240(4)	36(2)
C(27)	2121(3)	4255(6)	3642(4)	29(2)
C(28)	1969(3)	3497(6)	4340(5)	36(2)
C(29)	1482(3)	2704(6)	4266(6)	52(2)
C(30)	1132(3)	2656(7)	3505(8)	53(3)
C(31)	1274(3)	3383(8)	2815(6)	54(2)
C(32)	1766(3)	4192(6)	2866(5)	34(2)
C(33)	2629(3)	6520(5)	3026(4)	27(2)
C(34)	2021(3)	7045(5)	3058(4)	35(2)
C(35)	1911(4)	8049(6)	2559(5)	43(2)
C(36)	2392(4)	8554(6)	2073(4)	43(2)
C(37)	2988(4)	8058(6)	2046(5)	42(2)
C(38)	3099(3)	7035(6)	2541(4)	34(2)
C(39)	5000	0	8206(7)	50(3)
P(2)	5000	5000	6868(2)	35(1)

Table 3. Bond lengths [A] and angles [deg] for reopph.

Re(1)-O(3)	1.699(4)
Re(1)-O(2)	1.943(3)
Re(1)-O(1)	1.974(4)
Re(1)-N(1)	2.086(5)
Re(1)-N(2)	2.203(5)
Re(1)-P(1)	2.4923(16)
Cl(1)-C(39)	1.738(6)
P(1)-C(27)	1.810(7)
P(1)-C(21)	1.815(6)
P(1)-C(33)	1.840(6)

F(1)-P(2)	1.486(7)
O(1)-C(1)	1.349(7)
N(1)-C(3)	1.282(8)
N(1)-C(4)	1.435(7)
C(1)-C(2)	1.405(8)
C(1)-C(9)	1.414(8)
F(2)-P(2)	1.548(5)
O(2)-C(8)	1.364(7)
N(2)-C(5)	1.465(8)
N(2)-C(6)	1.517(7)
C(2)-C(12)	1.412(8)
C(2)-C(3)	1.432(9)
P(3)-F(7)#1	1.587(5)
P(3)-F(7)	1.587(5)
P(3)-F(6)#1	1.596(4)
P(3)-F(6)	1.596(4)
P(3)-F(5)	1.615(4)
P(3)-F(5)#1	1.615(4)
F(3)-P(2)	1.497(7)
C(3)-H(3)	0.9500
F(4)-P(2)	1.583(8)
C(4)-C(5)	1.381(9)
C(4)-C(13)	1.407(7)
C(5)-C(16)	1.413(10)
C(6)-C(7)	1.510(8)
C(6)-H(6A)	0.9900
C(6)-H(6B)	0.9900
C(7)-C(17)	1.375(8)
C(7)-C(8)	1.389(8)
C(8)-C(20)	1.384(8)
C(9)-C(10)	1.369(9)
C(9)-H(9)	0.9500
C(10)-C(11)	1.368(11)
C(10)-H(10)	0.9500
C(11)-C(12)	1.367(10)
C(11)-H(11)	0.9500
C(12)-H(12)	0.9500
C(13)-C(14)	1.357(10)
C(13)-H(13)	0.9500
C(14)-C(15)	1.389(10)
C(14)-H(14)	0.9500
C(15)-C(16)	1.386(9)
C(15)-H(15)	0.9500
C(16)-H(16)	0.9500
C(17)-C(18)	1.376(9)
C(17)-H(17)	0.9500

C(18)-C(19)	1.381(9)
C(18)-H(18)	0.9500
C(19)-C(20)	1.378(8)
C(19)-H(19)	0.9500
C(20)-H(20)	0.9500
C(21)-C(22)	1.368(8)
C(21)-C(26)	1.410(9)
C(22)-C(23)	1.379(8)
C(22)-H(22)	0.9500
C(23)-C(24)	1.365(9)
C(23)-H(23)	0.9500
C(24)-C(25)	1.379(9)
C(24)-H(24)	0.9500
C(25)-C(26)	1.366(9)
C(25)-H(25)	0.9500
C(26)-H(26)	0.9500
C(27)-C(32)	1.392(8)
C(27)-C(28)	1.398(9)
C(28)-C(29)	1.371(9)
C(28)-H(28)	0.9500
C(29)-C(30)	1.366(14)
C(29)-H(29)	0.9500
C(30)-C(31)	1.363(12)
C(30)-H(30)	0.9500
C(31)-C(32)	1.389(10)
C(31)-H(31)	0.9500
C(32)-H(32)	0.9500
C(33)-C(38)	1.363(9)
C(33)-C(34)	1.415(8)
C(34)-C(35)	1.389(9)
C(34)-H(34)	0.9500
C(35)-C(36)	1.375(10)
C(35)-H(35)	0.9500
C(36)-C(37)	1.378(10)
C(36)-H(36)	0.9500
C(37)-C(38)	1.402(9)
C(37)-H(37)	0.9500
C(38)-H(38)	0.9500
C(39)-Cl(1)#1	1.738(6)
C(39)-H(39A)	0.9900
C(39)-H(39B)	0.9900
P(2)-F(3)#2	1.497(7)
P(2)-F(2)#2	1.548(5)

O(3)-Re(1)-O(2)	165.6(2)
O(3)-Re(1)-O(1)	102.66(17)

O(2)-Re(1)-O(1)	91.64(19)
O(3)-Re(1)-N(1)	96.48(18)
O(2)-Re(1)-N(1)	84.53(17)
O(1)-Re(1)-N(1)	92.06(18)
O(3)-Re(1)-N(2)	85.50(18)
O(2)-Re(1)-N(2)	80.53(19)
O(1)-Re(1)-N(2)	169.18(17)
N(1)-Re(1)-N(2)	79.84(18)
O(3)-Re(1)-P(1)	91.93(13)
O(2)-Re(1)-P(1)	88.12(10)
O(1)-Re(1)-P(1)	82.94(12)
N(1)-Re(1)-P(1)	170.99(14)
N(2)-Re(1)-P(1)	104.09(13)
C(27)-P(1)-C(21)	104.7(3)
C(27)-P(1)-C(33)	107.4(3)
C(21)-P(1)-C(33)	102.7(3)
C(27)-P(1)-Re(1)	109.6(2)
C(21)-P(1)-Re(1)	118.8(2)
C(33)-P(1)-Re(1)	112.8(2)
C(1)-O(1)-Re(1)	124.6(4)
C(3)-N(1)-C(4)	122.2(5)
C(3)-N(1)-Re(1)	122.6(5)
C(4)-N(1)-Re(1)	115.1(4)
O(1)-C(1)-C(2)	125.5(5)
O(1)-C(1)-C(9)	115.7(5)
C(2)-C(1)-C(9)	118.8(5)
C(8)-O(2)-Re(1)	141.1(4)
C(5)-N(2)-C(6)	111.0(5)
C(5)-N(2)-Re(1)	108.1(4)
C(6)-N(2)-Re(1)	115.3(3)
C(1)-C(2)-C(12)	118.4(6)
C(1)-C(2)-C(3)	125.0(6)
C(12)-C(2)-C(3)	116.3(6)
F(7)#1-P(3)-F(7)	90.7(4)
F(7)#1-P(3)-F(6)#1	89.5(2)
F(7)-P(3)-F(6)#1	179.7(3)
F(7)#1-P(3)-F(6)	179.7(3)
F(7)-P(3)-F(6)	89.5(2)
F(6)#1-P(3)-F(6)	90.2(3)
F(7)#1-P(3)-F(5)	90.2(3)
F(7)-P(3)-F(5)	91.5(3)
F(6)#1-P(3)-F(5)	88.3(2)
F(6)-P(3)-F(5)	90.0(2)
F(7)#1-P(3)-F(5)#1	91.5(3)
F(7)-P(3)-F(5)#1	90.2(3)
F(6)#1-P(3)-F(5)#1	90.0(2)

F(6)-P(3)-F(5)#1	88.3(2)
F(5)-P(3)-F(5)#1	177.6(4)
N(1)-C(3)-C(2)	127.2(7)
N(1)-C(3)-H(3)	116.4
C(2)-C(3)-H(3)	116.4
C(5)-C(4)-C(13)	120.4(6)
C(5)-C(4)-N(1)	115.9(5)
C(13)-C(4)-N(1)	123.7(6)
C(4)-C(5)-C(16)	119.4(6)
C(4)-C(5)-N(2)	120.6(6)
C(16)-C(5)-N(2)	120.0(6)
C(7)-C(6)-N(2)	112.3(5)
C(7)-C(6)-H(6A)	109.2
N(2)-C(6)-H(6A)	109.2
C(7)-C(6)-H(6B)	109.2
N(2)-C(6)-H(6B)	109.2
H(6A)-C(6)-H(6B)	107.9
C(17)-C(7)-C(8)	119.1(6)
C(17)-C(7)-C(6)	120.2(5)
C(8)-C(7)-C(6)	120.8(5)
O(2)-C(8)-C(20)	119.9(5)
O(2)-C(8)-C(7)	120.2(6)
C(20)-C(8)-C(7)	119.8(5)
C(10)-C(9)-C(1)	120.3(6)
C(10)-C(9)-H(9)	119.8
C(1)-C(9)-H(9)	119.8
C(11)-C(10)-C(9)	121.2(7)
C(11)-C(10)-H(10)	119.4
C(9)-C(10)-H(10)	119.4
C(12)-C(11)-C(10)	119.8(7)
C(12)-C(11)-H(11)	120.1
C(10)-C(11)-H(11)	120.1
C(11)-C(12)-C(2)	121.4(7)
C(11)-C(12)-H(12)	119.3
C(2)-C(12)-H(12)	119.3
C(14)-C(13)-C(4)	119.2(8)
C(14)-C(13)-H(13)	120.4
C(4)-C(13)-H(13)	120.4
C(13)-C(14)-C(15)	121.7(7)
C(13)-C(14)-H(14)	119.1
C(15)-C(14)-H(14)	119.1
C(16)-C(15)-C(14)	119.7(6)
C(16)-C(15)-H(15)	120.2
C(14)-C(15)-H(15)	120.2
C(15)-C(16)-C(5)	119.5(7)
C(15)-C(16)-H(16)	120.2

C(5)-C(16)-H(16)	120.2
C(7)-C(17)-C(18)	121.5(6)
C(7)-C(17)-H(17)	119.3
C(18)-C(17)-H(17)	119.3
C(17)-C(18)-C(19)	119.2(6)
C(17)-C(18)-H(18)	120.4
C(19)-C(18)-H(18)	120.4
C(20)-C(19)-C(18)	120.2(6)
C(20)-C(19)-H(19)	119.9
C(18)-C(19)-H(19)	119.9
C(19)-C(20)-C(8)	120.2(6)
C(19)-C(20)-H(20)	119.9
C(8)-C(20)-H(20)	119.9
C(22)-C(21)-C(26)	118.3(6)
C(22)-C(21)-P(1)	120.2(5)
C(26)-C(21)-P(1)	121.5(5)
C(21)-C(22)-C(23)	120.6(7)
C(21)-C(22)-H(22)	119.7
C(23)-C(22)-H(22)	119.7
C(24)-C(23)-C(22)	120.7(7)
C(24)-C(23)-H(23)	119.6
C(22)-C(23)-H(23)	119.6
C(23)-C(24)-C(25)	119.7(7)
C(23)-C(24)-H(24)	120.1
C(25)-C(24)-H(24)	120.1
C(26)-C(25)-C(24)	120.0(7)
C(26)-C(25)-H(25)	120.0
C(24)-C(25)-H(25)	120.0
C(25)-C(26)-C(21)	120.6(7)
C(25)-C(26)-H(26)	119.7
C(21)-C(26)-H(26)	119.7
C(32)-C(27)-C(28)	118.6(6)
C(32)-C(27)-P(1)	121.5(5)
C(28)-C(27)-P(1)	119.8(5)
C(29)-C(28)-C(27)	121.0(7)
C(29)-C(28)-H(28)	119.5
C(27)-C(28)-H(28)	119.5
C(30)-C(29)-C(28)	120.0(8)
C(30)-C(29)-H(29)	120.0
C(28)-C(29)-H(29)	120.0
C(31)-C(30)-C(29)	120.0(7)
C(31)-C(30)-H(30)	120.0
C(29)-C(30)-H(30)	120.0
C(30)-C(31)-C(32)	121.6(8)
C(30)-C(31)-H(31)	119.2
C(32)-C(31)-H(31)	119.2

C(31)-C(32)-C(27)	118.8(7)
C(31)-C(32)-H(32)	120.6
C(27)-C(32)-H(32)	120.6
C(38)-C(33)-C(34)	119.7(6)
C(38)-C(33)-P(1)	121.5(5)
C(34)-C(33)-P(1)	118.5(5)
C(35)-C(34)-C(33)	118.6(7)
C(35)-C(34)-H(34)	120.7
C(33)-C(34)-H(34)	120.7
C(36)-C(35)-C(34)	120.7(7)
C(36)-C(35)-H(35)	119.6
C(34)-C(35)-H(35)	119.6
C(35)-C(36)-C(37)	121.0(7)
C(35)-C(36)-H(36)	119.5
C(37)-C(36)-H(36)	119.5
C(36)-C(37)-C(38)	118.5(7)
C(36)-C(37)-H(37)	120.8
C(38)-C(37)-H(37)	120.8
C(33)-C(38)-C(37)	121.4(7)
C(33)-C(38)-H(38)	119.3
C(37)-C(38)-H(38)	119.3
Cl(1)#1-C(39)-Cl(1)	114.6(7)
Cl(1)#1-C(39)-H(39A)	108.6
Cl(1)-C(39)-H(39A)	108.6
Cl(1)#1-C(39)-H(39B)	108.6
Cl(1)-C(39)-H(39B)	108.6
H(39A)-C(39)-H(39B)	107.6
F(1)-P(2)-F(3)#2	94.2(4)
F(1)-P(2)-F(3)	94.2(4)
F(3)#2-P(2)-F(3)	171.6(8)
F(1)-P(2)-F(2)#2	90.1(2)
F(3)#2-P(2)-F(2)#2	96.6(5)
F(3)-P(2)-F(2)#2	83.4(5)
F(1)-P(2)-F(2)	90.1(2)
F(3)#2-P(2)-F(2)	83.4(5)
F(3)-P(2)-F(2)	96.6(5)
F(2)#2-P(2)-F(2)	179.8(5)
F(1)-P(2)-F(4)	180.000(3)
F(3)#2-P(2)-F(4)	85.8(4)
F(3)-P(2)-F(4)	85.8(4)
F(2)#2-P(2)-F(4)	89.9(2)
F(2)-P(2)-F(4)	89.9(2)

Symmetry transformations used to generate equivalent atoms:
#1 -x+1,-y,z #2 -x+1,-y+1,z

Table 4. Anisotropic displacement parameters (A^2 x 10^3) for reopph.
The anisotropic displacement factor exponent takes the form:
-2 pi^2 [h^2 a*^2 U11 + ... + 2 h k a* b* U12]

	U11	U22	U33	U23	U13	U12
Re(1)	22(1)	18(1)	26(1)	0(1)	0(1)	0(1)
Cl(1)	46(2)	145(3)	128(2)	79(2)	-9(2)	-14(2)
P(1)	24(1)	21(1)	27(1)	-1(1)	-2(1)	3(1)
F(1)	640(30)	57(6)	17(4)	0	0	-94(10)
O(1)	26(2)	26(3)	34(3)	1(2)	1(2)	2(2)
N(1)	22(3)	19(3)	25(3)	-1(2)	-1(2)	-2(2)
C(1)	32(4)	24(3)	27(3)	1(3)	9(3)	-1(3)
F(2)	281(10)	51(4)	85(5)	12(3)	53(5)	49(5)
O(2)	25(2)	21(2)	20(2)	-2(2)	0(2)	-6(1)
N(2)	20(3)	22(3)	28(3)	-2(2)	-2(2)	6(2)
C(2)	26(4)	29(4)	30(4)	7(3)	4(3)	5(3)
P(3)	51(2)	39(2)	37(2)	0	0	13(1)
F(3)	82(6)	202(9)	254(11)	-17(8)	34(6)	-64(6)
O(3)	30(2)	22(2)	30(3)	2(2)	2(2)	-1(2)
C(3)	22(4)	24(4)	35(4)	1(3)	12(3)	-2(3)
F(4)	243(11)	61(5)	54(5)	0	0	-69(6)
C(4)	20(3)	21(3)	29(4)	1(3)	-6(2)	-2(2)
F(5)	59(3)	43(3)	76(3)	12(2)	20(2)	-2(2)
C(5)	20(4)	23(4)	37(4)	-8(3)	4(3)	-5(3)
F(6)	53(3)	50(3)	49(3)	-15(2)	6(2)	5(2)
C(6)	31(4)	30(4)	24(3)	-1(3)	-4(3)	-1(3)
F(7)	97(4)	73(4)	50(3)	-2(3)	-13(3)	40(3)
C(7)	27(4)	23(3)	26(3)	-1(3)	-1(3)	4(3)
C(8)	15(3)	21(3)	25(3)	1(3)	6(3)	3(2)
C(9)	25(4)	40(4)	29(4)	0(3)	1(3)	2(3)
C(10)	63(5)	25(4)	30(4)	5(3)	9(4)	-5(4)
C(11)	84(7)	27(4)	19(4)	10(3)	16(4)	-1(4)
C(12)	52(5)	34(4)	34(4)	3(3)	22(4)	8(4)
C(13)	29(3)	33(3)	34(3)	-9(5)	-6(5)	7(2)
C(14)	41(4)	31(4)	56(5)	-5(4)	-16(4)	13(3)
C(15)	53(5)	39(4)	36(4)	-1(3)	-25(4)	7(4)
C(16)	30(4)	36(4)	37(4)	-1(3)	-8(3)	2(3)
C(17)	29(4)	27(4)	27(3)	7(3)	-3(3)	1(3)
C(18)	39(4)	26(4)	44(4)	14(3)	8(3)	0(3)
C(19)	32(4)	25(4)	34(4)	2(3)	-3(3)	-5(3)

C(20)	33(3)	16(3)	32(3)	1(3)	0(2)	0(3)
C(21)	35(4)	15(3)	35(3)	-3(3)	0(3)	4(3)
C(22)	40(4)	21(3)	30(4)	6(3)	-3(3)	2(3)
C(23)	54(5)	31(4)	38(4)	-11(3)	-8(4)	-12(4)
C(24)	73(6)	25(4)	30(4)	-1(3)	10(4)	-5(4)
C(25)	43(5)	31(4)	42(4)	5(3)	9(4)	6(4)
C(26)	40(4)	32(4)	35(4)	-3(3)	-2(3)	6(3)
C(27)	18(3)	28(3)	40(4)	-4(3)	7(3)	7(3)
C(28)	25(4)	31(4)	53(5)	2(3)	3(3)	2(3)
C(29)	38(5)	26(4)	91(7)	-4(4)	14(4)	-5(4)
C(30)	33(4)	45(4)	82(9)	-24(5)	17(5)	-15(3)
C(31)	25(5)	70(6)	65(6)	-41(5)	-4(4)	11(4)
C(32)	24(4)	38(4)	39(4)	-13(4)	1(3)	8(4)
C(33)	33(4)	19(3)	29(3)	-3(3)	-9(3)	6(3)
C(34)	44(4)	24(4)	37(4)	-4(3)	-4(3)	6(3)
C(35)	51(5)	38(4)	41(4)	-7(4)	-18(4)	17(4)
C(36)	78(6)	15(4)	35(4)	-1(3)	-24(4)	-2(4)
C(37)	61(5)	28(4)	38(4)	8(3)	-5(4)	-1(4)
C(38)	41(4)	25(4)	36(4)	1(3)	-6(3)	2(3)
C(39)	45(6)	75(7)	30(8)	0	0	-14(5)
P(2)	44(2)	32(2)	29(1)	0	0	-8(1)

Table 5. Hydrogen coordinates (x 10^4) and isotropic displacement parameters (A^2 x 10^3) for reopph.

	x	y	z	U(eq)
H(3)	5082	2671	1970	32
H(6A)	3859	2881	5828	35
H(6B)	3317	3624	5338	35
H(9)	3193	5183	609	38
H(10)	3686	4827	-730	47
H(11)	4630	3795	-797	52
H(12)	5078	3053	482	48
H(13)	5419	1421	2814	38
H(14)	5900	463	3978	51
H(15)	5660	938	5442	51
H(16)	4860	2309	5747	41
H(17)	3398	1037	6049	33
H(18)	2941	-691	5535	44
H(19)	2659	-849	4042	36

H(20)	2829	720	3083	32
H(22)	3652	6075	5060	37
H(23)	3562	6954	6442	49
H(24)	2575	7321	7052	51
H(25)	1661	6747	6298	47
H(26)	1742	5817	4940	43
H(28)	2207	3533	4875	44
H(29)	1389	2188	4743	62
H(30)	790	2116	3457	64
H(31)	1030	3336	2286	64
H(32)	1858	4695	2380	41
H(34)	1694	6716	3415	42
H(35)	1500	8392	2552	52
H(36)	2311	9256	1750	51
H(37)	3316	8400	1701	51
H(38)	3511	6694	2539	41
H(39A)	5318	381	8594	60
H(39B)	4682	-381	8594	60

Table 6. Torsion angles [deg] for reopph.

O(3)-Re(1)-P(1)-C(27)	-179.6(3)
O(2)-Re(1)-P(1)-C(27)	-14.0(3)
O(1)-Re(1)-P(1)-C(27)	77.8(2)
N(1)-Re(1)-P(1)-C(27)	21.2(9)
N(2)-Re(1)-P(1)-C(27)	-93.8(3)
O(3)-Re(1)-P(1)-C(21)	-59.4(3)
O(2)-Re(1)-P(1)-C(21)	106.2(3)
O(1)-Re(1)-P(1)-C(21)	-162.0(3)
N(1)-Re(1)-P(1)-C(21)	141.4(9)
N(2)-Re(1)-P(1)-C(21)	26.4(3)
O(3)-Re(1)-P(1)-C(33)	60.8(2)
O(2)-Re(1)-P(1)-C(33)	-133.6(3)
O(1)-Re(1)-P(1)-C(33)	-41.7(2)
N(1)-Re(1)-P(1)-C(33)	-98.4(9)
N(2)-Re(1)-P(1)-C(33)	146.6(2)
O(3)-Re(1)-O(1)-C(1)	78.9(4)
O(2)-Re(1)-O(1)-C(1)	-102.8(4)
N(1)-Re(1)-O(1)-C(1)	-18.2(4)
N(2)-Re(1)-O(1)-C(1)	-59.4(11)
P(1)-Re(1)-O(1)-C(1)	169.3(4)
O(3)-Re(1)-N(1)-C(3)	-87.5(5)
O(2)-Re(1)-N(1)-C(3)	107.0(5)
O(1)-Re(1)-N(1)-C(3)	15.5(5)

N(2)-Re(1)-N(1)-C(3)	-171.7(5)
P(1)-Re(1)-N(1)-C(3)	71.6(11)
O(3)-Re(1)-N(1)-C(4)	90.8(4)
O(2)-Re(1)-N(1)-C(4)	-74.7(4)
O(1)-Re(1)-N(1)-C(4)	-166.2(4)
N(2)-Re(1)-N(1)-C(4)	6.6(4)
P(1)-Re(1)-N(1)-C(4)	-110.1(9)
Re(1)-O(1)-C(1)-C(2)	13.2(8)
Re(1)-O(1)-C(1)-C(9)	-168.0(4)
O(3)-Re(1)-O(2)-C(8)	-8.5(10)
O(1)-Re(1)-O(2)-C(8)	178.2(6)
N(1)-Re(1)-O(2)-C(8)	86.3(6)
N(2)-Re(1)-O(2)-C(8)	5.7(5)
P(1)-Re(1)-O(2)-C(8)	-98.9(5)
O(3)-Re(1)-N(2)-C(5)	-101.8(4)
O(2)-Re(1)-N(2)-C(5)	81.7(4)
O(1)-Re(1)-N(2)-C(5)	37.6(11)
N(1)-Re(1)-N(2)-C(5)	-4.4(4)
P(1)-Re(1)-N(2)-C(5)	167.3(3)
O(3)-Re(1)-N(2)-C(6)	133.4(4)
O(2)-Re(1)-N(2)-C(6)	-43.1(4)
O(1)-Re(1)-N(2)-C(6)	-87.2(10)
N(1)-Re(1)-N(2)-C(6)	-129.2(4)
P(1)-Re(1)-N(2)-C(6)	42.5(4)
O(1)-C(1)-C(2)-C(12)	176.1(6)
C(9)-C(1)-C(2)-C(12)	-2.6(9)
O(1)-C(1)-C(2)-C(3)	1.7(10)
C(9)-C(1)-C(2)-C(3)	-177.0(6)
C(4)-N(1)-C(3)-C(2)	174.4(6)
Re(1)-N(1)-C(3)-C(2)	-7.4(10)
C(1)-C(2)-C(3)-N(1)	-4.5(11)
C(12)-C(2)-C(3)-N(1)	-179.0(7)
C(3)-N(1)-C(4)-C(5)	170.5(6)
Re(1)-N(1)-C(4)-C(5)	-7.8(6)
C(3)-N(1)-C(4)-C(13)	-8.2(9)
Re(1)-N(1)-C(4)-C(13)	173.5(4)
C(13)-C(4)-C(5)-C(16)	3.0(9)
N(1)-C(4)-C(5)-C(16)	-175.8(5)
C(13)-C(4)-C(5)-N(2)	-177.4(5)
N(1)-C(4)-C(5)-N(2)	3.8(8)
C(6)-N(2)-C(5)-C(4)	129.0(6)
Re(1)-N(2)-C(5)-C(4)	1.7(7)
C(6)-N(2)-C(5)-C(16)	-51.4(7)
Re(1)-N(2)-C(5)-C(16)	-178.7(5)
C(5)-N(2)-C(6)-C(7)	-56.7(6)
Re(1)-N(2)-C(6)-C(7)	66.6(5)

N(2)-C(6)-C(7)-C(17)	137.3(6)
N(2)-C(6)-C(7)-C(8)	-42.7(8)
Re(1)-O(2)-C(8)-C(20)	-164.5(4)
Re(1)-O(2)-C(8)-C(7)	14.5(9)
C(17)-C(7)-C(8)-O(2)	-178.2(5)
C(6)-C(7)-C(8)-O(2)	1.8(9)
C(17)-C(7)-C(8)-C(20)	0.7(9)
C(6)-C(7)-C(8)-C(20)	-179.3(5)
O(1)-C(1)-C(9)-C(10)	-176.1(6)
C(2)-C(1)-C(9)-C(10)	2.8(9)
C(1)-C(9)-C(10)-C(11)	-1.8(10)
C(9)-C(10)-C(11)-C(12)	0.6(11)
C(10)-C(11)-C(12)-C(2)	-0.5(11)
C(1)-C(2)-C(12)-C(11)	1.5(10)
C(3)-C(2)-C(12)-C(11)	176.4(7)
C(5)-C(4)-C(13)-C(14)	-1.7(9)
N(1)-C(4)-C(13)-C(14)	177.0(6)
C(4)-C(13)-C(14)-C(15)	-1.2(10)
C(13)-C(14)-C(15)-C(16)	2.7(11)
C(14)-C(15)-C(16)-C(5)	-1.3(11)
C(4)-C(5)-C(16)-C(15)	-1.5(10)
N(2)-C(5)-C(16)-C(15)	178.9(6)
C(8)-C(7)-C(17)-C(18)	-1.1(9)
C(6)-C(7)-C(17)-C(18)	178.9(6)
C(7)-C(17)-C(18)-C(19)	0.8(10)
C(17)-C(18)-C(19)-C(20)	-0.2(10)
C(18)-C(19)-C(20)-C(8)	-0.2(9)
O(2)-C(8)-C(20)-C(19)	178.9(5)
C(7)-C(8)-C(20)-C(19)	-0.1(9)
C(27)-P(1)-C(21)-C(22)	150.1(5)
C(33)-P(1)-C(21)-C(22)	-97.9(5)
Re(1)-P(1)-C(21)-C(22)	27.4(6)
C(27)-P(1)-C(21)-C(26)	-32.8(6)
C(33)-P(1)-C(21)-C(26)	79.2(6)
Re(1)-P(1)-C(21)-C(26)	-155.5(4)
C(26)-C(21)-C(22)-C(23)	-0.6(9)
P(1)-C(21)-C(22)-C(23)	176.6(5)
C(21)-C(22)-C(23)-C(24)	-0.8(10)
C(22)-C(23)-C(24)-C(25)	1.2(10)
C(23)-C(24)-C(25)-C(26)	-0.1(10)
C(24)-C(25)-C(26)-C(21)	-1.3(10)
C(22)-C(21)-C(26)-C(25)	1.6(9)
P(1)-C(21)-C(26)-C(25)	-175.5(5)
C(21)-P(1)-C(27)-C(32)	137.9(5)
C(33)-P(1)-C(27)-C(32)	29.2(6)
Re(1)-P(1)-C(27)-C(32)	-93.6(5)

C(21)-P(1)-C(27)-C(28)	-44.5(6)
C(33)-P(1)-C(27)-C(28)	-153.2(5)
Re(1)-P(1)-C(27)-C(28)	83.9(5)
C(32)-C(27)-C(28)-C(29)	0.2(10)
P(1)-C(27)-C(28)-C(29)	-177.4(5)
C(27)-C(28)-C(29)-C(30)	-0.9(11)
C(28)-C(29)-C(30)-C(31)	1.1(12)
C(29)-C(30)-C(31)-C(32)	-0.7(12)
C(30)-C(31)-C(32)-C(27)	0.1(10)
C(28)-C(27)-C(32)-C(31)	0.1(9)
P(1)-C(27)-C(32)-C(31)	177.7(5)
C(27)-P(1)-C(33)-C(38)	-140.7(5)
C(21)-P(1)-C(33)-C(38)	109.2(5)
Re(1)-P(1)-C(33)-C(38)	-19.9(6)
C(27)-P(1)-C(33)-C(34)	46.3(5)
C(21)-P(1)-C(33)-C(34)	-63.8(5)
Re(1)-P(1)-C(33)-C(34)	167.1(4)
C(38)-C(33)-C(34)-C(35)	2.9(9)
P(1)-C(33)-C(34)-C(35)	176.0(5)
C(33)-C(34)-C(35)-C(36)	-2.8(9)
C(34)-C(35)-C(36)-C(37)	2.1(10)
C(35)-C(36)-C(37)-C(38)	-1.2(10)
C(34)-C(33)-C(38)-C(37)	-2.2(10)
P(1)-C(33)-C(38)-C(37)	-175.1(5)
C(36)-C(37)-C(38)-C(33)	1.3(10)

Symmetry transformations used to generate equivalent atoms:
#1 -x+1,-y,z #2 -x+1,-y+1,z

Appendix 2.1: Biodistribution of [^{99m}Tc-DTMA-β-Ala-BBN(7-14)NH_2] in normal CF-1 mice at 1h p.i. (n=5).

1 hr (11:33am)	Mouse #: Wt(g)	1.00 Bq(cps)	%ID	%ID/g		Mouse #: Wt(g)	2.00 Bq(cps)	%ID	%ID/g
Background		5.94					3.61		
Body Wt	20.86					22.24			
Cage Paper		70412.00	48.12				61338.00	48.63	
Urine		1687.00	1.15				901.00	0.71	
Bladder	0.02	8.00	0.01	0.27		0.02	7.00	0.01	0.28
Heart	0.09	40.00	0.03	0.30		0.09	33.00	0.03	0.29
Lung	0.13	118.00	0.08	0.62		0.15	109.00	0.09	0.58
Liver	1.02	9952.00	6.80	6.67		1.25	6234.00	4.94	3.95
Kidneys	0.24	1240.00	0.85	3.53		0.25	1032.00	0.82	3.27
Spleen	0.08	28.00	0.02	0.24		0.06	32.00	0.03	0.42
Stomach	0.29	362.00	0.25	0.85		0.46	255.00	0.20	0.44
S. Intestine	1.29	50245.00	34.34	26.62		1.47	43968.00	34.86	23.71
L. Intestine	0.75	2062.00	1.41	1.88		0.82	2856.00	2.26	2.76
Muscle	0.14	35.00	0.02	0.17		0.14	21.00	0.02	0.12
Bone	0.04	19.00	0.01	0.32		0.04	10.00	0.01	0.20
Brain	0.37	14.00	0.01	0.03		0.39	11.00	0.01	0.02
Pancreas	0.18	3142.00	2.15	11.93		0.23	2689.00	2.13	9.27
Tumor #1	0.14	180.00	0.12	0.88		0.27	310.00	0.25	0.91
Tumor #2	0.20	257.00	0.18	0.88		0.21	255.00	0.20	0.96
Blood	1.36	1601.00	1.09	0.80		1.45	3193.00	2.53	1.75
Carcass	13.29	4920.00	3.36	0.25		13.35	2886.00	2.29	0.17
Tail	0.61	728.00				0.63	1410.00		
Sac Time Total Bq		146322.00					126140.00		

	Mouse #: Wt(g)	3.00 Bq(cps)	%ID	%ID/g		Mouse #: Wt(g)	4.00 Bq(cps)	%ID	%ID/g
Background		2.67					3.06		
Body Wt	22.27					21.26			
Cage Paper		60298.00	50.01				77095.00	50.26	
Urine		3251.00	2.70				2291.00	1.49	
Bladder	0.02	9.00	0.01	0.37		0.02	19.00	0.01	0.62
Heart	0.11	29.00	0.02	0.22		0.09	42.00	0.03	0.30
Lung	0.20	108.00	0.09	0.45		0.14	133.00	0.09	0.62
Liver	1.29	6605.00	5.48	4.25		1.00	8191.00	5.34	5.34
Kidneys	0.28	934.00	0.77	2.77		0.29	1504.00	0.98	3.38
Spleen	0.07	28.00	0.02	0.33		0.09	71.00	0.05	0.51
Stomach	0.27	211.00	0.18	0.65		0.31	315.00	0.21	0.66
S. Intestine	1.25	41394.00	34.33	27.47		1.09	51497.00	33.57	30.80
L. Intestine	0.99	1330.00	1.10	1.11		0.84	2060.00	1.34	1.60
Muscle	0.10	18.00	0.01	0.15		0.12	36.00	0.02	0.20
Bone	0.07	13.00	0.01	0.15		0.03	13.00	0.01	0.28
Brain	0.40	13.00	0.01	0.03		0.35	17.00	0.01	0.03
Pancreas	0.20	1573.00	1.30	6.52		0.23	2337.00	1.52	6.62
Tumor #1	0.06	51.00	0.04	0.71		0.08	113.00	0.07	0.92
Tumor #2	0.17	211.00	0.18	1.03		0.11	145.00	0.09	0.86
Blood	1.45	689.00	0.57	0.39		1.38	919.00	0.60	0.43
Carcass	14.27	3801.00	3.15	0.22		14.27	6585.00	4.29	0.30
Tail	0.72	1046.00				0.71	947.00		
Sac Time Total Bq		120566.00					153383.00		

	Mouse #: Wt(g)	5.00 Bq(cps)	%ID	%ID/g		Averages Wt	STDev	%ID for as-measured mouse %ID	%STDev	%ID/g	%STDev
Background		4.72									
Body Wt	23.61					22.05	1.07				
Cage Paper		538.00	0.45					39.50	21.84		
Urine		58837.00	49.74					11.16	21.58		
Bladder	0.02	75.00	0.06	3.17		0.02	0.00	0.02	0.03	0.94	1.25
Heart	0.10	31.00	0.03	0.26		0.10	0.01	0.03	0.00	0.28	0.04
Lung	0.18	113.00	0.10	0.53		0.16	0.03	0.09	0.01	0.56	0.07
Liver	1.27	10065.00	8.51	6.70		1.17	0.14	6.21	1.46	5.38	1.30
Kidneys	0.31	845.00	0.71	2.30		0.27	0.03	0.83	0.10	3.05	0.51
Spleen	0.07	32.00	0.03	0.39		0.07	0.01	0.03	0.01	0.38	0.10
Stomach	0.52	1273.00	1.08	2.07		0.37	0.11	0.38	0.39	0.93	0.65
S. Intestine	1.60	34462.00	29.13	18.21		1.34	0.20	33.25	2.35	25.36	4.73
L. Intestine	1.02	1666.00	1.41	1.38		0.88	0.12	1.51	0.44	1.75	0.63
Muscle	0.15	28.00	0.02	0.16		0.13	0.02	0.02	0.00	0.16	0.03
Bone	0.04	11.00	0.01	0.23		0.04	0.02	0.01	0.00	0.24	0.07
Brain	0.44	10.00	0.01	0.02		0.39	0.03	0.01	0.00	0.03	0.00
Pancreas	0.24	1895.00	1.60	6.67		0.22	0.03	1.74	0.38	8.20	2.38
Tumor #1	0.06	83.00	0.07	1.17		0.12	0.09	0.11	0.08	0.92	0.17
Tumor #2	0.07	96.00	0.08	1.16		0.15	0.06	0.15	0.05	0.98	0.12
Blood	1.53	524.00	0.44	0.29		1.43	0.07	1.05	0.87	0.73	0.60
Carcass	15.00	7716.00	6.52	0.43		14.04	0.72	3.92	1.62	0.28	0.10
Tail	0.80	2222.00									
Sac Time Total Bq		118300.00				Total Inj Bq		Total Inj uCi			

Appendix 2.2: Biodistribution of [^{99m}Tc-DTMA-β-Ala-BBN(7-14)NH_2] in normal CF-1 mice at 4h p.i. (n=5).

Background		4.28					4.11		
Body Wt	23.50					17.28			
Cage Paper		112916.00	46.83				125061.00	56.17	
Urine		1081.00	0.45				494.00	0.22	
Bladder	0.02	29.00	0.01	0.60		0.02	11.00	0.00	0.25
Heart	0.09	33.00	0.01	0.15		0.07	30.00	0.01	0.19
Lung	0.17	98.00	0.04	0.24		0.12	109.00	0.05	0.41
Liver	1.24	5936.00	2.46	1.99		1.01	4515.00	2.03	2.01
Kidneys	0.31	859.00	0.36	1.15		0.17	999.00	0.45	2.64
Spleen	0.04	30.00	0.01	0.31		0.04	40.00	0.02	0.45
Stomach	0.40	283.00	0.12	0.29		0.27	320.00	0.14	0.53
S. Intestine	1.13	5613.00	2.33	2.06		1.13	4984.00	2.24	1.98
L. Intestine	1.01	105204.00	43.63	43.20		0.67	77334.00	34.74	51.85
Muscle	0.22	28.00	0.01	0.05		0.10	15.00	0.01	0.07
Bone	0.06	14.00	0.01	0.10		0.06	19.00	0.01	0.14
Brain	0.46	15.00	0.01	0.01		0.35	15.00	0.01	0.02
Pancreas	0.24	4768.00	1.98	8.24		0.12	3316.00	1.49	12.41
Tumor #1	0.02	22.00	0.01	0.46		0.13	171.00	0.08	0.59
Tumor #2	0.10	169.00	0.07	0.70		0.21	278.00	0.12	0.59
Blood	1.53	754.00	0.31	0.20		1.12	1508.00	0.68	0.60
Carcass	15.84	3282.00	1.36	0.09		10.85	3411.00	1.53	0.14
Tail	0.85	472.00				0.60	3312.00		
Sac Time Total Bq		241134.00					222630.00		
Inj Time Total Bq		383193.31					358349.80		

	Mouse #:	3.00				Mouse #:	4.00		
	Wt(g)	Bq(cps)	%ID	%ID/g		Wt(g)	Bq(cps)	%ID	%ID/g
Background		4.11					4.00		
Body Wt	24.35					18.53			
Cage Paper		173616.00	74.19				76128.00	54.88	
Urine		430.00	0.18				1057.00	0.76	
Bladder	0.02	1.00	0.00	0.02		0.02	11.00	0.01	0.40
Heart	0.12	48.00	0.02	0.17		0.10	24.00	0.02	0.17
Lung	0.16	109.00	0.05	0.29		0.17	61.00	0.04	0.26
Liver	1.21	4221.00	1.80	1.49		0.77	2777.00	2.00	2.60
Kidneys	0.25	805.00	0.34	1.38		0.20	779.00	0.56	2.81
Spleen	0.07	47.00	0.02	0.29		0.03	31.00	0.02	0.74
Stomach	0.90	208.00	0.09	0.10		0.14	110.00	0.08	0.57
S. Intestine	2.01	4095.00	1.75	0.87		1.04	5280.00	3.81	3.66
L. Intestine	0.96	39997.00	17.09	17.80		0.37	48142.00	34.70	93.80
Muscle	0.16	30.00	0.01	0.08		0.15	12.00	0.01	0.06
Bone	0.05	7.00	0.00	0.06		0.06	9.00	0.01	0.11
Brain	0.45	50.00	0.02	0.05		0.42	16.00	0.01	0.03
Pancreas	0.31	5534.00	2.36	7.63		0.10	989.00	0.71	7.13
Tumor #1	0.11	94.00	0.04	0.37		0.48	243.00	0.18	0.36
Tumor #2	0.23	286.00	0.12	0.53		0.20	134.00	0.10	0.48
Blood	1.58	710.00	0.30	0.19		1.20	1096.00	0.79	0.66
Carcass	14.74	3742.00	1.60	0.11		11.83	1819.00	1.31	0.11
Tail	0.84	2767.00				0.83	5818.00		
Sac Time Total Bq		234030.00					138718.00		
Inj Time Total Bq		375566.11					229237.80		

	Mouse #:	5.00				Averages		%ID for as-measured mouse			
	Wt(g)	Bq(cps)	%ID	%ID/g		Wt	STDev	%ID	%STDev	%ID/g	%STDev
Background		3.44									
Body Wt	25.45					21.82	3.67				
Cage Paper		124385.00	51.72					56.76	10.39		
Urine		6722.00	2.80					0.88	1.09		
Bladder	0.02	8.00	0.00	0.17		0.02	0.00	0.01	0.00	0.29	0.22
Heart	0.11	51.00	0.02	0.19		0.10	0.02	0.02	0.00	0.18	0.02
Lung	0.20	114.00	0.05	0.24		0.16	0.03	0.05	0.00	0.29	0.07
Liver	1.25	5578.00	2.32	1.86		1.10	0.21	2.12	0.26	1.99	0.40
Kidneys	0.29	1135.00	0.47	1.63		0.24	0.06	0.44	0.09	1.92	0.76
Spleen	0.04	36.00	0.01	0.37		0.04	0.02	0.02	0.00	0.43	0.19
Stomach	0.23	251.00	0.10	0.45		0.39	0.30	0.11	0.03	0.39	0.19
S. Intestine	1.58	9089.00	3.78	2.39		1.38	0.41	2.78	0.95	2.19	1.00
L. Intestine	0.75	83851.00	34.87	46.49		0.75	0.26	33.01	9.69	50.63	27.45
Muscle	0.15	18.00	0.01	0.05		0.16	0.04	0.01	0.00	0.06	0.01
Bone	0.06	33.00	0.01	0.23		0.06	0.00	0.01	0.00	0.13	0.06
Brain	0.47	24.00	0.01	0.02		0.43	0.05	0.01	0.01	0.03	0.01
Pancreas	0.28	3992.00	1.66	5.93		0.21	0.09	1.64	0.62	8.27	2.47
Tumor #1	0.23	310.00	0.13	0.56		0.19	0.18	0.09	0.07	0.47	0.11
Tumor #2	0.36	425.00	0.18	0.49		0.22	0.09	0.12	0.04	0.56	0.09
Blood	1.65	793.00	0.33	0.20		1.42	0.24	0.48	0.23	0.37	0.24
Carcass	16.80	3663.00	1.52	0.09		14.01	2.57	1.47	0.12	0.11	0.02
Tail	0.82	793.00									
Sac Time Total Bq		240478.00				Total Inj Bq		Total Inj uCi			
Inj Time Total Bq		382661.99				1729009.01		46.73			

Appendix 2.3: Biodistribution of [^{99m}Tc-DTMA-β-Ala-BBN(7-14)NH_2] in normal CF-1 mice at 24h p.i. (n=5).

24 hr (11:04am)	Mouse #: Wt(g)	1.00 Bq(cps)	%ID	%ID/g		Mouse #: Wt(g)	2.00 Bq(cps)	%ID	%ID/g
Background		5.00					4.22		
Body Wt	22.16					20.45			
Cage Paper		17825.00	96.07				11122.00	84.88	
Urine		5.00	0.03				20.00	0.15	
Bladder	0.02		0.00	0.00		0.02		0.00	0.00
Heart	0.09		0.00	0.00		0.09	1.00	0.01	0.08
Lung	0.15	2.00	0.01	0.07		0.16	2.00	0.02	0.10
Liver	1.19	111.00	0.60	0.50		0.94	117.00	0.89	0.95
Kidneys	0.20	17.00	0.09	0.46		0.20	21.00	0.16	0.80
Spleen	0.07	3.00	0.02	0.23		0.03	2.00	0.02	0.51
Stomach	1.00	11.00	0.06	0.06		0.41	497.00	3.79	9.25
S. Intestine	1.62	125.00	0.67	0.42		1.16	382.00	2.92	2.51
L. Intestine	1.10	52.00	0.28	0.25		0.60	672.00	5.13	8.55
Muscle	0.16		0.00	0.00		0.14	1.00	0.01	0.05
Bone	0.04		0.00	0.00		0.06		0.00	0.00
Brain	0.35		0.00	0.00		0.40		0.00	0.00
Pancreas	0.20	215.00	1.16	5.79		0.07	42.00	0.32	4.58
Tumor #1	0.20	5.00	0.03	0.13		0.49	11.00	0.08	0.17
Tumor #2	0.13	5.00	0.03	0.21		0.46	8.00	0.06	0.13
Blood	1.44	28.00	0.15	0.10		1.33	22.00	0.17	0.13
Carcass	13.22	151.00	0.81	0.06		12.76	183.00	1.40	0.11
Tail	0.65	20.00				0.71	42.00		
Sac Time Total Bq		18555.00					13103.00		
Inj Time Total Bq		295658.27					209228.96		

	Mouse #: Wt(g)	3.00 Bq(cps)	%ID	%ID/g		Mouse #: Wt(g)	4.00 Bq(cps)	%ID	%ID/g
Background		7.44					4.28		
Body Wt	25.53					22.50			
Cage Paper		13685.00	96.31				11124.00	95.61	
Urine		32.00	0.23				12.00	0.10	
Bladder	0.02		0.00	0.00		0.02		0.00	0.00
Heart	0.08	8.00	0.06	0.70		0.08		0.00	0.00
Lung	0.18		0.00	0.00		0.20	7.00	0.06	0.30
Liver	1.26	99.00	0.70	0.55		1.08	85.00	0.73	0.68
Kidneys	0.28	10.00	0.07	0.25		0.29	15.00	0.13	0.44
Spleen	0.10		0.00	0.00		0.10		0.00	0.00
Stomach	0.35	6.00	0.04	0.12		0.64	23.00	0.20	0.31
S. Intestine	1.66	84.00	0.59	0.36		1.66	103.00	0.89	0.53
L. Intestine	0.94	84.00	0.59	0.63		0.79	55.00	0.47	0.60
Muscle	0.14		0.00	0.00		0.18	1.00	0.01	0.05
Bone	0.06		0.00	0.00		0.06		0.00	0.00
Brain	0.47		0.00	0.00		0.39		0.00	0.00
Pancreas	0.22	86.00	0.61	2.75		0.17	87.00	0.75	4.40
Tumor #1	0.15		0.00	0.00		0.24	4.00	0.03	0.14
Tumor #2	0.32	1.00	0.01	0.02		0.19	4.00	0.03	0.18
Blood	1.66	13.00	0.09	0.06		1.46	28.00	0.24	0.16
Carcass	16.62	101.00	0.71	0.04		14.08	87.00	0.75	0.05
Tail	0.79	143.00				0.67	61.00		
Sac Time Total Bq		14209.00					11635.00		
Inj Time Total Bq		228440.78					186165.23		

	Mouse #: Wt(g)	5.00 Bq(cps)	%ID	%ID/g		Averages Wt	STDev	%ID for as-measured mouse %ID	%STDev	%ID/g	%STDev
Background		4.50									
Body Wt	22.45					22.62	1.83				
Cage Paper		11690.00	96.52					93.88	5.04		
Urine		17.00	0.14					0.13	0.07		
Bladder	0.02		0.00	0.00		0.02	0.00	0.00	0.00	0.00	0.00
Heart	0.08		0.00	0.00		0.08	0.01	0.01	0.02	0.16	0.31
Lung	0.20	1.00	0.01	0.04		0.18	0.02	0.02	0.02	0.10	0.12
Liver	1.13	69.00	0.57	0.50		1.12	0.12	0.70	0.13	0.64	0.19
Kidneys	0.29	15.00	0.12	0.43		0.25	0.05	0.12	0.03	0.48	0.20
Spleen	0.03	2.00	0.02	0.55		0.07	0.04	0.01	0.01	0.26	0.27
Stomach	0.45	3.00	0.02	0.06		0.57	0.26	0.82	1.66	1.96	4.08
S. Intestine	1.47	77.00	0.64	0.43		1.51	0.21	1.14	1.00	0.85	0.93
L. Intestine	0.78	35.00	0.29	0.37		0.84	0.19	1.35	2.12	2.08	3.62
Muscle	0.16		0.00	0.00		0.16	0.02	0.00	0.00	0.02	0.03
Bone	0.05		0.00	0.00		0.05	0.01	0.00	0.00	0.00	0.00
Brain	0.43	1.00	0.01	0.02		0.41	0.04	0.00	0.00	0.00	0.01
Pancreas	0.22	82.00	0.68	3.08		0.18	0.06	0.70	0.30	4.12	1.23
Tumor #1	0.21	3.00	0.02	0.12		0.26	0.13	0.03	0.03	0.11	0.07
Tumor #2	0.21	4.00	0.03	0.16		0.26	0.13	0.03	0.02	0.14	0.07
Blood	1.46	20.00	0.17	0.11		1.47	0.12	0.16	0.05	0.11	0.04
Carcass	14.41	92.00	0.76	0.05		14.22	1.50	0.89	0.29	0.06	0.03
Tail	0.72	54.00									
Sac Time Total Bq		12111.00				Total Inj Bq		Total Inj uCi			
Inj Time Total Bq		193630.30				1113123.53		30.08			

Appendix 3.1: Biodistribution of [^{64}Cu-NOTA-β-Ala-BBN(7-14)NH_2] in normal CF-1 mice at 1h p.i. (n=5).

	Mouse #:	1.00				Mouse #:	2.00		
	Wt(g)	Bq(cps)	%ID	%ID/g		Wt(g)	Bq(cps)	%ID	%ID/g
Background		8.44					9.83		
Body Wt	24.02					25.55			
Cage Paper		84864.00	62.07				111.00	0.08	
Urine		20929.00	15.31				########	69.17	
Bladder	0.02	43.00	0.03	1.57		0.02	189.00	0.13	6.41
Heart	0.14	28.00	0.02	0.15		0.09	9.00	0.01	0.07
Lung	0.17	95.00	0.07	0.41		0.19	150.00	0.10	0.54
Liver	1.42	2574.00	1.88	1.33		1.39	3215.00	2.18	1.57
Kidneys	0.32	1141.00	0.83	2.61		0.35	1299.00	0.88	2.52
Spleen	0.10	93.00	0.07	0.68		0.10	87.00	0.06	0.59
Stomach	0.56	514.00	0.38	0.67		0.43	533.00	0.36	0.84
S. Intestine	1.59	13936.00	10.19	6.41		1.31	11998.00	8.14	6.22
L. Intestine	0.89	2979.00	2.18	2.45		1.10	6219.00	4.22	3.84
Muscle	0.17	1.00	0.00	0.00		0.12	1.00	0.00	0.01
Bone	0.04	27.00	0.02	0.49		0.06	14.00	0.01	0.16
Brain	0.37	18.00	0.01	0.04		0.40	21.00	0.01	0.04
Pancreas	0.20	3973.00	2.91	14.53		0.19	4119.00	2.80	14.71
Blood	1.56	326.00	0.24	0.15		1.66	972.00	0.66	0.40
Carcass	15.82	5185.00	3.79	0.24		17.03	16492.00	11.19	0.66
Tail	0.82	725.00				0.72	675.00		
Sac Time Total Bq (less tail)		########					########		

	Mouse #:	3.00				Mouse #:	4.00		
	Wt(g)	Bq(cps)	%ID	%ID/g		Wt(g)	Bq(cps)	%ID	%ID/g
Background		6.89					7.50		
Body Wt	25.55					27.07			
Cage Paper		########	71.72				96144.00	65.25	
Urine		4949.00	3.45				18750.00	12.72	
Bladder	0.02	36.00	0.03	1.26		0.02	24.00	0.02	0.81
Heart	0.08	46.00	0.03	0.40		0.13	34.00	0.02	0.18
Lung	0.28	206.00	0.14	0.51		0.20	147.00	0.10	0.50
Liver	1.60	2548.00	1.78	1.11		1.84	2933.00	1.99	1.08
Kidneys	0.31	1155.00	0.81	2.60		0.41	2767.00	1.88	4.58
Spleen	0.11	142.00	0.10	0.90		0.13	127.00	0.09	0.66
Stomach	0.40	1078.00	0.75	1.88		0.44	419.00	0.28	0.65
S. Intestine	1.71	14218.00	9.92	5.80		1.77	12264.00	8.32	4.70
L. Intestine	1.06	3062.00	2.14	2.02		1.02	2423.00	1.64	1.61
Muscle	0.15	36.00	0.03	0.17		0.19	16.00	0.01	0.06
Bone	0.09	17.00	0.01	0.13		0.04	17.00	0.01	0.29
Brain	0.42	20.00	0.01	0.03		0.39	28.00	0.02	0.05
Pancreas	0.16	4238.00	2.96	18.49		0.24	4992.00	3.39	14.12
Blood	1.66	1383.00	0.97	0.58		1.76	442.00	0.30	0.17
Carcass	16.74	7383.00	5.15	0.31		17.71	5831.00	3.96	0.22
Tail	0.70	2985.00				0.70	1309.00		
Sac Time Total Bq (less tail)		########					########		
Inj Time Total Bq		#REF!					#REF!		

	Mouse #:	5.00				Averages		%ID for as-measured mouse			
	Wt(g)	Bq(cps)	%ID	%ID/g		Wt	STDev	%ID	%STDev	%ID/g	%STDev
Background		11.11									
Body Wt	26.48					25.73	1.16				
Cage Paper		99068.00	75.67					54.96	31.14		
Urine		1515.00	1.16					20.36	27.93		
Bladder	0.02	1.00	0.00	0.04		0.02	0.00	0.04	0.05	2.02	2.52
Heart	0.15	24.00	0.02	0.12		0.12	0.03	0.02	0.01	0.18	0.13
Lung	0.23	120.00	0.09	0.40		0.21	0.04	0.10	0.03	0.47	0.06
Liver	1.58	2826.00	2.16	1.37		1.57	0.18	2.00	0.17	1.29	0.20
Kidneys	0.39	1020.00	0.78	2.00		0.36	0.04	1.04	0.47	2.86	0.99
Spleen	0.09	85.00	0.06	0.72		0.11	0.02	0.08	0.02	0.71	0.12
Stomach	0.45	418.00	0.32	0.71		0.46	0.06	0.42	0.19	0.95	0.53
S. Intestine	1.59	12752.00	9.74	6.13		1.59	0.18	9.26	0.96	5.85	0.68
L. Intestine	0.80	2322.00	1.77	2.22		0.97	0.13	2.39	1.05	2.43	0.85
Muscle	0.12		0.00	0.00		0.15	0.03	0.01	0.01	0.05	0.07
Bone	0.05	1.00	0.00	0.02		0.06	0.02	0.01	0.01	0.22	0.18
Brain	0.42	1.00	0.00	0.00		0.40	0.02	0.01	0.01	0.03	0.02
Pancreas	0.31	5546.00	4.24	13.66		0.22	0.06	3.26	0.59	15.10	1.93
Blood	1.72	376.00	0.29	0.17		1.67	0.08	0.49	0.31	0.29	0.19
Carcass	17.65	4849.00	3.70	0.21		16.99	0.77	5.56	3.20	0.33	0.19
Tail	0.76	702.00									

Appendix 3.2: Biodistribution of [^{64}Cu-NOTA-5-Ava-BBN(7-14)NH_2] in normal CF-1 mouse biodistribution at 1h p.i. (n=4).

	Mouse #: 1.00					Mouse #: 2.00			
	Wt(g)	Bq(cps)	%ID	%ID/g		Wt(g)	Bq(cps)	%ID	%ID/g
Background		5.39					9.17		
Body Wt	25.02					25.32			
Cage Paper		101493.00	45.91				89426.00	61.08	
Urine		89846.00	40.64				28734.00	19.62	
Bladder	0.02	51.00	0.02	1.15		0.02	52.00	0.04	1.78
Heart	0.10	41.00	0.02	0.19		0.17	33.00	0.02	0.13
Lung	0.21	126.00	0.06	0.27		0.18	116.00	0.08	0.44
Liver	1.46	2901.00	1.31	0.90		1.51	3023.00	2.06	1.37
Kidneys	0.41	1166.00	0.53	1.29		0.38	1357.00	0.93	2.44
Spleen	0.14	94.00	0.04	0.30		0.14	128.00	0.09	0.62
Stomach	0.45	381.00	0.17	0.38		0.36	521.00	0.36	0.99
S. Intestine	1.60	9671.00	4.37	2.73		1.53	10595.00	7.24	4.73
L. Intestine	0.94	3575.00	1.62	1.72		0.99	2163.00	1.48	1.49
Muscle	0.14	50.00	0.02	0.16		0.13	16.00	0.01	0.08
Bone	0.07	32.00	0.01	0.21		0.04	4.00	0.00	0.07
Brain	0.37	14.00	0.01	0.02		0.43		0.00	0.00
Pancreas	0.18	3981.00	1.80	10.00		0.31	4204.00	2.87	9.26
Blood	1.63	572.00	0.26	0.16		1.65	532.00	0.36	0.22
Carcass	16.27	7063.00	3.20	0.20		16.50	5513.00	3.77	0.23
Tail	0.83	929.00				0.72	1424.00		
Sac Time Total Bq (less tail)		221057.00					146417.00		
Inj Time Total Bq		#REF!					#REF!		

	Mouse #: 3.00					Mouse #: 4.00			
	Wt(g)	Bq(cps)	%ID	%ID/g		Wt(g)	Bq(cps)	%ID	%ID/g
Background		10.00					7.67		
Body Wt	26.32					25.53			
Cage Paper		93838.00	70.32				73287.00	55.62	
Urine		2761.00	2.07				26132.00	19.83	
Bladder	0.02	21.00	0.02	0.79		0.02	21.00	0.02	0.80
Heart	0.11	6.00	0.00	0.04		0.10	21.00	0.02	0.16
Lung	0.26	99.00	0.07	0.29		0.20	107.00	0.08	0.41
Liver	1.56	2608.00	1.95	1.25		1.47	3461.00	2.63	1.79
Kidneys	0.33	1021.00	0.77	2.32		0.36	1389.00	1.05	2.93
Spleen	0.15	48.00	0.04	0.24		0.15	127.00	0.10	0.64
Stomach	0.52	5542.00	4.15	7.99		0.38	397.00	0.30	0.79
S. Intestine	1.56	13348.00	10.00	6.41		1.42	11957.00	9.08	6.39
L. Intestine	0.83	1892.00	1.42	1.71		0.73	1998.00	1.52	2.08
Muscle	0.14	4.00	0.00	0.02		0.19	8.00	0.01	0.03
Bone	0.06	1.00	0.00	0.01		0.07	9.00	0.01	0.10
Brain	0.50	4.00	0.00	0.01		0.45	10.00	0.01	0.02
Pancreas	0.26	4002.00	3.00	11.53		0.26	4969.00	3.77	14.51
Blood	1.71	335.00	0.25	0.15		1.66	447.00	0.34	0.20
Carcass	17.47	7921.00	5.94	0.34		16.83	7415.00	5.63	0.33
Tail	0.72	550.00				0.73	1433.00		
Sac Time Total Bq (less tail)		133451.00					131755.00		
Inj Time Total Bq		#REF!					#REF!		

	Averages		%ID for as-measured mouse			
	Wt	STDev	%ID	%STDev	%ID/g	%STDev
Background						
Body Wt	25.55	0.56				
Cage Paper			58.23	10.21		
Urine			20.54	15.78		
Bladder	0.02	0.00	0.02	0.01	1.13	0.46
Heart	0.12	0.03	0.02	0.01	0.13	0.06
Lung	0.21	0.03	0.07	0.01	0.35	0.08
Liver	1.50	0.05	1.99	0.54	1.33	0.37
Kidneys	0.37	0.03	0.82	0.23	2.24	0.69
Spleen	0.15	0.01	0.07	0.03	0.45	0.21
Stomach	0.43	0.07	1.25	1.94	2.54	3.64
S. Intestine	1.53	0.08	7.67	2.48	5.07	1.74
L. Intestine	0.87	0.12	1.51	0.08	1.75	0.24
Muscle	0.15	0.03	0.01	0.01	0.07	0.06
Bone	0.06	0.01	0.01	0.01	0.10	0.08
Brain	0.44	0.05	0.00	0.00	0.01	0.01
Pancreas	0.25	0.05	2.86	0.81	11.33	2.32
Blood	1.66	0.03	0.30	0.06	0.18	0.04
Carcass	16.77	0.52	4.63	1.35	0.27	0.07

Appendix 3.3: Biodistribution of [^{64}Cu-NOTA-6-Ahx-BBN(7-14)NH_2] in normal CF-1 mice at 1h p.i. (n=5).

	Mouse #:	1.00				Mouse #:	2.00		
	Wt(g)	Bq(cps)	%ID	%ID/g		Wt(g)	Bq(cps)	%ID	%ID/g
Background		5.06					7.61		
Body Wt	22.26					21.40			
Cage Paper		76488.00	66.88				60026.00	63.81	
Urine		5332.00	4.66				4604.00	4.89	
Bladder	0.02	12.00	0.01	0.52		0.02	18.00	0.02	0.96
Heart	0.10	48.00	0.04	0.42		0.11	1.00	0.00	0.01
Lung	0.17	101.00	0.09	0.52		0.15	98.00	0.10	0.69
Liver	1.19	1528.00	1.34	1.12		1.41	1984.00	2.11	1.50
Kidneys	0.31	823.00	0.72	2.32		0.29	827.00	0.88	3.03
Spleen	0.07	89.00	0.08	1.11		0.13	90.00	0.10	0.74
Stomach	0.44	611.00	0.53	1.21		0.48	431.00	0.46	0.95
S. Intestine	1.60	14546.00	12.72	7.95		1.33	12301.00	13.08	9.83
L. Intestine	0.81	2722.00	2.38	2.94		0.82	2491.00	2.65	3.23
Muscle	0.15	27.00	0.02	0.16		0.13	34.00	0.04	0.28
Bone	0.03	35.00	0.03	1.02		0.05	16.00	0.02	0.34
Brain	0.46	38.00	0.03	0.07		0.35	9.00	0.01	0.03
Pancreas	0.11	3904.00	3.41	31.03		0.24	5590.00	5.94	24.76
Blood	1.45	248.00	0.22	0.15		1.39	283.00	0.30	0.22
Carcass	14.68	7813.00	6.83	0.47		13.93	5272.00	5.60	0.40
Tail	0.63	929.00				0.61	3613.00		

	Mouse #:	3.00				Mouse #:	4.00		
	Wt(g)	Bq(cps)	%ID	%ID/g		Wt(g)	Bq(cps)	%ID	%ID/g
Background		6.83					7.83		
Body Wt	21.30					25.32			
Cage Paper		205.00	0.29				89336.00	69.40	
Urine		49209.00	69.90				1639.00	1.27	
Bladder	0.02	6.00	0.01	0.43		0.02	1.00	0.00	0.04
Heart	0.06	15.00	0.02	0.36		0.08	16.00	0.01	0.16
Lung	0.14	82.00	0.12	0.83		0.21	104.00	0.08	0.38
Liver	1.18	1163.00	1.65	1.40		1.57	2210.00	1.72	1.09
Kidneys	0.29	599.00	0.85	2.93		0.39	1052.00	0.82	2.10
Spleen	0.09	119.00	0.17	1.88		0.11	114.00	0.09	0.81
Stomach	0.38	311.00	0.44	1.16		0.50	682.00	0.53	1.06
S. Intestine	1.42	9605.00	13.64	9.61		1.63	14483.00	11.25	6.90
L. Intestine	0.84	1610.00	2.29	2.72		1.07	6106.00	4.74	4.43
Muscle	0.14	4.00	0.01	0.04		0.13	13.00	0.01	0.08
Bone	0.04	13.00	0.02	0.46		0.07	7.00	0.01	0.08
Brain	0.40	10.00	0.01	0.04		0.39	11.00	0.01	0.02
Pancreas	0.18	4156.00	5.90	32.80		0.25	6576.00	5.11	20.43
Blood	1.38	223.00	0.32	0.23		1.65	332.00	0.26	0.16
Carcass	13.65	3070.00	4.36	0.32		16.39	6039.00	4.69	0.29
Tail	0.68	957.00				0.77	630.00		
Sac Time Total Bq (less tail)		70400.00					128721.00		

	Mouse #:	5.00				Averages		%ID for as-measured mouse			
	Wt(g)	Bq(cps)	%ID	%ID/g		Wt	STDev	%ID	%STDev	%ID/g	%STDev
Background		7.44									
Body Wt	23.30					22.72	1.66				
Cage Paper		131.00	0.15					40.11	36.46		
Urine		62845.00	71.44					30.43	36.76		
Bladder	0.02	252.00	0.29	14.32		0.02	0.00	0.07	0.12	3.25	6.20
Heart	0.10	6.00	0.01	0.07		0.09	0.02	0.02	0.02	0.20	0.18
Lung	0.18	77.00	0.09	0.49		0.17	0.03	0.10	0.01	0.58	0.18
Liver	1.37	1318.00	1.50	1.09		1.34	0.16	1.66	0.29	1.24	0.19
Kidneys	0.34	844.00	0.96	2.82		0.32	0.04	0.85	0.09	2.64	0.41
Spleen	0.13	117.00	0.13	1.02		0.11	0.03	0.11	0.04	1.11	0.46
Stomach	0.43	417.00	0.47	1.10		0.45	0.05	0.49	0.04	1.10	0.10
S. Intestine	1.36	9265.00	10.53	7.74		1.47	0.14	12.24	1.30	8.41	1.26
L. Intestine	0.71	1875.00	2.13	3.00		0.85	0.13	2.84	1.08	3.27	0.68
Muscle	0.11	1.00	0.00	0.01		0.13	0.01	0.02	0.01	0.11	0.11
Bone	0.08	10.00	0.01	0.14		0.05	0.02	0.02	0.01	0.41	0.37
Brain	0.44	2.00	0.00	0.01		0.41	0.04	0.01	0.01	0.03	0.02
Pancreas	0.25	5575.00	6.34	25.35		0.21	0.06	5.34	1.17	26.87	5.02
Blood	1.51	160.00	0.18	0.12		1.48	0.11	0.25	0.06	0.17	0.05
Carcass	15.57	5074.00	5.77	0.37		14.84	1.14	5.45	0.97	0.37	0.07
Tail	0.68	582.00									

Appendix 3.4: Biodistribution of [^{64}Cu-NOTA-9-Anc-BBN(7-14)NH_2] in normal CF-1 mice at 1h p.i. (n=5).

	Mouse #: 1.00 Wt(g)	Bq(cps)	%ID	%ID/g		Mouse #: 2.00 Wt(g)	Bq(cps)	%ID	%ID/g
Background		5.28					5.28		
Body Wt	26.68					27.76			
Cage Paper		14690.00	31.44				29406.00	43.02	
Urine		6905.00	14.78				3621.00	5.30	
Bladder	0.02	3.00	0.01	0.32		0.02	12.00	0.02	0.88
Heart	0.14	43.00	0.09	0.66		0.11	26.00	0.04	0.35
Lung	0.19	107.00	0.23	1.21		0.17	120.00	0.18	1.03
Liver	1.71	1835.00	3.93	2.30		1.70	2400.00	3.51	2.07
Kidneys	0.37	463.00	0.99	2.68		0.36	603.00	0.88	2.45
Spleen	0.13	47.00	0.10	0.77		0.13	64.00	0.09	0.72
Stomach	0.62	217.00	0.46	0.75		0.50	372.00	0.54	1.09
S. Intestine	1.60	13456.00	28.80	18.00		1.69	20253.00	29.63	17.53
L. Intestine	1.05	1187.00	2.54	2.42		0.96	2252.00	3.29	3.43
Muscle	0.17	19.00	0.04	0.24		0.15	26.00	0.04	0.25
Bone	0.08	9.00	0.02	0.24		0.05	27.00	0.04	0.79
Brain	0.40	12.00	0.03	0.06		0.42	26.00	0.04	0.09
Pancreas	0.33	4298.00	9.20	27.87		0.24	3636.00	5.32	22.16
Blood	1.73	323.00	0.69	0.40		1.80	505.00	0.74	0.41
Carcass	17.17	3111.00	6.66	0.39		18.21	5008.00	7.33	0.40
Tail	0.79	1202.00				0.70	530.00		

	Mouse #: 3.00 Wt(g)	Bq(cps)	%ID	%ID/g		Mouse #: 4.00 Wt(g)	Bq(cps)	%ID	%ID/g
Background		6.72					6.39		
Body Wt	26.57					27.93			
Cage Paper		36.00	0.06				30892.00	51.99	
Urine		30687.00	51.73				924.00	1.56	
Bladder	0.02	5.00	0.01	0.42		0.02	1.00	0.00	0.08
Heart	0.15	38.00	0.06	0.43		0.15	22.00	0.04	0.25
Lung	0.20	119.00	0.20	1.00		0.17	98.00	0.16	0.97
Liver	1.59	2330.00	3.93	2.47		1.55	2868.00	4.83	3.11
Kidneys	0.37	505.00	0.85	2.30		0.41	495.00	0.83	2.03
Spleen	0.11	86.00	0.14	1.32		0.14	75.00	0.13	0.90
Stomach	0.57	467.00	0.79	1.38		0.84	394.00	0.66	0.79
S. Intestine	1.53	16549.00	27.90	18.23		1.60	7764.00	13.07	8.17
L. Intestine	0.88	914.00	1.54	1.75		0.81	8986.00	15.12	18.67
Muscle	0.17	15.00	0.03	0.15		0.20	5.00	0.01	0.04
Bone	0.08	12.00	0.02	0.25		0.05	14.00	0.02	0.47
Brain	0.43	12.00	0.02	0.05		0.45	10.00	0.02	0.04
Pancreas	0.29	3778.00	6.37	21.96		0.27	3518.00	5.92	21.93
Blood	1.73	245.00	0.41	0.24		1.82	199.00	0.33	0.18
Carcass	17.30	3521.00	5.94	0.34		18.43	3149.00	5.30	0.29
Tail	0.81	335.00				0.80	378.00		

	Mouse #: 5.00 Wt(g)	Bq(cps)	%ID	%ID/g		Averages Wt	STDev	%ID for as-measured mouse %ID	%STDev	%ID/g	%STDev
Background		5.94									
Body Wt	28.95										
Cage Paper		30414.00	46.05			27.58	0.98				
Urine		3569.00	5.40					34.51	20.66		
Bladder	0.02	4.00	0.01	0.30				15.75	20.70		
Heart	0.11	22.00	0.03	0.30		0.02	0.00	0.01	0.01	0.40	0.29
Lung	0.19	78.00	0.12	0.62		0.13	0.02	0.05	0.03	0.40	0.16
Liver	1.70	1997.00	3.02	1.78		0.18	0.01	0.18	0.04	0.97	0.21
Kidneys	0.39	592.00	0.90	2.30		1.65	0.07	3.84	0.66	2.35	0.50
Spleen	0.12	47.00	0.07	0.59		0.38	0.02	0.89	0.06	2.35	0.24
Stomach	1.15	362.00	0.55	0.48		0.13	0.01	0.11	0.03	0.86	0.28
S. Intestine	1.89	19563.00	29.62	15.67		0.74	0.26	0.60	0.13	0.90	0.35
L. Intestine	0.93	1373.00	2.08	2.24		1.66	0.14	25.80	7.15	15.52	4.23
Muscle	0.12	10.00	0.02	0.13		0.93	0.09	4.92	5.74	5.70	7.28
Bone	0.06	25.00	0.04	0.63		0.16	0.03	0.03	0.01	0.16	0.09
Brain	0.42	4.00	0.01	0.01		0.06	0.02	0.03	0.01	0.48	0.24
Pancreas	0.36	4773.00	7.23	20.08		0.42	0.02	0.02	0.01	0.05	0.03
Blood	1.88	226.00	0.34	0.18		0.30	0.05	6.81	1.51	22.80	2.96
Carcass	18.40	2983.00	4.52	0.25		1.79	0.06	0.50	0.20	0.28	0.11
Tail	0.71	813.00				17.90	0.62	5.95	1.10	0.33	0.07

Appendix 3.5: Biodistribution of [^{64}Cu-NOTA-PABA-BBN(7-14)NH_2] in normal CF-1 mice at 1h p.i. (n=5).

	Mouse #: 1.00 Wt(g)	Bq(cps)	%ID	%ID/g		Mouse #: 2.00 Wt(g)	Bq(cps)	%ID	%ID/g
Background		4.56					5.06		
Body Wt	25.10					23.27			
Cage Paper		48157.00	58.21				13185.00	17.45	
Urine		9918.00	11.99				30529.00	40.41	
Bladder	0.02	18.00	0.02	1.09		0.02	52.00	0.07	3.44
Heart	0.15	20.00	0.02	0.16		0.10	9.00	0.01	0.12
Lung	0.22	56.00	0.07	0.31		0.20	48.00	0.06	0.32
Liver	1.37	830.00	1.00	0.73		1.27	650.00	0.86	0.68
Kidneys	0.37	970.00	1.17	3.17		0.32	770.00	1.02	3.18
Spleen	0.19	161.00	0.19	1.02		0.18	189.00	0.25	1.39
Stomach	0.53	686.00	0.83	1.56		0.50	2867.00	3.79	7.59
S. Intestine	1.56	8283.00	10.01	6.42		1.42	12190.00	16.13	11.36
L. Intestine	0.95	3204.00	3.87	4.08		0.75	4248.00	5.62	7.50
Muscle	0.22	19.00	0.02	0.10		0.16	7.00	0.01	0.06
Bone	0.04	19.00	0.02	0.57		0.04	16.00	0.02	0.53
Brain	0.30	1.00	0.00	0.00		0.44	16.00	0.02	0.05
Pancreas	0.30	6281.00	7.59	25.31		0.25	5725.00	7.58	30.31
Blood	1.63	263.00	0.32	0.20		1.51	184.00	0.24	0.16
Carcass	16.27	3837.00	4.64	0.29		15.43	4870.00	6.45	0.42
Tail	0.74	526.00				0.80	592.00		

	Mouse #: 3.00 Wt(g)	Bq(cps)	%ID	%ID/g		Mouse #: 4.00 Wt(g)	Bq(cps)	%ID	%ID/g
Background		5.39					5.56		
Body Wt	22.76					22.29			
Cage Paper		45436.00	58.96				39286.00	49.36	
Urine		7616.00	9.88				15114.00	18.99	
Bladder	0.02	13.00	0.02	0.84		0.02	15.00	0.02	0.94
Heart	0.12	14.00	0.02	0.15		0.10	15.00	0.02	0.19
Lung	0.19	47.00	0.06	0.32		0.24	38.00	0.05	0.20
Liver	1.24	715.00	0.93	0.75		1.18	538.00	0.68	0.57
Kidneys	0.36	904.00	1.17	3.26		0.30	1373.00	1.73	5.75
Spleen	0.18	205.00	0.27	1.48		0.10	123.00	0.15	1.55
Stomach	0.52	537.00	0.70	1.34		0.39	583.00	0.73	1.88
S. Intestine	1.53	9224.00	11.97	7.82		1.50	7572.00	9.51	6.34
L. Intestine	0.83	3056.00	3.97	4.78		0.96	4176.00	5.25	5.47
Muscle	0.16	23.00	0.03	0.19		0.21	7.00	0.01	0.04
Bone	0.06	7.00	0.01	0.15		0.07	6.00	0.01	0.11
Brain	0.39	6.00	0.01	0.02		0.42	13.00	0.02	0.04
Pancreas	0.19	4857.00	6.30	33.17		0.27	7171.00	9.01	33.37
Blood	1.48	250.00	0.32	0.22		1.45	170.00	0.21	0.15
Carcass	14.73	4148.00	5.38	0.37		14.44	3383.00	4.25	0.29
Tail	0.77	486.00				0.68	594.00		

	Mouse #: 5.00 Wt(g)	Bq(cps)	%ID	%ID/g		Averages Wt	STDev	%ID for as-measured mouse %ID	%STDev	%ID/g	%STDev
Background		5.50									
Body Wt	21.15					22.91	1.45				
Cage Paper		54166.00	67.42					50.28	19.43		
Urine		1390.00	1.73					16.60	14.66		
Bladder	0.02	7.00	0.01	0.44		0.02	0.00	0.03	0.02	1.35	1.19
Heart	0.11	1.00	0.00	0.01		0.12	0.02	0.01	0.01	0.13	0.07
Lung	0.23	29.00	0.04	0.16		0.22	0.02	0.06	0.01	0.26	0.08
Liver	1.21	735.00	0.91	0.76		1.25	0.07	0.88	0.12	0.70	0.08
Kidneys	0.30	884.00	1.10	3.67		0.33	0.03	1.24	0.28	3.81	1.11
Spleen	0.10	142.00	0.18	1.77		0.15	0.05	0.21	0.05	1.44	0.27
Stomach	0.36	503.00	0.63	1.74		0.46	0.08	1.34	1.38	2.82	2.67
S. Intestine	1.32	8593.00	10.70	8.10		1.47	0.10	11.67	2.66	8.01	2.04
L. Intestine	0.83	4637.00	5.77	6.95		0.86	0.09	4.90	0.91	5.75	1.44
Muscle	0.20	6.00	0.01	0.04		0.19	0.03	0.02	0.01	0.09	0.06
Bone	0.04	2.00	0.00	0.06		0.05	0.01	0.01	0.01	0.28	0.25
Brain	0.48	9.00	0.01	0.02		0.41	0.07	0.01	0.01	0.03	0.02
Pancreas	0.23	5728.00	7.13	31.00		0.25	0.04	7.52	0.98	30.63	3.26
Blood	1.37	239.00	0.30	0.22		1.49	0.09	0.28	0.05	0.19	0.03
Carcass	13.86	3271.00	4.07	0.29		14.95	0.93	4.96	0.97	0.33	0.06
Tail	0.62	413.00									

Appendix 3.6: Biodistribution of [^{64}Cu-NOTA-6-Ahx-BBN(7-14)NH_2] in PC-3 tumor-bearing SCID mice at 1h p.i. (n=5).

1 hr	Mouse #:	1.00				Mouse #:	2.00				
	Wt(g)	Bq(cps)	%ID	%ID/g		Wt(g)	Bq(cps)	%ID	%ID/g		
Background		4.72					5.72				
Body Wt	27.99					27.07					
Cage Paper		48616.00	64.80				20.00	0.03			
Urine		876.00	1.17				49084.00	67.90			
Bladder	0.02	21.00	0.03	1.40		0.02	22.00	0.03	1.52		
Heart	0.12	35.00	0.05	0.39		0.07	31.00	0.04	0.61		
Lung	0.20	170.00	0.23	1.13		0.23	161.00	0.22	0.97		
Liver	1.39	2169.00	2.89	2.08		1.10	2297.00	3.18	2.89		
Kidneys	0.29	1036.00	1.38	4.76		0.33	988.00	1.37	4.14		
Spleen	0.15	94.00	0.13	0.84		0.06	103.00	0.14	2.37		
Stomach	0.62	709.00	0.95	1.52		0.35	298.00	0.41	1.18		
S. Intestine	1.49	7988.00	10.65	7.15		1.35	6344.00	8.78	6.50		
L. Intestine	1.25	1953.00	2.60	2.08		1.07	1539.00	2.13	1.99		
Muscle	0.24	35.00	0.05	0.19		0.21	18.00	0.02	0.12		
Bone	0.05	25.00	0.03	0.67		0.06	23.00	0.03	0.53		
Brain	0.42	16.00	0.02	0.05		0.28	19.00	0.03	0.09		
Pancreas	0.30	3335.00	4.45	14.82		0.25	2445.00	3.38	13.53		
Tumor #1	0.27	547.00	0.73	2.70		0.14	331.00	0.46	3.27		
Tumor #2	0.12	320.00	0.43	3.55		0.11	206.00	0.28	2.59		
Blood	1.82	1004.00	1.34	0.74		1.76	879.00	1.22	0.69		
Carcass	17.90	6070.00	8.09	0.45		18.10	7480.00	10.35	0.57		
Tail	0.84	897.00				1.01	2362.00				
Sac Time Total Bq (less tail)		75019.00					72288.00				
Inj Time Total Bq		80173.61					78836.61				

	Mouse #:	3.00				Mouse #:	4.00				
	Wt(g)	Bq(cps)	%ID	%ID/g		Wt(g)	Bq(cps)	%ID	%ID/g		
Background		4.94					5.39				
Body Wt	24.16					26.68					
Cage Paper		17.00	0.05				25.00	0.03			
Urine		25974.00	72.92				64025.00	70.45			
Bladder	0.02	20.00	0.06	2.81		0.02	15.00	0.02	0.83		
Heart	0.12	27.00	0.08	0.63		0.09	37.00	0.04	0.45		
Lung	0.19	78.00	0.22	1.15		0.25	183.00	0.20	0.81		
Liver	1.29	1624.00	4.56	3.53		1.16	2331.00	2.57	2.21		
Kidneys	0.34	485.00	1.36	4.00		0.29	1259.00	1.39	4.78		
Spleen	0.08	109.00	0.31	3.83		0.07	125.00	0.14	1.96		
Stomach	0.43	141.00	0.40	0.92		0.34	377.00	0.41	1.22		
S. Intestine	1.16	2445.00	6.86	5.92		1.40	7719.00	8.49	6.07		
L. Intestine	0.69	686.00	1.93	2.79		1.16	2433.00	2.68	2.31		
Muscle	0.20	7.00	0.02	0.10		0.19	19.00	0.02	0.11		
Bone	0.06	11.00	0.03	0.51		0.06	8.00	0.01	0.15		
Brain	0.46	16.00	0.04	0.10		0.44	1.00	0.00	0.00		
Pancreas	0.27	1033.00	2.90	10.74		0.31	4353.00	4.79	15.45		
Tumor #1	0.15	142.00	0.40	2.66		0.19	285.00	0.31	1.65		
Tumor #2	0.22	155.00	0.44	1.98		0.18	483.00	0.53	2.95		
Blood	1.57	469.00	1.32	0.84		1.73	941.00	1.04	0.60		
Carcass	15.61	2181.00	6.12	0.39		17.29	6258.00	6.89	0.40		
Tail	0.71	1640.00				0.97	1885.00				
Sac Time Total Bq (less tail)		35620.00					90877.00				
Inj Time Total Bq		39349.66					97964.39				

	Mouse #:	5.00			1 hr	Averages		%ID for as-measured mouse			
	Wt(g)	Bq(cps)	%ID	%ID/g		Wt	STDev	%ID	%STDev	%ID/g	%STDev
Background		5.83									
Body Wt	25.07					26.19	1.55				
Cage Paper		63322.00	67.54					26.49	36.24		
Urine		3355.00	3.58					43.20	37.33		
Bladder	0.02	15.00	0.02	0.80		0.02	0.00	0.03	0.02	1.47	0.82
Heart	0.13	52.00	0.06	0.43		0.11	0.03	0.05	0.01	0.50	0.11
Lung	0.23	135.00	0.14	0.63		0.22	0.02	0.20	0.03	0.94	0.22
Liver	1.40	2277.00	2.43	1.73		1.27	0.13	3.12	0.85	2.49	0.72
Kidneys	0.33	1513.00	1.61	4.89		0.32	0.02	1.42	0.11	4.52	0.41
Spleen	0.07	114.00	0.12	1.74		0.09	0.04	0.17	0.08	2.15	1.09
Stomach	0.43	492.00	0.52	1.22		0.43	0.11	0.54	0.23	1.21	0.21
S. Intestine	1.20	8378.00	8.94	7.45		1.32	0.14	8.74	1.35	6.62	0.67
L. Intestine	0.97	1958.00	2.09	2.15		1.03	0.22	2.28	0.33	2.26	0.32
Muscle	0.16	11.00	0.01	0.07		0.20	0.03	0.02	0.01	0.12	0.05
Bone	0.06	12.00	0.01	0.21		0.06	0.00	0.02	0.01	0.41	0.22
Brain	0.44	17.00	0.02	0.04		0.41	0.07	0.02	0.02	0.06	0.04
Pancreas	0.28	3521.00	3.76	13.41		0.28	0.02	3.85	0.77	13.59	1.81
Tumor #1	0.17	434.00	0.46	2.72		0.18	0.05	0.47	0.16	2.60	0.59
Tumor #2	0.11	315.00	0.34	3.05		0.15	0.05	0.40	0.10	2.83	0.59
Blood	1.63	1025.00	1.09	0.67		1.70	0.10	1.20	0.13	0.71	0.09
Carcass	16.40	6803.00	7.26	0.44		17.06	1.05	7.74	1.62	0.45	0.07
Tail	0.80	2896.00									
Sac Time Total Bq (less tail)		93749.00				Total Inj Bq		Total Inj uCi			
Inj Time Total Bq		102065.1				398389.4		10.77			

Appendix 3.7: Biodistribution of [^{64}Cu-NOTA-6-Ahx-BBN(7-14)NH_2] in PC-3 tumor-bearing SCID mice at 4h p.i. (n=5).

4 hr	Mouse #:	1.00				Mouse #:	2.00		
	Wt(g)	Bq(cps)	%ID	%ID/g		Wt(g)	Bq(cps)	%ID	%ID/g
Background		5.72					4.67		
Body Wt	24.43					25.77			
Cage Paper		36301.00	77.98				40803.00	80.53	
Urine		1092.00	2.35				759.00	1.50	
Bladder	0.02	1.00	0.00	0.11		0.02	8.00	0.02	0.79
Heart	0.11	15.00	0.03	0.29		0.08	25.00	0.05	0.62
Lung	0.23	85.00	0.18	0.79		0.18	83.00	0.16	0.91
Liver	0.93	953.00	2.05	2.20		1.17	1232.00	2.43	2.08
Kidneys	0.29	234.00	0.50	1.73		0.27	239.00	0.47	1.75
Spleen	0.09	49.00	0.11	1.17		0.07	76.00	0.15	2.14
Stomach	0.27	147.00	0.32	1.17		0.46	118.00	0.23	0.51
S. Intestine	1.72	1729.00	3.71	2.16		1.48	1126.00	2.22	1.50
L. Intestine	0.78	3147.00	6.76	8.67		0.80	2612.00	5.16	6.44
Muscle	0.20	1.00	0.00	0.01		0.19	4.00	0.01	0.04
Bone	0.05	7.00	0.02	0.30		0.06	1.00	0.00	0.03
Brain	0.36	3.00	0.01	0.02		0.41	1.00	0.00	0.00
Pancreas	0.21	912.00	1.96	9.33		0.29	1197.00	2.36	8.15
Tumor #1	0.40	278.00	0.60	1.49		0.16	140.00	0.28	1.73
Tumor #2	0.13	128.00	0.27	2.11		0.24	233.00	0.46	1.92
Blood	1.59	144.00	0.31	0.19		1.68	261.00	0.52	0.31
Carcass	15.86	1328.00	2.85	0.18		16.86	1749.00	3.45	0.20
Tail	0.82	221.00				0.69	203.00		

	Mouse #:	3.00				Mouse #:	4.00		
	Wt(g)	Bq(cps)	%ID	%ID/g		Wt(g)	Bq(cps)	%ID	%ID/g
Background		4.72					4.94		
Body Wt	24.58					25.89			
Cage Paper		49505.00	82.32				65779.00	78.23	
Urine		363.00	0.60				2586.00	3.08	
Bladder	0.02	1.00	0.00	0.08		0.02	6.00	0.01	0.36
Heart	0.10	21.00	0.03	0.35		0.10	35.00	0.04	0.42
Lung	0.20	69.00	0.11	0.57		0.17	91.00	0.11	0.64
Liver	1.10	1399.00	2.33	2.11		0.90	1701.00	2.02	2.25
Kidneys	0.28	253.00	0.42	1.50		0.32	373.00	0.44	1.39
Spleen	0.05	64.00	0.11	2.13		0.05	110.00	0.13	2.62
Stomach	0.38	127.00	0.21	0.56		0.28	264.00	0.31	1.12
S. Intestine	1.35	1336.00	2.22	1.65		1.17	2307.00	2.74	2.34
L. Intestine	0.68	3527.00	5.87	8.63		0.81	5952.00	7.08	8.74
Muscle	0.17	16.00	0.03	0.16		0.18	4.00	0.00	0.03
Bone	0.07	2.00	0.00	0.05		0.06	21.00	0.02	0.42
Brain	0.46	11.00	0.02	0.04		0.43	17.00	0.02	0.05
Pancreas	0.26	1278.00	2.13	8.17		0.25	1966.00	2.34	9.35
Tumor #1	0.24	304.00	0.51	2.11		0.12	133.00	0.16	1.32
Tumor #2	0.15	174.00	0.29	1.93		0.22	322.00	0.38	1.74
Blood	1.60	270.00	0.45	0.28		1.68	402.00	0.48	0.28
Carcass	16.18	1415.00	2.35	0.15		17.52	2019.00	2.40	0.14
Tail	0.83	205.00				0.94	454.00		

	Mouse #:	5.00			4 hr	Averages		%ID for as-measured mouse			
	Wt(g)	Bq(cps)	%ID	%ID/g		Wt	STDev	%ID	%STDev	%ID/g	%STDev
Background		4.67									
Body Wt	25.41					25.22	0.67				
Cage Paper		60767.00	77.14					79.24	2.13		
Urine		1285.00	1.63					1.83	0.93		
Bladder	0.02	9.00	0.01	0.57		0.02	0.00	0.01	0.01	0.38	0.30
Heart	0.09	9.00	0.01	0.13		0.10	0.01	0.03	0.01	0.36	0.18
Lung	0.18	91.00	0.12	0.64		0.19	0.02	0.14	0.03	0.71	0.14
Liver	1.22	1513.00	1.92	1.57		1.06	0.14	2.15	0.22	2.04	0.27
Kidneys	0.31	388.00	0.49	1.59		0.29	0.02	0.47	0.03	1.59	0.15
Spleen	0.06	87.00	0.11	1.84		0.06	0.02	0.12	0.02	1.98	0.53
Stomach	0.35	207.00	0.26	0.75		0.35	0.08	0.27	0.05	0.82	0.31
S. Intestine	1.31	2112.00	2.68	2.05		1.41	0.21	2.72	0.61	1.94	0.35
L. Intestine	0.83	7188.00	9.12	10.99		0.78	0.06	6.80	1.51	8.69	1.61
Muscle	0.21	4.00	0.01	0.02		0.19	0.02	0.01	0.01	0.05	0.06
Bone	0.04	16.00	0.02	0.51		0.06	0.01	0.01	0.01	0.26	0.21
Brain	0.41	15.00	0.02	0.05		0.41	0.04	0.01	0.01	0.03	0.02
Pancreas	0.30	2433.00	3.09	10.30		0.26	0.04	2.37	0.43	9.06	0.91
Tumor #1	0.11	206.00	0.26	2.38		0.21	0.12	0.36	0.18	1.80	0.44
Tumor #2	0.07	120.00	0.15	2.18		0.16	0.07	0.31	0.12	1.98	0.17
Blood	1.65	337.00	0.43	0.26		1.64	0.04	0.44	0.08	0.27	0.04
Carcass	16.60	1988.00	2.52	0.15		16.60	0.64	2.72	0.46	0.16	0.03
Tail	0.89	363.00									

Appendix 3.8: Biodistribution of [^{64}Cu-NOTA-6-Ahx-BBN(7-14)NH_2] in PC-3 tumor-bearing SCID mice at 24h p.i. (n=4).

24 hr	Mouse #:	1.00				Mouse #:	2.00		
	Wt(g)	Bq(cps)	%ID	%ID/g		Wt(g)	Bq(cps)	%ID	%ID/g
Background		4.06					4.94		
Body Wt	22.22					24.49			
Cage Paper		26421.00	85.77				22375.00	89.36	
Urine		22.00	0.07				1.00	0.00	
Bladder	0.02	11.00	0.04	1.79		0.02	1.00	0.00	0.20
Heart	0.10	6.00	0.02	0.19		0.10	10.00	0.04	0.40
Lung	0.18	45.00	0.15	0.81		0.22	38.00	0.15	0.69
Liver	1.15	416.00	1.35	1.17		1.32	448.00	1.79	1.36
Kidneys	0.30	78.00	0.25	0.84		0.26	95.00	0.38	1.46
Spleen	0.09	19.00	0.06	0.69		0.09	13.00	0.05	0.58
Stomach	0.47	67.00	0.22	0.46		0.38	27.00	0.11	0.28
S. Intestine	1.39	345.00	1.12	0.81		2.04	251.00	1.00	0.49
L. Intestine	0.65	263.00	0.85	1.31		0.91	200.00	0.80	0.88
Muscle	0.14	9.00	0.03	0.21		0.17	1.00	0.00	0.02
Bone	0.05	1.00	0.00	0.06		0.05	1.00	0.00	0.08
Brain	0.33	1.00	0.00	0.01		0.37	4.00	0.02	0.04
Feces	0.75	2171.00	7.05	9.40		1.02	919.00	3.67	3.60
Pancreas	0.25	191.00	0.62	2.48		0.25	113.00	0.45	1.81
Tumor #1	0.30	85.00	0.28	0.92		0.21	32.00	0.13	0.61
Tumor #2	0.21	108.00	0.35	1.67		0.37	55.00	0.22	0.59
Blood	1.44	33.00	0.11	0.07		1.59	52.00	0.21	0.13
Carcass	13.84	511.00	1.66	0.12		14.55	403.00	1.61	0.11
Tail	0.70	30.00				0.68	165.00		
Sac Time Total Bq (less tail)		30803.00					25039.00		
Inj Time Total Bq		114227.48					93373.64		

	Mouse #:	3.00				Mouse #:	4.00		
	Wt(g)	Bq(cps)	%ID	%ID/g		Wt(g)	Bq(cps)	%ID	%ID/g
Background		4.56					4.56		
Body Wt	20.71					23.77			
Cage Paper		24756.00	85.52				20712.00	89.09	
Urine		3.00	0.01				4.00	0.02	
Bladder	0.02	1.00	0.00	0.17		0.02	1.00	0.00	0.22
Heart	0.06	10.00	0.03	0.58		0.12	12.00	0.05	0.43
Lung	0.13	34.00	0.12	0.90		0.16	22.00	0.09	0.59
Liver	1.01	393.00	1.36	1.34		1.14	336.00	1.45	1.27
Kidneys	0.22	95.00	0.33	1.49		0.32	74.00	0.32	0.99
Spleen	0.04	13.00	0.04	1.12		0.05	2.00	0.01	0.17
Stomach	0.36	35.00	0.12	0.34		0.37	23.00	0.10	0.27
S. Intestine	1.12	215.00	0.74	0.66		1.40	201.00	0.86	0.62
L. Intestine	0.53	177.00	0.61	1.15		0.93	224.00	0.96	1.04
Muscle	0.16	8.00	0.03	0.17		0.13	1.00	0.00	0.03
Bone	0.06	8.00	0.03	0.46		0.04	1.00	0.00	0.11
Brain	0.35	7.00	0.02	0.07		0.40	8.00	0.03	0.09
Feces	0.81	2305.00	7.96	9.83		0.75	946.00	4.07	5.43
Pancreas	0.20	140.00	0.48	2.42		0.24	114.00	0.49	2.04
Tumor #1	0.33	96.00	0.33	1.00		0.12	52.00	0.22	1.86
Tumor #2	0.48	127.00	0.44	0.91		0.18	64.00	0.28	1.53
Blood	1.35	28.00	0.10	0.07		1.55	9.00	0.04	0.02
Carcass	12.91	498.00	1.72	0.13		15.14	442.00	1.90	0.13
Tail	0.69	27.00				0.72	53.00		
Sac Time Total Bq (less tail)		28949.00					23248.00		
Inj Time Total Bq		107347.83					86323.57		

	Averages		%ID for as-measured mouse			
	Wt	STDev	%ID	%STDev	%ID/g	%STDev
Background						
Body Wt	22.80	1.68				
Cage Paper			87.44	2.07		
Urine			0.03	0.03		
Bladder	0.02	0.00	0.01	0.02	0.59	0.80
Heart	0.10	0.03	0.04	0.01	0.40	0.16
Lung	0.17	0.04	0.13	0.03	0.75	0.14
Liver	1.16	0.13	1.49	0.21	1.29	0.08
Kidneys	0.28	0.04	0.32	0.05	1.20	0.33
Spleen	0.07	0.03	0.04	0.02	0.64	0.39
Stomach	0.40	0.05	0.14	0.05	0.34	0.09
S. Intestine	1.49	0.39	0.93	0.16	0.64	0.13
L. Intestine	0.76	0.20	0.81	0.15	1.10	0.18
Muscle	0.15	0.02	0.02	0.01	0.11	0.09
Bone	0.05	0.01	0.01	0.01	0.18	0.19
Brain	0.36	0.03	0.02	0.01	0.05	0.03
Feces	0.83	0.13	5.69	2.14	7.06	3.04
Pancreas	0.24	0.02	0.51	0.07	2.19	0.32
Tumor #1	0.24	0.09	0.24	0.09	1.10	0.54
Tumor #2	0.31	0.14	0.32	0.10	1.18	0.51
Blood	1.48	0.11	0.11	0.07	0.08	0.04
Carcass	14.11	0.96	1.72	0.13	0.12	0.01

Appendix 3.9: Biodistribution of [^{64}Cu-NOTA-9-Anc-BBN(7-14)NH_2] in PC-3 tumor-bearing SCID mice at 1h p.i. (n=5).

1 hr	Mouse #: Wt(g)	1.00 Bq(cps)	%ID	%ID/g		Mouse #: Wt(g)	2.00 Bq(cps)	%ID	%ID/g
Background		5.33					5.06		
Body Wt	24.26					24.16			
Cage Paper		42.00	0.06				101.00	0.08	
Urine		41451.00	55.90				62487.00	51.00	
Bladder	0.02	27.00	0.04	1.82		0.02	37.00	0.03	1.51
Heart	0.10	20.00	0.03	0.27		0.10	61.00	0.05	0.50
Lung	0.15	133.00	0.18	1.20		0.17	216.00	0.18	1.04
Liver	1.13	1584.00	2.14	1.89		1.09	3841.00	3.13	2.88
Kidneys	0.24	1129.00	1.52	6.34		0.32	2073.00	1.69	5.29
Spleen	0.09	62.00	0.08	0.93		0.09	126.00	0.10	1.14
Stomach	0.50	351.00	0.47	0.95		0.42	682.00	0.56	1.33
S. Intestine	1.41	16592.00	22.38	15.87		1.29	32677.00	26.67	20.67
L. Intestine	0.76	2023.00	2.73	3.59		0.78	2864.00	2.34	3.00
Muscle	0.20	39.00	0.05	0.26		0.16	25.00	0.02	0.13
Bone	0.05	19.00	0.03	0.51		0.06	37.00	0.03	0.50
Brain	0.46	9.00	0.01	0.03		0.43	34.00	0.03	0.06
Pancreas	0.24	3281.00	4.42	18.44		0.21	6714.00	5.48	26.09
Tumor #1	0.18	330.00	0.45	2.47		0.22	1051.00	0.86	3.90
Tumor #2	0.18	434.00	0.59	3.25		0.08	360.00	0.29	3.67
Blood	1.58	774.00	1.04	0.66		1.57	1195.00	0.98	0.62
Carcass	15.53	5850.00	7.89	0.51		16.02	7941.00	6.48	0.40
Tail	0.86	1241.00				0.77	1604.00		

	Mouse #: Wt(g)	3.00 Bq(cps)	%ID	%ID/g		Mouse #: Wt(g)	4.00 Bq(cps)	%ID	%ID/g
Background		5.89					4.50		
Body Wt	23.20					22.72			
Cage Paper		125.00	0.12				139.00	0.07	
Urine		48150.00	46.37				96509.00	45.85	
Bladder	0.02	16.00	0.02	0.77		0.02	103.00	0.05	2.45
Heart	0.04	28.00	0.03	0.67		0.08	110.00	0.05	0.65
Lung	0.18	162.00	0.16	0.87		0.15	462.00	0.22	1.46
Liver	1.03	2325.00	2.24	2.17		0.87	5951.00	2.83	3.25
Kidneys	0.31	1874.00	1.80	5.82		0.28	5766.00	2.74	9.78
Spleen	0.06	66.00	0.06	1.06		0.02	76.00	0.04	1.81
Stomach	0.43	620.00	0.60	1.39		0.22	877.00	0.42	1.89
S. Intestine	1.38	24302.00	23.41	16.96		0.90	58595.00	27.83	30.93
L. Intestine	0.85	2564.00	2.47	2.91		0.49	3414.00	1.62	3.31
Muscle	0.16	31.00	0.03	0.19		0.09	73.00	0.03	0.39
Bone	0.03	10.00	0.01	0.32		0.07	61.00	0.03	0.41
Brain	0.38	23.00	0.02	0.06		0.42	89.00	0.04	0.10
Pancreas	0.28	7044.00	6.78	24.23		0.20	6703.00	3.18	15.92
Tumor #1	0.24	704.00	0.68	2.83		0.29	2697.00	1.28	4.42
Tumor #2	0.32	1117.00	1.08	3.36		0.13	1936.00	0.92	7.07
Blood	1.51	799.00	0.77	0.51		1.48	3048.00	1.45	0.98
Carcass	14.74	13868.00	13.36	0.91		15.76	23901.00	11.35	0.72
Tail	0.68	1157.00				0.67	8115.00		

	Mouse #: Wt(g)	5.00 Bq(cps)	%ID	%ID/g		Averages Wt	STDev	%ID for as-measured mouse %ID	%STDev	%ID/g	%STDev
Background		4.67									
Body Wt	21.88					23.24	1.00				
Cage Paper		66.00	0.05					0.08	0.03		
Urine		73157.00	55.34					50.89	4.76		
Bladder	0.02	156.00	0.12	5.90		0.02	0.00	0.05	0.04	2.49	2.00
Heart	0.09	54.00	0.04	0.45		0.08	0.02	0.04	0.01	0.51	0.16
Lung	0.21	255.00	0.19	0.92		0.17	0.02	0.18	0.02	1.10	0.24
Liver	0.95	2712.00	2.05	2.16		1.01	0.11	2.48	0.48	2.47	0.57
Kidneys	0.26	2267.00	1.71	6.60		0.28	0.03	1.89	0.48	6.77	1.76
Spleen	0.01	81.00	0.06	6.13		0.05	0.04	0.07	0.03	2.21	2.21
Stomach	0.21	571.00	0.43	2.06		0.36	0.13	0.50	0.08	1.52	0.45
S. Intestine	1.11	25797.00	19.52	17.58		1.22	0.21	23.96	3.35	20.40	6.15
L. Intestine	0.71	5427.00	4.11	5.78		0.72	0.14	2.65	0.91	3.72	1.19
Muscle	0.19	68.00	0.05	0.27		0.16	0.04	0.04	0.01	0.25	0.10
Bone	0.03	44.00	0.03	1.11		0.05	0.02	0.03	0.01	0.57	0.31
Brain	0.46	29.00	0.02	0.05		0.43	0.03	0.03	0.01	0.06	0.03
Pancreas	0.25	6326.00	4.79	19.14		0.24	0.03	4.93	1.33	20.76	4.24
Tumor #1	0.35	1464.00	1.11	3.16		0.26	0.07	0.87	0.33	3.36	0.79
Tumor #2	0.18	749.00	0.57	3.15		0.18	0.09	0.69	0.31	4.10	1.67
Blood	1.42	1295.00	0.98	0.69		1.51	0.07	1.04	0.25	0.69	0.17
Carcass	14.20	11672.00	8.83	0.62		15.25	0.76	9.58	2.76	0.63	0.19
Tail	0.80	1925.00									

Appendix 3.10: Biodistribution of [^{64}Cu-NOTA-9-Anc-BBN(7-14)NH_2] in PC-3 tumor-bearing SCID mice at 4h p.i. (n=5).

4 hr	Mouse #:	1.00				Mouse #:	2.00		
	Wt(g)	Bq(cps)	%ID	%ID/g		Wt(g)	Bq(cps)	%ID	%ID/g
Background		5.50					5.94		
Body Wt	22.54					30.60			
Cage Paper		28618.00	66.30				71991.00	62.02	
Urine		1883.00	4.36				636.00	0.55	
Bladder	0.02	1.00	0.00	0.12		0.02	8.00	0.01	0.34
Heart	0.15	17.00	0.04	0.26		0.14	14.00	0.01	0.09
Lung	0.22	57.00	0.13	0.60		0.23	69.00	0.06	0.26
Liver	1.01	845.00	1.96	1.94		1.21	1942.00	1.67	1.38
Kidneys	0.27	171.00	0.40	1.47		0.34	293.00	0.25	0.74
Spleen	0.09	27.00	0.06	0.69		0.13	57.00	0.05	0.38
Stomach	0.31	143.00	0.33	1.07		0.41	220.00	0.19	0.46
S. Intestine	1.06	1574.00	3.65	3.44		1.31	5131.00	4.42	3.37
L. Intestine	0.83	8109.00	18.79	22.63		0.91	31397.00	27.05	29.73
Muscle	0.18	7.00	0.02	0.09		0.22	8.00	0.01	0.03
Bone	0.06	1.00	0.00	0.04		0.07	2.00	0.00	0.02
Brain	0.47	1.00	0.00	0.00		0.49	13.00	0.01	0.02
Pancreas	0.28	298.00	0.69	2.47		0.29	1829.00	1.58	5.43
Tumor #1	0.13	47.00	0.11	0.84		0.13	182.00	0.16	1.21
Tumor #2	0.04	5.00	0.01	0.29		0.24	272.00	0.23	0.98
Blood	1.47	472.00	1.09	0.74		1.99	439.00	0.38	0.19
Carcass	14.94	890.00	2.06	0.14		21.36	1567.00	1.35	0.06
Tail	0.83	646.00				0.87	418.00		

	Mouse #:	3.00				Mouse #:	4.00		
	Wt(g)	Bq(cps)	%ID	%ID/g		Wt(g)	Bq(cps)	%ID	%ID/g
Background		4.61					5.33		
Body Wt	21.31					24.37			
Cage Paper		55.00	0.05				47505.00	80.55	
Urine		61840.00	55.80				346.00	0.59	
Bladder	0.02	35.00	0.03	1.58		0.02	5.00	0.01	0.42
Heart	0.13	36.00	0.03	0.25		0.10	7.00	0.01	0.12
Lung	0.20	126.00	0.11	0.57		0.22	20.00	0.03	0.15
Liver	0.92	2072.00	1.87	2.03		1.15	741.00	1.26	1.09
Kidneys	0.24	817.00	0.74	3.07		0.32	193.00	0.33	1.02
Spleen	0.06	45.00	0.04	0.68		0.10	29.00	0.05	0.49
Stomach	0.23	202.00	0.18	0.79		0.48	107.00	0.18	0.38
S. Intestine	1.06	25179.00	22.72	21.43		1.66	1266.00	2.15	1.29
L. Intestine	0.46	15231.00	13.74	29.88		0.60	5636.00	9.56	15.93
Muscle	0.12	11.00	0.01	0.08		0.18	1.00	0.00	0.01
Bone	0.05	16.00	0.01	0.29		0.06	9.00	0.02	0.25
Brain	0.47	19.00	0.02	0.04		0.46	1.00	0.00	0.00
Pancreas	0.20	939.00	0.85	4.24		0.29	641.00	1.09	3.75
Tumor #1	0.65	827.00	0.75	1.15		0.38	251.00	0.43	1.12
Tumor #2	0.41	501.00	0.45	1.10		0.27	146.00	0.25	0.92
Blood	1.39	536.00	0.48	0.35		1.58	115.00	0.20	0.12
Carcass	13.57	2333.00	2.11	0.16		15.24	1955.00	3.32	0.22
Tail	0.88	1147.00				0.93	704.00		

	Mouse #:	5.00				Averages		%ID for as-measured mouse			
	Wt(g)	Bq(cps)	%ID	%ID/g		Wt	STDev	%ID	%STDev	%ID/g	%STDev
Background		5.28									
Body Wt	20.28					23.82	4.08				
Cage Paper		85902.00	68.00					55.38	31.69		
Urine		236.00	0.19					12.30	24.38		
Bladder	0.02	4.00	0.00	0.16		0.02	0.00	0.01	0.01	0.52	0.60
Heart	0.06	43.00	0.03	0.57		0.12	0.04	0.03	0.01	0.26	0.19
Lung	0.14	130.00	0.10	0.74		0.20	0.04	0.09	0.04	0.46	0.25
Liver	0.72	2239.00	1.77	2.46		1.00	0.19	1.71	0.27	1.78	0.54
Kidneys	0.24	612.00	0.48	2.02		0.28	0.05	0.44	0.19	1.66	0.92
Spleen	0.02	33.00	0.03	1.31		0.08	0.04	0.05	0.01	0.71	0.36
Stomach	0.18	286.00	0.23	1.26		0.32	0.12	0.22	0.06	0.79	0.38
S. Intestine	0.88	3915.00	3.10	3.52		1.19	0.30	7.21	8.71	6.61	8.34
L. Intestine	0.40	26639.00	21.09	52.72		0.64	0.22	18.04	6.74	30.18	13.86
Muscle	0.15	15.00	0.01	0.08		0.17	0.04	0.01	0.01	0.06	0.04
Bone	0.03	12.00	0.01	0.32		0.05	0.02	0.01	0.01	0.18	0.14
Brain	0.36	12.00	0.01	0.03		0.45	0.05	0.01	0.01	0.02	0.01
Pancreas	0.15	806.00	0.64	4.25		0.24	0.06	0.97	0.38	4.03	1.07
Tumor #1	0.41	702.00	0.56	1.36		0.34	0.22	0.40	0.27	1.13	0.19
Tumor #2	0.36	441.00	0.35	0.97		0.26	0.14	0.26	0.16	0.85	0.32
Blood	1.32	793.00	0.63	0.48		1.55	0.26	0.56	0.34	0.38	0.25
Carcass	13.47	3504.00	2.77	0.21		15.72	3.25	2.32	0.75	0.16	0.06
Tail	0.79	1864.00									

Appendix 3.11: Biodistribution of [^{64}Cu-NOTA-9-Anc-BBN(7-14)NH_2] in PC-3 tumor-bearing SCID mice at 24h p.i. (n=4).

24 hr	Mouse #:	1.00				Mouse #:	2.00		
	Wt(g)	Bq(cps)	%ID	%ID/g		Wt(g)	Bq(cps)	%ID	%ID/g
Background		4.83					4.39		
Body Wt	21.55					26.14			
Cage Paper		16346.00	73.68				18068.00	74.95	
Urine		10.00	0.05				1.00	0.00	
Bladder	0.02	1.00	0.00	0.23		0.02	1.00	0.00	0.21
Heart	0.09	1.00	0.00	0.05		0.14	3.00	0.01	0.09
Lung	0.15	6.00	0.03	0.18		0.20	12.00	0.05	0.25
Liver	0.90	293.00	1.32	1.47		1.37	334.00	1.39	1.01
Kidneys	0.29	40.00	0.18	0.62		0.33	55.00	0.23	0.69
Spleen	0.07	5.00	0.02	0.32		0.07	16.00	0.07	0.95
Stomach	0.30	25.00	0.11	0.38		1.05	35.00	0.15	0.14
S. Intestine	1.34	158.00	0.71	0.53		1.90	141.00	0.58	0.31
L. Intestine	0.72	312.00	1.41	1.95		0.93	232.00	0.96	1.03
Muscle	0.15	1.00	0.00	0.03		0.18	1.00	0.00	0.02
Bone	0.03	1.00	0.00	0.15		0.08	4.00	0.02	0.21
Brain	0.41	1.00	0.00	0.01		0.43	9.00	0.04	0.09
Feces	0.34	4504.00	20.30	59.71		0.54	4735.00	19.64	36.37
Pancreas	0.26	61.00	0.27	1.06		0.34	94.00	0.39	1.15
Tumor #1	0.27	38.00	0.17	0.63		0.12	19.00	0.08	0.66
Tumor #2	0.09	12.00	0.05	0.60		0.17	25.00	0.10	0.61
Blood	1.40	11.00	0.05	0.04		1.70	79.00	0.33	0.19
Carcass	13.85	360.00	1.62	0.12		15.96	243.00	1.01	0.06
Tail	0.71	237.00				0.85	24.00		

	Mouse #:	3.00				Mouse #:	4.00		
	Wt(g)	Bq(cps)	%ID	%ID/g		Wt(g)	Bq(cps)	%ID	%ID/g
Background		4.28					4.33		
Body Wt	22.85					18.22			
Cage Paper		17578.00	77.81				12778.00	75.08	
Urine			0.00				1.00	0.01	
Bladder	0.02	3.00	0.01	0.66		0.02	5.00	0.03	1.47
Heart	0.12	1.00	0.00	0.04		0.08	1.00	0.01	0.07
Lung	0.17	16.00	0.07	0.42		0.20	19.00	0.11	0.56
Liver	1.16	245.00	1.08	0.93		0.85	298.00	1.75	2.06
Kidneys	0.24	32.00	0.14	0.59		0.24	48.00	0.28	1.18
Spleen	0.05	13.00	0.06	1.15		0.06	6.00	0.04	0.59
Stomach	0.36	29.00	0.13	0.36		0.17	36.00	0.21	1.24
S. Intestine	1.22	115.00	0.51	0.42		0.80	182.00	1.07	1.34
L. Intestine	0.74	139.00	0.62	0.83		0.32	143.00	0.84	2.63
Muscle	0.18	9.00	0.04	0.22		0.13	1.00	0.01	0.05
Bone	0.06		0.00	0.00		0.06	6.00	0.04	0.59
Brain	0.42	1.00	0.00	0.01		0.37	5.00	0.03	0.08
Feces	0.73	3948.00	17.48	23.94		0.32	2963.00	17.41	54.41
Pancreas	0.29	78.00	0.35	1.19		0.17	41.00	0.24	1.42
Tumor #1	0.20	30.00	0.13	0.66		0.20	16.00	0.09	0.47
Tumor #2	0.26	32.00	0.14	0.54		0.39	52.00	0.31	0.78
Blood	1.49	53.00	0.23	0.16		1.18	34.00	0.20	0.17
Carcass	14.49	270.00	1.20	0.08		12.06	384.00	2.26	0.19
Tail	0.72	23.00				0.63	38.00		

	Averages		%ID for as-measured			
	Wt	STDev	%ID	%STDev	%ID/g	%STDev
Background						
Body Wt	22.19	3.28				
Cage Paper			75.38	1.74		
Urine			0.01	0.02		
Bladder	0.02	0.00	0.01	0.01	0.64	0.59
Heart	0.11	0.03	0.01	0.00	0.06	0.02
Lung	0.18	0.02	0.06	0.04	0.35	0.17
Liver	1.07	0.24	1.39	0.28	1.37	0.52
Kidneys	0.28	0.04	0.21	0.06	0.77	0.27
Spleen	0.06	0.01	0.05	0.02	0.75	0.37
Stomach	0.47	0.39	0.15	0.04	0.53	0.49
S. Intestine	1.32	0.45	0.72	0.25	0.65	0.47
L. Intestine	0.68	0.26	0.96	0.33	1.61	0.83
Muscle	0.16	0.02	0.01	0.02	0.08	0.09
Bone	0.06	0.02	0.01	0.02	0.24	0.25
Brain	0.41	0.03	0.02	0.02	0.05	0.04
Feces	0.48	0.19	18.71	1.48	43.61	16.48
Pancreas	0.27	0.07	0.31	0.07	1.20	0.15
Tumor #1	0.20	0.06	0.12	0.04	0.61	0.09
Tumor #2	0.23	0.13	0.15	0.11	0.63	0.10
Blood	1.44	0.22	0.20	0.12	0.14	0.07
Carcass	14.09	1.62	1.52	0.55	0.11	0.05

Appendix 3.12: Biodistribution of [^{64}Cu-NOTA-PABA-BBN(7-14)NH_2] in PC-3 tumor-bearing SCID mice at 1h p.i. (n=5).

	Mouse #: 1.00					Mouse #: 2.00			
	Wt(g)	Bq(cps)	%ID	%ID/g		Wt(g)	Bq(cps)	%ID	%ID/g
Background		5.00					7.61		
Body Wt	21.28			0.00		21.03			0.00
Cage Paper		80.00	0.03				273.00	0.13	
Urine		138643.00	53.63				113252.00	55.52	
Bladder	0.02	934.00	0.36	18.07		0.02	92.00	0.05	2.26
Heart	0.05	117.00	0.05	0.91		0.10	106.00	0.05	0.52
Lung	0.20	440.00	0.17	0.85		0.20	519.00	0.25	1.27
Liver	1.05	3815.00	1.48	1.41		1.03	2720.00	1.33	1.29
Kidneys	0.26	3295.00	1.27	4.90		0.25	6739.00	3.30	13.21
Spleen	0.06	171.00	0.07	1.10		0.09	83.00	0.04	0.45
Stomach	0.44	2313.00	0.89	2.03		0.36	1497.00	0.73	2.04
S. Intestine	1.40	31738.00	12.28	8.77		1.31	19340.00	9.48	7.24
L. Intestine	0.92	6561.00	2.54	2.76		0.93	5877.00	2.88	3.10
Muscle	0.09	102.00	0.04	0.44		0.17	112.00	0.05	0.32
Bone	0.06	101.00	0.04	0.65		0.07	66.00	0.03	0.46
Brain	0.38	80.00	0.03	0.08		0.38	64.00	0.03	0.08
Pancreas	0.22	25680.00	9.93	45.16		0.21	13741.00	6.74	32.08
Tumor #1	0.13	2574.00	1.00	7.66		0.36	3892.00	1.91	5.30
Tumor #2	0.23	3483.00	1.35	5.86		0.16	2124.00	1.04	6.51
Blood	1.38	4190.00	1.62	1.17		1.37	4169.00	2.04	1.49
Carcass	13.42	34185.00	13.22	0.99		13.19	29319.00	14.37	1.09
Tail	0.75	5189.00				0.79	13385.00		

	Mouse #: 3.00					Mouse #: 4.00			
	Wt(g)	Bq(cps)	%ID	%ID/g		Wt(g)	Bq(cps)	%ID	%ID/g
Background		7.17					8.11		
Body Wt	23.90			0.00		25.72			0.00
Cage Paper		45.00	0.02				283.00	0.13	
Urine		134628.00	63.46				127748.00	60.53	
Bladder	0.02	71.00	0.03	1.67		0.02	62.00	0.03	1.47
Heart	0.10	91.00	0.04	0.43		0.07	51.00	0.02	0.35
Lung	0.17	360.00	0.17	1.00		0.16	246.00	0.12	0.73
Liver	1.20	2576.00	1.21	1.01		1.13	3114.00	1.48	1.31
Kidneys	0.26	3340.00	1.57	6.06		0.28	3247.00	1.54	5.49
Spleen	0.06	124.00	0.06	0.97		0.06	113.00	0.05	0.89
Stomach	0.36	1457.00	0.69	1.91		0.38	1336.00	0.63	1.67
S. Intestine	1.25	20748.00	9.78	7.82		1.14	25552.00	12.11	10.62
L. Intestine	0.81	4348.00	2.05	2.53		0.74	4019.00	1.90	2.57
Muscle	0.15	82.00	0.04	0.26		0.20	56.00	0.03	0.13
Bone	0.06	48.00	0.02	0.38		0.05	45.00	0.02	0.43
Brain	0.46	51.00	0.02	0.05		0.44	59.00	0.03	0.06
Pancreas	0.23	17667.00	8.33	36.21		0.23	17273.00	8.18	35.59
Tumor #1	0.31	3003.00	1.42	4.57		0.16	1472.00	0.70	4.36
Tumor #2	0.19	2383.00	1.12	5.91		0.08	1346.00	0.64	7.97
Blood	1.55	2771.00	1.31	0.84		1.67	2291.00	1.09	0.65
Carcass	15.42	18351.00	8.65	0.56		17.53	22728.00	10.77	0.61
Tail	0.75	3351.00				0.80	3478.00		

	Mouse #: 5.00					Averages		%ID for as-measured			
	Wt(g)	Bq(cps)	%ID	%ID/g		Wt	STDev	%ID	%STDev	%ID/g	%STDev
Background		6.61									
Body Wt	22.81			0.00		22.95	1.94			0.00	0.00
Cage Paper		218.00	0.09					0.08	0.05		
Urine		155023.00	65.97					59.82	5.20		
Bladder	0.02	142.00	0.06	3.02		0.02	0.00	0.11	0.14	5.30	7.16
Heart	0.10	52.00	0.02	0.22		0.08	0.02	0.04	0.01	0.48	0.26
Lung	0.18	212.00	0.09	0.50		0.18	0.02	0.16	0.06	0.87	0.29
Liver	1.22	3031.00	1.29	1.06		1.13	0.09	1.36	0.12	1.22	0.17
Kidneys	0.29	2217.00	0.94	3.25		0.27	0.02	1.73	0.92	6.58	3.85
Spleen	0.09	261.00	0.11	1.23		0.07	0.02	0.07	0.03	0.93	0.30
Stomach	0.28	1690.00	0.72	2.57		0.36	0.06	0.73	0.10	2.04	0.33
S. Intestine	1.33	24555.00	10.45	7.86		1.29	0.10	10.82	1.30	8.46	1.33
L. Intestine	0.92	6450.00	2.74	2.98		0.86	0.09	2.42	0.43	2.79	0.25
Muscle	0.17	83.00	0.04	0.21		0.16	0.04	0.04	0.01	0.27	0.12
Bone	0.06	35.00	0.01	0.25		0.06	0.01	0.03	0.01	0.43	0.15
Brain	0.40	57.00	0.02	0.06		0.41	0.04	0.03	0.00	0.07	0.01
Pancreas	0.25	22132.00	9.42	37.67		0.23	0.01	8.52	1.24	37.34	4.83
Tumor #1	0.10	1528.00	0.65	6.50		0.21	0.12	1.13	0.53	5.68	1.39
Tumor #2	0.17	2340.00	1.00	5.86		0.17	0.06	1.03	0.26	6.42	0.91
Blood	1.48	1646.00	0.70	0.47		1.49	0.13	1.35	0.51	0.93	0.41
Carcass	14.37	13314.00	5.67	0.39		14.79	1.77	10.54	3.51	0.73	0.30
Tail	0.71	3205.00									

Appendix 3.13: Biodistribution of [^{64}Cu-NOTA-PABA-BBN(7-14)NH_2] in PC-3 tumor-bearing SCID mice at 4h p.i. (n=5).

	Mouse #:	1.00				Mouse #:	2.00		
	Wt(g)	Bq(cps)	%ID	%ID/g		Wt(g)	Bq(cps)	%ID	%ID/g
Background		5.44					5.78		
Body Wt	21.94			0.00		23.05			0.00
Cage Paper		129654.00	74.69				135371.00	71.90	
Urine		1638.00	0.94				6823.00	3.62	
Bladder	0.02	9.00	0.01	0.26		0.02	18.00	0.01	0.48
Heart	0.10	52.00	0.03	0.30		0.11	32.00	0.02	0.15
Lung	0.17	115.00	0.07	0.39		0.17	141.00	0.07	0.44
Liver	1.02	1920.00	1.11	1.08		1.07	1928.00	1.02	0.96
Kidneys	0.27	536.00	0.31	1.14		0.25	446.00	0.24	0.95
Spleen	0.06	98.00	0.06	0.94		0.08	81.00	0.04	0.54
Stomach	0.37	1021.00	0.59	1.59		0.30	630.00	0.33	1.12
S. Intestine	1.71	9680.00	5.58	3.26		1.36	8655.00	4.60	3.38
L. Intestine	0.85	13842.00	7.97	9.38		0.86	17407.00	9.25	10.75
Muscle	0.17	17.00	0.01	0.06		0.19	30.00	0.02	0.08
Bone	0.05	22.00	0.01	0.25		0.08	29.00	0.02	0.19
Brain	0.42	28.00	0.02	0.04		0.42	22.00	0.01	0.03
Feces									
Pancreas	0.17	7703.00	4.44	26.10		0.25	10087.00	5.36	21.43
Tumor #1	0.13	946.00	0.54	4.19		0.10	759.00	0.40	4.03
Tumor #2	0.25	1801.00	1.04	4.15		0.11	843.00	0.45	4.07
Blood	1.43	297.00	0.17	0.12		1.50	223.00	0.12	0.08
Carcass	13.72	4201.00	2.42	0.18		15.02	4746.00	2.52	0.17

	Mouse #:	3.00				Mouse #:	4.00		
	Wt(g)	Bq(cps)	%ID	%ID/g		Wt(g)	Bq(cps)	%ID	%ID/g
Background		6.67					5.94		
Body Wt	23.54			0.00		24.43			0.00
Cage Paper		152208.00	76.16				137652.00	74.64	
Urine		2827.00	1.41				6255.00	3.39	
Bladder	0.02	6.00	0.00	0.15		0.02	13.00	0.01	0.35
Heart	0.08	40.00	0.02	0.25		0.08	21.00	0.01	0.14
Lung	0.23	171.00	0.09	0.37		0.16	98.00	0.05	0.33
Liver	1.12	2566.00	1.28	1.15		1.16	1926.00	1.04	0.90
Kidneys	0.28	856.00	0.43	1.53		0.29	523.00	0.28	0.98
Spleen	0.06	106.00	0.05	0.88		0.06	117.00	0.06	1.06
Stomach	0.37	563.00	0.28	0.76		0.47	644.00	0.35	0.74
S. Intestine	1.64	8498.00	4.25	2.59		1.48	8676.00	4.70	3.18
L. Intestine	0.60	15102.00	7.56	12.59		0.81	12510.00	6.78	8.37
Muscle	0.16	13.00	0.01	0.04		0.16	18.00	0.01	0.06
Bone	0.05	12.00	0.01	0.12		0.06	14.00	0.01	0.13
Brain	0.45	21.00	0.01	0.02		0.42	23.00	0.01	0.03
Feces									
Pancreas	0.21	7470.00	3.74	17.80		0.24	10202.00	5.53	23.05
Tumor #1	0.35	2586.00	1.29	3.70		0.05	302.00	0.16	3.28
Tumor #2	0.31	1599.00	0.80	2.58		0.15	791.00	0.43	2.86
Blood	1.53	342.00	0.17	0.11		1.59	310.00	0.17	0.11
Carcass	14.81	4870.00	2.44	0.16		15.86	4323.00	2.34	0.15

	Mouse #:	5.00				Averages		%ID for as-measured mouse			
	Wt(g)	Bq(cps)	%ID	%ID/g		Wt	STDev	%ID	%STDev	%ID/g	%STDev
Background		6.94									
Body Wt	23.11			0.00		23.21	0.90			0.00	0.00
Cage Paper		139550.00	77.23					74.93	2.01		
Urine		5071.00	2.81					2.44	1.20		
Bladder	0.02	1.00	0.00	0.03		0.02	0.00	0.01	0.00	0.25	0.17
Heart	0.08	9.00	0.00	0.06		0.09	0.01	0.02	0.01	0.18	0.09
Lung	0.21	81.00	0.04	0.21		0.19	0.03	0.06	0.02	0.35	0.09
Liver	1.22	2004.00	1.11	0.91		1.12	0.08	1.11	0.10	1.00	0.11
Kidneys	0.32	559.00	0.31	0.97		0.28	0.03	0.31	0.07	1.11	0.25
Spleen	0.05	61.00	0.03	0.68		0.06	0.01	0.05	0.01	0.82	0.21
Stomach	0.44	1026.00	0.57	1.29		0.39	0.07	0.42	0.14	1.10	0.36
S. Intestine	1.59	6382.00	3.53	2.22		1.56	0.14	4.53	0.74	2.93	0.50
L. Intestine	0.78	8957.00	4.96	6.36		0.78	0.11	7.30	1.59	9.49	2.36
Muscle	0.17	2.00	0.00	0.01		0.17	0.01	0.01	0.01	0.05	0.03
Bone	0.05	4.00	0.00	0.04		0.06	0.01	0.01	0.01	0.15	0.08
Brain	0.38	16.00	0.01	0.02		0.42	0.02	0.01	0.00	0.03	0.01
Pancreas	0.24	10469.00	5.79	24.14		0.22	0.03	4.97	0.86	22.50	3.13
Tumor #1	0.23	1697.00	0.94	4.08		0.17	0.12	0.67	0.45	3.86	0.37
Tumor #2	0.14	915.00	0.51	3.62		0.19	0.08	0.64	0.27	3.46	0.71
Blood	1.50	298.00	0.16	0.11		1.51	0.06	0.16	0.02	0.11	0.02
Carcass	14.25	3587.00	1.99	0.14		14.73	0.81	2.34	0.21	0.16	0.02

Appendix 3.14: Biodistribution of [^{64}Cu-NOTA-PABA-BBN(7-14)NH_2] in PC-3 tumor-bearing SCID mice at 24h p.i. (n=5).

	Mouse #:	1.00				Mouse #:	2.00		
	Wt(g)	Bq(cps)	%ID	%ID/g		Wt(g)	Bq(cps)	%ID	%ID/g
Background		6.56					6.67		
Body Wt	24.03			0.00		19.95			0.00
Cage Paper		75085.00	80.77				89657.00	85.76	
Urine		57.00	0.06				20.00	0.02	
Bladder	0.02	8.00	0.01	0.43		0.02	4.00	0.00	0.19
Heart	0.12	26.00	0.03	0.23		0.06	29.00	0.03	0.46
Lung	0.22	83.00	0.09	0.41		0.14	103.00	0.10	0.70
Liver	1.29	1039.00	1.12	0.87		0.79	1259.00	1.20	1.52
Kidneys	0.34	200.00	0.22	0.63		0.22	246.00	0.24	1.07
Spleen	0.07	31.00	0.03	0.48		0.06	37.00	0.04	0.59
Stomach	0.55	121.00	0.13	0.24		0.23	156.00	0.15	0.65
S. Intestine	1.52	1175.00	1.26	0.83		0.83	954.00	0.91	1.10
L. Intestine	1.25	804.00	0.86	0.69		0.69	785.00	0.75	1.09
Muscle	0.20	7.00	0.01	0.04		0.14	7.00	0.01	0.05
Bone	0.07	5.00	0.01	0.08		0.07	13.00	0.01	0.18
Brain	0.45	22.00	0.02	0.05		0.37	15.00	0.01	0.04
Feces	1.07	11115.00	11.96	11.17		0.79	6550.00	6.27	7.93
Pancreas	0.24	1391.00	1.50	6.23		0.17	1851.00	1.77	10.41
Tumor #1	0.13	273.00	0.29	2.26		0.18	577.00	0.55	3.07
Tumor #2	0.15	152.00	0.16	1.09		0.19	591.00	0.57	2.98
Blood	1.56	179.00	0.19	0.12		1.30	202.00	0.19	0.15
Carcass	15.00	1191.00	1.28	0.09		13.50	1493.00	1.43	0.11

	Mouse #:	3.00				Mouse #:	4.00		
	Wt(g)	Bq(cps)	%ID	%ID/g		Wt(g)	Bq(cps)	%ID	%ID/g
Background		8.22					7.72		
Body Wt	24.10			0.00		21.82			0.00
Cage Paper		77513.00	83.49				51148.00	76.93	
Urine		5.00	0.01				9.00	0.01	
Bladder	0.02	1.00	0.00	0.05		0.02	1.00	0.00	0.08
Heart	0.10	24.00	0.03	0.26		0.10	4.00	0.01	0.06
Lung	0.14	69.00	0.07	0.53		0.16	61.00	0.09	0.57
Liver	1.14	1375.00	1.48	1.30		1.02	927.00	1.39	1.37
Kidneys	0.33	336.00	0.36	1.10		0.22	143.00	0.22	0.98
Spleen	0.03	30.00	0.03	1.08		0.06	38.00	0.06	0.95
Stomach	0.36	125.00	0.13	0.37		0.77	126.00	0.19	0.25
S. Intestine	1.41	1434.00	1.54	1.10		1.58	943.00	1.42	0.90
L. Intestine	0.67	674.00	0.73	1.08		1.01	733.00	1.10	1.09
Muscle	0.18	19.00	0.02	0.11		0.11	1.00	0.00	0.01
Bone	0.09	1.00	0.00	0.01		0.06	1.00	0.00	0.03
Brain	0.37	5.00	0.01	0.01		0.43	3.00	0.00	0.01
Feces	1.05	6157.00	6.63	6.32		1.26	8200.00	12.33	9.79
Pancreas	0.23	2146.00	2.31	10.05		0.29	1943.00	2.92	10.08
Tumor #1	0.31	783.00	0.84	2.72		0.30	587.00	0.88	2.94
Tumor #2	0.13	339.00	0.37	2.81		0.10	181.00	0.27	2.72
Blood	1.57	156.00	0.17	0.11		1.42	141.00	0.21	0.15
Carcass	15.75	1651.00	1.78	0.11		13.08	1296.00	1.95	0.15

	Mouse #:	5.00				Averages		%ID for as-measured mouse			
	Wt(g)	Bq(cps)	%ID	%ID/g		Wt	STDev	%ID	%STDev	%ID/g	%STDev
Background		7.22									
Body Wt	23.67			0.00		22.71	1.80			0.00	0.00
Cage Paper		65146.00	79.74					81.34	3.41		
Urine		14.00	0.02					0.02	0.02		
Bladder	0.02	3.00	0.00	0.18		0.02	0.00	0.00	0.00	0.19	0.15
Heart	0.09	14.00	0.02	0.19		0.09	0.02	0.02	0.01	0.24	0.15
Lung	0.20	58.00	0.07	0.35		0.17	0.04	0.08	0.01	0.51	0.14
Liver	1.12	1022.00	1.25	1.12		1.07	0.18	1.29	0.15	1.23	0.25
Kidneys	0.25	159.00	0.19	0.78		0.27	0.06	0.24	0.07	0.91	0.20
Spleen	0.07	25.00	0.03	0.44		0.06	0.02	0.04	0.01	0.71	0.29
Stomach	0.50	182.00	0.22	0.45		0.48	0.20	0.17	0.04	0.39	0.17
S. Intestine	1.82	1708.00	2.09	1.15		1.43	0.37	1.45	0.43	1.01	0.14
L. Intestine	1.15	1396.00	1.71	1.49		0.95	0.26	1.03	0.41	1.09	0.28
Muscle	0.16	5.00	0.01	0.04		0.16	0.03	0.01	0.01	0.05	0.04
Bone	0.04	1.00	0.00	0.03		0.07	0.02	0.00	0.00	0.06	0.07
Brain	0.38	9.00	0.01	0.03		0.40	0.04	0.01	0.01	0.03	0.02
Feces	0.84	8075.00	9.88	11.77		1.00	0.19	9.41	2.87	9.40	2.27
Pancreas	0.30	1933.00	2.37	7.89		0.25	0.05	2.17	0.56	8.93	1.81
Tumor #1	0.17	270.00	0.33	1.94		0.22	0.08	0.58	0.28	2.59	0.47
Tumor #2	0.16	371.00	0.45	2.84		0.15	0.03	0.36	0.16	2.49	0.79
Blood	1.54	121.00	0.15	0.10		1.48	0.12	0.18	0.02	0.12	0.02
Carcass	14.60	1181.00	1.45	0.10		14.39	1.09	1.58	0.28	0.11	0.02

Appendix 4.1: Biodistribution of [^{205}Bi-CHX-A´´-8-Aoc-BBN(7-14)NH_2] in PC-3 tumor-bearing nude mice at 0.5h p.i. (n=5).

Mouse	Tissue	(mg)	CPM	CPM/mg	%ID	%ID/gm	Tiss:Blood	Tum:Tiss	Panc:Tiss
1.00	Blood	739.00	47069.90	63.69	0.94	1.27	1.00	0.98	0.66
	Tumor	908.00	56585.90	62.32	1.13	1.24	0.98	1.00	0.68
	Liver	1173.00	38558.60	32.87	0.77	0.65	0.52	1.90	1.28
	Spleen	102.00	16606.80	162.81	0.33	3.24	2.56	0.38	0.26
	Kidney	331.00	80432.90	243.00	1.60	4.83	3.82	0.26	0.17
	Lung	170.00	9377.40	55.16	0.19	1.10	0.87	1.13	0.76
	Heart	143.00	4032.50	28.20	0.08	0.56	0.44	2.21	1.49
	Femur	40.00	2063.10	51.58	0.04	1.03	0.81	1.21	0.82
	Pancreas	60.00	2524.40	42.07	0.05	0.84	0.66	1.48	1.00
	Tail	640.00	66171.90	103.39	1.32	2.06	1.62	0.60	0.41
	Carcass	20490.00	795535.90	38.83	15.82	0.77	0.61	1.61	1.08
2.00	Blood	780.00	22484.80	28.83	0.45	0.57	1.00	3.23	2.85
	Tumor	100.00	9309.30	93.09	0.19	1.85	3.23	1.00	0.88
	Liver	950.00	22664.60	23.86	0.45	0.47	0.83	3.90	3.44
	Spleen	56.00	2996.70	53.51	0.06	1.06	1.86	1.74	1.53
	Kidney	310.00	43533.50	140.43	0.87	2.79	4.87	0.66	0.58
	Lung	153.00	4628.10	30.25	0.09	0.60	1.05	3.08	2.71
	Heart	140.00	2717.50	19.41	0.05	0.39	0.67	4.80	4.23
	Femur	62.00	1538.90	24.82	0.03	0.49	0.86	3.75	3.31
	Pancreas	23.00	1888.10	82.09	0.04	1.63	2.85	1.13	1.00
	Tail	604.00	51163.10	84.71	1.02	1.68	2.94	1.10	0.97
	Carcass	19470.00	552229.30	28.36	10.98	0.56	0.98	3.28	2.89
3.00	Blood	812.00	14674.30	18.07	0.29	0.36	1.00	2.01	2.08
	Tumor	131.00	4760.20	36.34	0.09	0.72	2.01	1.00	1.03
	Liver	1043.00	26590.50	25.49	0.53	0.51	1.41	1.43	1.47
	Spleen	72.00	2835.60	39.38	0.06	0.78	2.18	0.92	0.95
	Kidney	330.00	38251.90	115.91	0.76	2.31	6.41	0.31	0.32
	Lung	155.00	4775.20	30.81	0.09	0.61	1.70	1.18	1.22
	Heart	150.00	2507.40	16.72	0.05	0.33	0.92	2.17	2.25
	Femur	41.00	1281.80	31.26	0.03	0.62	1.73	1.16	1.20
	Pancreas	58.00	2179.20	37.57	0.04	0.75	2.08	0.97	1.00
	Tail	591.00	34767.60	58.83	0.69	1.17	3.26	0.62	0.64
	Carcass	21040.00	838597.00	39.86	16.68	0.79	2.21	0.91	0.94
4.00	Blood	495.00	9013.70	18.21	0.18	0.36	1.00	2.31	6.27
	Tumor	580.00	24413.60	42.09	0.49	0.84	2.31	1.00	2.71
	Liver	1007.00	21996.40	21.84	0.44	0.43	1.20	1.93	5.22
	Spleen	50.00	2547.40	50.95	0.05	1.01	2.80	0.83	2.24
	Kidney	283.00	55440.00	195.90	1.10	3.90	10.76	0.21	0.58
	Lung	139.00	3652.20	26.27	0.07	0.52	1.44	1.60	4.34
	Heart	105.00	2024.10	19.28	0.04	0.38	1.06	2.18	5.92
	Femur	37.00	1407.90	38.05	0.03	0.76	2.09	1.11	3.00
	Pancreas	20.00	2282.30	114.12	0.05	2.27	6.27	0.37	1.00
	Tail	524.00	30093.90	57.43	0.60	1.14	3.15	0.73	1.99
	Carcass	16430.00	534948.75	32.56	10.64	0.65	1.79	1.29	3.50
5.00	Blood	659.00	6619.60	10.04	0.13	0.20	1.00	3.21	4.60
	Tumor	139.00	4475.90	32.20	0.09	0.64	3.21	1.00	1.44
	Liver	1374.00	19430.90	14.14	0.39	0.28	1.41	2.28	3.27
	Spleen	110.00	6252.00	56.84	0.12	1.13	5.66	0.57	0.81
	Kidney	353.00	42042.80	119.10	0.84	2.37	11.86	0.27	0.39
	Lung	196.00	2998.70	15.30	0.06	0.30	1.52	2.10	3.02
	Heart	133.00	1624.90	12.22	0.03	0.24	1.22	2.64	3.78
	Femur	49.00	1557.90	31.79	0.03	0.63	3.17	1.01	1.45
	Pancreas	31.00	1432.90	46.22	0.03	0.92	4.60	0.70	1.00
	Tail	796.00	52390.80	65.82	1.04	1.31	6.55	0.49	0.70
	Carcass	21708.00	651424.80	30.01	12.96	0.60	2.99	1.07	1.54

AVERAGE	CPM/mg	%ID/gm	Tiss:Blood	Tum:Tiss	STDEV
Blood	27.77	0.55	1.00	2.35	0.42
Tumor	53.21	1.06	2.35	1.00	0.50
Liver	23.64	0.47	1.07	2.29	0.13
Spleen	72.70	1.45	3.01	0.89	1.01
Kidney	162.87	3.24	7.54	0.34	1.10
Lung	31.56	0.63	1.32	1.82	0.29
Heart	19.16	0.38	0.86	2.80	0.12
Femur	35.50	0.71	1.73	1.65	0.20
Pancreas	64.41	1.28	3.29	0.93	0.65
Tail	74.04	1.47	3.50	0.71	0.39
Carcass	33.92	0.67	1.71	1.63	0.10

Appendix 4.2: Biodistribution of [^{205}Bi-CHX-A´´-8-Aoc-BBN(7-14)NH_2] in PC-3 tumor-bearing nude mice at 1h p.i. (n=5).

Mouse	Tissue	(mg)	CPM	CPM/mg	%ID	%ID/gm	Tiss:Blood	Tum:Tiss	Panc:Tiss
1.00	Blood	437.00	7407.80	16.95	0.15	0.34	1.00	2.97	2.55
	Tumor	144.00	7246.50	50.32	0.14	1.00	2.97	1.00	0.86
	Liver	1091.00	22302.80	20.44	0.44	0.41	1.21	2.46	2.12
	Spleen	64.00	3057.70	47.78	0.06	0.95	2.82	1.05	0.91
	Kidney	297.00	55558.50	187.07	1.11	3.72	11.04	0.27	0.23
	Lung	179.00	4005.50	22.38	0.08	0.45	1.32	2.25	1.93
	Heart	121.00	1855.00	15.33	0.04	0.30	0.90	3.28	2.82
	Femur	63.00	2634.50	41.82	0.05	0.83	2.47	1.20	1.03
	Pancreas	36.00	1557.90	43.28	0.03	0.86	2.55	1.16	1.00
	Tail	623.00	48485.50	77.83	0.96	1.55	4.59	0.65	0.56
	Carcass	19738.00	881704.40	44.67	17.54	0.89	2.64	1.13	0.97
2.00	Blood	647.00	9191.00	14.21	0.18	0.28	1.00	2.80	2.96
	Tumor	452.00	17968.00	39.75	0.36	0.79	2.80	1.00	1.06
	Liver	986.00	15871.30	16.10	0.32	0.32	1.13	2.47	2.61
	Spleen	133.00	5017.50	37.73	0.10	0.75	2.66	1.05	1.11
	Kidney	295.00	42101.20	142.72	0.84	2.84	10.05	0.28	0.29
	Lung	160.00	3015.70	18.85	0.06	0.37	1.33	2.11	2.23
	Heart	107.00	1547.90	14.47	0.03	0.29	1.02	2.75	2.91
	Femur	49.00	1611.90	32.90	0.03	0.65	2.32	1.21	1.28
	Pancreas	32.00	1345.80	42.06	0.03	0.84	2.96	0.95	1.00
	Tail	546.00	51323.00	94.00	1.02	1.87	6.62	0.42	0.45
	Carcass	17607.00	573626.10	32.58	11.41	0.65	2.29	1.22	1.29
3.00	Blood	502.00	6582.50	13.11	0.13	0.26	1.00	4.61	4.59
	Tumor	540.00	32657.30	60.48	0.65	1.20	4.61	1.00	1.00
	Liver	928.00	26968.70	29.06	0.54	0.58	2.22	2.08	2.07
	Spleen	57.00	5899.60	103.50	0.12	2.06	7.89	0.58	0.58
	Kidney	234.00	42828.90	183.03	0.85	3.64	13.96	0.33	0.33
	Lung	135.00	3147.80	23.32	0.06	0.46	1.78	2.59	2.58
	Heart	132.00	1600.90	12.13	0.03	0.24	0.92	4.99	4.96
	Femur	40.00	1144.80	28.62	0.02	0.57	2.18	2.11	2.10
	Pancreas	28.00	1685.00	60.18	0.03	1.20	4.59	1.00	1.00
	Tail	540.00	54263.30	100.49	1.08	2.00	7.66	0.60	0.60
	Carcass	17036.00	675252.70	39.64	13.43	0.79	3.02	1.53	1.52
4.00	Blood	726.00	3616.10	4.98	0.07	0.10	1.00	8.43	6.14
	Tumor	290.00	12173.00	41.98	0.24	0.83	8.43	1.00	0.73
	Liver	1162.00	175259.30	150.83	3.49	3.00	30.28	0.28	0.20
	Spleen	75.00	4015.50	53.54	0.08	1.06	10.75	0.78	0.57
	Kidney	311.00	38281.30	123.09	0.76	2.45	24.71	0.34	0.25
	Lung	157.00	2178.20	13.87	0.04	0.28	2.79	3.03	2.20
	Heart	85.00	1162.80	13.68	0.02	0.27	2.75	3.07	2.23
	Femur	38.00	1099.80	28.94	0.02	0.58	5.81	1.45	1.06
	Pancreas	50.00	1527.90	30.56	0.03	0.61	6.14	1.37	1.00
	Tail	590.00	37146.00	62.96	0.74	1.25	12.64	0.67	0.49
	Carcass	20052.00	561541.30	28.00	11.17	0.56	5.62	1.50	1.09
5.00	Blood	572.00	3191.80	5.58	0.06	0.11	1.00	7.26	11.60
	Tumor	644.00	26101.70	40.53	0.52	0.81	7.26	1.00	1.60
	Liver	1193.00	23409.30	19.62	0.47	0.39	3.52	2.07	3.30
	Spleen	99.00	6749.80	68.18	0.13	1.36	12.22	0.59	0.95
	Kidney	289.00	47119.30	163.04	0.94	3.24	29.22	0.25	0.40
	Lung	207.00	2683.50	12.96	0.05	0.26	2.32	3.13	4.99
	Heart	124.00	1114.80	8.99	0.02	0.18	1.61	4.51	7.20
	Femur	44.00	1031.80	23.45	0.02	0.47	4.20	1.73	2.76
	Pancreas	16.00	1035.80	64.74	0.02	1.29	11.60	0.63	1.00
	Tail	652.00	23040.50	35.34	0.46	0.70	6.33	1.15	1.83
	Carcass		588040.80	#DIV/0!	11.70	#DIV/0!	#DIV/0!	#DIV/0!	#DIV/0!

AVERAGE	CPM/mg	%ID/gm	Tiss:Blood	Tum:Tiss	STDEV
Blood	10.97	0.22	1.00	5.21	0.11
Tumor	46.61	0.93	5.21	1.00	0.18
Liver	47.21	0.94	7.67	1.87	1.16
Spleen	62.14	1.24	7.27	0.81	0.51
Kidney	164.06	3.26	19.73	0.30	0.58
Lung	18.28	0.36	1.91	2.62	0.09
Heart	12.92	0.26	1.44	3.72	0.05
Femur	31.15	0.62	3.40	1.54	0.14
Pancreas	48.16	0.96	5.57	1.02	0.28
Tail	74.12	1.47	7.57	0.70	0.52
Carcass	#DIV/0!	#DIV/0!	#DIV/0!	#DIV/0!	#DIV/0!

Appendix 4.3: Biodistribution of [^{205}Bi-CHX-A´´-8-Aoc-BBN(7-14)NH_2] in PC-3 tumor-bearing nude mice at 4h p.i. (n=5).

Mouse	Tissue	(mg)	CPM	CPM/mg	%ID	%ID/gm	Tiss:Blood	Tum:Tiss	Panc:Tiss
1.00	Blood	566.00	1402.90	2.48	0.03	0.05	1.00	4.97	12.74
	Tumor	142.00	1751.00	12.33	0.03	0.25	4.97	1.00	2.56
	Liver	1125.00	13551.80	12.05	0.27	0.24	4.86	1.02	2.62
	Spleen	120.00	1640.00	13.67	0.03	0.27	5.51	0.90	2.31
	Kidney	303.00	19534.30	64.47	0.39	1.28	26.01	0.19	0.49
	Lung	160.00	1276.80	7.98	0.03	0.16	3.22	1.55	3.96
	Heart	127.00	878.70	6.92	0.02	0.14	2.79	1.78	4.56
	Femur	68.00	1000.70	14.72	0.02	0.29	5.94	0.84	2.14
	Pancreas	26.00	820.70	31.57	0.02	0.63	12.74	0.39	1.00
	Tail	583.00	7101.30	12.18	0.14	0.24	4.91	1.01	2.59
	Carcass	21130.00	384161.50	18.18	7.64	0.36	7.34	0.68	1.74
2.00	Blood	470.00	1353.90	2.88	0.03	0.06	1.00	5.61	9.95
	Tumor	450.00	7268.60	16.15	0.14	0.32	5.61	1.00	1.77
	Liver	930.00	11658.70	12.54	0.23	0.25	4.35	1.29	2.29
	Spleen	65.00	3001.70	46.18	0.06	0.92	16.03	0.35	0.62
	Kidney	232.00	26531.10	114.36	0.53	2.27	39.70	0.14	0.25
	Lung	167.00	984.70	5.90	0.02	0.12	2.05	2.74	4.86
	Heart	59.00	817.70	13.86	0.02	0.28	4.81	1.17	2.07
	Femur	45.00	774.70	17.22	0.02	0.34	5.98	0.94	1.67
	Pancreas	25.00	716.70	28.67	0.01	0.57	9.95	0.56	1.00
	Tail	488.00	7048.20	14.44	0.14	0.29	5.01	1.12	1.98
	Carcass	15990.00	264018.00	16.51	5.25	0.33	5.73	0.98	1.74
3.00	Blood	645.00	1216.80	1.89	0.02	0.04	1.00	8.18	13.91
	Tumor	299.00	4612.10	15.43	0.09	0.31	8.18	1.00	1.70
	Liver	964.00	12751.60	13.23	0.25	0.26	7.01	1.17	1.98
	Spleen	57.00	2369.30	41.57	0.05	0.83	22.03	0.37	0.63
	Kidney	250.00	27768.40	111.07	0.55	2.21	58.88	0.14	0.24
	Lung	183.00	1068.80	5.84	0.02	0.12	3.10	2.64	4.49
	Heart	139.00	772.70	5.56	0.02	0.11	2.95	2.77	4.72
	Femur	49.00	663.70	13.54	0.01	0.27	7.18	1.14	1.94
	Pancreas	40.00	1049.80	26.25	0.02	0.52	13.91	0.59	1.00
	Tail	510.00	5567.10	10.92	0.11	0.22	5.79	1.41	2.40
	Carcass	18736.00	297665.50	15.89	5.92	0.32	8.42	0.97	1.65
4.00	Blood	680.00	1219.80	1.79	0.02	0.04	1.00	8.36	16.52
	Tumor	803.00	12043.70	15.00	0.24	0.30	8.36	1.00	1.98
	Liver	1080.00	10888.80	10.08	0.22	0.20	5.62	1.49	2.94
	Spleen	89.00	1589.90	17.86	0.03	0.36	9.96	0.84	1.66
	Kidney	270.00	24941.30	92.38	0.50	1.84	51.50	0.16	0.32
	Lung	217.00	1273.80	5.87	0.03	0.12	3.27	2.56	5.05
	Heart	133.00	801.70	6.03	0.02	0.12	3.36	2.49	4.92
	Femur	59.00	819.70	13.89	0.02	0.28	7.75	1.08	2.13
	Pancreas	34.00	1007.70	29.64	0.02	0.59	16.52	0.51	1.00
	Tail	661.00	2650.50	4.01	0.05	0.08	2.24	3.74	7.39
	Carcass	22023.00	289158.50	13.13	5.75	0.26	7.32	1.14	2.26
5.00	Blood	768.00	1662.00	2.16	0.03	0.04	1.00	8.15	12.95
	Tumor	272.00	4796.30	17.63	0.10	0.35	8.15	1.00	1.59
	Liver	1150.00	10421.70	9.06	0.21	0.18	4.19	1.95	3.09
	Spleen	66.00	1322.80	20.04	0.03	0.40	9.26	0.88	1.40
	Kidney	333.00	24191.30	72.65	0.48	1.44	33.57	0.24	0.39
	Lung	192.00	1124.80	5.86	0.02	0.12	2.71	3.01	4.78
	Heart	118.00	1011.80	8.57	0.02	0.17	3.96	2.06	3.27
	Femur	37.00	890.70	24.07	0.02	0.48	11.12	0.73	1.16
	Pancreas	35.00	980.70	28.02	0.02	0.56	12.95	0.63	1.00
	Tail	554.00	4970.50	8.97	0.10	0.18	4.15	1.97	3.12
	Carcass	19334.00	284832.90	14.73	5.67	0.29	6.81	1.20	1.90

AVERAGE	CPM/mg	%ID/gm	Tiss:Blood	Tum:Tiss	STDEV
Blood	2.24	0.04	1.00	7.05	0.01
Tumor	15.31	0.30	7.05	1.00	0.04
Liver	11.39	0.23	5.21	1.38	0.03
Spleen	27.86	0.55	12.56	0.67	0.30
Kidney	85.14	1.69	42.49	0.18	0.42
Lung	6.29	0.13	2.87	2.50	0.02
Heart	8.19	0.16	3.57	2.05	0.07
Femur	16.69	0.33	7.59	0.95	0.09
Pancreas	28.83	0.57	13.21	0.54	0.04
Tail	10.10	0.20	4.42	1.85	0.08
Carcass	15.69	0.31	7.12	0.99	0.04

Appendix 4.4: Biodistribution of [^{205}Bi-CHX-A´´-8-Aoc-BBN(7-14)NH_2] in PC-3 tumor-bearing nude mice at 8h p.i. (n=5).

Mouse	Tissue	(mg)	CPM	CPM/mg	%ID	%ID/gm	Tiss:Blood	Tum:Tiss	Panc:Tiss
1.00	Blood	582.00	1398.90	2.40	0.03	0.05	1.00	5.11	25.77
	Tumor	196.00	2409.30	12.29	0.05	0.24	5.11	1.00	5.04
	Liver	1040.00	8896.50	8.55	0.18	0.17	3.56	1.44	7.24
	Spleen	59.00	1622.90	27.51	0.03	0.55	11.44	0.45	2.25
	Kidney	308.00	20303.60	65.92	0.40	1.31	27.43	0.19	0.94
	Lung	195.00	1241.80	6.37	0.02	0.13	2.65	1.93	9.72
	Heart	113.00	1092.80	9.67	0.02	0.19	4.02	1.27	6.40
	Femur	64.00	1000.70	15.64	0.02	0.31	6.51	0.79	3.96
	Pancreas	17.00	1052.80	61.93	0.02	1.23	25.77	0.20	1.00
	Tail	518.00	5871.50	11.33	0.12	0.23	4.72	1.08	5.46
	Carcass	22183.00	213277.30	9.61	4.24	0.19	4.00	1.28	6.44
2.00	Blood	741.00	1433.90	1.94	0.03	0.04	1.00	7.75	42.67
	Tumor	417.00	6252.00	14.99	0.12	0.30	7.75	1.00	5.51
	Liver	1033.00	9759.20	9.45	0.19	0.19	4.88	1.59	8.74
	Spleen	76.00	2206.20	29.03	0.04	0.58	15.00	0.52	2.84
	Kidney	308.00	21270.00	69.06	0.42	1.37	35.69	0.22	1.20
	Lung	159.00	1309.80	8.24	0.03	0.16	4.26	1.82	10.02
	Heart	100.00	1098.80	10.99	0.02	0.22	5.68	1.36	7.51
	Femur	49.00	1128.80	23.04	0.02	0.46	11.90	0.65	3.58
	Pancreas	29.00	2394.30	82.56	0.05	1.64	42.67	0.18	1.00
	Tail	567.00	6796.80	11.99	0.14	0.24	6.19	1.25	6.89
	Carcass	20170.00	167830.60	8.32	3.34	0.17	4.30	1.80	9.92
3.00	Blood	814.00	1710.00	2.10	0.03	0.04	1.00	7.55	19.03
	Tumor	239.00	3790.30	15.86	0.08	0.32	7.55	1.00	2.52
	Liver	1152.00	9914.50	8.61	0.20	0.17	4.10	1.84	4.64
	Spleen	119.00	2524.40	21.21	0.05	0.42	10.10	0.75	1.88
	Kidney	335.00	20164.00	60.19	0.40	1.20	28.65	0.26	0.66
	Lung	219.00	1583.90	7.23	0.03	0.14	3.44	2.19	5.53
	Heart	140.00	1371.90	9.80	0.03	0.19	4.66	1.62	4.08
	Femur	41.00	1202.80	29.34	0.02	0.58	13.96	0.54	1.36
	Pancreas	37.00	1478.90	39.97	0.03	0.80	19.03	0.40	1.00
	Tail	641.00	8772.20	13.69	0.17	0.27	6.51	1.16	2.92
	Carcass	22125.00	206016.70	9.31	4.10	0.19	4.43	1.70	4.29
4.00	Blood	670.00	1789.00	2.67	0.04	0.05	1.00	5.85	17.17
	Tumor	244.00	3812.30	15.62	0.08	0.31	5.85	1.00	2.93
	Liver	1197.00	10587.10	8.84	0.21	0.18	3.31	1.77	5.18
	Spleen	125.00	3066.70	24.53	0.06	0.49	9.19	0.64	1.87
	Kidney	347.00	23664.60	68.20	0.47	1.36	25.54	0.23	0.67
	Lung	213.00	1782.00	8.37	0.04	0.17	3.13	1.87	5.48
	Heart	121.00	1395.90	11.54	0.03	0.23	4.32	1.35	3.97
	Femur	45.00	1393.90	30.98	0.03	0.62	11.60	0.50	1.48
	Pancreas	34.00	1558.90	45.85	0.03	0.91	17.17	0.34	1.00
	Tail	644.00	4562.00	7.08	0.09	0.14	2.65	2.21	6.47
	Carcass	17965.00	225355.00	12.54	4.48	0.25	4.70	1.25	3.66
5.00	Blood	478.00	1798.00	3.76	0.04	0.07	1.00	2.78	11.85
	Tumor	753.00	7872.60	10.45	0.16	0.21	2.78	1.00	4.26
	Liver	998.00	10442.70	10.46	0.21	0.21	2.78	1.00	4.26
	Spleen	56.00	2574.40	45.97	0.05	0.91	12.22	0.23	0.97
	Kidney	239.00	21931.10	91.76	0.44	1.83	24.39	0.11	0.49
	Lung	192.00	1539.90	8.02	0.03	0.16	2.13	1.30	5.56
	Heart	144.00	1484.90	10.31	0.03	0.21	2.74	1.01	4.32
	Femur	62.00	1318.80	21.27	0.03	0.42	5.65	0.49	2.10
	Pancreas	31.00	1381.90	44.58	0.03	0.89	11.85	0.23	1.00
	Tail	537.00	6321.10	11.77	0.13	0.23	3.13	0.89	3.79
	Carcass	18144.00	151416.20	8.35	3.01	0.17	2.22	1.25	5.34

AVERAGE	CPM/mg	%ID/gm	Tiss:Blood	Tum:Tiss	STDEV
Blood	2.57	0.05	1.00	5.81	0.01
Tumor	13.84	0.28	5.81	1.00	0.05
Liver	9.18	0.18	3.73	1.53	0.02
Spleen	29.65	0.59	11.59	0.52	0.19
Kidney	71.52	1.42	26.50	0.20	0.28
Lung	7.64	0.15	3.12	1.82	0.02
Heart	10.46	0.21	4.29	1.32	0.02
Femur	24.05	0.48	9.93	0.59	0.12
Pancreas	54.98	1.09	23.30	0.27	0.35
Tail	11.17	0.22	4.64	1.32	0.05
Carcass	9.63	0.19	3.93	1.46	0.03

Appendix 4.5: Biodistribution of [^{205}Bi-CHX-A´´-8-Aoc-BBN(7-14)NH_2] in PC-3 tumor-bearing nude mice at 24h p.i. (n=5).

Mouse	Tissue	(mg)	CPM	CPM/mg	%ID	%ID/gm	Tiss:Blood	Tum:Tiss	Panc:Tiss
1.00	Blood	579.00	534.70	0.92	0.01	0.02	1.00	9.53	29.88
	Tumor	637.00	5603.20	8.80	0.12	0.19	9.53	1.00	3.14
	Liver	964.00	6352.20	6.59	0.14	0.14	7.14	1.33	4.19
	Spleen	60.00	827.70	13.80	0.02	0.29	14.94	0.64	2.00
	Kidney	261.00	9661.00	37.02	0.21	0.79	40.08	0.24	0.75
	Lung	150.00	617.70	4.12	0.01	0.09	4.46	2.14	6.70
	Heart	115.00	474.60	4.13	0.01	0.09	4.47	2.13	6.69
	Femur	46.00	418.60	9.10	0.01	0.19	9.85	0.97	3.03
	Pancreas	23.00	634.70	27.60	0.01	0.59	29.88	0.32	1.00
	Tail	527.00	3704.20	7.03	0.08	0.15	7.61	1.25	3.93
	Carcass	16089.00	78255.60	4.86	1.66	0.10	5.27	1.81	5.67
2.00	Blood	470.00	586.70	1.25	0.01	0.03	1.00	16.26	20.93
	Tumor	64.00	1298.80	20.29	0.03	0.43	16.26	1.00	1.29
	Liver	1154.00	5172.70	4.48	0.11	0.10	3.59	4.53	5.83
	Spleen	80.00	1303.80	16.30	0.03	0.35	13.06	1.25	1.60
	Kidney	282.00	10154.10	36.01	0.22	0.77	28.85	0.56	0.73
	Lung	165.00	651.70	3.95	0.01	0.08	3.16	5.14	6.61
	Heart	130.00	556.70	4.28	0.01	0.09	3.43	4.74	6.10
	Femur	40.00	533.70	13.34	0.01	0.28	10.69	1.52	1.96
	Pancreas	22.00	574.70	26.12	0.01	0.56	20.93	0.78	1.00
	Tail	471.00	1890.10	4.01	0.04	0.09	3.21	5.06	6.51
	Carcass	17334.00	78289.10	4.52	1.67	0.10	3.62	4.49	5.78
3.00	Blood	654.00	678.70	1.04	0.01	0.02	1.00	8.88	28.16
	Tumor	319.00	2938.60	9.21	0.06	0.20	8.88	1.00	3.17
	Liver	1175.00	5615.20	4.78	0.12	0.10	4.60	1.93	6.12
	Spleen	73.00	1039.80	14.24	0.02	0.30	13.73	0.65	2.05
	Kidney	285.00	9352.40	32.82	0.20	0.70	31.62	0.28	0.89
	Lung	156.00	664.70	4.26	0.01	0.09	4.11	2.16	6.86
	Heart	115.00	563.70	4.90	0.01	0.10	4.72	1.88	5.96
	Femur	41.00	527.70	12.87	0.01	0.27	12.40	0.72	2.27
	Pancreas	25.00	730.70	29.23	0.02	0.62	28.16	0.32	1.00
	Tail	487.00	2111.20	4.34	0.04	0.09	4.18	2.12	6.74
	Carcass	19667.00	65136.00	3.31	1.39	0.07	3.19	2.78	8.83
4.00	Blood	496.00	603.70	1.22	0.01	0.03	1.00	13.25	27.45
	Tumor	970.00	15648.50	16.13	0.33	0.34	13.25	1.00	2.07
	Liver	886.00	6046.80	6.82	0.13	0.15	5.61	2.36	4.89
	Spleen	47.00	896.70	19.08	0.02	0.41	15.68	0.85	1.75
	Kidney	226.00	11418.10	50.52	0.24	1.07	41.51	0.32	0.66
	Lung	176.00	795.70	4.52	0.02	0.10	3.71	3.57	7.39
	Heart	94.00	567.70	6.04	0.01	0.13	4.96	2.67	5.53
	Femur	34.00	526.70	15.49	0.01	0.33	12.73	1.04	2.16
	Pancreas	19.00	634.70	33.41	0.01	0.71	27.45	0.48	1.00
	Tail	635.00	2451.30	3.86	0.05	0.08	3.17	4.18	8.65
	Carcass	15120.00	96010.30	6.35	2.04	0.14	5.22	2.54	5.26
5.00	Blood	835.00	567.70	0.68	0.01	0.01	1.00	11.09	32.12
	Tumor	245.00	1847.00	7.54	0.04	0.16	11.09	1.00	2.90
	Liver	1278.00	5299.80	4.15	0.11	0.09	6.10	1.82	5.27
	Spleen	91.00	773.70	8.50	0.02	0.18	12.51	0.89	2.57
	Kidney	299.00	10614.10	35.50	0.23	0.76	52.21	0.21	0.62
	Lung	176.00	524.70	2.98	0.01	0.06	4.38	2.53	7.33
	Heart	117.00	437.60	3.74	0.01	0.08	5.50	2.02	5.84
	Femur	41.00	408.60	9.97	0.01	0.21	14.66	0.76	2.19
	Pancreas	21.00	458.60	21.84	0.01	0.46	32.12	0.35	1.00
	Tail	643.00	2648.50	4.12	0.06	0.09	6.06	1.83	5.30
	Carcass	22030.00	70357.40	3.19	1.50	0.07	4.70	2.36	6.84

AVERAGE	CPM/mg	%ID/gm	Tiss:Blood	Tum:Tiss	STDEV
Blood	1.02	0.02	1.00	11.80	0.00
Tumor	12.39	0.26	11.80	1.00	0.12
Liver	5.36	0.11	5.41	2.39	0.03
Spleen	14.38	0.31	13.98	0.85	0.08
Kidney	38.96	0.83	41.36	0.26	0.17
Lung	3.97	0.08	3.97	3.11	0.01
Heart	4.62	0.10	4.62	2.69	0.02
Femur	12.15	0.26	12.07	1.00	0.06
Pancreas	27.64	0.59	27.71	0.45	0.09
Tail	4.67	0.10	4.85	2.89	0.03
Carcass	4.45	0.09	4.40	2.80	0.03

VITA

Stephanie Lane was born on April 20, 1982, in Lafayette, Indiana. After attending public schools in the Springfield, Missouri school district, she graduated from Kickapoo High School (2000). She earned a Bachelors of Science with Honors in Chemistry from the University of Missouri-Columbia (2005). She received a Ph.D. in Chemistry with a specialization in Radiopharmaceutical Chemistry from the University of Missouri-Columbia (2009). She married Charlie Gordon Doll in 2009. She is planning to complete a postdoctoral appointment where she will continue her research in the area of radiochemistry.